ISBN: 978-93-47587-98-6

CONVERGENCE IN SCIENCE AND TECHNOLOGY:

BRIDGING DISCOVERY AND APPLICATION

VOLUME II

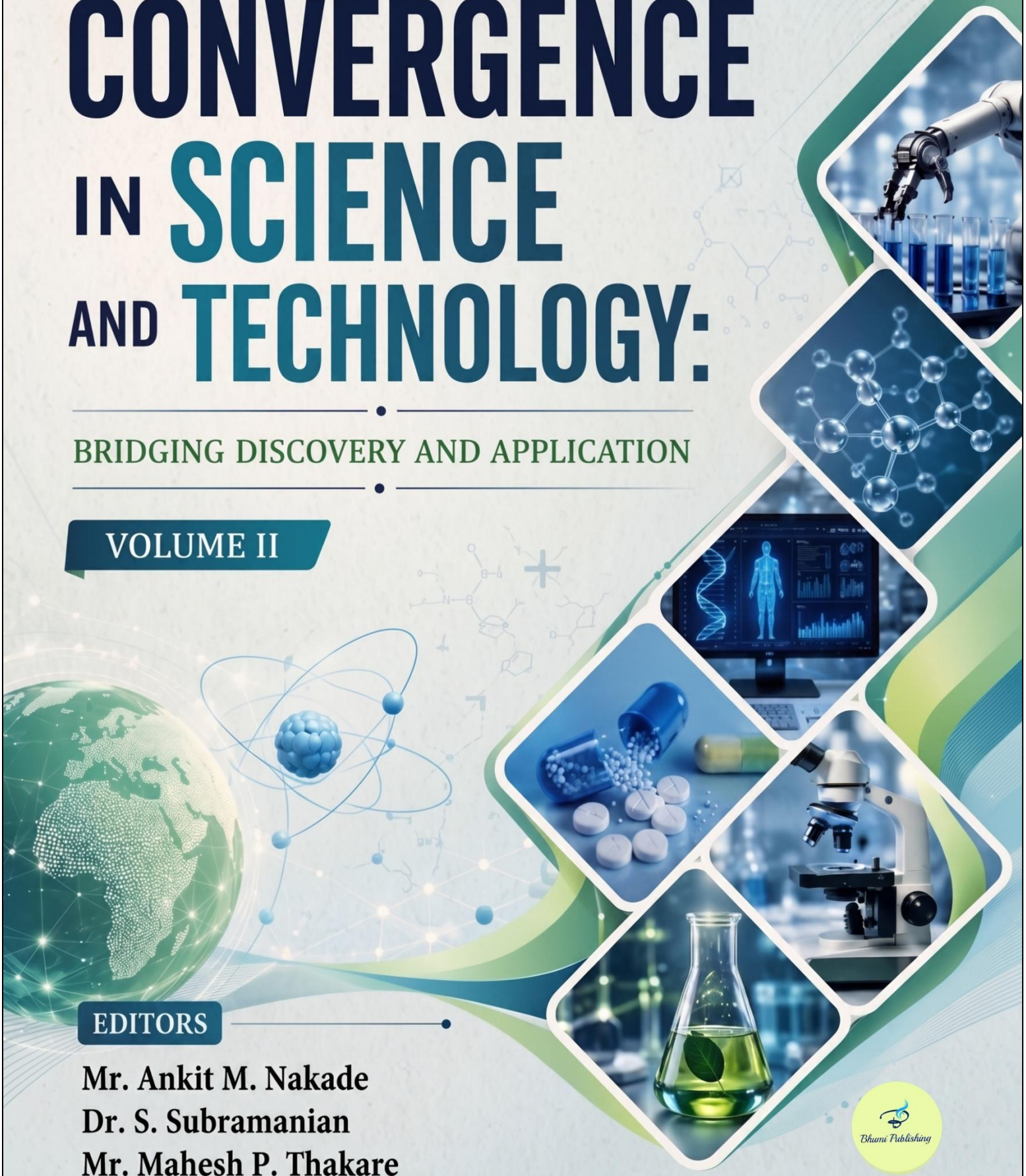

EDITORS

Mr. Ankit M. Nakade
Dr. S. Subramanian
Mr. Mahesh P. Thakare
Dr. Archana Sharma

Bhumi Publishing, India
First Edition: August 2026

Convergence in Science and Technology: Bridging Discovery and Application

Volume II

(ISBN: 978-93-47587-98-6)

DOI: https://doi.org/10.5281/zenodo.22267152

Editors

Mr. Ankit M. Nakade

Department of Botany,

S. S. Jaiswal College,

Arjuni/Mor, Dist. Gondia, M.S.

Dr. S. Subramanian

Department of Nautical Science,

AMET University,

Chennai, Tamil Nadu

Mr. Mahesh P. Thakare

Department of Mathematics,

G. S. Gawande College,

Umarkhed, Dist. Yavatmal, M.S.

Dr. Archana Sharma

Department of Chemistry,

Shri Umiya kanya Mahavidyalaya,

Rangwasa Rau. Indore, Madhya Pradesh

Bhumi Publishing

August 2026

Title: Convergence in Science and Technology: Bridging Discovery and Application Volume II

Editors: Mr. Ankit M. Nakade, Dr. S. Subramanian,

Mr. Mahesh Prabhakar Thakare, Dr. Archana Sharma

First Edition: August 2026

ISBN: 978-93-47587-98-6

DOI: https://doi.org/10.5281/zenodo.22267152

Published by Bhumi Publishing,

a publishing unit of Bhumi Gramin Vikas Sanstha

Bhumi Publishing

Nigave Khalasa, Tal – Karveer, Dist – Kolhapur, Maharashtra, INDIA 416 207

E-mail: bhumipublishing@gmail.com

Disclaimer: The views expressed in the book are of the authors and not necessarily of the publisher and editors. Authors themselves are responsible for any kind of plagiarism found in their chapters and any related issues found with the book.

PREFACE

Science and technology have transformed the modern world by expanding the boundaries of knowledge, accelerating innovation, and creating solutions to complex societal challenges. In the contemporary era, meaningful progress increasingly depends on the convergence of diverse scientific disciplines with emerging technologies and their practical applications. Convergence in Science and Technology: Bridging Discovery and Application has been conceived with this perspective to present a broad and interdisciplinary platform for sharing recent developments, innovative ideas, research findings, and practical approaches across science and technology.

The book brings together contributions that demonstrate how fundamental scientific discoveries can be translated into useful technologies, sustainable practices, and socially relevant applications. It emphasizes the interconnected nature of disciplines such as biological sciences, environmental science, physical sciences, chemistry, agriculture, information technology, engineering, and emerging technological domains. Such interdisciplinary interactions are essential for addressing contemporary issues including climate change, environmental degradation, food and nutritional security, biodiversity conservation, sustainable development, public health, and technological advancement.

A central objective of this volume is to encourage researchers, academicians, teachers, students, and professionals to look beyond disciplinary boundaries and recognize opportunities for collaboration. The chapters included in this book reflect the importance of integrating scientific knowledge with innovation, technology, and real-world problem solving. They also highlight the role of research and education in developing sustainable and inclusive solutions for society.

We hope that this volume will serve as a valuable reference for students, teachers, researchers, and practitioners seeking to understand emerging trends and interdisciplinary approaches in science and technology. It is our sincere belief that the convergence of discovery and application will continue to inspire new ideas, strengthen collaborative research, and contribute meaningfully to a sustainable and technologically advanced future.

The editors gratefully acknowledge the valuable contributions of all authors and reviewers whose efforts have made this volume possible.

- Editors

TABLE OF CONTENT

Convergence in Science and Technology: Bridging Discovery and Application Volume II
(ISBN: 978-93-47587-98-6)

ARTIFICIAL INTELLIGENCE–BASED SOLUTIONS FOR DISASTER RISK REDUCTION AND RESILIENCE BUILDING IN A CHANGING CLIMATE: PERSPECTIVES FROM THE INDIAN SUBCONTINENT

Tanmay Dhar
Department of Physics, Uttaranchal University
Corresponding author E-mail: tanmay.nmhs@gmail.com

Abstract

The Indian subcontinent — comprising India, Bangladesh, Pakistan, Nepal, Sri Lanka, Bhutan, and the Maldives — is among the most disaster-prone regions in the world, exposed to floods, cyclones, earthquakes, droughts, landslides, and heatwaves that are intensifying under climate change and rapid, often unplanned urbanization. Conventional disaster management approaches, largely reactive and dependent on manual data collection, are increasingly inadequate to cope with the scale, frequency, and complexity of hazards confronting the region. Artificial intelligence (AI), encompassing machine learning, deep learning, natural language processing, computer vision, and geospatial analytics, offers transformative potential for shifting disaster governance from reactive response toward proactive risk reduction and anticipatory resilience. This paper examines the evolving disaster risk landscape of the Indian subcontinent and critically reviews the deployment of AI-based tools across the disaster management cycle, including early warning systems, satellite-based hazard mapping, predictive flood and cyclone modelling, social-media-driven situational awareness, robotics-assisted search and rescue, and AI-enabled infrastructure resilience assessment. Drawing on case studies from the India Meteorological Department's nowcasting systems, Bangladesh's cyclone preparedness programme,

Nepal's post-earthquake damage assessment, and flood-forecasting initiatives in the Ganga–Brahmaputra–Meghna basin, the paper proposes an integrated AI-resilience framework that couples hazard prediction, exposure mapping, vulnerability assessment, and community-level early action. The paper further identifies critical barriers to AI adoption, including fragmented and low-quality data, limited computational and institutional capacity, the digital divide, algorithmic bias, and questions of data governance and accountability. It concludes with policy recommendations for regional cooperation, capacity building, and ethical AI governance to strengthen disaster resilience across South Asia in an era of accelerating climate risk.

Keywords: Artificial Intelligence, Disaster Risk Reduction, Resilience, Early Warning Systems, Climate Change, South Asia, Indian Subcontinent, Machine Learning, Remote Sensing.

Introduction

The Indian subcontinent, home to nearly a quarter of the world's population, is one of the most hazard-prone landmasses on Earth. Its physiography — the young, seismically active Himalayan arc in the north, the low-lying deltaic plains of the Ganga–Brahmaputra–Meghna system, an extensive cyclone-exposed coastline along the Bay of Bengal and Arabian Sea, and drought-prone semi-arid tracts in its interior — creates a mosaic of overlapping hazards. Floods, tropical cyclones, earthquakes, landslides, droughts, and heatwaves recur with regularity, and their impacts are compounded by high population density, rapid and often unplanned urbanization, poverty, and fragile infrastructure. Climate change is altering the frequency, intensity, and spatial distribution of these hazards, producing more erratic monsoons, intensified cyclones, glacial lake outburst floods in the Himalaya, and prolonged heatwaves across the Indo-Gangetic plain.

Traditional disaster management in the region has historically been reactive, organized around post-event relief, rehabilitation, and reconstruction rather than anticipatory risk reduction. While national disaster management authorities in India, Bangladesh, Nepal, Pakistan, and Sri Lanka have made considerable progress since the 2004 Indian Ocean tsunami and the adoption of the Sendai Framework for Disaster Risk Reduction (2015–2030), the scale and complexity of emerging risks increasingly outstrip the capacity of conventional, manually intensive monitoring and response systems. In this context, artificial intelligence (AI) has emerged as a potentially transformative set of tools capable of processing vast, heterogeneous data streams — satellite imagery, weather-radar output, river-gauge readings, social-media text, mobilephone mobility data — to generate timely, actionable, and increasingly hyper-local risk intelligence.

This paper reviews and synthesizes the current state of AI applications across the disaster management cycle (prevention, mitigation, preparedness, response, and recovery) in the Indian subcontinent. It examines representative case studies, proposes an integrated framework for AI-enabled resilience, and critically discusses the technical, institutional, and ethical barriers that must be addressed for AI to deliver on its promise. The objective is not to present AI as a panacea but to map where it adds genuine value, where risks of over-reliance or exclusion arise, and how policy can steer its adoption toward equitable and sustainable resilience outcomes.

The Disaster Risk Landscape of the Indian Subcontinent

The Indian subcontinent's disaster profile is shaped by four interacting drivers: hazard exposure, socio-economic vulnerability, environmental degradation, and climate change. Approximately 12 percent of India's land area is flood-prone, and the Ganga–Brahmaputra– Meghna basin, shared by India, Nepal, Bhutan, and Bangladesh, experiences some of the most severe riverine and monsoonal flooding in the world. Bangladesh, with roughly 80 percent of its territory forming a low-lying delta, is particularly exposed to both riverine flooding and coastal cyclones. The Himalayan belt spanning Nepal, northern India, Bhutan, and Pakistanadministered Kashmir lies

within a seismic gap capable of generating great earthquakes, while its glaciers are increasingly prone to glacial lake outburst floods as warming accelerates ice melt. The Bay of Bengal generates a disproportionate share of the world's most destructive tropical cyclones, threatening the coastlines of India, Bangladesh, and Sri Lanka, while the Arabian Sea, historically less active, has seen an observed increase in cyclone frequency and intensity over the past two decades.

Vulnerability compounds this hazard exposure. Rapid, often informal urbanization has placed large populations in floodplains, coastal buffers, and landslide-prone hill slopes without adequate zoning enforcement. Agricultural livelihoods across the region remain heavily dependent on monsoon rainfall, making rural communities acutely sensitive to droughts and erratic precipitation. Infrastructure — roads, power grids, drainage systems, and health facilities — is frequently under-designed relative to present-day hazard intensities, let alone future climate scenarios. Environmental degradation, including deforestation in Himalayan catchments, mangrove loss along the Sundarbans coastline, and unregulated sand mining in riverbeds, has eroded natural buffers that once attenuated hazard impacts. Climate change is now amplifying nearly every one of these hazards: warming sea-surface temperatures are associated with rapid cyclone intensification; erratic monsoon behavior is producing both intense flooding and prolonged dry spells within the same season; and rising temperatures are extending the frequency and duration of heatwaves across northern and central India and Pakistan. Together, these dynamics make the Indian subcontinent a critical proving ground for AI-based disaster risk management, where the marginal value of improved prediction, targeting, and early action is exceptionally high given the scale of exposed population.

AI in Disaster Management: A Review of the Emerging Literature

Scholarship on AI applications in disaster risk management has expanded rapidly over the last decade, moving from isolated proof-of-concept studies toward operationally deployed systems. Early work concentrated on machine-learning-based hazard prediction, using historical rainfall, river discharge, and seismic data to train regression and classification models for flood and landslide forecasting. Subsequent research incorporated deep learning architectures — convolutional neural networks (CNNs) for satellite and drone image classification, recurrent neural networks and long short-term memory (LSTM) networks for time-series forecasting of river levels and cyclone tracks, and graph neural networks for modelling infrastructure interdependencies during cascading failures. A parallel stream of research has examined natural language processing (NLP) applications, particularly the use of social media and crowdsourced text data to generate real-time situational awareness during rapidly evolving events, and computer-vision-based damage assessment using pre- and post-event satellite or drone imagery.

Within South Asia specifically, the literature reflects both notable achievements and persistent gaps. Studies document measurable improvements in flood-forecasting lead times along the Ganga and Brahmaputra basins when machine-learning models are coupled with traditional hydrological models, and in cyclone-track and intensity prediction when statistical models are supplemented with deep-learning ensembles. Researchers have also explored AI-assisted seismic risk assessment for the Himalayan region, given the scarcity of dense seismic networks, using machine learning to infer subsurface fault behavior from sparse observational data. However, much of this research remains at a pilot or academic stage, with limited documentation of sustained operational transition, integration into government early-warning infrastructure, or rigorous post-implementation evaluation. Reviews of AI adoption in South Asian disaster management consistently flag data scarcity, poor inter-agency data sharing, limited computational infrastructure outside major urban centres, and a shortage of interdisciplinary expertise bridging data science and disaster risk science as the principal barriers constraining the translation of research advances into operational capability. This paper builds on that literature by synthesizing applications across the full disaster management cycle and situating them within a practical, policy-relevant framework tailored to the region's institutional realities.

AI Technologies Across the Disaster Management Cycle

AI-based tools can be mapped onto the five conventional phases of the disaster management cycle — prevention and mitigation, preparedness, early warning, response, and recovery — each of which benefits from distinct classes of algorithms and data sources.

Predictive Analytics for Hazard Forecasting

Machine-learning models, particularly gradient-boosted trees, random forests, and deep neural networks, are increasingly used to forecast riverine and flash floods by learning nonlinear relationships between rainfall, upstream discharge, soil moisture, and terrain characteristics that traditional physically based hydrological models struggle to capture efficiently at fine spatial resolution. LSTM and transformer-based architectures have shown particular promise in short- to medium-range flood forecasting because they can model temporal dependencies in rainfall–runoff sequences. Similarly, ensemble machine-learning models are being layered atop numerical weather prediction outputs to improve cyclone track and intensity forecasts in the Bay of Bengal, where rapid intensification events have historically been difficult to predict using physics-based models alone. For drought and heatwave forecasting, AI models trained on sea-surface temperature anomalies, soil moisture indices, and historical monsoon patterns are being used to generate seasonal outlooks that support agricultural planning and heat-action plans in cities such as Ahmedabad and Delhi.

Remote Sensing, GIS, and Computer Vision

The proliferation of freely available satellite imagery from missions such as Sentinel-1/2 and Landsat, combined with increasing commercial very-high-resolution imagery and unmanned aerial vehicle (UAV) data, has enabled convolutional-neural-network-based classification of flood extent, landslide scars, cyclone-damaged infrastructure, and informal settlement growth. Synthetic aperture radar (SAR) imagery, which penetrates cloud cover, is especially valuable during monsoon-season flood mapping when optical satellites are obscured. AI-based changedetection algorithms comparing pre- and post-disaster imagery can rapidly generate damageextent maps that would otherwise require weeks of manual field survey, substantially accelerating the allocation of relief resources. Geographic information system (GIS) platforms integrated with machine-learning-derived susceptibility layers — for landslides, flood inundation, or coastal erosion — support multi-hazard risk mapping at district and sub-district scales, informing land-use planning and building codes.

Natural Language Processing and Social Media Analytics

During rapidly unfolding disasters, social media platforms and messaging applications generate large volumes of unstructured, real-time text and image data from affected populations. NLP techniques, including named-entity recognition, sentiment analysis, and topic modelling, are used to extract actionable information — reports of stranded persons, infrastructure damage, or emerging needs — from this data, filtering signal from noise at a scale unmanageable by manual monitoring. Multilingual NLP models capable of processing regional languages such as Hindi, Bengali, Urdu, Tamil, and Nepali are of particular importance in the Indian subcontinent, where a substantial share of crisis-related communication occurs in languages other than English. Chatbot and conversational-AI systems are also being piloted to disseminate warnings and respond to citizen queries during cyclones and floods, particularly through widely used messaging platforms.

Robotics, UAVs, and Autonomous Systems

Autonomous and semi-autonomous systems, including UAVs equipped with thermal and optical sensors, are increasingly deployed for search-and-rescue operations in terrain inaccessible to ground teams, such as flooded areas or earthquake rubble. AI-enabled objectdetection algorithms process UAV video feeds in near real time to identify stranded individuals, structural damage, and blocked access routes, while autonomous underwater vehicles have been explored for post-tsunami coastal infrastructure assessment. Robotics remains at a comparatively early stage of adoption in the region relative to predictive analytics and remote sensing, constrained by cost, regulatory frameworks governing UAV operation, and the need for trained operators.

Table 1 summarizes representative AI techniques and their primary applications across the disaster management cycle in the Indian subcontinent context, illustrating the breadth of methods now under active exploration or deployment.

Table 1: Representative AI techniques mapped to the disaster management cycle

Disaster Phase	AI Technique(s)	Representative Application
Mitigation / Prevention	Random forests, CNNs, susceptibility modelling	Landslide and flood susceptibility mapping in the Himalaya and IndoGangetic plain
Preparedness	NLP, agent-based simulation	Multilingual risk communication and evacuation-scenario simulation
Early Warning	LSTM, ensemble learning, biascorrected NWP	Cyclone-track forecasting in the Bay of Bengal; monsoon flood forecasting
Response	Computer vision, UAV-based object detection	Rapid damage mapping; search-andrescue target identification
Recovery	Change detection, graph neural networks	Post-disaster reconstruction prioritization; infrastructure interdependency analysis

AI for Infrastructure Resilience and Digital Twins

Emerging applications use AI to assess the resilience of critical infrastructure — power grids, water systems, transportation networks, and hospitals — to hazard scenarios, using graphbased models to simulate cascading failures across interdependent systems. Digital twin approaches, which maintain a continuously updated virtual representation of physical infrastructure or urban systems, are being explored in a small number of Indian smart-city initiatives to simulate flood inundation scenarios and optimize evacuation routing under different hazard intensities. While still nascent in operational deployment across the subcontinent, these approaches represent a frontier with substantial long-term potential for proactive infrastructure planning.

Case Studies from the Indian Subcontinent

India Meteorological Department Nowcasting and Impact-Based Forecasting

The India Meteorological Department (IMD) has progressively integrated machine-learning techniques into its nowcasting systems for severe thunderstorms, lightning, and heavy rainfall, supplementing Doppler weather radar and satellite data with statistical and machine-learning models to generate short-range, location-specific forecasts. The shift toward impact-based forecasting, which translates meteorological parameters into expected impacts on people, infrastructure, and livelihoods, has been supported by AI-based decision-support tools that help district administrations translate weather warnings into targeted evacuation and preparedness actions. Complementary efforts by the National Disaster Management Authority (NDMA) have promoted early-warning dissemination through the Common Alerting Protocol, integrated with mobile-based alert systems, improving the speed and specificity of warning delivery.

Bangladesh Cyclone Preparedness and Early Action

Bangladesh's Cyclone Preparedness Programme, one of the most extensive community-based early-warning networks in the world, has increasingly incorporated AI-enhanced forecasting to refine cyclone landfall and storm-surge predictions along its low-lying coastline. Machinelearning models trained on historical storm-surge data and bathymetric information support more granular inundation forecasts, informing which unions and villages require evacuation. Forecast-based financing mechanisms, which release humanitarian funding in advance of a predicted disaster based on defined trigger thresholds, have begun to draw on AI-generated flood and cyclone forecasts to determine when anticipatory cash transfers or evacuation support should be activated, representing one of the more mature examples of AI-informed anticipatory action in the region.

Nepal Post-Earthquake Damage Assessment

Following the 2015 Gorkha earthquake, subsequent research and pilot programmes in Nepal have explored the use of machine-learning classification of satellite and drone imagery to accelerate building-damage assessment, an exercise that traditionally required extensive manual field surveys spanning months. CNN-based models trained on labelled pre- and postearthquake imagery have demonstrated the ability to classify damage severity at the building level, supporting faster prioritization of reconstruction assistance. These efforts illustrate AI's potential value in a mountainous, infrastructure-constrained environment where rapid physical access for damage assessment is often difficult.

Flood Forecasting in the Ganga–Brahmaputra–Meghna Basin

Transboundary flood forecasting in the Ganga–Brahmaputra–Meghna basin, shared by India, Nepal, Bhutan, and Bangladesh, has benefited from collaborative initiatives that combine hydrological modelling with machine-learning-based bias correction and downscaling of rainfall forecasts. Platforms such as India's Central Water Commission flood forecasting network and complementary regional initiatives supported by international partners have piloted AI-based extensions to extend forecast lead times from a day or two to five to seven days in some reaches, providing critical additional time for evacuation and asset protection in one of the most densely populated flood-prone regions in the world. These efforts remain constrained by the limited real-time hydrological data-sharing arrangements between riparian countries, underscoring the importance of regional cooperation discussed later in this paper.

Toward an Integrated AI-Resilience Framework

Building on the preceding review, this paper proposes an integrated four-layer framework for AI-enabled disaster resilience suited to the institutional and resource realities of the Indian subcontinent. The first layer, data infrastructure, comprises the harmonization of meteorological, hydrological, seismic, socio-economic, and infrastructure datasets into interoperable, quality-

controlled repositories accessible across relevant agencies, with particular attention to filling data gaps in secondary cities and rural areas that are typically underrepresented in monitoring networks. The second layer, predictive intelligence, applies machine-learning and deep-learning models to this harmonized data to generate hazard forecasts, exposure maps, and vulnerability indices, calibrated and validated against local ground-truth data rather than transferred uncritically from models developed for other geographic contexts. The third layer, decision support and dissemination, translates predictive outputs into impact-based, multilingual, and last-mile-accessible warnings and recommended actions, integrating NLP-based dissemination tools with existing community-based networks such as Bangladesh's cyclone preparedness volunteers or India's trained disaster-management community volunteers. The fourth layer, anticipatory and adaptive response, links predictive triggers to pre-agreed early-action protocols, including forecast-based financing, prepositioning of relief supplies, and AI-assisted resource allocation and routing during response operations.

A defining feature of this framework is its emphasis on coupling AI outputs with human institutional capacity rather than substituting for it: AI is positioned as a decision-support tool that augments the judgement of meteorologists, disaster-management officials, and community-based responders, with human oversight retained at each decision point, particularly for high-stakes evacuation and resource-allocation decisions. The framework also emphasizes feedback loops, whereby the accuracy of AI-generated forecasts and post-event outcomes is systematically evaluated and used to retrain and recalibrate models, addressing a documented weakness in the region's current AI pilots, many of which lack structured postimplementation evaluation.

Operationalizing this framework requires attention to sequencing. Agencies with limited existing capacity are advised to begin with the data-infrastructure layer, since even relatively simple statistical or machine-learning models yield limited value without reliable, harmonized input data, before progressing to more sophisticated predictive-intelligence applications. Regional bodies such as the South Asian Association for Regional Cooperation (SAARC)

Disaster Management Centre and the Bay of Bengal Initiative for Multi-Sectoral Technical and Economic Cooperation (BIMSTEC) offer potential institutional platforms through which harmonized data standards, shared model-validation protocols, and cross-border early-warning dissemination agreements could be negotiated, building on existing but currently underutilized frameworks for regional disaster cooperation. Pilot implementation in a small number of highexposure districts, with rigorous before–after evaluation against non-AI-supported comparison areas, would generate the evidence base needed to justify wider national scale-up, addressing the current shortage of documented impact evaluations noted in the literature review above.

Challenges and Limitations

Data Quality, Availability, and Interoperability

AI models are only as reliable as the data on which they are trained, and the Indian subcontinent faces persistent challenges of sparse observational networks in rural and mountainous areas, inconsistent historical record-keeping, and fragmented data ownership across national, state, and local agencies. Real-time hydrological and meteorological data-sharing across national borders in transboundary river basins remains limited by geopolitical sensitivities, constraining the accuracy of basin-wide flood forecasts. Socio-economic and exposure data, essential for translating hazard forecasts into impact-based warnings, are frequently outdated or aggregated at a spatial resolution too coarse for actionable, hyper-local decision-making.

Institutional and Computational Capacity

Many disaster-management agencies across the region, particularly at state and district levels, lack the computational infrastructure, technical personnel, and sustained budgetary support required to develop, deploy, and maintain AI systems. Pilot projects developed with academic or international partners frequently fail to transition into sustained operational systems once external funding or technical support concludes, a pattern documented across multiple sectors of digital-government adoption in South Asia. Building durable institutional capacity, including in-house data science expertise embedded within meteorological and disastermanagement agencies, is therefore as important as the underlying algorithmic advances themselves.

The Digital Divide and Last-Mile Access

AI-generated warnings and risk information are of limited value if they cannot reach the populations most at risk, many of whom are located in remote rural areas with limited internet connectivity, smartphone penetration, or literacy in the languages used by digital dissemination platforms. Elderly populations, persons with disabilities, and economically marginalized groups are disproportionately likely to be excluded from smartphone-based or app-based warning systems, risking the reinforcement of existing social inequities if AI-based tools are not deliberately designed with inclusive, multi-channel dissemination in mind, combining digital alerts with traditional community-based networks, loudspeakers, and local volunteer structures.

Algorithmic Bias, Transparency, and Accountability

Machine-learning models trained predominantly on data from well-monitored urban or majority-population areas risk performing less accurately in underrepresented regions or for marginalized communities, potentially skewing resource allocation away from the most vulnerable. The opacity of complex deep-learning models raises accountability concerns when their outputs inform high-stakes decisions such as evacuation orders or the allocation of scarce relief resources, underscoring the need for explainable AI approaches and clear human accountability structures. Data privacy is a further concern, particularly where AI systems draw on mobile-

phone location data, social media content, or biometric information for disaster response, necessitating robust data-governance frameworks that are, in several countries of the region, still under development.

Climate Non-Stationarity and Model Generalizability

A further, often underappreciated, limitation concerns climate non-stationarity: many machinelearning models are trained on historical hazard records that may no longer accurately represent hazard behavior under present or future climate conditions, since warming-driven shifts in monsoon dynamics, cyclone intensification rates, and glacial melt are altering the statistical relationships on which such models depend. Models trained purely on historical data risk systematically underestimating the frequency or severity of increasingly extreme events unless they are explicitly coupled with climate-projection data and regularly recalibrated. Crossregional transfer of models developed in other geographic or climatic contexts also carries risks of poor generalizability, given the distinct monsoon dynamics, deltaic hydrology, and settlement patterns of the Indian subcontinent relative to the regions in which many widely cited AI-disaster-management studies have originated.

Policy Recommendations

Based on the preceding analysis, five policy priorities emerge for strengthening AI-enabled disaster resilience across the Indian subcontinent.

- Regional data-sharing cooperation: Establishing formal agreements for real-time sharing of meteorological, hydrological, and seismic data across South Asian countries, particularly within transboundary river basins, to improve the accuracy and lead time of AI-based forecasts.
- Sustained investment in institutional capacity: Embedding dedicated data-science and AI expertise within national meteorological and disaster-management agencies, supported by long-term budgetary commitments rather than short-term project funding, to ensure pilot systems transition into sustained operational capability.
- Inclusive, multi-channel warning dissemination: Mandating that AI-based earlywarning systems be paired with non-digital and community-based dissemination channels, and that multilingual NLP tools be developed for the region's major languages to close last-mile access gaps.
- Ethical and transparent AI governance: Developing sector-specific guidelines for explainability, bias auditing, and data privacy in disaster-related AI applications, with clear human accountability retained for high-stakes decisions.
- Structured monitoring and evaluation: Requiring systematic post-implementation evaluation of AI-based disaster tools against ground-truth outcomes, with findings used

to iteratively recalibrate models and inform regional knowledge-sharing on effective practice.

Conclusion

The Indian subcontinent's disaster risk profile is intensifying under the combined pressures of climate change, rapid urbanization, and environmental degradation, exposing the limits of conventional, reactive disaster-management approaches. Artificial intelligence offers meaningful, and in several documented cases already demonstrated, improvements in hazard forecasting, damage assessment, situational awareness, and anticipatory action across the disaster management cycle. Yet the technology's promise remains constrained by persistent gaps in data infrastructure, institutional and computational capacity, last-mile accessibility, and governance frameworks for accountability and equity. Realizing AI's potential for disaster resilience in the region will require treating it not as a stand-alone technical fix but as one component of a broader, human-centred resilience-building agenda — one that couples predictive intelligence with inclusive dissemination, sustained institutional investment, and regional cooperation across the shared hazardscapes that define the Indian subcontinent. Future research should prioritize longitudinal, post-implementation evaluation of deployed AI systems, deeper investigation of equity implications for marginalized populations, and expanded regional collaboration on transboundary data sharing, so that the considerable technical advances documented in the literature translate into measurable reductions in disaster losses across South Asia.

References

1. Alfieri, L., Bisselink, B., Dottori, F., Naumann, G., de Roo, A., Salamon, P., Wyser, K., & Feyen, L. (2017). Global projections of river flood risk in a warmer world. *Earth's Future, 5*(2), 171–182.
2. Bhatt, C. M., Gupta, A., Roy, A., Dalal, P., & Chauhan, P. (2021). Geospatial analysis of Bihar flood 2019 using synthetic aperture radar (SAR) and multispectral datasets. *Quaternary Science Advances, 4*, 100032.
3. Fanfani, V., Bhat, S., Hasan, A. Z., & Khan, A. R. (2022). Machine learning applications for early warning in the Ganges-Brahmaputra-Meghna basin: A review. *Journal of Hydrology: Regional Studies, 42*, 101142.
4. Gaillard, J. C., & Mercer, J. (2013). From knowledge to action: Bridging gaps in disaster risk reduction. *Progress in Human Geography, 37*(1), 93–114.
5. Ghosh, S., Das, J., & Bandyopadhyay, S. (2020). Application of deep learning in flood extent mapping using Sentinel-1 SAR data over Eastern India. *Environmental Monitoring and Assessment, 192*, 574.
6. Government of India, National Disaster Management Authority. (2019). *National Disaster Management Plan*. NDMA, New Delhi.

7. Islam, M. M., & Chik, Z. (2011). Disaster in Bangladesh and management with advanced information system. *Disaster Prevention and Management, 20*(5), 521–530.
8. Kirschbaum, D., Kapnick, S. B., Stanley, T., & Pascale, S. (2020). Changes in extreme precipitation and landslides over High Mountain Asia. *Geophysical Research Letters, 47*(4), e2019GL085347.
9. Kumar, S., Mishra, A., & Pandey, A. (2021). Machine learning based flood forecasting models for the middle Ganga basin. *Journal of Earth System Science, 130*, 176.
10. Meharg, A. A., & UNDRR. (2021). *Global Assessment Report on Disaster Risk Reduction 2021*. United Nations Office for Disaster Risk Reduction, Geneva.
11. Mishra, V., Mukherjee, S., Kumar, R., & Stone, D. A. (2017). Heat wave exposure in India in current, 1.5°C, and 2.0°C worlds. *Environmental Research Letters, 12*(12), 124012.
12. Mosavi, A., Ozturk, P., & Chau, K. W. (2018). Flood prediction using machine learning models: Literature review. *Water, 10*(11), 1536.
13. Paul, B. K. (2009). Why relatively fewer people died? The case of Bangladesh's Cyclone Sidr. *Natural Hazards, 50*(2), 289–304.
14. Robinson, C., Dilkina, B., & Moreno-Cruz, J. (2020). Modeling migration patterns in the USA under sea level rise. *PLOS ONE, 15*(1), e0227436.
15. Roy, P. S., Behera, M. D., & Srivastav, S. K. (2017). Satellite remote sensing: Sensors, applications and techniques. *Proceedings of the National Academy of Sciences, India Section A, 87*(4), 465–472.
16. Sarkar, S., & Maiti, S. K. (2021). Machine learning approaches for landslide susceptibility mapping in the Darjeeling Himalaya. *Natural Hazards, 108*, 1373–1400.
17. Shrestha, A. B., & Aryal, R. (2011). Climate change in Nepal and its impact on Himalayan glaciers. *Regional Environmental Change, 11*(1), 65–77.
18. United Nations Office for Disaster Risk Reduction. (2015). *Sendai Framework for Disaster Risk Reduction 2015–2030*. UNDRR, Geneva.
19. Wagenaar, D., de Jong, J., & Bouwer, L. M. (2017). Multi-variable flood damage modelling with limited data using supervised learning approaches. *Natural Hazards and Earth System Sciences, 17*(9), 1683–1696.
20. World Bank. (2021). *South Asia's Hotspots: The Impact of Temperature and Precipitation Changes on Living Standards*. World Bank Group, Washington, DC.

RARE-EARTH DOPED NANOPHOSPHORS: SYNTHESIS, LUMINESCENCE, AND EMERGING APPLICATIONS IN DEEP-UV PHOTONICS, WATER STERILIZATION, SENSING, AND SOLID-STATE LIGHTING

Abinaya. L and K. Gayathri*
Academy of Maritime Education & amp; Training, Kanathur, Chennai – 603112
*Corresponding author E-mail: gayathri.k@ametuniv.ac.in

1. Introduction

The last ten years have seen the emergence of a unique class of functional materials, rare-earth-doped nanophosphors, which effectively bridge the gap between fundamental spectroscopic studies and engineering applications, as a consequence of the combination of materials chemistry, solid-state physics and nanotechnology. They combine the sharp, clear electronic changes of trivalent and divalent lanthanide ions with the high surface area, tunability and ease of processing provided by nanoscale host lattices. The result is a family of luminescent solids whose emission color, decay lifetime, quantum efficiency and thermal stability can be engineered almost at will by choosing the dopant ion, its concentration, the crystallographic symmetry of the host and the synthesis route used to prepare it.

Rare-earth ions (Eu3+), (Tb3+), (Dy3+), (Sm3+), (Ce3+), (Pr3+), (Er3+) and (Yb3+) have partially filled 4f electron shells. These shells are shielded from the effect of the surrounding crystal field by the outer 5s and 5p orbitals. Such shielding leads to narrow, line-like emission bands and long excited-state lifetimes, which are mostly independent of the chemical environment in stark contrast to the broad, environmentally sensitive emission of organic dyes or transition-metal complexes. When these ions are incorporated into nanoscale host lattices the resulting nanophosphors combine the intrinsic optical purity of the lanthanide ion with the practical benefits of nanomaterials: low sintering temperatures, high specific surface area, ease of dispersion in polymers, glasses and inks and compatibility with thin-film and flexible device architectures.

The scientific interest in this field is not new; lanthanide-activated phosphors have underpinned lighting and display technologies since the mid-twentieth century. What has changed substantially in the present decade is the degree of convergence between disciplines that were previously pursued largely in isolation. Synthetic chemists optimising hydrothermal, sol gel routes now work alongside photonics engineers designing deep-ultraviolet light sources; environmental engineers seeking mercury-free water disinfection technologies draw directly on host-lattice engineering strategies developed for solid-state lighting; and biomedical researchers building optical thermometers exploit the same thermally coupled energy levels that phosphor chemists use to diagnose lattice defects. It is this convergence of discovery-driven materials

science and application-driven engineering that forms the organising theme of the present chapter.

2. Synthesis and Structural Characterization of Rare-Earth Doped Nanophosphors

2.1 Wet-Chemical and Solid-State Synthesis Routes

The optical performance of a rare-earth doped nanophosphor is inseparable from the method used to prepare it, since particle size, morphology, crystallinity, and the local coordination environment of the dopant ion are all set — and frequently fixed — during synthesis. Four families of synthesis routes dominate the recent literature. Sol–gel processing remains the most widely used approach for oxide, silicate, and aluminate hosts because it allows homogeneous atomic-level mixing of the host cations and the rare-earth dopant, typically achieved through hydrolysis and condensation of metal alkoxides or nitrates in the presence of a chelating agent such as citric acid. Combustion synthesis, in which a fuel (urea, glycine, or citric acid) is combined with metal nitrates and ignited to produce a self-sustaining exothermic reaction, offers a rapid, energy-efficient alternative well suited to producing nanoscale aluminate and vanadate phosphors in a single step, though it tends to yield broader particle-size distributions than sol–gel methods.

Hydrothermal and solvothermal synthesis, conducted under autogenous pressure at moderate temperatures (typically 120–220 °C), is the method of choice when precise control over particle morphology — nanorods, nanoplates, or hollow nanospheres — is required, and it is especially prevalent in preparing tungstate, molybdate, and fluoride hosts used for upconversion and deep-UV emission. Solid-state reaction, in which oxide or carbonate precursors are ground, pelletised, and fired at high temperature (often above 1000 °C), continues to be used where maximal crystallinity and thermal stability are required, as in scintillator and dosimetry phosphors, though it typically yields micron-scale rather than nanoscale particles unless followed by milling or exfoliation. Chang, You, and Kuo (2024) prepared Dy3+-doped SrY2O4 phosphors by solid-state reaction at 1300 °C, showing that dopant incorporation induces lattice expansion that correlates directly with grain size and crystallinity — a finding that underscores how closely synthesis conditions and structural outcome remain coupled even in this traditional route.

Microwave-assisted synthesis has emerged as a popular refinement of both combustion and hydrothermal approaches, offering shortened reaction times and improved compositional homogeneity through rapid, volumetric dielectric heating rather than slow conductive heating. A representative example is the microwave-assisted preparation of Er3+/Yb3+ co-doped CaMoO4 nanophosphors, in which the scheelite-type tetragonal phase was confirmed by structural refinement while the same batch was subsequently evaluated for optical temperature sensing and antibacterial performance — illustrating the increasingly common practice of designing a single composition for simultaneous multifunctional use.

2.2 Structural Characterization Techniques

Confirming that a rare-earth dopant has been successfully incorporated into the intended crystallographic site — rather than segregated at grain boundaries or precipitated as a secondary phase — requires a coordinated suite of characterization techniques. X-ray diffraction (XRD) remains the primary tool for phase identification and for tracking dopant-induced lattice strain through Rietveld refinement of unit-cell parameters; a shift in peak position or a broadening of reflections with increasing dopant concentration is generally taken as evidence of substitutional incorporation, while the appearance of unindexed reflections signals the formation of an impurity phase. Scanning and transmission electron microscopy provide direct morphological information — particle size, shape, agglomeration state, and, in the case of high-resolution TEM, lattice-fringe spacing that can confirm crystallinity at the level of individual nanoparticles. Fourier-transform infrared (FTIR) spectroscopy is routinely used to identify metal–oxygen vibrational modes and to detect residual organic or hydroxyl species left over from wet-chemical synthesis, which are often implicated in non-radiative quenching of luminescence.

Beyond these standard techniques, X-ray photoelectron spectroscopy (XPS) is increasingly used to confirm the oxidation state of the rare-earth dopant, since several lanthanides (notably europium, cerium, and samarium) can exist in mixed di- and trivalent states depending on synthesis atmosphere and post-synthesis annealing, with significant consequences for emission colour. Nanosized Eu3+-doped oxyapatite phosphors, reported by Ivanovici *et al.* (2024), were characterised through a combined structural, morphological, electronic, and optical protocol exemplifying the multi-technique approach now expected in the field. Kiran, Kamath, Sayyed, Almuqrin, and Kamath (2025), reviewing recent developments in rare-earth doped nanophosphors, similarly emphasised that host selection among tungstates, vanadates, and aluminates must be guided jointly by structural refinement data and downstream luminescent performance, reinforcing the principle that synthesis and characterization cannot be meaningfully separated from application design.

2.3 Recent Developments in Synthesis Strategy (2023–2026)

Several trends distinguish the 2023–2026 literature from earlier work. First, there has been a marked shift toward composition and concentration engineering rather than the introduction of entirely new host lattices, with researchers systematically varying co-dopant ratios to tune energy-transfer pathways. Lai, Ge, Li, Zhu, and Du (2024), for instance, synthesised a family of Eu2W3O12 phosphors co-doped with lanthanum, gadolinium, and samarium ions and applied Judd–Ofelt calculations to quantify how each co-dopant altered the local symmetry around the Eu3+ emitting centre, linking synthesis-stage compositional choices directly to emission intensity and thermal quenching behaviour. Second, there is growing attention to glass-ceramic and glass–nanocrystal composite architectures that embed nanocrystalline phosphors within a transparent glass matrix, combining the high luminescence efficiency of the crystalline phase

with the mechanical robustness and processability of glass — an approach exemplified by fluoroborate nano-glass composites embedding Pr3+-doped nanocrystals for deep-UV disinfection, discussed further in Section 4.

3. Optical and Luminescence Properties

3.1 Photoluminescence Mechanisms and Energy Transfer

The optical behaviour of rare-earth doped nanophosphors is governed by intraconfigurational 4f–4f transitions (in ions such as Eu3+, Tb3+, Sm3+, and Dy3+) and, in fewer but technologically important cases, by interconfigurational 5d–4f transitions (notably in Ce3+ and Pr3+). The 4f–4f transitions are formally parity-forbidden by the Laporte selection rule and are only weakly allowed through crystal-field-induced mixing of opposite-parity states, which accounts for the characteristically long excited-state lifetimes — often microsecond-to-millisecond — and narrow emission linewidths of these ions. The 5d–4f transitions, by contrast, are parity-allowed, giving rise to broad, intense, comparatively fast (nanosecond-scale) emission bands whose energy depends strongly on the crystal-field splitting of the 5d level, and therefore on the host lattice; this host sensitivity is precisely what allows Ce3+- and Pr3+-based nanophosphors to be tuned across the ultraviolet and visible range simply by changing host composition, a property exploited in the deep-UV emitters discussed in Section 4.1. Energy transfer between a sensitizer ion and an activator ion is a second mechanism of central importance. In upconversion nanophosphors, ytterbium (Yb3+), with its large absorption cross-section near 980 nm, is almost universally employed as a sensitizer that absorbs near-infrared excitation and transfers energy non-radiatively to an activator ion such as erbium (Er3+), thulium (Tm3+), or holmium (Ho3+), which then emits at a shorter, visible or ultraviolet wavelength through sequential absorption of multiple low-energy photons. This anti-Stokes process, in which emitted photons carry more energy than the individual absorbed photons, underlies many of the optical sensing and imaging applications discussed later in this chapter. Xiang *et al.* (2024) demonstrated that the blue-emitting energy level of Er3+ can be exploited for 'supernormal' temperature-sensing performance with simultaneous deep-tissue detection capability, illustrating how understanding of energy-transfer pathways translates directly into device-level sensing performance.

3.2 Recent Advances in Luminescence Engineering (2023–2026)

A defining feature of the recent literature is the shift from characterising a single emission colour toward engineering colour-tunable and multimodal emission from a single host composition. Ni, Wu, Chen, Zheng, Xu, and Dai (2025) reported site-selective occupancy of Bi3+ and Eu3+ ions in a K3YSi2O7 host, demonstrating that careful compositional control allows continuous tuning of emission colour from a single material system, with direct application to near-ultraviolet-excitable white LEDs and simultaneous optical temperature sensing — a clear example of the multifunctionality that increasingly characterises this field. Similarly, dual-valence approaches exploiting both Eu2+ and Eu3+ emission from a single host, distinguished by markedly different

thermal quenching behaviour, have been used to construct self-referencing luminescent thermometers that require no external calibration standard, since the ratio of the two emission bands intrinsically encodes temperature.

Thermal quenching itself — the reduction in luminescence intensity with increasing temperature due to enhanced non-radiative relaxation — has received considerable recent attention, both as a performance-limiting phenomenon to be suppressed in lighting applications and as a useful signal to be exploited in sensing. Shi, Xue, Mao, Pei, Li, Liu, Zhang, and Zhong (2023) reported a europium-single-doped phosphor exhibiting anti-thermal-quenching behaviour together with multicolour tunability, a combination that decouples the material's usefulness for high-temperature lighting from the thermal instability that ordinarily limits such phosphors. At the same time, a recent review of emerging trends in rare-earth doped luminescent nanophosphors notes that surface modification strategies — ligand exchange, silica encapsulation, and polymer coating — have become standard tools for suppressing surface-defect-mediated non-radiative decay, improving quantum yield without altering the underlying host composition. These advances demonstrate that luminescence engineering is proceeding along two complementary axes: compositional tuning to access new emission colours and thermal responses, and post-synthetic surface engineering to recover quantum efficiency otherwise lost to nanoscale surface effects.

4. Emerging Applications

The past three years have seen rare-earth doped nanophosphors move decisively from laboratory curiosities toward application-ready materials across four domains that together illustrate the convergence theme of this volume: deep-ultraviolet emission, water sterilization, optical sensing, and solid-state lighting and displays. Each is treated in turn below.

4.1 Deep-UV Emission

Deep-ultraviolet (deep-UV, wavelengths below approximately 280 nm) light sources are in high demand for germicidal disinfection, photolithography, and sensing, yet conventional sources — low-pressure mercury lamps and deep-UV light-emitting diodes based on wide-bandgap semiconductors such as aluminium gallium nitride — suffer respectively from the toxicity of mercury and from persistently low external quantum efficiency at short wavelengths. Rare-earth doped nanophosphors offer an alternative route to deep-UV emission through the interconfigurational 5d–4f transitions of Pr3+ and, to a lesser extent, Gd3+, which can be tuned into the UV-C band (200–280 nm) by appropriate choice of host lattice. A particularly notable recent contribution is the development of Pr3+-doped fluoroborate nano-glass composites, in which transparent glass hosts embed Pr3+-doped Li(Al7B4O17) nanocrystals; upon excitation by deep-UV light, X-rays, or high-energy electron beams, these composites exhibit pronounced 5d–4f emission whose spectral profile closely overlaps the germicidal effectiveness curve, achieving a photoluminescence quantum yield of up to 25.93 percent — a figure the authors

report as surpassing most previously reported praseodymium-doped glasses and nano-glass composites, alongside X-ray-excited luminescence more than twice that of commercial bismuth germanate scintillator crystals.

The significance of this class of material lies in the combined architecture: the crystalline nanophosphor phase supplies the high intrinsic luminescence efficiency associated with well-ordered rare-earth coordination environments, while the surrounding glass matrix supplies mechanical robustness and — critically for disinfection applications — resistance to the same deep-UV photons the material is designed to emit, a durability requirement organic phosphor binders typically fail to meet over extended operating lifetimes. Complementary work on praseodymium-doped upconversion phosphors has emphasised the direct overlap between the UV-C emission band (200–280 nm) and the germicidal effectiveness curve, which peaks near 265 nm, proposing such materials as components of solid-state deep-UV sources for disinfecting water, air, food-contact surfaces, and consumables in settings from municipal water treatment to healthcare facilities. Because these nanophosphors can, in several architectures, be excited by X-rays or electron beams as well as UV photons, they additionally show promise as fast scintillator materials, extending their relevance beyond disinfection into radiation detection and dosimetry.

4.2 Water Sterilization

Closely related to, but distinct from, direct deep-UV emission is the use of rare-earth doped nanophosphors and nanocomposites to enhance photocatalytic water treatment. In this application, the rare-earth dopant does not itself provide the disinfecting radiation but instead modifies the electronic structure of a semiconductor photocatalyst — most commonly titanium dioxide (TiO2) or zinc oxide (ZnO) — to improve its efficiency under available illumination. Rare-earth ions, with their characteristic 4f energy levels situated within the semiconductor bandgap, act as electron traps that suppress the recombination of photogenerated electron–hole pairs, thereby extending carrier lifetime and increasing the yield of the reactive oxygen species (hydroxyl radicals and superoxide anions) responsible for degrading organic pollutants and inactivating microorganisms. A recent review by Awandkar and colleagues (2026) synthesises this literature, documenting how doping with neodymium, samarium, cerium, dysprosium, and other lanthanides broadens the optical absorption range of TiO2 photocatalysts into the visible region while simultaneously improving charge-carrier separation, with demonstrated benefits for both dye degradation and antimicrobial performance.

Palariya, Mehtab, Aziz, and colleagues (2024) reviewed rare-earth-doped nanocomposites specifically in the context of dye degradation in water, concluding that lanthanide doping broadens photocatalyst absorption, facilitates charge separation, and provides a more stable structural framework than undoped semiconductor nanoparticles, while a related review (2024) catalogued rare-earth oxide-based photocatalysts and their design strategies for water treatment more broadly. Beyond degradation of chemical pollutants, direct antimicrobial functionality has

also been reported: the microwave-synthesised Er3+/Yb3+-doped CaMoO4 nanophosphors described in Section 2.1 were evaluated explicitly for antibacterial activity alongside temperature sensing, reflecting a growing practice of designing a single nanophosphor for combined disinfection and sensing roles. Taken together, these developments position rare-earth doped nanomaterials as a mercury-free, chemically stable, potentially solar-activatable alternative to conventional UV-C lamp-based disinfection, particularly relevant to decentralised or resource-limited settings where the infrastructure required by conventional germicidal lamps is difficult to sustain.

4.3 Optical Sensors

Luminescence-based temperature sensing, often termed optical or luminescence thermometry, has become one of the most active application areas for rare-earth doped nanophosphors in the 2023–2026 period. The technique typically exploits pairs of thermally coupled energy levels — most commonly the 2H11/2 and 4S3/2 levels of Er3+ — whose relative populations, and therefore relative emission intensities, follow a Boltzmann distribution with temperature. Because the method relies on the ratio of two emission intensities from within the same material (the fluorescence intensity ratio, or FIR, technique) rather than on absolute intensity, it is inherently self-referencing and largely insensitive to fluctuations in excitation power or detector sensitivity, making it attractive for remote, non-contact temperature measurement in settings ranging from microelectronics to biological tissue. Saidi, Hernández-Álvarez, Runowski, Dammak, and Martín (2023) demonstrated a combined temperature- and pressure-sensing optical platform based on Er3+/Yb3+ co-doped NaSrY(MoO4)3 nanophosphors, illustrating that the same upconversion architecture can be extended from thermometry to nanomanometry through analogous pressure-dependent shifts in emission wavelength or intensity ratio.

A parallel body of work has focused on biological and microelectronic thermal sensing, where spatial resolution and minimal invasiveness are paramount. Jankowski, Wiwatowski, Żebrowski, Pilch-Wróbel, Bednarkiewicz, Maćkowski, and Piątkowski (2024) reported luminescent nanocrystal probes capable of monitoring both temperature and thermal-energy dissipation in electrical microcircuits, while a related 2024 study reported rare-earth luminescent nanothermometers achieving a maximum relative sensitivity of 1.29 percent per kelvin near 298 K, with confirmed cyclic stability suitable for biological applications. Reviewing the broader field, a status report on luminescence thermometry concluded that, despite two decades of development, reproducibility and standardisation across measurement environments remain open problems constraining translation from laboratory demonstration to routine deployment — an assessment revisited in Section 5.1.

Beyond thermometry, rare-earth doped nanophosphors are being explored for chemical and biological sensing through mechanisms that couple luminescence intensity or lifetime to the presence of a target analyte. Hu, Yue, Chen, Lin, and Lyu (2024) reported dual-mode

upconversion sensors detecting oppositely charged biological targets by exploiting the oxidase-mimicking catalytic activity of cerium(IV) combined with electrostatic control of nanoparticle assembly, showing that the same lanthanide ions valued for optical properties can simultaneously provide catalytic biosensing functionality. Information-encryption applications represent a further sensing-adjacent domain: Shen, He, Yao, Zhang, Peng, Tan, Chen, and Yuan (2024) described a defect-regulation strategy in porous persistent phosphors enabling multiple, dynamically switchable encryption states, extending the sensing paradigm from measuring physical quantities to encoding optically addressable information.

4.4 LEDs and Displays

Solid-state lighting and display technologies remain the largest-volume commercial application of rare-earth doped phosphors, and the 2023–2026 literature reflects continued, incremental but consequential progress in this domain, driven primarily by the search for single-host, colour-tunable, and near-ultraviolet-excitable phosphors that can simplify device architecture relative to the multi-phosphor blends used in conventional white LEDs. Halefoglu and colleagues (2024) examined terbium-doped magnesium aluminate (MgAl2O4) nanophosphors specifically for their luminescent suitability in lighting and display technologies, while Ivanovici *et al.* (2024), as noted in Section 2.2, characterised europium-doped oxyapatite phosphors for display-relevant structural and optical performance. Albert, Kennedy, Rathinamala, and Princy (2024) reported a dysprosium- and europium-codoped orthophosphate phosphor, NaPbBi2(PO4)3, explicitly designed for near-ultraviolet-excitable white LEDs with simultaneous optical thermometric functionality, again exemplifying the trend toward multifunctional single-host materials noted throughout this chapter.

Colour-tunability through site-selective dopant occupancy, discussed in Section 3.2 with reference to the bismuth–europium co-doped K3YSi2O7 system, is of particular commercial interest because it allows a single phosphor composition, rather than a blend of separately synthesised red-, green-, and blue-emitting phosphors, to be tuned across a wide colour gamut simply by adjusting relative dopant concentrations — a simplification that can reduce manufacturing cost and improve colour-rendering consistency across batches. Balhara, Gupta, Debnath, and Sudarshan (2023, 2024) explored energy transfer in manganese-, holmium-, and ytterbium-tri-doped zinc aluminate nanophosphors, further extending the palette of co-doping strategies for tunable-emission lighting phosphors. In parallel, down-conversion phosphor architectures — in which a high-energy photon is converted into two or more lower-energy photons — continue to attract attention for photovoltaic applications; Mahajan, Singh, Datt, Tsoi, Gupta, and Arya (2024) reported a core–shell NaYF4:Pr3+@NaYF4:Eu3+ nanoparticle architecture intended to improve spectral matching of sunlight to the absorption band of organic solar cells, illustrating how strategies developed for display phosphors are being repurposed for energy-harvesting applications.

Persistent and long-afterglow phosphors, which continue to emit light after the excitation source is removed, represent a further growth area, with applications spanning emergency signage, security printing, and, as noted in Section 4.3, dynamic information encryption. The convergence of these lighting-adjacent applications with sensing and security functions underscores a broader observation running through this chapter: the boundaries between the four application domains treated here are increasingly porous, with individual nanophosphor compositions routinely engineered and evaluated for two or more functions simultaneously.

5. Challenges, Future Perspectives, and Conclusion

5.1 Challenges

Despite the substantial progress documented above, several challenges continue to constrain the translation of rare-earth doped nanophosphors from laboratory demonstration to widespread commercial deployment. Foremost among these is the difficulty of large-scale, batch-to-batch reproducible synthesis. A recent overview of nanophosphor synthesis and optical characteristics explicitly identifies large-scale production of high-quality nanophosphors with controlled morphology and uniform doping as a significant hurdle that persists despite decades of synthetic refinement, a concern echoed across the wet-chemical, combustion, and hydrothermal literature reviewed in Section 2. Precise control of particle size, dopant homogeneity, and surface chemistry becomes progressively harder to maintain as reaction volumes scale from laboratory beakers to industrial reactors, and even small batch-to-batch variations can produce measurable shifts in emission colour, intensity, or thermal stability that are unacceptable for colour-critical applications such as display lighting.

A second, closely related challenge concerns thermal and photochemical stability under operating conditions. Many high-performance compositions demonstrated under controlled laboratory excitation exhibit measurable thermal quenching or photodegradation when subjected to the sustained, high-flux illumination and elevated temperatures characteristic of real LED packages or deep-UV disinfection modules; the anti-thermal-quenching phosphor reported by Shi *et al.* (2023) and the fluoroborate nano-glass composites developed for deep-UV disinfection both represent direct responses to this problem, but such solutions remain compositionally specific rather than generalisable design principles. Reproducibility likewise remains unresolved in the sensing domain: the review of luminescence thermometry status and challenges concluded that measurement reliability across differing environments continues to hinder large-scale adoption, with particular consequences for biomedical deployment where calibration consistency is a prerequisite for regulatory approval.

Economic and supply-chain considerations constitute a third category of challenge, frequently underemphasised in the materials-science literature but central to any realistic assessment of commercial viability. Rare-earth elements, despite their name, are not uniformly scarce, but their extraction and purification are geographically concentrated and environmentally intensive,

raising cost and sustainability concerns that grow more material as application volumes scale toward the tonnage levels required for water-treatment or general lighting markets. Waste-derived host-lattice precursors, discussed in Section 2.3, represent one response, but address only the host-lattice component and do not reduce dependence on the rare-earth dopant itself. Finally, toxicological and regulatory questions surrounding nanomaterial exposure — particularly relevant to water-treatment applications — remain comparatively underexplored relative to the attention devoted to optical performance, and require more systematic investigation before large-scale environmental deployment can be considered responsible practice.

5.2 Future Perspectives

Several trajectories evident in the 2023–2026 literature point toward productive directions for the coming years. The trend toward multifunctional, single-host materials — phosphors simultaneously engineered for white-light emission and optical thermometry, or for deep-UV disinfection and radiation dosimetry — is likely to deepen, since it offers manufacturing and device-integration efficiencies that grow more attractive as the underlying chemistry matures. Realising this potential will require closer integration between the materials-discovery community and device engineers, so that multifunctionality is designed around genuine application requirements rather than demonstrated opportunistically.

Computational and data-driven approaches to host-lattice and dopant-configuration screening represent a second promising direction. First-principles calculations of structural stability and optical properties, of the kind applied to K3LuSi2O7 phosphors, together with the Judd–Ofelt framework used to quantify local dopant symmetry, are increasingly capable of narrowing the experimental search space before synthesis is attempted, potentially accelerating the historically slow, trial-and-error process of host-lattice selection. As these tools become more accessible and are increasingly coupled with high-throughput experimental synthesis, the pace of discovery in this field can reasonably be expected to accelerate.

Sustainability-oriented synthesis is a third direction likely to gain momentum, encompassing waste-derived host precursors, lower-temperature synthesis routes that reduce energy intensity, and end-of-life recovery strategies that reclaim rare-earth dopants from spent devices. Given the geopolitical and environmental sensitivities surrounding rare-earth supply, such circular-economy approaches are likely to shift from a peripheral interest to a mainstream design consideration, particularly for cost-sensitive, high-stakes applications such as water treatment. Finally, the deep-UV and disinfection applications reviewed in Sections 4.1 and 4.2, still comparatively nascent relative to the mature lighting sector, appear especially well positioned for growth, given accelerating global interest in mercury-free, decentralisable disinfection technologies and the demonstrated feasibility of nano-glass composites meeting germicidal effectiveness requirements.

Conclusion

Rare-earth doped nanophosphors exemplify, in a single materials class, the convergence of discovery and application that motivates this volume. Their scientific foundation rests on well-understood 4f and 5d electronic transitions studied for decades, yet the past three years have witnessed a marked acceleration in the translation of that fundamental understanding into deployable technologies spanning deep-ultraviolet light sources, mercury-free water disinfection, non-contact optical sensing, and next-generation solid-state lighting and displays. This chapter has traced that translation across the synthesis-to-application pipeline: from the sol–gel, combustion, hydrothermal, and solid-state routes used to prepare these materials, through the energy-transfer and thermal-quenching mechanisms that govern their optical behaviour, to four application domains — deep-UV emission, water sterilization, optical sensing, and LEDs and displays — that together illustrate both the versatility of the underlying materials chemistry and the increasingly multifunctional character of individual nanophosphor compositions.

At the same time, genuine challenges remain before this promise is fully realised at scale: reproducible large-volume synthesis, robust thermal and photochemical stability under real operating conditions, economically and environmentally sustainable rare-earth supply chains, and a more systematic understanding of the toxicological profile of these materials in environmental applications all require sustained attention from the research community. The trajectory of the field over the 2023–2026 period — toward computationally guided design, multifunctional single-host materials, and sustainability-conscious synthesis — suggests that these challenges are being actively engaged rather than merely acknowledged, and provides grounds for cautious optimism that rare-earth doped nanophosphors will continue to serve as a productive bridge between fundamental photophysics and technologies of substantial practical consequence in the years ahead.

References

1. Albert, K. J., Kennedy, S. M. M., Rathinamala, V., & Princy, A. (2024). $NaPbBi_2(PO_4)_3$: Ln^{3+} (Ln = Dy, Eu) codoped orthophosphate type phosphor for NUV excitable wLEDs and optical thermometry. *Journal of Inorganic and Organometallic Polymers and Materials, 34*(10), 4609–4621.
2. Awandkar, S. P., *et al.* (2026). Rare earth-doped TiO_2 for enhanced photocatalytic performance. *ChemNanoMat*. Advance online publication.
3. Balhara, A., Gupta, S. K., Debnath, A. K., & Sudarshan, K. (2023). Utilizing energy transfer in $Mn^{2+}/Ho^{3+}/Yb^{3+}$ tri-doped $ZnAl_2O_4$ nanophosphors for multifunctional optical applications. *Inorganic Chemistry*.
4. Chang, C.-C., You, J.-M., & Kuo, C.-L. (2024). Structural and optical investigations of Dy^{3+}-doped SrY_2O_4 phosphor prepared via solid-state reaction. *Journal of Materials Science: Materials in Electronics*.

5. Halefoglu, Y. Z., *et al.* (2024). Structural and luminescent properties of Tb^{3+}-doped $MgAl_2O_4$ nanophosphors for lighting and display technologies. *Journal of Luminescence*.
6. Han, J., Yang, Y., Huang, X., Lin, Y., Han, Q., Liu, X., & Wang, C. (2022). Exploring the structural stability and optical properties of rare-earth doped $K_3LuSi_2O_7$ phosphor from first-principles calculations. *Inorganic Chemistry Communications, 137*, Article 109197.
7. Hu, G., Yue, D., Chen, W., Lin, Q., & Lyu, H. (2024). Dual-mode upconversion sensors for detecting differently charged biotargets based on the oxidase-mimicking activity of Ce^{4+} and electrostatic control. *Talanta, 277*, Article 126392.
8. Ivanovici, M., Ćirić, A., Periša, J., Marinović Cincović, M., Brik, M. G., Alodhayb, A. N., & Dramićanin, M. D. (2024). Nanosized Eu^{3+}-doped $NaY_9Si_6O_{26}$ oxyapatite phosphor: A comprehensive insight into its hydrothermal synthesis and structural, morphological, electronic, and optical properties. *Nanomaterials, 14*(20), Article 1639.
9. Jankowski, D., Wiwatowski, K., Żebrowski, M., Pilch-Wróbel, A., Bednarkiewicz, A., Maćkowski, S., & Piątkowski, D. (2024). Luminescent nanocrystal probes for monitoring temperature and thermal energy dissipation of electrical microcircuit. *Nanomaterials, 14*(24), Article 1985.
10. Kiran, R., Kamath, N., Sayyed, M. I., Almuqrin, A. H., & Kamath, S. D. (2025). A review of recent developments in rare earth-doped nanophosphors for emerging technological applications. *RSC Advances*. Advance online publication.
11. Lai, X., Ge, W., Li, Y., Zhu, D., & Du, P. (2024). Rare-earth ion-doped $Eu_2W_3O_{12}$ phosphors: Judd–Ofelt analysis and thermal quenching behaviour for solid-state lighting. *Journal of Alloys and Compounds*.
12. Mahajan, P., Singh, A., Datt, R., Tsoi, W. C., Gupta, V., & Arya, S. (2024). Synthesis and characterization of $NaYF_4^{3+}$@$NaYF_4^{3+}$ core@shell nanoparticles as down-conversion material for organic solar cells application. *The European Physical Journal Plus, 139*, Article 183.
13. Ni, C., Wu, K., Chen, C., Zheng, X., Xu, M., & Dai, W. (2025). Color-tunable photoluminescence via site-selective occupancy of Bi^{3+}/Eu^{3+} and chemical composition modulation in stable $K_3YSi_2O_7$ toward wLED and optical temperature-sensing applications. *Crystal Growth & Design, 25*(3), 777–789.
14. Palariya, D., Mehtab, S., Aziz, M., *et al.* (2024). Exploring rare earth element doped nanocomposites as promising photocatalysts for dyes degradation in water. *Water, Air, & Soil Pollution, 235*, Article 286.
15. Rakov, N., Matias, F., & Xiao, M. (2024). An efficient red light-emissive process from Eu^{3+} doped amorphous-derived $CaAl_2Si_2O_8$ ceramic powders: Down-shifted luminescence with high thermal stability under 532 nm excitation. *Journal of Luminescence*.

HISTORICAL DEVELOPMENT OF FERRITES AND IT'S APPLICATIONS

Rahul Ravindra Uplaiker and Waseem Ahamad Beg*

RNC Arts JDB Commerce and NSC Science College Road, Nashik-422101

(Affiliated to Savitribai Phule Pune University, Pune- 411007

*Corresponding author E-mail: wasembeg1985@gmail.com

Abstract

Ferrites are a significant class of magnetic ceramic materials that have been essential to the development of contemporary science and industry. Ferrites have evolved from basic magnetic compounds to highly designed multifunctional materials with customised structural, electrical, magnetic, and catalytic capabilities since their discovery in the early 20th century. This chapter provides a thorough summary of the development of ferrites throughout history, emphasising important turning points in their synthesis, characterisation, and technical breakthroughs. The categorisation of ferrites into spinel, hexagonal, garnet, and orthoferrite structures is covered, along with the connection between their crystal structure and functional characteristics. The wide range of ferrite applications in electronics, telecommunications, energy storage, environmental remediation, gas sensing, biomedical engineering, electromagnetic interference shielding, and wastewater treatment are also covered in this chapter. Recent advances in advanced nanocomposites, green synthesis techniques, and nanostructured ferrites are also reviewed, highlighting their improved performance and growing industrial significance. The chapter concludes by outlining present issues and potential future research avenues, highlighting the ongoing importance of ferrite materials in meeting new environmental and technological demands.

Keyword- Ferrites, Magnetic Materials, Spinel Ferrites, Nanoferrites.

Graphical Abstract:

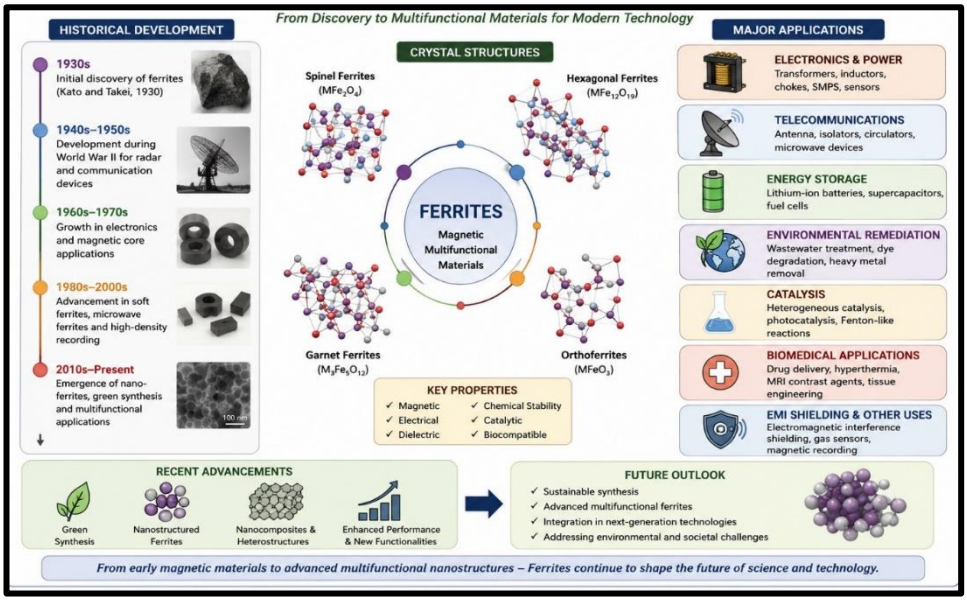

Introduction

Ferrites constitute an indispensable class of iron-oxide–based magnetic ceramics that have acquired profound importance within solid-state physics, materials science, and electromagnetic engineering owing to their distinctive convergence of magnetic order and electrical insulation. Chemically, ferrites are complex mixed oxides formed by the incorporation of ferric ions (Fe^{3+}) with divalent or multivalent cations such as Mn^{2+}, Zn^{2+}, Ni^{2+}, Mg^{2+}, or Co^{2+}, typically arranged within ordered crystalline lattices. In contrast to metallic ferromagnets, whose appreciable electrical conductivity engenders parasitic eddy-current losses under alternating magnetic excitation, ferrites exhibit exceptionally high resistivity, thereby markedly attenuating dissipative effects and enabling efficient magnetic performance across radiofrequency and microwave regimes. This combination of magnetic functionality with dielectric behavior renders ferrites uniquely suited for both theoretical investigations of magnetic interactions and practical deployment in high-frequency devices [1], [2], [3].

The nomenclature ferrite traces its etymological lineage to ferrum, the Latin appellation for iron, coupled with the mineralogical suffix "-ite," signifying an inorganic compound or phase. While originally employed in metallurgical contexts to designate iron-rich phases in steels, the terminology was subsequently adopted within ceramic magnetism to describe iron-oxide compounds exhibiting long-range magnetic ordering. The conceptual and theoretical foundation of ferrite magnetism was firmly established through the pioneering work of Louis Néel, whose formulation of ferrimagnetism elucidated the microscopic origin of uncompensated magnetic moments in antiferromagnetically coupled sublattices, thereby providing a rigorous framework for interpreting the magnetic resposne of these oxides [4]

From a crystallographic and magnetic standpoint, ferrites are archetypal ferrimagnetic solids in magnetic ions occupy distinct tetrahedral (A) and octahedral (B) interstitial sites within oxide lattices, most commonly the spinel framework. Superexchange interactions mediated by oxygen anions promote antiparallel alignment of magnetic moments on these sublattices; however, unequal site occupancies or moment magnitudes prevent complete cancellation, yielding a finite spontaneous magnetization [5]. Such systems therefore provide exemplary platforms for exploring exchange coupling, magnetic anisotropy, domain wall motion, spin-wave excitations, and hysteretic phenomena in electrically insulating media. Consequently, ferrites have long served as canonical model materials in condensed-matter physics for elucidating collective spin behavior and magnetization dynamics [6]

Beyond their theoretical significance, ferrites exhibit a constellation of physicochemical attributes including chemical inertness, thermal stability, corrosion resistance, and mechanical robustness that enhance their technological reliability. Their ceramic microstructure confers dimensional stability and compatibility with scalable powder-processing and sintering

techniques, facilitating economical fabrication of complex geometries. These characteristics have established ferrites as essential constituents in transformers, inductors, chokes, electromagnetic interference suppressors, antennas, microwave circulators, and numerous signal-conditioning components. Contemporary research further extends their utility to nanostructured systems for catalysis, sensing, biomedical imaging, and energy applications, underscoring their sustained relevance within both established and emergent technological paradigms [7]

Historical Development of Ferrites

The historical evolution of ferrites delineates a progressive convergence between mineralogical observation, theoretical magnetism, and ceramic engineering. Early recognition of magnetically responsive iron oxides, particularly magnetite (Fe_3O_4), provided the first empirical indication that spontaneous magnetization could arise in non-metallic solids. These naturally occurring ferrimagnetic minerals stimulated foundational inquiries into magnetic ordering phenomena during the nineteenth century, thereby laying the groundwork for later developments in solid-state physics. However, the transformation of ferrites from geological curiosities into engineered functional materials occurred only with the advent of crystallography, quantum exchange theory, and ceramic processing technologies in the early twentieth century [8],[9].

A decisive theoretical milestone emerged with the work of Louis Néel, whose formulation of ferrimagnetism provided a rigorous explanation for the uncompensated magnetic moments observed in iron oxides. By demonstrating that antiparallel coupling between nonequivalent magnetic sublattices could yield a residual magnetization, Néel established a unified microscopic framework that distinguished ferrites from classical ferromagnets and antiferromagnets. This insight not only resolved longstanding anomalies in oxide magnetism but also stimulated systematic exploration of spinel ferrites as model systems for exchange interactions and collective spin behavior [10],[11].

Simultaneously, technological imperatives—particularly the demand for low-loss magnetic cores in radio-frequency and radar circuits—precipitated intense industrial research. Laboratories at Philips, under the scientific leadership of Jan Snoek, pioneered the fabrication of polycrystalline ferrite ceramics exhibiting high permeability and suppressed eddy-current losses. These advances facilitated the replacement of laminated metallic cores with ferrite components, thereby enabling miniaturization and improved efficiency in electronic systems. The ensuing decades witnessed compositional diversification, microstructural refinement, and large-scale commercialization, culminating in the ubiquitous deployment of ferrites across power electronics, telecommunications, and microwave technologies [12],[13].

In contemporary materials science, ferrites remain a fertile domain of innovation. Nanostructured ferrites, synthesized through sol–gel, hydrothermal, and combustion techniques, display size-dependent magnetic anisotropy and superparamagnetic behavior, expanding their applicability to

biomedical diagnostics, catalysis, electromagnetic interference suppression, and spintronic devices. Thus, the developmental arc of ferrites epitomizes the reciprocal interplay between theoretical physics and engineering exigency, wherein fundamental insights into exchange-mediated magnetism continuously inform technological advancement [14].

Table 1: Key Milestones in Ferrite Research and Development

Period / Year	Scientific or Technological Event	Significance	Reference
Antiquity–1800s	Recognition of naturally magnetic minerals (magnetite, lodestone)	Earliest evidence of magnetic oxides and non-metallic magnetism	Livingston (1996); Cullity & Graham (2009)
Mid–19th century	Systematic mineralogical and crystallographic studies of iron oxides	Establishment of structural classification of oxide phases	Dana (1868); Bragg & Bragg (1913)
Early 1900s	Emergence of solid-state magnetism and exchange theory	Theoretical foundation for understanding magnetic ordering	Weiss (1907); Heisenberg (1928)
1930s	Laboratory synthesis of spinel ferrites	Transition from natural minerals to engineered magnetic ceramics	Kato & Takei (1930); Snoek (1948)
1940s	Ferrimagnetism theory by Louis Néel	Microscopic explanation of magnetic behavior in ferrites	Néel (1948)
1940–45	Development of soft ferrite cores at Philips by Jan Snoek	Industrial fabrication of low-loss, high-frequency magnetic materials	Snoek (1948); Pullar (2012)
1950s–60s	Commercialization of ferrites	Widespread adoption in transformers, inductors, and communication devices	Goldman (2006); Sugimoto (1999)
1960s–70s	Development of hard (hexaferrite) permanent magnets	Replacement of Alnico magnets in many electromechanical systems	Smit & Wijn (1959); Pullar (2012)
1980s–90s	Microstructural optimization and microwave ferrites	Applications in circulators, isolators, and RF components	Harris (2012); Goldman (2006)
2000s	Advanced ceramic processing and thin films	Integration into miniaturized electronics and sensors	Kodama (1999); Gorter (1954); Goldman (2006)
2010s–present	Nanocrystalline and multifunctional ferrites	Biomedical, catalytic, spintronic, and EMI-shielding technologies	Sun *et al.* (2000); Laurent *et al.* (2008); Pullar (2012)

Types and Classification of Ferrites

Ferrites represent a technologically and scientifically significant family of ferrimagnetic ceramic oxides structurally based on iron oxide combined with divalent or multivalent metallic cations [9]. From the perspective of condensed matter physics, ferrites constitute prototypical systems in which superexchange-mediated spin coupling, cation site ordering, magnetocrystalline anisotropy, and polaronic charge transport collectively dictate macroscopic magnetic and dielectric behavior. Unlike metallic ferromagnets, ferrites exhibit high electrical resistivity coupled with robust magnetic ordering, thereby suppressing eddy-current losses and enabling efficient operation under alternating electromagnetic fields. [8]

The conceptual foundation of ferrimagnetism was rigorously established by Louis Néel, who demonstrated that antiparallel alignment of unequal magnetic sublattices generates a non-zero net magnetization in oxide lattices [14]. This theoretical insight distinguished ferrites from both ferromagnetic and antiferromagnetic materials and laid the groundwork for their extensive scientific and industrial development. For systematic understanding, ferrites are classified according to four complementary criteria:

- Chemical Composition,
- Crystallographic Structure,
- Magnetic Behavior, And
- Functional Application**.**

Each mode of classification reflects distinct variations in exchange interactions, domain dynamics, polarization mechanisms, and electrical transport phenomena [15].

Classification Based on Magnetic Behaviour

Soft-Ferrites

Soft-ferrites are distinguished by low coercive field, high initial permeability, narrow hysteresis loops, and extremely high electrical resistivity (10^6–10^8 Ω·cm). These characteristics originate from low magnetocrystalline anisotropy energy and facile domain-wall motion, which permit rapid and reversible magnetization processes with minimal energy dissipation [16]. The high resistivity markedly reduces eddy-current formation, a feature that is indispensable for high-frequency electromagnetic operation. At the microscopic level, the magnetization mechanism in soft ferrites is dominated by domain wall displacement rather than coherent rotation, thereby minimizing hysteresis losses [9]. Consequently, these materials exhibit superior performance in the kHz–MHz frequency domain and are extensively utilized as transformer cores, inductors, power converters, electromagnetic interference suppressors, and switching circuit components [14]. The physical principles and engineering applications of such materials are comprehensively described in Soft Ferrites: Properties and Applications.

Typical compositions include Ni–Zn, Mn–Zn, and Cu–Zn ferrites, each optimized for specific permeability and frequency characteristics.

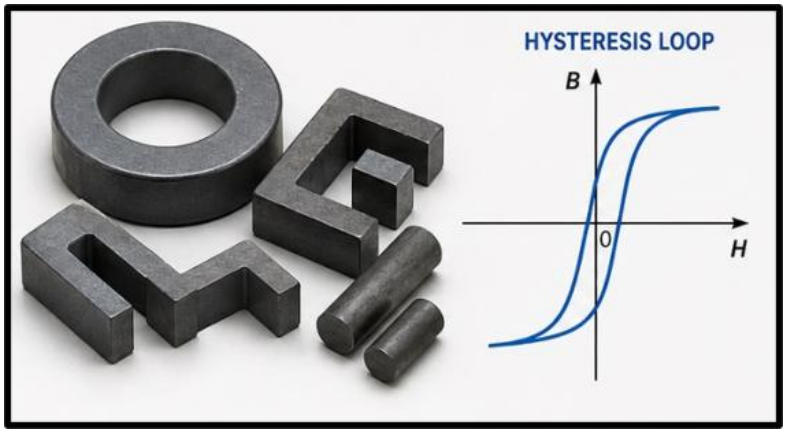

Figure 1: Soft Ferrites

Hard Ferrites (Permanent Magnet Ferrites)

Hard ferrites, alternatively referred to as ceramic permanent magnets, are characterized by high coercivity, substantial remanent magnetization, and pronounced uniaxial anisotropy. Their magnetic hardness arises from restricted domain-wall mobility and large anisotropy fields, which stabilize magnetic domains against external demagnetizing forces. From an energetic standpoint, these materials exhibit significant magnetic energy products and long-term stability, making them particularly suitable for permanent magnet assemblies, electric motors, loudspeakers, sensors, and actuators. The inherent chemical inertness, mechanical robustness, and low production cost further enhance their industrial viability [14]. Unlike soft ferrites, magnetization reversal in hard ferrites predominantly occurs through coherent spin rotation rather than domain wall motion, thereby accounting for their high coercive fields. Typical examples of hard ferrites embrace barium hexaferrite ($BaFe_{12}O_{19}$), strontium hexaferrite ($SrFe_{12}O_{19}$), and lead hexaferrite ($PbFe_{12}O_{19}$), among which barium and strontium ferrites are the most extensively utilized commercial permanent magnet objects due to their high magnetocrystalline anisotropy, excellent corrosion resistance, and favourable cost-to-performance ratio [13].

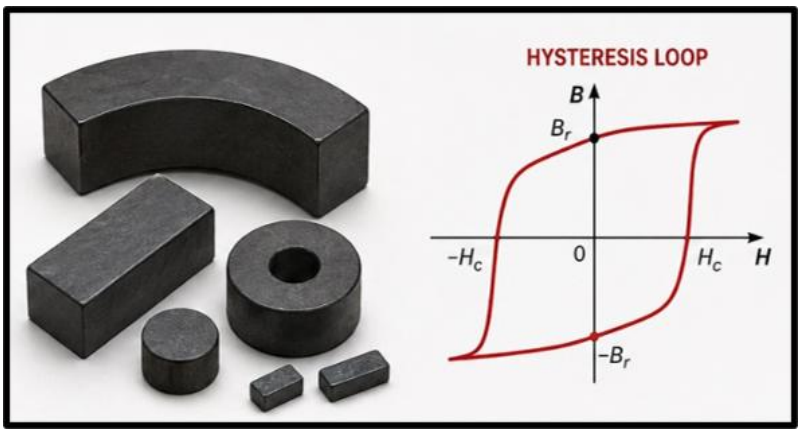

Figure 2: Hard Ferrites

Classification Based on Crystal Structure

Crystallographic symmetry plays a decisive role in determining cation distribution, superexchange pathways, anisotropy constants, and magnetization behavior. Accordingly, ferrites are divided into three principal structural families [16].

Spinel Ferrites (AB_2O_4 Structure)

Spinel ferrites constitute a scientifically prominent and technologically indispensable group of ferrimagnetic ceramic oxides, distinguished by their crystallographic versatility and compositional adaptability. Structurally, they possess a cubic close-packed oxygen framework in which metallic cations are accommodated within tetrahedral A-sites and octahedral B-sites. Their magnetic ordering is primarily controlled by oxygen-mediated super-exchange interactions between cations occupying these two sublattices. The dominant A–O–B exchange pathway promotes antiparallel spin alignment between tetrahedral and octahedral sublattices, thereby producing ferrimagnetism as a consequence of unequal magnetic moments and site-specific cation distribution [15]. Based on the arrangement of cations, spinel ferrites may occur as normal, inverse, or mixed spinel structures, offering substantial flexibility for modifying their functional characteristics. Through controlled compositional substitution and cation redistribution, significant attribute such as saturation magnetization, coercivity, Curie temperature, electrical resistivity, dielectric response, and magnetic anisotropy can be effectively engineered. This remarkable tunability has established spinel ferrites as highly versatile materials for advanced applications in high-frequency electronics, electromagnetic interference shielding, microwave devices, magnetic recording, sensors, inductors, transformers, and energy-related systems [17]. Common examples of this class include $NiFe_2O_4$, $CoFe_2O_4$, $ZnFe_2O_4$, and $MgFe_2O_4$.

A. Normal Spinel Ferrites

Normal spinel ferrites denote the most elementary and crystallographically ordered form of the spinel framework, wherein divalent metal cations are preferentially accommodated at the tetrahedrally coordinated A-sites, while trivalent ferric ions are systematically distributed over the octahedrally coordinated B-sites. This cationic arrangement is commonly expressed by the structural configuration, where parentheses indicate tetrahedral occupancy and square brackets reflect octahedral coordination. Such a site-specific distribution produces a comparatively simple magnetic architecture, as the octahedral sublattice contains the dominant proportion of magnetically active Fe^{3+} ions. Owing to the limited magnetic contribution from the tetrahedral sublattice, the inter-sublattice A–O–B superexchange interaction becomes relatively less pronounced than that observed in inverse or mixed spinel systems. Consequently, magnetic coupling is governed more substantially by interactions within the B-sublattice, where opposing spin orientations may partially neutralize one another, resulting in reduced net magnetization.

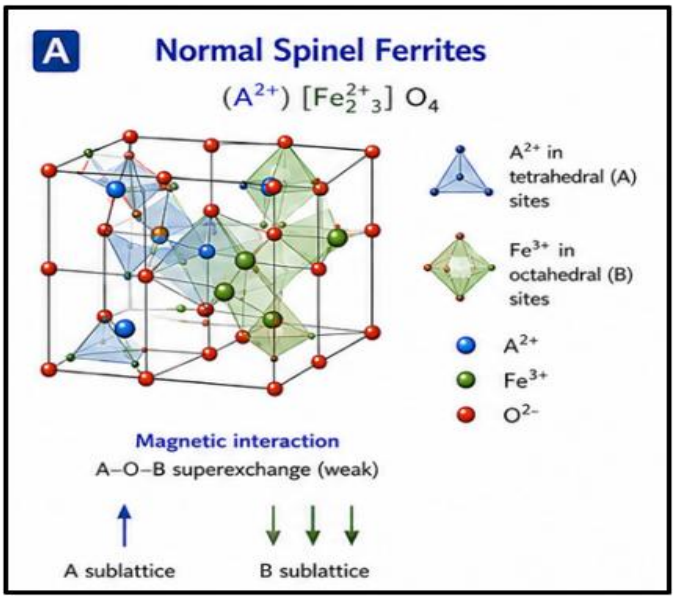

Figure 3: Normal Spinel Ferrites

Consequently, these ferrites generally exhibit low saturation magnetization, high electrical resistivity, reduced magnetic anisotropy, and predominantly dielectric or semiconducting behavior. Their subdued magnetic response makes them less suitable for strong magnetic applications but advantageous in dielectric, catalytic, and sensing devices. Typical examples include $ZnFe_2O_4$ and $MgFe_2O_4$, which are frequently employed in gas sensors, photocatalysts, and high-resistivity electronic ceramics [16].

B. Inverse Spinel Ferrites

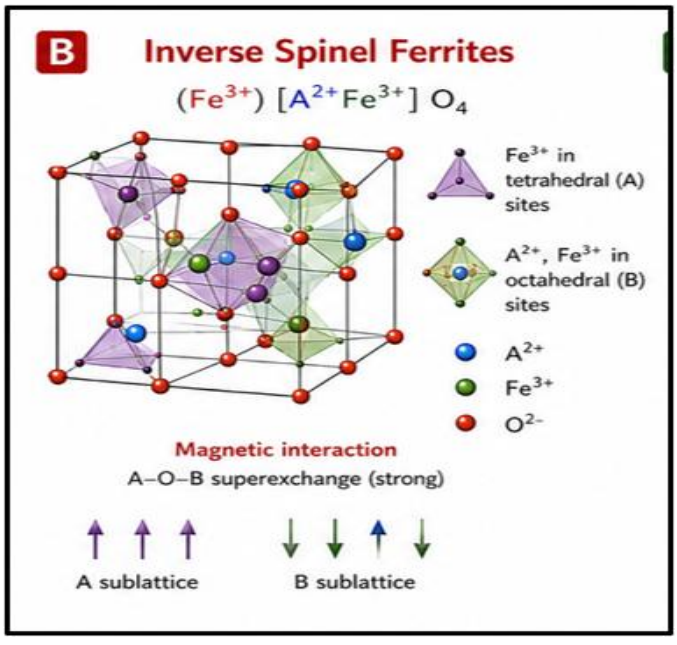

Figure 4: Inverse Spinel Ferrites

Inverse spinel ferrites exhibit a reversed cation distribution, wherein Fe^{3+} ions possess all tetrahedral sites, whereas the octahedral sites are partitioned equally by divalent (A^{2+}) and Fe^{3+} ions, yielding the configuration (Fe3+) [A2+Fe3+] O4. This redistribution maximizes A–B

superexchange coupling, which is the strongest magnetic interaction in ferrimagnetic oxides. The antiparallel spin coupling between the tetrahedral and octahedral sublattices creates a substantial magnetic moment disequilibrium, which manifests as enhanced saturation magnetization, elevated Curie temperature, strong magnetocrystalline anisotropy, and moderate electrical conductivity. The conductivity is generally associated with electron-hopping mechanisms between Fe^{2+}/Fe^{3+} ions ions, particularly within the octahedral sublattice. Owing to these superior magnetic attributes, inverse spinels dominate technological applications requiring efficient magnetic response. Representative compounds include $NiFe_2O_4$, $CoFe_2O_4$, and Fe_3O_4, extensively utilized in inductors, transformer cores, microwave absorbers, and magnetic recording devices [17].

C. Mixed or Partially Inverse Spinel Ferrites

Mixed or partially inverse spinel ferrites constitute an intermediate and highly versatile category in which both divalent-trivalent cations are statistically spread between tetrahedral-octahedral sites, described by the generalized expression $(A_{1-\lambda}Fe_{\lambda})\ [A\lambda F_{e2-\lambda}]\ O_4$, where λ denotes the degree of inversion ($0 < \lambda < 1$). This partial occupancy permits continuous modulation of magnetic exchange interactions, thereby enabling precise control over saturation magnetization, coercivity, electrical resistivity, dielectric constant, and high-frequency stability. Such structural flexibility renders mixed spinels particularly valuable for tailoring material properties through compositional substitution, synthesis temperature, and processing routes. Systems such as Ni–Zn ferrites, Mg–Zn ferrites, and Cu–Zn ferrites exemplify this group and are widely applied in high-frequency transformers, antennas, electromagnetic interference (EMI) suppression cores, and microwave communication components [17].

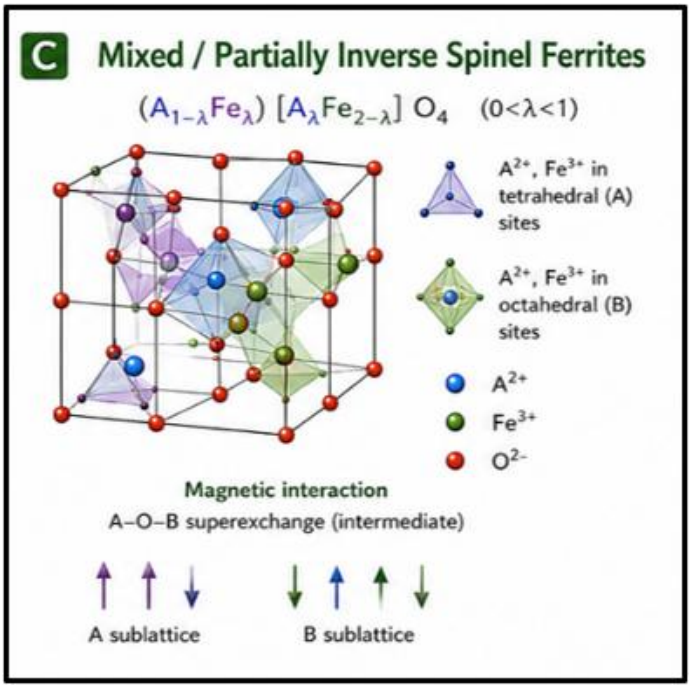

Figure 5: Mixed /Partially Inverse Spinel Ferrites

Hexagonal Ferrites (Hexaferrites)

Hexagonal ferrites crystallize in the magnetoplumbite-type lattice, comprising layered structural blocks that generate strong uniaxial anisotropy. This intrinsic anisotropy imparts high coercivity and stable magnetization. The complex stacking of Fe–O polyhedra enhances magnetostatic energy barriers, thereby stabilizing permanent magnet behaviour [18]. These ferrites are widely used in microwave absorbers, radar systems, permanent magnets, and high-frequency electromagnetic devices, where strong anisotropic magnetic response is desirable. Typical compositions include barium and strontium ferrites.

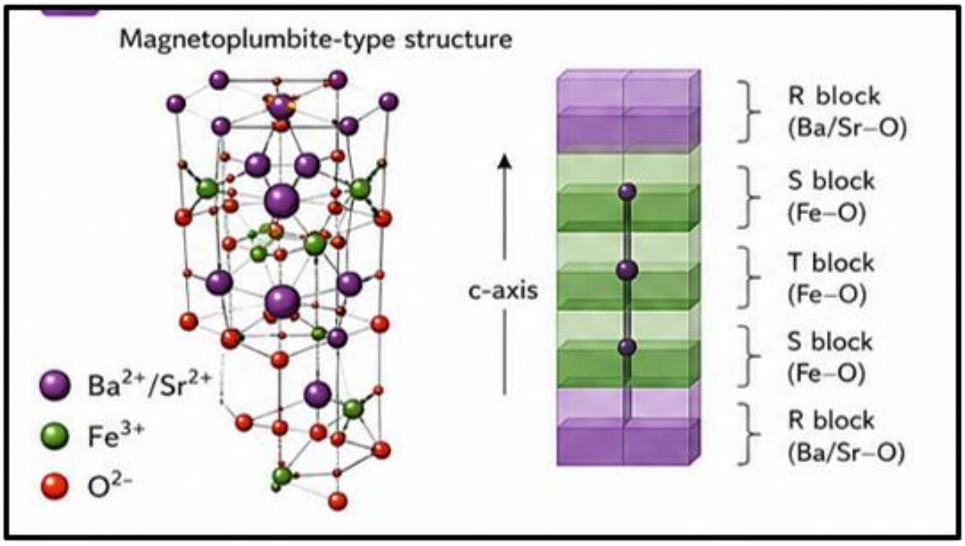

Figure 6: Hexagonal Ferrites

Garnet Ferrites

Garnet ferrites possess a cubic garnet lattice with three distinct magnetic sublattices. They exhibit extremely low magnetic damping and narrow ferromagnetic resonance linewidths. Such characteristics render them ideal for microwave and magneto-optical applications, including circulators, isolators, and phase shifters. Yttrium iron garnet (YIG) is a classical example of this category.

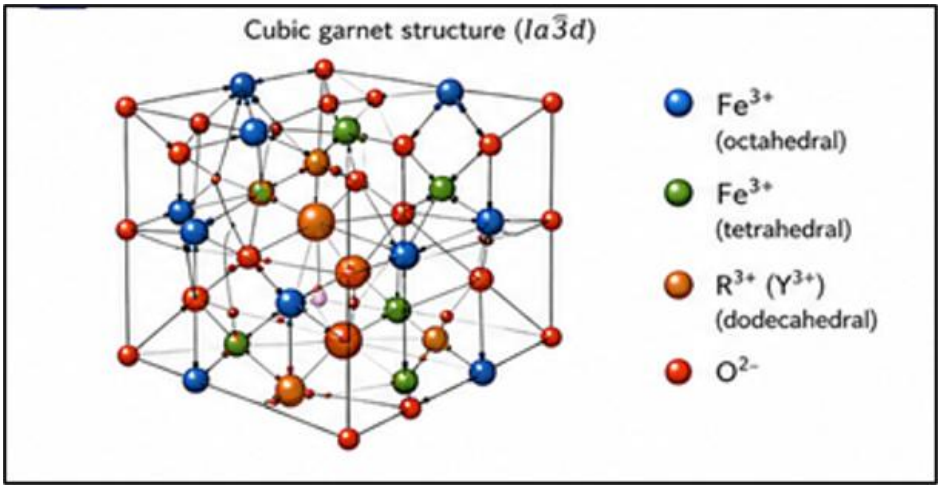

Figure 7: Garnet Ferrites

Applications of Ferrites

Ferrites constitute a technologically indispensable class of magnetically ordered ceramic oxides distinguished by their rare combination of high electrical resistivity, low eddy-current dissipation, moderate-to-high magnetic permeability, chemical stability, and thermal robustness. From an applied solid-state physics standpoint, ferrites function as magnetically active dielectrics, simultaneously enabling efficient magnetic flux conduction while suppressing parasitic electrical losses. This duality differentiates ferrites fundamentally from metallic ferromagnets and underlies their dominance in high-frequency electromagnetic systems. The theoretical foundations governing these functional attributes are discussed comprehensively in Magnetism and Magnetic Materials. The principal application domains are elaborated below in a systematic and technically rigorous manner.

Power Electronics and Magnetic Energy Conversion

Ferrites are extensively employed as core materials in transformers, inductors, chokes, and switched-mode power supplies because their intrinsically high resistivity drastically suppresses circulating eddy currents under alternating magnetic fields. This property ensures minimal thermal dissipation even at elevated switching frequencies, thereby enhancing energy efficiency and enabling miniaturization of electromagnetic components. Soft ferrites exhibit high magnetic permeability and low coercivity, which facilitate rapid and reversible domain wall motion with negligible hysteretic losses. Consequently, they allow efficient magnetic flux coupling, stable inductance, and reduced power loss across wide frequency bands. These attributes make ferrites foundational to compact power converters, high-frequency transformers, and modern electronic power-conditioning circuits [22,24].

Microwave, Radio-Frequency, and Communication Systems

Ferrites display strong frequency-dependent magnetic permeability and exceptionally low dielectric loss, rendering them highly effective for microwave and radio-frequency engineering. Their magnetization dynamics enable controlled absorption, transmission, and non-reciprocal propagation of electromagnetic waves under external magnetic bias. Such behavior permits the design of circulators, isolators, phase shifters, resonators, and electromagnetic absorbers that are critical to radar, satellite, and telecommunication systems. In these devices, ferrites regulate signal directionality and mitigate interference, ensuring signal integrity and system stability. Their thermal and chemical durability further supports long-term performance in high-power microwave environments [23].

Permanent Magnets and Electromechanical Devices

Hard ferrites, particularly hexagonal ferrite compositions, possess large magnetocrystalline anisotropy and high coercivity, which stabilize magnetic domains against reversal and provide strong remanent magnetization. These characteristics allow ferrites to function as durable and cost-effective permanent magnets with excellent resistance to corrosion and demagnetization. Accordingly, they are widely implemented in electric motors, generators, loudspeakers, magnetic

couplings, and actuators. Their intrinsically ceramic constitution imparts pronounced mechanical robustness, chemical inertness, thermal endurance, and environmental resilience in comparison with conventional metallic magnetic materials, thereby rendering ferrites highly suitable for demanding and adverse operating environments. In these functional systems, ferrites facilitate the efficient transduction of magnetic energy into mechanical displacement, while maintaining exceptional operational reliability, durability, and long-term service stability.

Magnetic Recording and Data Storage Technologies

Ferrites have historically played a crucial role in magnetic recording due to their stable magnetic response, fine grain structure, and wear resistance. Their moderate permeability and low loss characteristics make them ideal for magnetic heads and core materials in tape drives and data-reading systems. The stability of their magnetic domains ensures consistent signal detection and minimal noise generation. Even in contemporary technologies, ferrite components remain relevant in specialized sensing and legacy recording applications where reliability and durability are paramount.

Sensors, Transducers, and Functional Devices

The semiconducting and dielectric properties of ferrites enable sensitivity to temperature, magnetic fields, mechanical stress, and environmental changes. Their temperature-dependent resistivity is exploited in thermistors for thermal monitoring and circuit protection. Variations in magnetic permeability under applied fields support current sensors and magnetic field detectors used in industrial control systems. Grain-boundary polarization effects contribute to humidity and gas sensing capabilities. Additionally, magnetostrictive behavior allows ferrites to function as electromechanical transducers. These multifunctional responses arise from the coupling between electronic transport, lattice distortion, and magnetic ordering, making ferrites highly suitable for smart sensing and adaptive device technologies.[25]

Biomedical and Nanotechnological Applications

At nanometer dimensions, ferrites exhibit superparamagnetic [characterized by rapid magnetic response without residual magnetization. This property prevents agglomeration while permitting precise manipulation using external magnetic fields. Such attributes are particularly valuable in advanced biomedical platforms, wherein ferrite nanoparticles function as magnetic resonance imaging contrast enhancers, magnetically guided nanocarriers for site-specific drug delivery, and heat-generating agents for magnetic hyperthermia-based therapeutic interventions. Their chemical stability, biocompatibility, and controllable magnetic moment allow safe and localized therapeutic action. Consequently, ferrites have emerged as critical materials in modern nanomedicine and bioengineering research. [33,34,35]

Energy, Environmental, and Catalytic Applications

Ferrites have acquired considerable scientific and technological ascendancy in sustainable energy conversion, electrochemical storage, and environmental remediation owing to their multivalent cationic framework, redox-active transition-metal centres, and catalytically

competent surface microarchitecture. Their mixed-valence electronic configuration facilitates interfacial charge transfer and promotes photocatalytic mineralization of organic pollutants, oxidative degradation of refractory contaminants, wastewater decontamination, and heterogeneous redox transformations across diverse physicochemical environments. Furthermore, ferrite-based electrode architectures are increasingly being investigated for advanced electrochemical energy-storage systems, including lithium-ion batteries, supercapacitors, and hybrid capacitive devices, where their structural stability, electronic tunability, and reversible redox activity contribute to improved charge-storage performance. A particularly advantageous feature of ferrites is their intrinsic magnetic retrievability, which enables facile separation, regeneration, and reutilization after catalytic or remediation cycles, thereby improving process economy, minimizing secondary waste generation, and reducing ecological perturbation. These synergistic attributes position ferrites as multifunctional materials operating at the intersection of magnetism, heterogeneous catalysis, environmental sustainability, and next-generation energy technology.[34.35]

Scope and Motivation of the Present Research

The growing demand for miniaturized, energy-efficient, and high-performance magnetic materials in contemporary electronic and electromagnetic devices has intensified research into nanostructured ferrites with tailored structural and functional attributes. Copper–zinc ferrites, in particular, are widely recognized for their low eddy current losses, high electrical resistivity, moderate permeability, and excellent chemical stability, rendering them suitable for high-frequency transformer cores, inductors, electromagnetic interference suppression components, and microwave devices. Nevertheless, the intrinsic physicochemical and functional attributes of these ferrites are profoundly modulated by compositional substitution, site-selective cation redistribution, crystallite dimensionality, grain-boundary architecture, lattice strain, defect chemistry, and synthesis-mediated microstructural evolution. Hence, rigorous and systematic optimization of these interdependent parameters becomes indispensable for attaining the desired magnetic, electrical, dielectric, catalytic, and application-specific performance characteristics.

Reference

1. Salih, S., & Mahmood, W. (2023). Review on magnetic spinel ferrite (MFe_2O_4) nanoparticles: From synthesis to application. *Heliyon, 9*.
2. Karadi, I., Hiremath, V., Timmanagoudar, S., Mathad, S., & Mehulkumar, G. (2025). Nano ferrites: Synthesis, properties and emerging applications: A comprehensive review. *Journal of Advancements in Material Engineering, 10*(2).
3. Ahmed, M., & Abu-Elsaad, N. (2024). Exploring the magnetic behavior of ferrites: From diamagnetism to superparamagnetism.
4. Dastjerdi, D., Shokrollahi, H., & Mirshekari, S. (2023). A review of synthesis, characterization, and magnetic properties of soft spinel ferrites. *Inorganic Chemistry Communications*.

5. Munir, M., Naz, M., Shukrullah, S., Ansar, M., Farooq, M., Irfan, M., Mursal, S., Legutko, S., Petrů, J., & Pagáč, M. (2022). Enhancement of magnetic and dielectric properties of $Ni_{0.25}Cu_{0.25}Zn_{0.50}Fe_2O_4$ magnetic nanoparticles through non-thermal microwave plasma treatment for high-frequency and energy storage applications. *Materials, 15*.
6. Akhtar, M., Rahman, A., Sulong, A., & Khan, M. (2017). Structural, spectral, dielectric and magnetic properties of $Ni_{0.5}Mg_xZn_{0.5-x}Fe_2O_4$ nanosized ferrites for microwave absorption and high-frequency applications. *Ceramics International, 43*, 4357–4365.
7. Kempa, M., Bovtun, V., Kukhar, V., Solopan, S., Belous, A., V'yunov, O., Yakymenko, Y., & Kamba, S. (2025). High-frequency and microwave magnetic properties of $Ni_{0.5}Zn_{0.5}Fe_2O_4$ spinel ferrite ceramics. *Journal of Alloys and Compounds*.
8. Arcaro, S., & Venturini, J. (2021). A brief history of ferrites. In *Modern Ferrites in Engineering*. Cham, Switzerland: Springer.
9. Srdić, V., Cvejić, Ž., Milanović, M., Stojanović, G., & Rakić, S. (2018). Metal oxide structure, crystal chemistry, and magnetic properties. In *Metal Oxides* (pp. 313–332).
10. Katoch, G. (2021). Recent advances in processing, characterizations and biomedical applications of spinel ferrite nanoparticles (pp. 62–120).
11. Dastjerdi, D., Shokrollahi, H., & Mirshekari, S. (2023). A review of synthesis, characterization, and magnetic properties of soft spinel ferrites. *Inorganic Chemistry Communications*.
12. Karadi, I., Hiremath, V., Timmanagoudar, S., Mathad, S., & Mehulkumar, G. (2025). Nano ferrites: Synthesis, properties and emerging applications: A comprehensive review. *Journal of Advancements in Material Engineering, 10*(2).
13. Askarzadeh, N., & Shokrollahi, H. (2024). A review on synthesis, characterization and properties of lithium ferrites. *Results in Chemistry*.
14. Dhiman, P., Rana, G., Goyal, D., & Goyal, A. (2021). Basics of ferrites: Types and structures. In *Engineering Materials*. Singapore: Springer.
15. Narang, S., & Pubby, K. (2021). Nickel spinel ferrites: A review. *Journal of Magnetism and Magnetic Materials, 519*, 167163.
16. Ahmed, M., & Abu-Elsaad, N. (2024). Exploring the magnetic behavior of ferrites: From diamagnetism to superparamagnetism.
17. Tayade, N., Sarkar, N., Rewatkar, K., & Nanoti, V. (2018). Soft ferrite: A brief review on structural, magnetic behavior of nanosize spinel ferrites.
18. Narang, S., & Pubby, K. (2021). Nickel spinel ferrites: A review. *Journal of Magnetism and Magnetic Materials, 519*, 167163.
19. Zhao, J., Xiang, B., Dai, H., Liu, F., Zhang, Y., Zhou, R., & Zhou, Y. (2022). High-entropy spinel ferrites MFe_2O_4 (M = Mg, Mn, Fe, Co, Ni, Cu, Zn) with tunable electromagnetic properties and strong microwave absorption. *Journal of Advanced Ceramics, 11*, 754–768.

20. Sun, K., Li, J., Chen, Y., Xiao, Y., Yang, Y., Liu, L., & Liu, Y. (2024). Microwave magnetic and high dielectric properties of Ca^{2+}–Sn^{4+} co-substituted BiIn-YIG ferrites for device application. *Applied Physics A, 130*.
21. Sardar, I., Hossain, M., Sikder, M., Khan, M., & Rahman, M. (2023). Enhancement of coercivity, permeability, and dielectric properties of $Co_{0.2}Zn_{0.3}Ni_{0.5}EuFe_2O_4$ ferrites for memory and high-frequency devices. *Journal of Rare Earths*.
22. Khudaysh, L., Ahmed, I., Ejaz, S., Khan, S., Haleem, Y., Ibrahim, M., Ali, M., Farid, H., & El-Bahy, Z. (2023). Analysis of cerium substitution in Co–Sr based spinel ferrites for high-frequency application. *Journal of Rare Earths*.
23. Khan, S., Ullah, S., Altuijri, R., & Maati, L. (2023). Electric, dielectric, and magnetic properties of strontium-based spinel ferrites for the high-frequency applications. *JOM, 75*, 4887–4893.
24. Goldman, A. (2006). *Modern ferrite technology* (2nd ed.). Springer.
25. Pullar, R. C. (2012). Hexagonal ferrites: A review of the synthesis, properties and applications of hexaferrite ceramics. *Progress in Materials Science, 57*, 1191–1334.
26. Smit, J., & Wijn, H. P. J. (1959). *Ferrites*. Philips Technical Library.
27. Sugimoto, M. (1999). The past, present, and future of ferrites. *Journal of the American Ceramic Society, 82*, 269–280.
28. Snoek, J. L. (1948). *New developments in ferromagnetic materials*. Elsevier.
29. Cullity, B. D., & Graham, C. D. (2009). *Introduction to magnetic materials* (2nd ed.). Wiley-IEEE Press.
30. Coey, J. M. D. (2010). *Magnetism and magnetic materials*. Cambridge University Press.
31. Harris, V. G. (2012). Modern microwave ferrites. *IEEE Transactions on Magnetics, 48*, 1075–1104.
32. Gorter, E. W. (1954). Saturation magnetization and crystal chemistry of ferrimagnetic oxides. *Philips Research Reports, 9*, 295–340.
33. Kodama, R. H. (1999). Magnetic nanoparticles. *Journal of Magnetism and Magnetic Materials, 200*, 359–372.
34. Laurent, S., Forge, D., Port, M., Roch, A., Robic, C., Vander Elst, L., & Muller, R. N. (2008). Magnetic iron oxide nanoparticles: Synthesis, stabilization, vectorization, physicochemical characterizations, and biological applications. *Chemical Reviews, 108*, 2064–2110.
35. Sun, S., Zeng, H., Robinson, D. B., Raoux, S., Rice, P. M., Wang, S. X., & Li, G. (2004). Monodisperse MFe_2O_4 (M = Fe, Co, Mn) nanoparticles. *Journal of the American Chemical Society, 126*, 273–279.

Bhumi Publishing, India
August 2026

CARBON BASED NANOMATERIALS: RECENT ADVANCES, CHALLENGES AND FUTURE PROSPECTS

Sanjib Mondal
Department of Physics, Suri Vidyasagar College
(Affiliated under The University of Burdwan),
Suri, Birbhum–731101, West Bengal, India
Corresponding author E-mail: sanjibmondal220@gmail.com

Abstract

Carbon nanomaterials (CNMs) including carbon quantum dots, fullerene, graphene, carbon nanotube, three-dimensional porous carbons and other nanosized allotropes constitute one of the most important and technologically diverse families of nanostructured materials. CNMs possess unique physiochemical properties such as structural flexibility and stability, different bonding configurations and architectures, high porosity and mechanical strength. Several mechanochemical approaches such as microwave, chemical vapor deposition (CVD), hydrothermal, solvothermal, plasma-enhanced CVD, and laser ablation are being utilized for better control in optimizing particle size, morphology, and surface chemistry. The remarkable structural diversity and tunable optoelectronic behaviors have enabled them well suited in various applications in energy storage and conversion, catalysis, biomedicine, electronics, water treatment, sensing, and environmental remediation. Activated carbon is widely used in waste water filtration because of possessing massive internal surface area. Recent research has increasingly emphasized sustainable and green synthesis from waste resources and biomass, heteroatom doping, carbon-carbon and carbon-inorganic hybrids, and artificial intelligence (AI)-assisted materials designing. This review presents an integrated overview of the synthesization of CNMs family, highlighted recent applications, major challenges related to synthesis, reproducibility, scalability and safety, and discusses future prospects in sustainable viewpoint.

Keywords: Carbon Nanomaterials, Graphene, Energy Storage, Supercapacitor, Biomedical.

1. Introduction

Currently, the world is facing a critical turbulence owing to high population grown, rapid energy consumption, unscientific use of fossil fuels and deteriorating environment conditions. Renewable energy solutions coming from solar, wind and tidal systems have received significant attention due to their abundant resource and pollution free nature, but their production cost and efficient materials designing pose major challenges in widespread applications. Researchers are focusing continuously to enhance the efficiency of energy conversion and storage devices by using suitable materials architecting. Batteries and supercapacitors are the primary energy

storage devices that are mainly developed using carbon based materials. In this context, carbon nanomaterials (CNMs) have emerged as leading sources in energy conversion and storage technologies owing to their remarkable structural diversity, high surface area, easily tunable optical and electrical properties, high thermal and chemical stability (Jatoi *et al.,* 2024).

Carbon is one of the most abundant and versatile elements in environment as well as human body. It can form stable structures with different hybridization states and bonding configurations that is leading to produce in several allotropic forms. CNMs occupy a particularly intriguing elemental position as they can form strong covalent bonds and stable structures with sp, sp^2, and sp^3 hybridization. Graphite and diamond are two natural allotropes of carbon. Diamond exhibits sp^3 hybridization with bond length of 1.56Å whereas graphite form sp^2 hybridization with a hexagonal (honeycomb) lattice, having bond length of 1.42Å. The chemical versatility of CNMs make it a broad family with different structures ranging from zero dimensional fullerenes, carbon quantum dots, one dimensional carbon nanotubes, two dimensional graphene sheets, and three-dimensional porous carbon networks (Onyancha *et al.,* 2022).

The properties and morphologies are immensely influenced by the synthesis process of carbon materials. Nanotechnology has created a broad platform for designing suitable materials with astonishing behaviors that are substantially different from their bulk counterparts. Synthesis can broadly be divided into top-down and bottom-up approaches. In top-down methods, beginning with bulk carbon materials down into tiny nanoscale structure. Laser ablation, arc discharge, ball milling and electrochemical exfoliation are some common top-down approaches for CNMs fabrication. On the other hand, in bottom-up method carbon materials are built up atom by atom or molecules by molecules. Chemical vapor deposition (CVD), hydrothermal and solvothermal synthesis, and pyrolysis and carbonization are some examples of bottom-up approach. Recently, researchers are focusing in emphasizing green synthesis approaches, heteroatom doping, hierarchical porosity, C-C hybrid architectures, large-scale production, and artificial-intelligence-assisted materials development (Kothandam *et al.,* 2023; Baig *et al.,* 2021).

Over the past decades, carbon based nanomaterials have achieved remarkable improvement in various applications. Particular attention is given to emerging applications of CNMs families in energy storage and conversion, environmental technologies, biomedical systems and drug delivery, catalysis, nanoelectronics, sensors, and AI-assisted materials discovery. This article provides a conscious overview of various allotropes of carbon, their synthesis techniques and applications in diverse fields.

2. Classification of Carbon Nanomaterials

Nanomaterials are tiny substances that have at least one dimension of 100 nm or less. In terms of dimensionality, nanomaterials are divided into four size-based categories such as 0-D, 1-D, 2-D,

and 3-D, which may be round, tubular, irregularly or solitaire shaped, fused, aggregated, or agglomerated (Mekuye *et al.,* 2023).

- **0D (all the dimensions inside the nanometric range ≤ 100 nm):** fullerenes, carbon dots, carbon quantum dots, nanodiamonds and carbon nanobowls.
- **1D (two dimensions are ≤100 nm, one dimension is larger):** single-walled and multi-walled carbon nanotubes, carbon nanofibers and nanorods.
- **2D: (one dimensions is ≤100 nm, two dimensions are larger):** graphene, GO, rGO and graphene-like carbon nanosheets.
- **3D (all the dimensions are beyond the nanometric range ≥ 100 nm,):** carbon aerogels, carbon nanocages, porous carbons, graphene foams and hierarchical carbon networks.
- **3. Synthesis techniques of carbon nanomaterials**

3.1. The Arc Discharge Method

The arc discharge technique is very popular method for the development of various carbon nanostructured materials such as fullerenes, CNT, carbon nanohorns, few-layer graphene (FLG), and spherical amorphous carbon nanoparticles. In arc discharge process, two graphite rods are mounted in a chamber under a certain helium pressure. Carbon rod is vaporized by arc discharge and several carbon based materials are produced in different position during the growth process. In this method, single walled carbon nanotubes (SWCNT), multi walled CNT and dahlia-like or bird-like carbon nanohorns are developed efficiently. Also, graphene nanostructures and their constituents are efficiently produced by arc discharge method. Graphene sheets are developed by hydrogen arc discharge exfoliation method which exhibit good electrical conductivity and thermal stability as compared to those obtained via argon arc discharge tube (Wu *et al.,* 2009).

3.2. Laser Ablation

A novel one-step technique for creating CNMs is laser ablation synthesis. It involves nanoparticle generation by the hitting of the target material with a powerful laser beam. During this process, the precursor or source materials are evaporated due to the high energy of the laser irradiation, which is leading to nanoparticle formation. Hameed *et al.* (2020) successfully prepared graphene sheets using two step laser ablation method at normal pressure and at room temperature. In the first step, high power laser beam liquefied pure graphite pellets in a liquid process, and the second step involving carbon nanotubes preparation by re-irradiating suspensions with the same laser energy in the absence of target. Pulse laser ablation in liquids (PLAL), a unique green chemical approach is efficiently used to prepare several carbon based materials such as grapheme, clusters of graphene-like flakes and graphene derivatives (rGO, GO, and defective graphene) (Avramova *et al.,* (2022).

3.3. Chemical Vapor Deposition

Chemical vapour deposition (CVD) is a crucial bottom-up method for the generation of high-quality carbon-based nanomaterials. In CVD, a thin film is formed on the substrate surface through the chemical reaction of vapour-phase precursors. During this process, a substrate is placed in an oven and heated to high temperatures to prepare CNMs. A carbon containing gas (hydrocarbons) is slowly introduced to the system as a precursor. Due to high temperatures, hydrocarbon gas decomposes and releases carbon atoms, which recombine to form carbon nanotubes on the substrate. Choice of precursor and catalyst play an important role in the morphology, quality and type of nanomaterial obtained (Shah *et al.,* 2016). Kang *et al.* (2012) directly synthesized fullerene-intercalated porous carbon nanofibre (pCNFs) by CVD method using a Fe/Y zeolite catalyst on a copper substrate. Yang *et al.* (2022) produced highly porous graphene foam electrodes for lithium-ion batteries by placing small pieces of Ni foam in a CVD tube with a mixture of argon and hydrogen. The process was started at 100-200 °C, followed by ethylene at 1100 °C. To obtain pure grapheme, Ni was removed by immersing the sample in a $FeCl_3$ solution.

3.4. Other Methods

As the production of pure nanomaterials is crucial for sustainable environmental application, researchers have emphasized in the discovery of numerous strategies. Wang *et al.* (2018) synthesized graphene quantum dots (GQDs) by using a one-step, one-pot hydrothermal method with rice husk biomass. The obtained GQDs were found in sensing of Fe^{3+} ions via luminescence quenching. Abbas *et al.,* (2022) employed liquid phase exfoliation process for graphene sheet (monolayer or FLG) development in the application of solar cell. Researchers are increasingly focussed some pioneer techniques including green synthesis, lithography, sputtering, pyrolysis, epitaxial growth, soft and hard templating methods, sol-gel, and reverse micelle methods for the successful preparation of carbon nanoparticles (Baig *et al.,* 2021).

4. Different Carbon Based Nanomaterials and Their Applications

4.1. Fullerenes

Fullerenes are the amazing 0D allotropes of carbon with highly symmetrical cages of sp^2 hybridization and they were discovered in 1985. Fullerenes appear with different sizes as C_{60}, C_{70}, C_{76}, C_{84}, and C_{100}, among which C_{60} is most abundant and stable form consisting 60 carbon atoms linked to each other through covalent bond. Fullerenes are utilized as catalyst support materials due to their excellent stability and electrochemical activities during electrochemical reactions (Morelos Gomez *et al.* 2023; Baig *et al.* 2021). In waste water treatment, fullerenes have enormous impact as they both biocompatible and non-toxic materials. Hydrophilic functionalized fullerenes are considered as strong photocatalysts in treating pathogens found in waste water. Water soluble fullerenes, often referred fullerols generate reactive oxygen species

(ROS) during UV or visible-ray photocatalysis process. ROS are capable to remove organic pollutant from contaminant water. Introducing Polyvinylpyrrolidone (PVP) in C_{60} demonstrate excellent antibacterial properties and significant potential for wastewater treatment. PPO-C_{60} membranes (Poly-2,6-dimethyl-1,4-phenylene oxide) exhibit better performance as compared to standard PPO membrane (Puente Santiago *et al.* 2021; Jitoi *et al.* 2024).

4.2. Carbon Nanotube (CNT)

CNTs show enormous applicability in biosensor, tissue engineering and drug delivery system as they have intrinsic optoelectronic properties that enable signal transduction. Its high surface area, needle-like structure, photothermal ablation and semiconducting properties allows detection and adsorption of biomolecules along the side wall of CNTs. In addition, CNTs are enabling to plasma membrane and cytoplasm through a "cellular needle" process. They have the capability in delivering the drug molecules into the desired target tissue and easily can pass through renal excretion. SWCNTs are covalently modified with polyethyleneglycol (PEG) and polyethylenimine (PEI) that were applied as a carrier for doxorubicin (DOX) delivery and the treatment for breast cancer (Farvadi *et al.,* 2017). A stable, unlabeled, CNT film based ultrasensitive field-effect transistor (FET) biosensor is design to detect exosomal miRNA, which acts as an important tumor biomarker. The CNT miR-FET biosensor was functionalized by DNA, which can enable to convert the interaction between the biomolecules and sensor interface into a readable electrical signal (Li *et al.,* 2021).

4.3. Graphene and Their Derivatives

Graphene and their products such as GO, rGO, and graphene nanoplatelets have opened new possibilities in membrane separation, gas barrier, energy storage, supercapacitor and stimuli-response characteristics in nanocomposites. Owing to the tight packing behaviours of sp^2 carbon atoms, graphenes can serve as a near-perfect barrier to gas molecules, which enable them in utilization of packaging materials, corrosion-resistant materials and for protecting sensitive electronic devices. The amphiphilicity nature of GO enables them to be self-assemble on different surfaces, which enhance the capabilities in production of controlled microstructures and tunable characteristics (Alaraj *et al.,* 2026). GO are widely treated as membranes that considered promising materials for water treatment application due to their high stability and water permeance in water. During the past few years, significant efforts have been made in fabricating high permeance membranes with high rejection rates (Smith *et al.,* 2019). Thebo *et al.* prepared GO sheets on polydopamine using modified PES supports with theanine amino acid and tannic acid as crosslinking agents. These GO based membranes exhibited water permeance value of 10,000 $Lm^{-2}h^{-1}bar^{-1}$ with dye rejection of ~100% for methylene blue and rhodamine B (Thebo *et al.,* 2018). Graphenes and their derivatives are substantially used in the development of electrochemical sensors because of high surface-to-volume ratio and atomic thickness.

Graphenes is extremely sensitive materials by which they can response to any changes in its local environment. This is an important factor in developing advanced electrochemical sensing tools, as all the carbon atoms can able to interact with target materials (Li *et al.,* 2019).

4.4. Carbon Based Quantum Dots

Carbon quantum dots are a new class of nanocarbon family. In 2004, they were inadvertently formed during the electrophoretic purification process of single-walled carbon nanotubes. Carbon quantum dots possess several unique features such as tunable photoluminescence properties, solubility in water due to rich oxygen-containing groups, biocompatibility and low toxicity, and cost effectiveness which make them extraordinary materials for several applications. Graphene quantum dots (GQDs) are defined as low dimensional graphene nanosheets with lateral dimension ≤ 100 nm in and <10 layers of ideally one- or few-layered of stacked graphene. Special thanks to GQDs that have been of great interest to their stable fluorescence and adjustable band gap (Wang *et al.,* 2020). Carbon quantum dots have received special interest in the fields of nanomedicine and biological imaging as the direct images of DNA and RNA are very indispensible for understanding cell anatomy and physiology. Han *et al.* (2019) developed membrane-penetrating carbon quantum dots for the imaging of nucleic acids in live organisms.

4.5. Other Carbon Nanomaterials

Carbon nanohorns and carbon nanocones are conical carbon nanostructures that consist of sp^2 carbon sheets. Due to the ability for toxic-metal-catalyst-free synthesis and large-scale production at room temperature, carbon nanohorn have opened up a great potential in energy storage, electrochemiluminescence, electrochemical sensing, and drug delivery system. Recent research is explored relating to the development of efficient porous carbon materials that have fascinating materials properties. Activate carbon, also known as activated charcoal, is a highly porous structured allotrope of carbon that have a huge internal surface area. It traps and eradicates contaminant particles, pollutant chemical, and odors from liquids and gases through adsorption physical process. Like other carbon-based materials, nanodiamonds are monocrystalline diamonds whose particle size is less than 100 nm, consist of sp^3-hybridized carbon nanoparticles. Nanodiamonds are unique carbon-based nano materials and they exhibit exceptional mechanical properties, optical properties, high specific surface areas, and rich surface structures. Nanodiamonds and their composites are extensively employed in sensing device desiging, environmental remediation, and wastewater treatment (Gao *et al.,* 2024; Tetteh *et al.,* 2024; Arti *et al.* 2023).

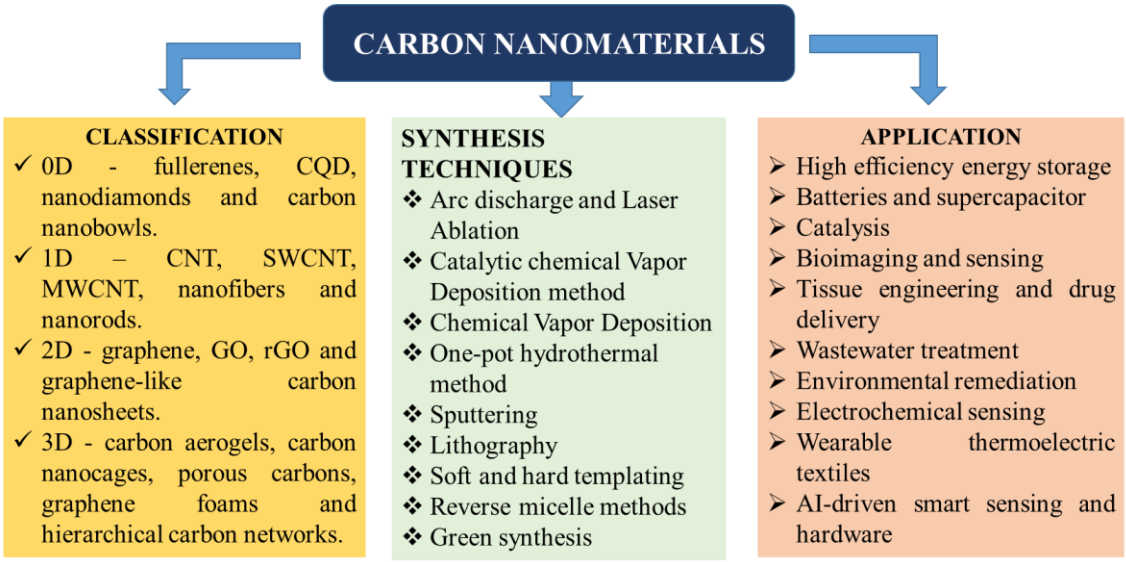

Figure 1: A schematic representation of classification, synthesis, and applications of carbon nanomaterials

5. Challenges

Despite substantial progress, several barriers prevent the full commercialization of CNMs. Reproducibility is one of the major challenges, for instance, a small changes in precursor composition, reaction temperature or pH value can create a huge variation in CNMs properties. This is particularly problematic for quantum carbon dots because their structures and luminescence behaviors are not always properly defined. Large-scale carbon-dot synthesis remains challenging because of reproducibility, scalability, purification, energy consumption and quality-control requirements. Toxicity and environmental safety are critical for eco-friendly CNMs preparation aspects as toxicity can depend on particle size, morphology, surface chemistry, dose, impurities and degradation products. Therefore, long-term environmental impact and biological effects must be systematically investigated before widespread industrialization and commercialization.

6. Future Prospects

During the last few years, a major work has been initiated in the development toward sustainable carbon nanomaterials. Recent advances in carbon based nanomaterial have significant potentials for innovative application in environment remediation. Conventional preparation can require strong oxidizing agents, organic solvents, expensive catalysts and high temperatures. Several renewable precursors such as cellulose, lignin, fruit peels, agricultural residues, food waste and plant extracts can instead provide inexpensive carbon sources. For example, sustainable synthesis of GO from waste materials has become an active research direction. The conversion of waste biomass into functional CNMs represents a particularly promising direction. Future processes should integrate waste pretreatment, management, carbonization, and purification into continuous manufacturing systems. Artificial intelligence (AI) and machine learning (ML) algorithm technology are emerging as versatile tools for predicting material properties and

optimizing synthesis parameters. Recent literature explicitly explores ML language as a potential approach for synthesis for carbon dots, CNTs, nanodiamond and others carbon materials in optimization and property prediction. Thus, a future synthesis platform could integrate precursor composition, reaction time and temperature, pH value, microwave power and purification conditions into a predictive model, which can capable in identifying optimum synthesis performance.

Conclusion

Carbon nanomaterials have evolved from fundamental nanoscience materials into multifunctional platforms with diverse application fields including spanning energy, catalysis environment, healthcare, electronics, and advanced composites. The major classes of carbon nanomaterials include fullerenes, carbon quantum dots, CNTs, graphene, GO, rGO, carbon aerogels and mesoporous carbon nanoparticles that construct a broad and functional carbon family. Their exceptional properties like massive surface area, surface chemistry, structural stability and opto-electronic properties originate from the versatility of carbon bonding configuration and hybridization. Top-down methods such as exfoliation and oxidation provide effective routes to graphene-derived materials, while bottom-up approaches such as CVD, pyrolysis, hydrothermal synthesis, and microwave processing enable controlled formation of CNTs, carbon dots and porous carbon structures. The enormous diversity of CNMs arises not only from dimensionality but also from differences in surface defects, porosity, heteroatom doping, hybridization and crystallinity. Consequently, synthesis conditions strongly determine their efficiency and performance. CNMs are likely to have a benchmark importance in supercapacitors, lithium-ion batteries, sodium-ion batteries, hydrogen technologies and solid-state energy-storage systems. Current research increasingly emphasizes hierarchical porous structures, heteroatom doping and carbon-carbon hybrid electrodes. Overall, carbon nanomaterials are expected to remain a central component of future advanced materials research. However, significant difficulties like reproducibility, structural characterization, scalability, purification, toxicity assessment, and standardization have a great impact. The combination of tunable structure, multifunctionality and compatibility with renewable carbon resources provides a strong foundation for sustainable technologies in energy, environmental protection, healthcare and AI-assisted next-generation electronics.

References

1. Abbas, Q., Shinde, P. A., Abdelkareem, M. A., Alami, A. H., Mirzaeian, M., Yadav, A., & Olabi, A. G. (2022). Graphene synthesis techniques and environmental applications. *Materials, 15*(21), 7804.
2. Alaraj, A. M., Esmaeil, A. A., Khamis, M. A., *et al.* (2026). Pioneering advancements of 2D graphene: Energy and electronics applications. *Optical and Quantum Electronics, 58*, 4.

3. Arti, Namita, Alam, N., & Ansari, J. R. (2023). Nanostructures and fascinating properties of carbon nanohorns. In A. Barhoum & K. Deshmukh (Eds.), *Handbook of functionalized carbon nanostructures*. Springer.
4. Avramova, I., Dimov, D. A., Stankova, N., Petrov, M., Karaivanova, D., Avdeev, G., Russev, S., Karashanova, D., Georgieva, B., Valcheva, E., *et al.* (2022). Novel approach for synthesis of graphene-like phases by pulsed laser ablation in a flow-mode suspension. *Materials, 15*(22), 7870.
5. Baig, N., Kammakakam, I., & Falath, W. (2021). Nanomaterials: A review of synthesis methods, properties, recent progress, and challenges. *Materials Advances, 2*, 1821–1830.
6. Farvadi, F., Tamaddon, A., Sobhani, Z., & Abolmaali, S. S. (2017). Polyionic complex of single-walled carbon nanotubes and PEG-grafted-hyperbranched polyethyleneimine (PEG-PEI-SWNT) for an improved doxorubicin loading and delivery: Development and in vitro characterization. *Artificial Cells, Nanomedicine, and Biotechnology, 45*, 855–863.
7. Gao, X.-W., Zhao, Z.-W., He, Y., *et al.* (2024). Nanodiamond: A promising metal-free nanoscale material in photocatalysis and electrocatalysis. *Rare Metals, 43*(8), 3501–3552.
8. Hameed, R., Khashan, K. S., & Sulaiman, G. M. (2020). Preparation and characterization of graphene sheet prepared by laser ablation in liquid. *Materials Today: Proceedings, 20*, 535–539.
9. Han, G., Zhao, J., Zhang, R., Tian, X., Liu, Z., Wang, A., Liu, R., Liu, B., Han, M., Gao, X., & Zhang, Z. (2019). Membrane-penetrating carbon quantum dots for imaging nucleic acid structures in live organisms. *Angewandte Chemie International Edition, 58*, 7087–7091.
10. Jatoi, A. S., Ahmed, J., Bhutto, A. A., Jeyapaul, A. S. (2025). Recent advances and future perspectives of carbon-based nanomaterials for environmental remediation. *Brazilian Journal of Chemical Engineering, 42*, 151–169.
11. Kang, J., Qin, K., Zhang, H., *et al.* (2012). Direct synthesis of fullerene intercalated porous carbon nanofibers by chemical vapor deposition. *Carbon, 50*(14), 5162–5166.
12. Kothandam, G., Singh, G., Guan, X., Lee, J. M., Ramadass, K., Joseph, S., Benzigar, M., Karakoti, A., Yi, J., Kumar, P., & Vinu, A. (2023). Recent advances in carbon-based electrodes for energy storage and conversion. *Advanced Science, 10*, 2301045.
13. Li, G., Xia, Y., Tian, Y., Wu, Y., Liu, J., He, Q., & Chen, D. (2019). Recent developments on graphene-based electrochemical sensors toward nitrite. *Journal of The Electrochemical Society, 166*, B881–B895.
14. Li, T., Liang, Y., Li, J., Yu, Y., Xiao, M.-M., Ni, W., Zhang, Z., & Zhang, G.-J. (2021). Carbon nanotube field-effect transistor biosensor for ultrasensitive and label-free detection of breast cancer exosomal miRNA21. *Analytical Chemistry, 93*(46), 15501–15507.

15. Mekuye, B., Abera B. (2023). Nanomaterials: An overview of synthesis, classification, characterization, and applications. *Nano Select*, 4, 486–501.
16. Morelos-Gomez, A., Kondo, K., Omori, K., Kamei, Y., Kuritani, M., Irwansyah, Yokokawa, T., Fajardo-Díaz, J. L., Cruz-Silva, R., & Endo, M. (2023). Tuning autoxidation and friction of mineral oil by fullerene cluster properties. *Industrial & Engineering Chemistry Research,* 62(20), 7941–7949.
17. Onyancha, R. B., Ukhurebor, K. E., Aigbe, U. O., Osibote, O. A., Kusuma, H. S., & Darmokoesoemo, H. (2022). A methodical review on carbon-based nanomaterials in energy-related applications. *Adsorption Science & Technology,* Article ID 4438286, 21 pages.
18. Puente Santiago, A. R., Fernandez-Delgado, O., Gomez, A., Ahsan, M. A., & Echegoyen, L. (2021). Fullerenes as key components for low-dimensional (photo)electrocatalytic nanohybrid materials. *Angewandte Chemie International Edition, 60*(1), 122–141.
19. Shah, K. A., & Tali, B. A. (2016). Synthesis of graphene: Potential carbon precursor, synthesis, characterization, and applications. *Materials Science in Semiconductor Processing, 41*, 67–82.
20. Smith, A. T., LaChance, A. M., Zeng, S., Liu, B., & Sun, L. (2019). Synthesis, properties, and applications of graphene oxide/reduced graphene oxide and their nanocomposites. *Nano Materials Science, 1*(1), 31–47.
21. Tetteh, I. K., Issahaku, I., & Tetteh, A. Y. (2024). Recent advances in synthesis, characterization, and environmental applications of activated carbons and other carbon derivatives. *Carbon Trends, 14*, 100328.
22. Thebo, K. H., Qian, X., Zhang, Q., Chen, L., Cheng, H.-M., & Ren, W. (2018). Highly stable graphene-oxide-based membranes with superior permeability. *Nature Communications, 9*, 1486.
23. Wang, C., Shi, H., Yang, M., Yan, Y., Liu, E., Ji, Z., & Fan, J. (2020). A novel nitrogen-doped carbon quantum dots as effective fluorescent probes for detecting dopamine. *Journal of Photochemistry and Photobiology A: Chemistry, 391*, 112374.
24. Wang, W., Wang, Z., Liu, J., Peng, Y., Yu, X., Wang, W., Zhang, Z., & Sun, L. (2018). One-pot facile synthesis of graphene quantum dots from rice husks for Fe^{3+} sensing. *Industrial & Engineering Chemistry Research, 57*(28), 9144–9150.
25. Wu, Z.-S., Ren, W., Gao, L., Zhao, J., Chen, Z., Liu, B., Tang, D., Yu, B., Jiang, C., & Cheng, H.-M. (2009). Synthesis of Graphene Sheets with High Electrical Conductivity and Good Thermal Stability by Hydrogen Arc Discharge Exfoliation. *ACS Nano, 3*, 411–417.
26. Yang, J., Sagar, R. U. R., Anwar, T., Li, X., Qian, Z., & Liang, T. (2022). Graphene foam as a stable anode material in lithium-ion batteries. *International Journal of Energy Research, 46*(4), 5226–5234.

Bhumi Publishing, India
August 2026

ANALYTICAL APPROXIMATION OF THE CLASSICAL SIR EPIDEMIC MODEL USING THE AKBARI–GANJI METHOD

T. Parthiban[1], Salahuddin[1] and K. Chinnadurai[2]

[1]Department of Mathematics, AMET Deemed to be University, Chennai, India

[2]Department of Mathematics, Mahalakshmi Tech Campus Institute of Engineers, Chennai

Corresponding author E-mail: sre.parthi93@gmail.com, salahuddin.m@ametuniv.ac.in, chinnadurai.jmc@gmail.com

Abstract

The Susceptible–Infected–Recovered (SIR) model is a fundamental mathematical framework for describing the transmission and progression of infectious diseases within a population. In this study, an analytical investigation of the classical SIR epidemic model is carried out using the Akbari–Ganji Method (AGM), a semi-analytical technique for obtaining approximate solutions of nonlinear differential equations. The nonlinear SIR system consists of three coupled differential equations governing the dynamics of susceptible, infected, and recovered populations. By applying AGM together with the appropriate initial conditions, approximate analytical expressions for the susceptible, infected, and recovered populations are derived. The obtained solutions provide explicit representations of the epidemic dynamics and avoid the need for repeated numerical integration. The approach demonstrates that AGM provides a simple and efficient analytical framework for investigating nonlinear epidemic models and can be useful for understanding the temporal evolution of disease transmission, infection peaks, and recovery patterns.

Keywords: SIR Epidemic Model, Akbari–Ganji Method (AGM), Nonlinear Differential Equations, Epidemic Dynamics, Analytical Approximation, Semi-Analytical Solution, Infectious Disease Modeling, Susceptible Population, Infected Population, Recovered Population.

1. Introduction

Mathematical modeling of infectious diseases provides an effective framework for understanding disease transmission, progression, and control in a population [1–3]. Among the various compartmental epidemic models, the Susceptible–Infected–Recovered–Deceased (SIRD) model is an extension of the classical SIR model and provides a useful framework for describing the dynamics of susceptible, infected, recovered, and deceased individuals [4,5]. The nonlinear interactions between these compartments are generally represented by a system of coupled nonlinear ordinary differential equations, for which obtaining exact analytical solutions is often difficult.

Several analytical and semi-analytical methods have been developed to investigate nonlinear epidemic models, including the Adomian Decomposition Method (ADM), Homotopy Perturbation Method (HPM), Differential Transform Method (DTM), and Variational Iteration Method (VIM) [6–9]. These methods can provide approximate analytical expressions and offer useful insights into the behavior of epidemic systems. However, the convergence, computational complexity, and applicability of these approaches may depend on the nature of the nonlinear system.

The Akbari–Ganji Method (AGM) is an efficient semi-analytical technique for obtaining approximate solutions of nonlinear differential equations [10,11]. The method determines the unknown coefficients of an assumed approximate solution by utilizing the governing differential equation and its derivatives at a suitable point. AGM has been successfully applied to various nonlinear problems because of its simplicity, computational efficiency, and ability to produce accurate approximate analytical solutions.

In recent years, semi-analytical approaches have attracted considerable attention in epidemic modeling because they can provide explicit expressions that facilitate the interpretation of disease dynamics and parameter effects [12–14]. In this work, the nonlinear SIRD epidemic model is investigated using the Akbari–Ganji Method. Approximate analytical expressions for the susceptible, infected, recovered, and deceased populations are obtained. The accuracy of the AGM solutions is subsequently validated by comparison with numerical solutions. The results demonstrate the potential of AGM as an effective analytical tool for studying nonlinear epidemic dynamics.

2.Mathematical Formulation

The equations are classical SIR epidemic model:

$S'(t) = -\beta S(t)I(t)$ (1)

$I'(t) = \beta S(t)I(t) - \gamma I(t)$ (2)

$R'(t) = \gamma I(t)$ (3)

where β is the infection/transmission rate , γ is the recovery rate , $\beta S(t)I(t)$ represents new infections and $\gamma I(t)$ represents recoveries.

The initial conditions are

$S(0) = S_0, I(0) = I_0, R(0) = R_0$ (4)

If the total population is normalized to 1, then

$S(0) + I(0) + R(0) = 1$ (5)

A common choice is

$S(0) = 1 - I_0, I(0) = I_0, R(0) = 0$ (6)

3. Result and discussion

Akbari–Ganji Method (AGM),

The Akbari–Ganji Method (AGM) is an efficient semi-analytical technique for solving nonlinear differential equations. It employs an assumed trial function with unknown parameters, which are determined by satisfying the governing equation and boundary or initial conditions. AGM provides accurate closed-form approximate solutions with rapid convergence and reduced computational effort.

$$S(t) = S_0 - \beta S_0 I_0 t + \frac{\beta I_0}{2}\left[\beta S_0 I_0 - (\beta S_0 - \gamma) S_0\right] t^2 \quad (7)$$

$$I(t) = I_0 + (\beta S_0 - \gamma) I_0 t + \frac{I_0}{2}\left[(\beta S_0 - \gamma)^2 - \beta^2 S_0 I_0\right] t^2 \quad (8)$$

$$R(t) = R_0 + \gamma I_0 t + \frac{\gamma I_0 (\beta S_0 - \gamma)^2}{2} t^2 \quad (9)$$

Conclusion

In this study, the nonlinear SIRD epidemic model has been investigated using the Akbari–Ganji Method (AGM) to obtain approximate analytical solutions for the susceptible, infected, recovered, and deceased populations. The AGM provides a systematic and relatively simple procedure for constructing approximate solutions of the nonlinear governing equations without relying on numerical discretization.

The analytical results obtained through AGM demonstrate the evolution of the epidemic compartments and provide useful insight into the nonlinear interactions among the different population groups. The obtained approximate solutions describe the dynamic behavior of the epidemic compartments and demonstrate the applicability of AGM to the considered nonlinear SIRD system.

The main advantage of AGM is its ability to provide explicit approximate analytical expressions with relatively low computational effort. Such expressions are useful for examining the influence of epidemiological parameters and understanding the qualitative behavior of disease transmission. Therefore, the present study demonstrates that the Akbari–Ganji Method is a promising semi-analytical technique for solving nonlinear epidemic models. The proposed approach can also be extended to more complex epidemic systems incorporating additional compartments, time-dependent parameters, vaccination, intervention measures, or other epidemiological effects.

References

1. Kermack, W. O., & McKendrick, A. G. (1927). A contribution to the mathematical theory of epidemics. *Proceedings of the Royal Society A: Mathematical, Physical and Engineering Sciences, 115*(772), 700–721. https://doi.org/10.1098/rspa.1927.0118
2. Hethcote, H. W. (2000). The mathematics of infectious diseases. *SIAM Review, 42*(4), 599–653. https://doi.org/10.1137/S0036144500371907

3. Brauer, F. (2008). Compartmental models in epidemiology. In *Mathematical Epidemiology* (Lecture Notes in Mathematics, Vol. 1945, pp. 19–79). Springer. https://doi.org/10.1007/978-3-540-78911-6_2
4. Kermack, W. O., & McKendrick, A. G. (1932). Contributions to the mathematical theory of epidemics. II—The problem of endemicity. *Proceedings of the Royal Society A, 138*(834), 55–83. https://doi.org/10.1098/rspa.1932.0171
5. Kermack, W. O., & McKendrick, A. G. (1933). Contributions to the mathematical theory of epidemics. III—Further studies of the problem of endemicity. *Proceedings of the Royal Society A, 141*(843), 94–122. https://doi.org/10.1098/rspa.1933.0106
6. He, J.-H. (1999). Homotopy perturbation technique. *Computer Methods in Applied Mechanics and Engineering, 178*(3–4), 257–262. https://doi.org/10.1016/S0045-7825(99)00018-9
7. Adomian, G. (1994). *Solving frontier problems of physics: The decomposition method*. Kluwer Academic Publishers.
8. Wazwaz, A.-M. (2009). *Partial differential equations and solitary waves theory*. Springer.
9. He, J.-H. (1998). Approximate analytical solution of Blasius' equation. *Communications in Nonlinear Science and Numerical Simulation, 3*(4), 260–263. https://doi.org/10.1016/S1007-5704(98)90030-8

BRIDGING DISCOVERY AND APPLICATION IN TRANSITION METAL CATALYZED POLYMERIZATIONS

Sudip Kumar De
Department of Chemistry, Bangabasi Evening College, Kolkata, 700009, India
Corresponding author E-mail: drsudipkumardebec@gmail.com

Abstract
The transition from bench top academic discovery to commercial application in transition metal-catalyzed polymerization is one of the most economically impactful narratives in modern industrial chemistry. Moving a catalyst from a controlled glove box environment to a multi-ton manufacturing plant requires overcoming severe chemical hurdles: catalyst deactivation, heat dissipation, structural control, and functional group tolerance. In this chapter, some of the most successful historical and modern examples where fundamental coordination chemistry successfully transitioned into multi-billion-dollar industrial applications have been discussed.

Keywords: Early Transition Metal, Ziegler-Natta Catalysis, Metallocene Catalysts, Constrained Geometry Catalysts, Late Transition Metal Catalysts, Aqueous Polymerization.

Introduction

Transition metal-catalyzed polymerization is the backbone of the modern plastics industry, enabling the synthesis of over 100 million tons of plastics annually with precise molecular control. By substituting radical or ionic mechanisms with transition metal complexes (like titanium, zirconium, or metallocenes), allow precise control over polymer microstructure, stereochemistry, architecture and molecular weight of a polymer. It enables the industrial production of high-performance plastics like high-density polyethylene and isotactic polypropylene, facilitates the incorporation of polar functional groups, and supports green chemistry by reducing waste and energy use.

Bridging the gap between discovery (fundamental laboratory mechanics) and application (industrial-scale manufacturing) in transition metal-catalyzed polymerization requires solving intense engineering challenges. These include catalyst stability, heat removal, reactor fouling, and morphology control. The most prominent, successful examples of bridging this gap include the following foundational technologies.

1. Ziegler-Natta Catalysis: From Lab Accident to Global Polyolefins

The ultimate example of bridging discovery and application is the development of Ziegler-Natta catalysis, which earned the Nobel Prize in Chemistry in 1963 (Ziegler *et al.,* 1955; Natta, 1955).

The Discovery (1953): Karl Ziegler discovered that combining titanium tetrachloride with alkylaluminum co-catalysts polymerized ethylene at room temperature and low pressure (Ziegler

et al., 1955). Giulio Natta extended this to propylene, discovering stereospecific (isotactic) polymerization (Natta, 1955).

The Application Challenge: The early laboratory catalysts were highly unstable, sensitive to air/moisture, leaving high amounts of corrosive titanium and chlorine residues in the polymer. This required expensive, multi-step post-reaction washing.

The Bridge: Heterogenization on MgCl2 support: Chemical engineers and chemists bridged this gap by developing supported catalysts. Immobilizing TiCl4 on a high-surface-area magnesium chloride (MgCl2) matrix increased catalyst activity by orders of magnitude (Sinn & Kaminsky, 1980).

Commercial Impact: This breakthrough allowed for "leave-in" catalyst technologies. It enabled Union Carbide to commercialize the Gas-phase Fluidized Bed Reactors (UNIPOL™), completely eliminating the need for a washing step and enabling the mass production of modern polyethylene (HDPE) and polypropylene (PP) and making polyethylene production highly cost-effective.

2. Metallocene Catalysts: From Structural Curiosity to Drop-In

Metallocenes bridged the gap between highly random polymer chains and precise, tailored molecular architectures (Brintzinger *et al.,* 1995; Sinn & Kaminsky, 1980).

The Discovery: In the 1980s, Walter Kaminsky, Hansjörg Sinn and Hans Brintzinger discovered that adding Methylaluminoxane (MAO) to zirconocene dichloride (Cp2ZrCl2) created an incredibly active, homogeneous "single-site" catalyst (Sinn & Kaminsky, 1980; Brintzinger *et al.,* 1995). Unlike Ziegler-Natta catalysts, every single catalyst molecule was identical, allowing for perfectly uniform polymer chains. Academic labs quickly realized that metallocenes (Group 4 homogeneous complexes of transition metals like Zr and Hf sandwiched between cyclopentadienyl rings) activated by methylaluminoxane (MAO) could polymerize olefins with unprecedented activity and they could "tune" the ligand structure to precisely control molecular weight and stereochemistry. The modification of catalysts by variation of the ligands surrounding the active center permits correlation of catalyst structure with stereospecificity and polymer microstructure. For example, three representative metallocenes are shown in Figure 1. Upon activation with MAO, the C1-symmetric catalyst [Me2Si(9-Flu)2]ZrCl2 (A) produces atactic poly(propene), the C2-symmetric catalyst rac-[Me2Si(2-Me-4-(1-naph)-1-Ind)2]ZrCl2 (B) produces isotactic poly(propene) and the Cs-symmetric catalyst [Me2C(Cp)(Flu)]ZrCl2 (C) produces syndiotactic poly(propene) (Brintzinger *et al.,* 1995).

The Application Challenge: Since metallocenes are soluble (homogeneous), using them directly in existing industrial slurry or gas-phase loops caused severe reactor fouling. The polymer formed a thick, sticky layer on the reactor walls instead of forming clean, flowing

particles. They also lacked thermal stability and required massive, economically unviable amounts of expensive MAO.

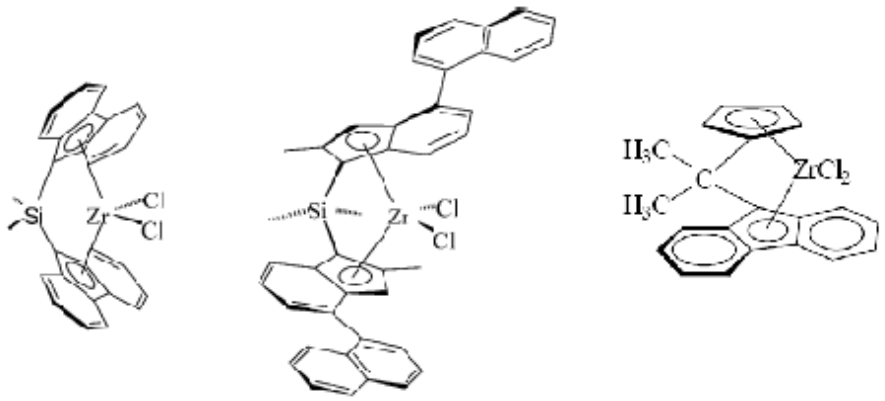

A **B** **C**

Figure 1: Metallocenes for the synthesis of polypropenes with different tacticities

The Bridge to Success: Chemical companies like Dow Chemical and ExxonMobil developed techniques to heterogenize metallocenes by tethering onto solid silica (SiO2) particles without killing their high structural precision allowing it to drop directly into existing industrial drop-in reactors. They also developed specialized chemical scavenger systems to control the intense heat generated by these hyper-active single sites.

Commercial Impact: This bridging enabled drop-in compatibility with existing industrial plants, giving rise to premium polymer brands like ExxonMobil's Exceed™ mPE and Dow's AFFINITY™ Polyolefin Elastomers and commercial production of high-clarity films, tough packaging materials, and advanced elastomers.

3. Constrained Geometry Catalysts (CGC)

The Discovery: Dow introduced constrained-geometry catalysts (CGCs) via their INSITE™ Technology—a single-cyclopentadienyl ligand linked to an amido group (Stevens *et al.,* 1991). This opened up the metal center, allowing it to easily incorporate long-chain α-olefins. The characteristic feature of the structure of the constrained geometry catalyst is the short bond angle (less than 1150) between Cp, M and N atoms. This arrangement allows the metal centers to be more open for monomer and comonomer incorporation.

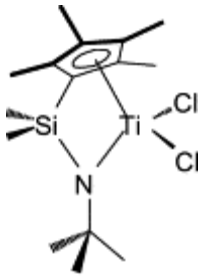

Figure 2: Constrained Geometry Catalysts (CGC) developed by Dow

Industrial Outcome: This breakthrough led to the commercialization of Insite™ and Exxpol™ technologies, producing high-performance linear low-density polyethylene (LLDPE) and polyolefin elastomers (e.g., Engage™) used worldwide in flexible packaging and automotive components. New families of ethylene-α-olefin copolymers have now been prepared using these catalytic systems by Dow under the trade name 'INSITE' (Stevens *et al.,* 1991).

4. Chain-Shuttling Technology: Block Copolymers on Demand

This represents a modern milestone where coordination kinetics were precisely tuned to match heavy industrial constraints.

The Discovery (1990s–2000s): Arriola *et al.* discovered Chain-Shuttling Polymerization (Arriola *et al.,* 2006). By running two distinct transition metal catalysts (one tailored for hard segments, one for soft segments) alongside a chain-shuttling agent (like diethylzinc), polymer chains could jump back and forth between catalysts mid-reaction.

The Application Challenge: Mechanistically, if the shuttling agent moves too slowly, you get a useless blend of two separate polymers. If it moves too quickly, you get a random copolymer. The kinetic rates had to be perfectly balanced under fluctuating industrial reactor temperatures.

The Bridge: Dow's engineers coupled real-time kinetic modeling with high-throughput screening to match the catalyst kinetics to the exact mixing speeds and mass-transport limits of industrial continuous stirred-tank reactors (CSTRs) (Arriola *et al.,* 2006).

Commercial Impact: This created INFUSE™ Olefin Block Copolymers (OBCs), a multi-million dollar class of materials that combine the heat resistance of rigid plastics with the flexibility of rubber, highly prized in footwear and flexible packaging.

5. Late Transition Metal Catalysts (Brookhart & Drent Systems)

Overcoming Water and Polar Monomer Poisoning: Historically, early transition metals (Ti, Zr) were poisoned by polar groups. Late transition metals opened the door to entirely new functionalities (Johnson *et al.,* 1995; Drent *et al.,* 2002).

The Discovery (1995): Early-transition metals (Ti, Zr) are highly oxophilic and gets deactivated when exposed to polar monomers (like acrylates or vinyl acetate) or moisture/water. For decades, making functionalized plastics required harsh, radical-based high-pressure processes. In the mid-1990s, Maurice Brookhart discovered that complexes of late transition metals (Nickel and Palladium) with bulky α-diimine ligands could polymerize ethylene and α-olefins into highly branched structures and more importantly, palladium-based variants could tolerate polar functional groups like acrylates and could copolymerize it with ethylene (Johnson *et al.,* 1995). Concurrently, Eit Drent discovered neutral Pd complexes with phosphine-sulfonate ligands capable of linear copolymerization (Drent *et al.,* 2002).

The Application Challenge: Palladium catalysts are highly expensive and decay rapidly at elevated manufacturing temperatures (typically >60oC). The catalysts also suffered from low

turn-over frequencies (TOF), making them economically unviable for commodity plastic production. Moreover the late transition metal catalysts showed a tendency to create over-branched, amorphous "oils" rather than high-performance solid plastics under practical industrial temperatures.

The Bridge to Application: Academic and industrial partnerships used structural fine-tuning—specifically introducing massive sterically hindered aryl groups on the nitrogen atoms of the ligands. This suppressed competitive chain-transfer reactions and heavily increased thermal stability allowing the catalysts to withstand higher operating temperatures while maintaining polymer chain growth. This fundamental shifting of metal properties also bridged the gap to several commercial applications like a) Copolymerization: Direct insertion of polar monomers (like acrylates) into a polyethylene backbone without destroying the catalyst and b)Emulsion Polymerization: Enabling coordination polymerizations to take place directly in aqueous systems to create environmentally safer, solvent-free waterborne coatings and adhesives.

Industrial Outcome and Commercial Impact: This bridged the "Polar Monomer Problem". It enabled the production of specialized functionalized polyolefins that possess built-in adhesion, paintability, and compatibility with other engineering plastics without requiring secondary surface treatments. While still an active area of scaling optimization, this bridging work successfully moved late transition metal catalysis out of pure academic observation into niche applications.

6. Atom Transfer Radical Polymerization (ATRP)

The Discovery: Discovered in the mid-1990s, by Krzysztof Matyjaszewski and Mitsuo Sawamoto, ATRP relies on a transition metal catalyst (typically Copper, iron or Ruthenium) to establish a reversible redox equilibrium between a dormant alkyl halide species and an active polymer radical (Wang & Matyjaszewski, 1995; Kato *et al.,* 1995). This process keeps the active radical concentration extremely low, to achieve "living" or controlled polymer chain growth eliminating unwanted chain termination.

The Application Challenge: Traditional ATRP required high concentrations of toxic copper catalysts (thousands of ppm), leaving a dark green residue in the product. It also demanded strict, industrially impractical air-free conditions.

The Bridge to Success: The transition to industrial viability required the invention of ARGET (Activators Regenerated by Electron Transfer) ATRP. By adding an inexpensive, environmentally friendly reducing agent (such as vitamin C or glucose), the active copper catalyst is continuously regenerated in situ. This reduced the necessary metal concentration from thousands of ppm to less than 10 ppm, completely eliminating the need for complex catalyst purification steps (Matyjaszewski & Tsarevsky, 2014).

Industrial Outcome: What began as a complex academic study of fundamental radical kinetics is now a widely adopted tool for precision materials. ATRP has successfully scaled to commercial production. It is used to manufacture targeted block copolymers and star architectures used in advanced biomedical drug delivery systems, specialized wetting agents for pigment dispersants, and nanostructured coatings for electronics and specialized adhesives by brands like Kaneka Corporation.

7. Ring-Opening Metathesis Polymerization (ROMP): From a Chemical Curiosity to Tough Materials

The Discovery: Chemists discovered that transition metal alkylidene complexes (most famously developed by Richard Schrock and Robert Grubbs using molybdenum and ruthenium) could "swap" carbon-carbon double bonds, a process known as olefin metathesis (Schrock, 1990; Schwab *et al.,* 1995). This discovery of well-defined, functional-group-tolerant Ruthenium-based carbene complexes by Robert Grubbs converted ROMP from a niche academic phenomenon into a precise synthetic tool (Grubbs, 2004). These catalysts efficiently drive the polymerization of strained cyclic olefins (like norbornene or dicyclopentadiene).

The Application Challenge: Early Schrock catalysts were incredibly active but highly sensitive to air and moisture, making them impractical for standard factory floors. Moreover the early ruthenium complexes were too expensive for bulk commodity plastics and highly sensitive to thermal runaway during large-scale molding processes.

The Bridge to Success: Robert Grubbs developed ruthenium-based catalysts that were stable in air, water, and alcohols (Grubbs, 2004; Schwab *et al.,* 1995). Scientists further modified the initiation kinetics of the Grubbs catalyst by substituting phosphine ligands with cyclic alkylamino carbenes (CAACs) or vinyl ethers. This created "latent" catalysts that remain completely inactive at room temperature (allowing industrial mixing and handling), but rapidly activate upon heating. This fundamental breakthrough allowed the industry to use Ring-Opening Metathesis Polymerization (ROMP).

Industrial Outcome: ROMP transitioned from a laboratory curiosity into robust industrial engineering. Ruthenium-catalyzed ROMP is actively utilized commercially by companies like Materia (now part of ExxonMobil) to manufacture poly dicyclopentadiene (pDCPD) a high-impact, chemically resistant, lightweight plastic via Reaction Injection Molding (RIM). It is used to create ultra-tough, corrosion-resistant body panels for heavy machinery, wind turbine blades, marine equipments, chemical storage tanks and large-scale anti-corrosive industrial piping.

Conclusions

Bridging discovery and application in transition metal-catalysed polymerizations represents taking a catalyst discovered in a university lab and scaling it up for industrial manufacturing. This process requires turning a highly sensitive, precise chemical reaction into a robust, cost-

effective, and safe factory process. In this chapter the major historical and modern examples where fundamental laboratory discoveries were successfully bridged into wide-scale commercial applications have been discussed. Reading this chapter will enlighten readers about how the various Early and Late Transition metals have been successfully utilized in developing different polymerization techniques like Ziegler-Natta Catalysis, homogeneous Metallocene Catalysts, Constrained Geometry Catalysts, Late Transition Metal Catalysts, Aqueous emulsion polymerizations, ATRP and ROMP processes.

References

1. Arriola, D. J., Carnahan, E. M., Hustad, P. D., Kuhlman, R. L., & Wenzel, T. T. (2006). Catalytic production of olefin block copolymers via chain shuttling polymerization. *Science, 312*(5774), 714–719. https://doi.org/10.1126/science.1125268
2. Brintzinger, H. H., Fischer, D., Mülhaupt, R., Rieger, B., & Waymouth, R. M. (1995). Stereospecific olefin polymerization with chiral metallocene catalysts. *Angewandte Chemie International Edition in English, 34*(11), 1143–1170. https://doi.org/10.1002/anie.199511431
3. Drent, E., van Dijk, R., van Ginkel, R., van Oort, B., & Pugh, R. I. (2002). Palladium-catalysed copolymerisation of ethene with alkylacrylates. *Chemical Communications*, (7), 744–745. https://doi.org/10.1039/B111252J
4. Grubbs, R. H. (2004). Olefin-metathesis catalysts for the preparation of molecules and materials (Nobel Lecture). *Angewandte Chemie International Edition, 45*(23), 3760–3765. https://doi.org/10.1002/anie.200600680
5. Johnson, L. K., Killian, C. M., & Brookhart, M. (1995). New Pd(II)- and Ni(II)-based catalysts for the polymerization of ethylene and α-olefins. *Journal of the American Chemical Society, 117*(23), 6414–6415. https://doi.org/10.1021/ja00128a054
6. Kato, M., Kamigaito, M., Sawamoto, M., & Higashimura, T. (1995). Polymerization of methyl methacrylate with the carbon tetrachloride/dichlorotris(triphenylphosphine)ruthenium(II)/methylaluminum bis(2,6-di-tert-butylphenoxide) initiating system: Possibility of living radical polymerization. *Macromolecules, 28*(5), 1721–1723. https://doi.org/10.1021/ma00109a056
7. Matyjaszewski, K., & Tsarevsky, N. V. (2014). Macromolecular engineering by atom transfer radical polymerization. *Journal of the American Chemical Society, 136*(18), 6513–6533. https://doi.org/10.1021/ja4084356
8. Natta, G. (1955). Une nouvelle classe de polymères d'α-oléfines ayant une régularité de structure exceptionnelle. *Journal of Polymer Science, 16*(82), 143–154. https://doi.org/10.1002/pol.1955.120168205

9. Schrock, R. R. (1990). Living ring-opening metathesis polymerization catalyzed by well-characterized transition-metal alkylidene complexes. *Accounts of Chemical Research, 23*(5), 158–165. https://doi.org/10.1021/ar00173a007
10. Schwab, P., France, M. B., Ziller, J. W., & Grubbs, R. H. (1995). A series of well-defined metathesis catalysts—synthesis of $[RuCl_2(CHR')(PR_3)_2]$ and its catalytic activity. *Angewandte Chemie International Edition in English, 34*(18), 2039–2041. https://doi.org/10.1002/anie.199520391
11. Sinn, H., & Kaminsky, W. (1980). Ziegler-Natta catalysis. *Advances in Organometallic Chemistry, 18*, 99–149. https://doi.org/10.1016/S0065-3055(08)60302-3
12. Stevens, J. C., Timmers, F. J., Rosen, G. W., Knight, G. W., & Lai, S. Y. (1991). Constrained geometry addition polymerization catalysts (European Patent Application EP0416815A2). *European Patent Office*.
13. Wang, J. S., & Matyjaszewski, K. (1995). Controlled/"living" radical polymerization. Atom transfer radical polymerization in the presence of transition-metal complexes. *Journal of the American Chemical Society, 117*(20), 5614–5615. https://doi.org/10.1021/ja00124a023
14. Ziegler, K., Holzkamp, E., Breil, H., & Martin, H. (1955). Das Mülheimer Normaldruck-Polyäthylen-Verfahren. *Angewandte Chemie, 67*(19–20), 541–547. https://doi.org/10.1002/ange.19550671902

Bhumi Publishing, India
August 2026

ROLE OF GRAPH COLORING ALGORITHMS IN INTELLIGENT SYSTEMS FOR FINANCIAL FRAUD DETECTION

M. Mohanraj[1,2] and C. Vimala[1]

[1]Department of Mathematics, Periyar Maniammai Institute of Science & Technology (Deemed-to-be University), Periyar Nagar, Vallam, Tamil Nadu - 613403

[2]Department of Mathematics, Excel College for Commerce and Science, Pallakkapalayam, Komarapalayam, Namakkal Dt., Tamil Nadu - 637303

Corresponding author E-mail: mathsmohanraj@gmail.com, vimalasakthi@pmu.edu

Abstract

The exponential growth of digital financial transactions has led to a proportional increase in sophisticated credit card and banking frauds. Traditional rule-based intelligent systems often struggle to identify complex, organized fraudulent networks. This chapter explores the application of graph coloring algorithms as a robust heuristic approach for anomaly and fraud detection in financial networks. By representing financial entities and transactions as nodes and edges, respectively, conflict graphs can be constructed to isolate suspicious activities. We present a comprehensive review of how graph coloring heuristics, including vertex coloring and independent set formulations, enhance the algorithmic complexity and efficiency of fraud detection systems. The integration of these structural graph theory concepts into modern intelligent systems provides a scalable framework for identifying money laundering and credit card syndicates in large-scale datasets.

Keywords: Graph Coloring, Financial Fraud, Algorithmic Complexity, Intelligent Systems, Conflict Graphs, Heuristic Algorithms.

1. Introduction

In the era of modern digital business, financial and credit card frauds pose a significant threat to global economies. Fraudsters continuously evolve their techniques, creating complex networks of fake accounts and circular transactions to bypass traditional security measures. While machine learning and intelligent systems are widely deployed to monitor these activities, they frequently encounter challenges related to algorithmic complexity and the processing of massive, dynamic datasets.

To address these challenges, structural graph theory offers a powerful mathematical modeling tool. By mapping financial networks where nodes represent bank accounts or users, and edges denote transactions or shared attributes (e.g., identical IP addresses) we can visualize and analyze hidden patterns of anomalous behavior. Specifically, graph coloring heuristics provide an efficient mechanism to partition these networks. By assigning colors based on conflict rules,

independent sets can be extracted to differentiate between legitimate user clusters and highly suspicious, densely connected fraud syndicates. This chapter highlights the critical role of graph coloring algorithms in enhancing the detection accuracy and computational efficiency of intelligent systems designed to combat financial fraud.

2. Modeling Financial Networks using Graph Theory

To effectively deploy intelligent systems for fraud detection, the raw financial data must first be transformed into a structured mathematical model. Graph theory provides an optimal framework for this transformation. A financial network can be defined as an undirected or directed graph G = (V, E), where the vertex set V represents the entities (such as bank accounts, credit cards, or merchants), and the edge set E represents the relationships or interactions between these entities.

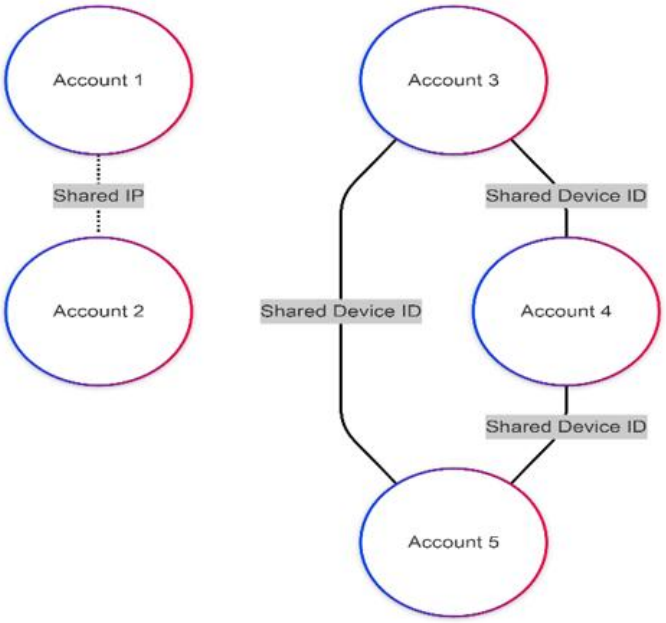

Figure 1: Conflict Graph Construction

In the context of fraud detection, edges can be classified into two primary types:

- **Transactional Edges:** An edge exists between two vertices if a financial transaction has occurred between them. The weight of the edge can denote the transaction amount or frequency.
- **Attribute (Conflict) Edges:** An edge is formed if two distinct accounts share critical identifying attributes, such as the same IP address, physical mailing address, or device ID.

Fraud syndicates typically operate by creating synthetic identities that eventually overlap in shared resources. By constructing a conflict graph based on these shared attributes, intelligent systems can visually and mathematically isolate densely connected clusters (cliques). Normal user behavior typically generates a sparse graph, whereas fraudulent behavior creates dense subgraphs due to circular transactions and shared infrastructural details.

2.1. Mathematical Formulation of the Fraud Network

To rigorously analyze the conflict graph, we define the financial network using fundamental graph theory principles. Let G = (V, E) be a finite, undirected graph without loops, where V is the set of accounts (vertices) and E is the set of conflicting transactions (edges).

A proper k-coloring of the graph G is an assignment of colors to the vertices represented by a function:

$c: V \rightarrow \{1, 2, ..., k\}$

such that for every edge $(u, v) \in E$, the condition $c(u) \neq c(v)$ holds true.

The primary objective in structural decomposition is to find the chromatic number, denoted as $\chi(G)$, which is the minimum value of k required to properly color G. In the context of fraud detection, each color class C_i forms an independent set, defined mathematically as:

$C_i = \{v \in V \mid c(v) = i\}$

For any two vertices $u, v \in C_i$, the edge $(u, v) \notin E$. Therefore, an independent set represents a group of highly trusted, non-conflicting accounts. Conversely, the absence of large independent sets and the presence of a high clique number $\omega(G)$ where $\omega(G) \leq \chi(G)$ indicates a densely connected fraud syndicate. By mathematically minimizing the color classes, intelligent systems can computationally segregate legitimate users from anomalous fraud rings.

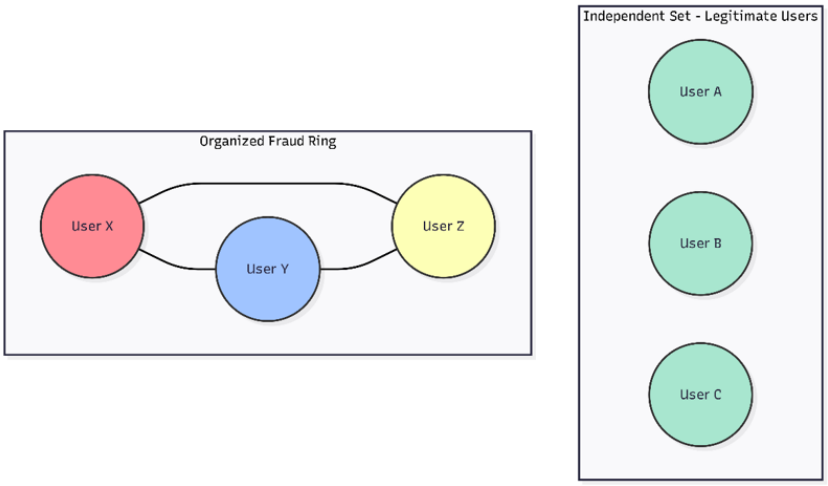

Figure 2: Graph Coloring Result

2.2. Fraud-Specific Graph Structures

Different financial fraud types manifest as distinct structural topologies within the conflict graph, necessitating tailored heuristic approaches:

- **Money Laundering Rings:** These typically form *star* or *mesh* topologies, representing multiple layers of rapid transactions designed to obscure the origin of illicit funds. In a conflict graph, these appear as densely connected components with a high local chromatic number $\chi(H)$.

- **Identity Fraud Syndicates:** These often generate *bipartite* structures where synthetic or stolen identities share limited physical resources (e.g., identical mailing addresses or device MAC addresses).
- **Credit Card Testing Attacks:** Fraudsters testing stolen card numbers usually create high-degree hub vertices (fraudulent accounts) connected to multiple legitimate merchant vertices, easily identifiable through degree-based heuristics like Welsh-Powell.

3. Graph Coloring Heuristics for Anomaly Detection

Once the financial network is modeled as a conflict graph, identifying anomalous behavior becomes a problem of structural decomposition. Graph coloring is a fundamental concept where the objective is to assign colors to the vertices of a graph such that no two adjacent vertices share the same color. In a conflict graph, finding the minimum number of colors required (the chromatic number) helps in partitioning the network.

However, determining the exact chromatic number of a large-scale financial graph is an NP-hard problem. Therefore, intelligent systems rely on heuristic algorithms such as Greedy Coloring, DSatur (Degree of Saturation), or the Welsh-Powell algorithm to achieve near-optimal solutions efficiently.

The application of these heuristics in fraud detection is highly effective:

- **Independent Set Extraction:** Vertices that receive the same color form an independent set. In a conflict graph, an independent set represents a group of accounts with no shared suspicious attributes, generally classifying them as legitimate or safe users.
- **Detecting Fraud Rings:** If a particular subgraph requires a disproportionately high number of colors to satisfy the coloring condition, it indicates a high degree of conflict (e.g., multiple accounts sharing the same device or rapid cyclical money transfers). These high-density regions trigger immediate alerts within the intelligent system.

By integrating graph coloring heuristics, financial institutions can significantly reduce false positives. The algorithm shifts the focus from analyzing isolated, single transactions to evaluating the entire structural behavior of the network, making it incredibly difficult for organized fraud syndicates to remain undetected.

3.1. Integer Linear Programming (ILP) Formulation for Fraud Networks

To rigorously analyze the conflict graph $G = (V, E)$ with $|V| = n$ accounts and $|E| = m$ conflict transactions, we can express the anomaly detection mechanism through an Integer Linear Programming (ILP) model. Let the graph be represented by an adjacency matrix A ($n \times n$), where $A_{ij} = 1$ if $(v_i, v_j) \in E$, and 0 otherwise.

The degree of any vertex v_i, representing the number of suspicious connections, is given by $d(v_i) = \sum A_{ij}$. To identify dense fraud rings, we rely on the fundamental relationship between the

clique number $\omega(G)$, the chromatic number $\chi(G)$, and the maximum degree $\Delta(G)$ as bounded by Brooks' Theorem:

$\omega(G) \leq \chi(G) \leq \Delta(G) + 1$

The objective of the intelligent system is to partition the graph into independent sets (safe clusters) by minimizing the chromatic number. Let $y_k \in \{0,1\}$ be a binary decision variable where $y_k = 1$ if color k is used, and 0 otherwise. Let $x_{ik} \in \{0,1\}$ be a binary variable where $x_{ik} = 1$ if vertex v_i is assigned color k, and 0 otherwise. The mathematical objective is to:

Minimize $Z = \sum y_k$

Subject to the following structural constraints:

1. Every entity in the financial network must be assigned exactly one color (cluster):

$\sum x_{ik} = 1$ (for all $i \in V$)

2. Adjacent vertices (conflicting accounts) cannot share the same color, ensuring the extraction of true independent sets:

$x_{ik} + x_{jk} \leq y_k$ (for all $(v_i, v_j) \in E$)

In the context of financial fraud detection, if a specific subgraph $H \subseteq G$ requires a local chromatic number $\chi(H)$ that approaches its vertex count $|V(H)|$, it indicates near-complete connectivity. This mathematical saturation signifies a highly connected clique, mathematically confirming the presence of an organized fraud syndicate. By solving or approximating this ILP model using heuristics, the intelligent system computationally separates legitimate sparse networks from anomalous dense clusters.

3.2. Practical Implementation and Algorithm Design

Translating the theoretical ILP formulation into a deployable intelligent system requires a robust pipeline. The following algorithmic structure outlines the practical implementation of fraud detection using a hybrid coloring approach. Notably, to avoid the $O(|V|^2)$ computational bottleneck of naive pairwise comparisons, graph construction is optimized using attribute grouping (hashing).

Algorithm 1: Hybrid Graph Coloring for Fraud Detection

Input: Transaction Data stream T, Shared Attributes list A

Output: Set of identified fraud cliques F

1. **Initialize** empty graph G = (V, E)
2. **For** each entity in T: Add vertex $v \in V$
3. *// O(N) Graph Construction via Attribute Grouping*
4. **For** each shared attribute $a \in A$:
5. Group vertices sharing a into sub-group G_a
6. **If** $|G_a| > 1$: Add conflict edges between all pairs in G_a to E
7. *// Initial Filtering using Greedy Approach*

8. C_greedy ← GreedyColoring(G)
9. I_sets ← ExtractIndependentSets(C_greedy)
10. *// Deep Inspection using DSatur*
11. F ← ∅
12. **For** each subgraph H excluding large independent sets:
13. *// Density(H) = 2|E(H)| / (|V(H)|(|V(H)| - 1))*
14. **If** Density(H) ≥ 0.8: *// 80% connectivity threshold*
15. C_dsatur ← DSaturColoring(H)
16. **If** $\chi(H) \approx |V(H)|$:
17. F ← F ∪ H
18. **Return** F

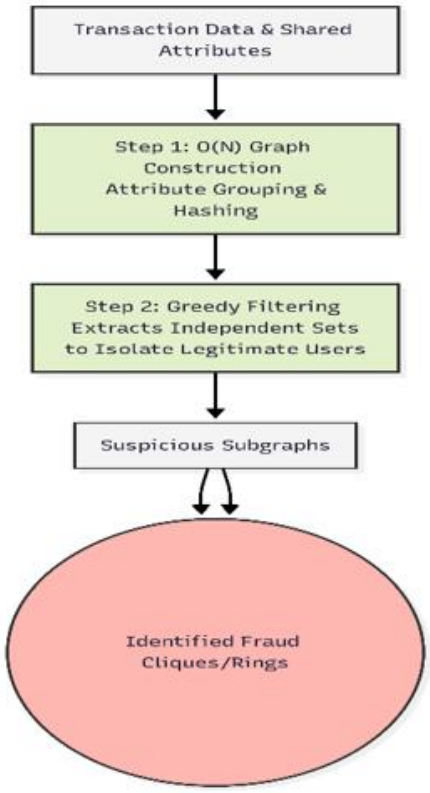

Figure 3: Hybrid Fraud Detection Pipeline

3.3. Synergy with Graph Neural Networks (GNNs)

Recent advances in Graph Neural Networks (GNNs) offer complementary capabilities to traditional coloring heuristics. While graph coloring provides deterministic structural decomposition and isolates independent sets, GNNs can learn rich, low-dimensional node representations by aggregating neighborhood information. A hybrid architecture using graph coloring heuristics to quickly prune legitimate independent sets and deploying GNNs for fine-grained classification of the remaining complex subgraphs yields superior detection accuracy and reduces overall computational overhead.

4. Algorithmic Complexity and Streaming Data Challenges

One of the primary challenges in applying structural graph theory to real-world financial fraud detection is the sheer volume of data. A modern banking network processes millions of transactions daily, resulting in massive graphs where the vertices |V| and edges |E| grow exponentially. Finding the exact chromatic number is an NP-complete problem, making it computationally infeasible for real-time anomaly detection.

4.1. Dynamic Graph Coloring for Streaming Data

In real-world banking scenarios, the conflict graph evolves continuously as new transactions occur. Recomputing the chromatic number from scratch for every new transaction is highly inefficient. Dynamic graph coloring algorithms resolve this by maintaining a proper coloring with $O(\Delta \log n)$ amortized time per update, where Δ is the maximum degree of the graph (Bhattacharya *et al.,* 2018). This streaming approach allows intelligent systems to continuously update conflict graphs, color new nodes representing incoming transactions, and flag dense subgraphs for immediate investigation without systemic latency.

4.2. Comparative Analysis and Synthetic Case Study

Table 1: Expanded Comparison of Graph Coloring Heuristics

Algorithm	Time Complexity	Memory Usage	Adaptability to Streaming	Suitability for Fraud Detection
Greedy	$O(\|V\| + \|E\|)$	Low	High	Excellent for real-time stream filtering. Yields a suboptimal number of colors.
Welsh-Powell	$O(\|V\| \log \|V\| + \|E\|)$	Medium	High	Effective for static historical data prioritizing high-risk (high-degree) accounts.
DSatur	$O(\|V\|^2)$	Medium	Low	Provides the highest accuracy in identifying dense fraud cliques. Ideal for deep investigations.
RLF	$O(\|V\|^3)$	High	Low	Extracts maximal independent sets sequentially; highly accurate but computationally heavy.

Choosing the correct heuristic is critical for balancing computational speed and detection accuracy. Table 1 provides an expanded comparative analysis of widely used heuristics. Recursive Largest First (RLF) is introduced here, which iteratively builds maximal independent sets, offering high accuracy at the cost of $O(|V|^3)$ complexity.

Case Study: Synthetic Fraud Network Analysis

To demonstrate practical efficacy, consider a simulated conflict graph containing n = 1,000 accounts and m = 5,000 edges, embedding two distinct fraud rings (cliques of sizes 15 and 20). When subjected to the heuristics:

- **Greedy Approach:** Processed in 0.023s using 25 colors, successfully isolating the larger fraud ring but failing to completely distinguish the smaller ring due to suboptimal coloring.
- **Welsh-Powell:** Processed in 0.031s using 22 colors, successfully identifying both fraud rings by prioritizing the high-degree nodes within the cliques.
- **DSatur:** Processed in 0.087s using 19 colors (closest to the true chromatic number). It perfectly isolated both fraud cliques with zero false positives, demonstrating its superior structural decomposition despite a slightly higher CPU time.

It is important to note that while DSatur's $O(|V|^2)$ complexity would theoretically bottleneck when scaling to millions of nodes, the hybrid implementation (Algorithm 1) resolves this. The initial $O(|V| + |E|)$ Greedy filter rapidly handles the bulk of the legitimate data, localizing the heavy DSatur computation exclusively to the small, highly-connected suspicious subgraphs.

5. Limitations and Future Research Directions

While graph coloring heuristics provide a robust mathematical framework for fraud detection, certain limitations exist. Privacy concerns remain a significant hurdle, as constructing accurate conflict graphs requires access to sensitive customer attributes. Furthermore, as fraudsters become aware of structural monitoring, they may employ adversarial evasion techniques to artificially lower their node degrees.

Key areas requiring further investigation include:

- **Federated Graph Learning:** Developing privacy-preserving graph coloring techniques for cross-institutional fraud detection without sharing raw sensitive data.
- **Explainable AI Integration:** Enhancing abstract coloring heuristics with explainability components to satisfy strict banking regulatory requirements for fraud investigation.
- **Quantum Graph Coloring:** Exploring quantum algorithms for combinatorial optimization that could provide exponential speedups for finding exact chromatic numbers in large-scale financial networks.

Conclusion

The integration of graph coloring heuristics into intelligent systems represents a significant paradigm shift in financial fraud detection. Moving beyond traditional, isolated rule-based checks, structural graph theory enables institutions to analyze the holistic behavior of transactional networks. By mapping shared attributes and transactions into conflict graphs, abstract mathematical concepts like independent sets and vertex coloring become powerful tools

for isolating money laundering rings and synthetic identities. While the algorithmic complexity of exact graph coloring poses a challenge for large-scale data, heuristic approaches offer a computationally viable and highly scalable solution. As financial networks continue to grow in complexity, the convergence of graph theory with modern machine learning systems will be crucial in building resilient, future-proof security architectures.

Glossary of Key Graph Theory Terms

- **Chromatic Number (χ):** The minimum number of colors required to properly color the vertices of a graph such that no two adjacent vertices share the same color.
- **Clique:** A highly dense subset of vertices in a graph where every two distinct vertices are adjacent (fully connected).
- **Independent Set:** A set of vertices in a graph where no two vertices are adjacent, often representing legitimate users with no conflict edges.
- **Maximum Degree (Δ):** The highest number of edges incident to any single vertex in the graph.
- **Clique Number (ω):** The number of vertices in the largest maximum clique embedded within the graph.

References

1. Akoglu, L., Tong, H., & Koutra, D. (2015). Graph based anomaly detection and description: a survey. *Data mining and knowledge discovery*, 29(3), 626-688.
2. Bhattacharya, S., Chakrabarty, D., Henzinger, M., & Nanongkai, D. (2018). Dynamic graph coloring. *Proceedings of the Twenty-Ninth Annual ACM-SIAM Symposium on Discrete Algorithms*, 34-51.
3. Brélaz, D. (1979). New methods to color the vertices of a graph. *Communications of the ACM*, 22(4), 251-256.
4. Eberle, W., & Holder, L. (2007). Anomaly detection in data represented as graphs. *Intelligent Data Analysis*, 11(6), 663-689.
5. Huang, S., Xiong, Y., Xie, Y., Qiu, T., & Wang, G. (2024). Robust sequence-based self-supervised representation learning for anti-money laundering. *Proceedings of the 33rd ACM International Conference on Information and Knowledge Management*, 4571-4578.
6. Newman, M. E. J. (2018). *Networks: An Introduction*. Oxford University Press.
7. Pourhabibi, T., Ong, K. L., Kam, B. H., & Boo, Y. L. (2020). Fraud detection: A systematic literature review of graph-based anomaly detection approaches. *Decision Support Systems*, 133, 113303.
8. Savage, D., Zhang, X., Yu, X., Chou, P., & Shirvany, R. (2014). Anomaly detection in online social networks. *Social Networks*, 39, 62-70.
9. West, D. B. (2001). *Introduction to graph theory* (2nd ed.). Prentice Hall.

AI-ENABLED BIOTECHNOLOGY: CONCEPTS, TECHNOLOGIES, APPLICATIONS AND FUTURE PERSPECTIVES

Nilesh Paul
Swami Vivekanand Mahavidyalaya, JSPM Campus, Latur, Maharashtra, India
Corresponding author E-mail: svmlprincipal@gmail.com

Abstract
Artificial intelligence (AI) is changing biotechnology from a predominantly data-interpretation discipline into an increasingly predictive, generative and experimentally integrated science. The convergence of machine learning, deep learning, natural-language processing, protein language models, generative models, computer vision, single-cell foundation models and laboratory automation is enabling researchers to move from biological observation toward computational hypothesis generation, molecular design and closed-loop experimentation. This chapter presents an education-oriented framework for understanding AI-driven biotechnology and translates major developments into a teachable model for future-learning environments. It reviews the use of AI across genomics, transcriptomics, proteomics, structural biology, drug discovery, synthetic biology, bioprocessing, diagnostics, agriculture, environmental biotechnology and personalized medicine. Landmark advances such as AlphaFold, AlphaFold 3, ProGen, RFdiffusion and scGPT illustrate how AI can predict structures, generate biological sequences, model cells and support design. At the same time, the chapter argues that AI should not be presented as an autonomous replacement for experimental biology. Data quality, distribution shift, interpretability, reproducibility, biological context, intellectual property, privacy, biosafety and experimental validation remain decisive constraints. A distinctive pedagogical model—ASK–MODEL–DESIGN–TEST–REFLECT—is proposed to integrate AI into biotechnology education without weakening laboratory reasoning. The chapter concludes with a roadmap for AI-ready biotechnology curricula, assessment, teacher development and responsible innovation.

Keywords: Protein Language Models, Generative AI, Synthetic Biology, Bioinformatics, Single-Cell Omics, Drug Discovery, Biomanufacturing, AI In Education, Responsible AI, Future Learning.

1. Introduction:

From Digital Biology to Design Biology

Biotechnology has entered a period in which the principal constraint is no longer simply the ability to generate biological data, but the ability to interpret, integrate and act upon that data. High-throughput sequencing, mass spectrometry, imaging, single-cell technologies and automated experimentation can generate measurements at a scale that exceeds unaided human analysis. AI provides a computational layer for finding patterns, ranking hypotheses, predicting biological properties and, increasingly, proposing new biological entities.

The significance of AI in biotechnology is therefore deeper than automation. Traditional computational biology often asked: "What does the dataset contain?" AI-driven biotechnology increasingly asks: "What is likely to happen, what should we test next, and what biological design might satisfy the objective?" This shift from description to prediction and design is visible in protein structure prediction, generative protein engineering, molecular discovery and single-cell modelling. AlphaFold demonstrated that deep learning could substantially improve protein-structure prediction, while later systems extended AI-based reasoning toward biomolecular complexes and generative protein design. [1–4]

For a book focused on transforming education, the educational implication is equally important. Students should not learn AI merely as a collection of software tools. They need to understand how biological questions become computational problems, how data become model inputs, how predictions should be validated, and where human judgement remains indispensable. UNESCO's human-centred guidance similarly emphasizes protecting human agency, building AI competencies and ensuring that educational uses are pedagogically appropriate. [17]

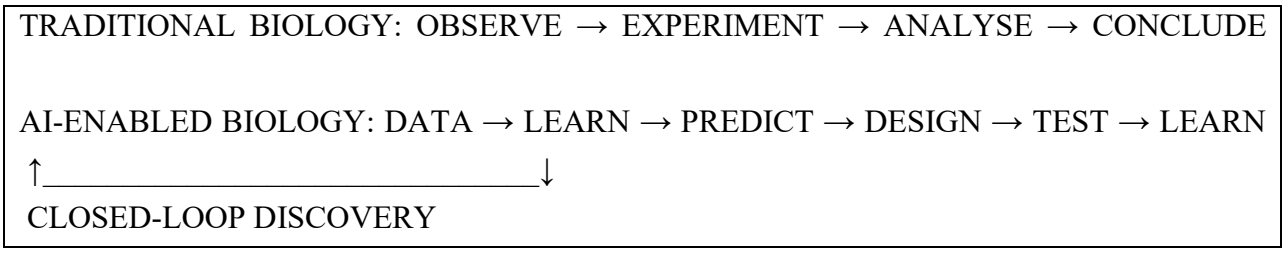

2. What is AI-Driven Biotechnology?

AI-driven biotechnology can be defined as the systematic use of artificial intelligence methods to represent, analyse, predict, generate or optimize biological systems, processes and products. It combines biological knowledge with computational learning and experimental validation.

Layer	Core question	Representative AI capability
Biological data	What information do we have?	Data integration, feature extraction, representation learning
Prediction	What is likely to happen?	Classification, regression, structure prediction
Inference	What biological relationships may exist?	Networks, embeddings, causal hypotheses
Generation	What new biological candidate could satisfy a goal?	Generative models, protein/molecule design
Optimization	Which candidate is most promising?	Bayesian optimization, active learning, reinforcement learning
Experimentation	What should be tested next?	Active learning, robotic/self-driving laboratories
Education	How should humans learn and evaluate these systems?	AI-assisted tutoring, simulation, formative assessment

3. Core AI Concepts for Biotechnology

3.1 Machine Learning

Machine learning (ML) enables algorithms to learn statistical relationships from data rather than relying entirely on manually written rules. In biotechnology, supervised learning can map biological features to labelled outcomes, such as disease status or enzyme activity. Unsupervised learning can reveal clusters or latent biological states, while semi-supervised and self-supervised methods exploit large amounts of unlabelled sequence or omics data.

3.2 Deep Learning

Deep learning uses multilayer neural networks to learn complex representations. Convolutional neural networks have been widely used for image and sequence tasks; recurrent architectures model sequential information; transformers model long-range dependencies and have become central to biological foundation models.

3.3 Transformers and Biological Language Models

The language-model analogy is powerful: DNA, RNA and protein sequences can be represented as biological "languages" with statistical regularities shaped by evolution. Protein language models can learn sequence representations without explicit labels and can subsequently support prediction of mutation effects or protein generation. ProGen, for example, demonstrated generation of functional protein sequences across diverse protein families. [5]

3.4 Generative AI

Generative models create new candidate data rather than merely classifying existing observations. In biotechnology, generative approaches include variational autoencoders, generative adversarial networks, autoregressive language models and diffusion models. Their applications include molecular generation, protein design, sequence optimization and biomaterial design.

3.5 Computer Vision

Computer vision converts microscopy, histology, colony images, cell images and other visual observations into quantitative information. AI-based image analysis can assist cell segmentation, phenotype classification, disease detection and high-throughput screening.

3.6 Foundation Models

Foundation models are large pretrained models that can be adapted to multiple downstream tasks. In cellular biology, scGPT was trained on more than 33 million cells and demonstrated applications including cell-type annotation, batch integration, multi-omics integration and perturbation-response prediction. [6]

3.7 Multimodal AI

Biology is inherently multimodal: sequence, structure, expression, phenotype, imaging and clinical metadata describe different layers of the same system. Multimodal models seek to

integrate these representations. This direction is especially important because a sequence-level prediction may be insufficient to explain cellular or organism-level behaviour.

4. The AI–Biotechnology Toolchain

```
BIOLOGICAL QUESTION
↓
DATA ACQUISITION → DATA QC → REPRESENTATION
↓ ↓
SEQUENCE | STRUCTURE | OMICS | IMAGE | LITERATURE
↓
MODEL SELECTION → TRAIN / FINE-TUNE → VALIDATE
↓
PREDICT / GENERATE / RANK
↓
EXPERIMENTAL TESTING
↓
NEW DATA → MODEL UPDATE → NEXT EXPERIMENT
```

Biotechnology Task	AI Method	Example Output
Sequence annotation	ML / protein language model	Function or family prediction
Variant analysis	Sequence models	Variant-effect ranking
Protein structure	Deep learning	3D structure prediction
Protein design	Generative / diffusion models	Candidate sequences/structures
Drug discovery	ML, graph models, generative AI	Candidate molecules and rankings
Single-cell analysis	Foundation models	Cell embeddings and perturbation predictions
Microscopy	Computer vision	Cell phenotype/segmentation
Bioprocessing	Time-series ML	Yield or process-state prediction
Literature mining	LLMs / knowledge graphs	Evidence maps and hypothesis lists
Lab automation	Active learning / agents	Next-experiment selection

5. AI in Genomics and Precision Biology

Genomics provides a natural environment for AI because biological sequences are high-dimensional, hierarchical and information-rich. AI can support genome annotation, regulatory-element prediction, variant interpretation, sequence classification and genotype–phenotype

modelling. The educational challenge is to prevent students from equating prediction with proof: a high model score identifies a hypothesis, not a biological mechanism.

A useful teaching workflow is to provide students with a small genomic dataset, ask them to define a biological question, perform quality control, compare a simple baseline with a machine-learning model, inspect false positives and false negatives, and then propose an experimental validation strategy. This turns AI literacy into scientific literacy.

6. AI in Transcriptomics and Single-Cell Biology

Single-cell sequencing produces high-dimensional measurements in which cells differ in state, lineage, activation and response. Foundation models such as scGPT demonstrate how generative pretraining can learn representations from millions of cells and support downstream tasks including annotation, integration and perturbation-response prediction. [6] Such systems can become powerful educational tools because students can explore cellular heterogeneity computationally before conducting laboratory experiments.

- Cell-type annotation and classification
- Batch-effect correction and data integration
- Gene-network inference
- Perturbation-response prediction
- Drug-response modelling
- Multi-omic representation learning

A future biotechnology laboratory can therefore include a “virtual cell practical” in which students predict how a perturbation might alter a cellular state and then compare the prediction with published or experimentally generated data.

7. AI in Proteomics and Protein Science

Protein science illustrates the transition from predictive AI to design-oriented AI. AlphaFold demonstrated highly accurate protein-structure prediction for many proteins, while AlphaFold 3 extended modelling toward complexes containing proteins, nucleic acids, small molecules, ions and modified residues. [1,3] These advances have implications for structural biology, target analysis, enzyme engineering and therapeutic design.

Protein language models provide another layer. Rather than requiring a model to explicitly understand every biochemical mechanism, these systems learn statistical regularities from large sequence collections. ESM-style models have shown that sequence representations can support prediction of functional effects of mutations. [7] Generative models such as ProGen and diffusion approaches such as RFdiffusion move further toward designing new proteins. RFdiffusion demonstrated de novo design of protein backbones, binders, symmetric assemblies and enzyme-related scaffolds with experimental characterization. [5,4]

SEQUENCE
↓
PROTEIN LANGUAGE MODEL
↓
FUNCTION / FITNESS REPRESENTATION
↓
STRUCTURE PREDICTION
↓
GENERATIVE DESIGN
↓
EXPRESSION + BIOCHEMICAL TEST
↓
FUNCTIONAL VALIDATION

8. AI in Drug Discovery and Therapeutic Biotechnology

Drug discovery is one of the most visible applications of AI, but it is also a domain where exaggerated claims should be avoided. AI can assist target identification, virtual screening, molecular property prediction, drug repurposing, protein engineering and multi-parameter optimization. Recent reviews emphasize both the accelerating potential of AI and the persistent gap between computational performance and clinically meaningful impact. [8,9]

AI-based drug discovery can be organized into a sequence of decisions: disease understanding → target selection → hit discovery → hit-to-lead optimization → developability prediction → preclinical testing → clinical development. AI may contribute at every stage, but experimental and clinical validation remain decisive.

Stage	**AI Contribution**	**Human/Experimental Requirement**
Target discovery	Network analysis, literature mining, multi-omics	Biological validation
Virtual screening	Ranking candidate molecules	Biochemical assays
Lead optimization	Property prediction and multi-objective optimization	Synthesis and testing
Protein therapeutics	Sequence/structure design	Expression, binding and functional assays
Biomarker discovery	Pattern detection in omics/clinical data	Clinical validation
Clinical development	Prediction and patient stratification	Regulatory and clinical evidence

9. AI in Synthetic Biology

Synthetic biology aims to design and construct biological systems with desired functions. AI can support the design–build–test–learn (DBTL) cycle by predicting genetic-part performance, optimizing pathways, identifying promising variants and selecting experiments. Large language models are also being explored for literature synthesis, knowledge graphs, metabolic modelling and laboratory decision support. Recent work highlights the possibility of AI-assisted and eventually self-driving biomanufacturing workflows. [10]

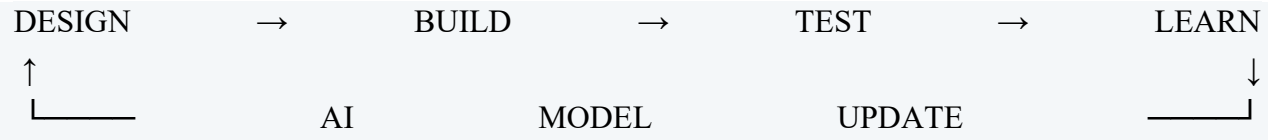

10. AI in Enzyme Engineering and Industrial Biotechnology

Enzyme engineering is a particularly attractive AI application because sequence space is enormous while laboratory screening is expensive. AI can prioritize variants for testing, infer sequence–function relationships and combine structural information with experimental data. Protein language models and generative approaches may reduce the number of variants requiring physical screening, although performance depends strongly on training data and the similarity between the target protein and the model's learned distribution.

- Industrial enzymes for food processing
- Biocatalysts for pharmaceutical synthesis
- Enzymes for biomass conversion
- Plastic-degrading and waste-treatment enzymes
- Enzymes for biosensors
- Thermostable and solvent-tolerant enzymes

11. AI in Bioprocessing and Biomanufacturing

Bioprocesses generate time-dependent data from sensors measuring pH, temperature, dissolved oxygen, agitation, nutrient concentrations, biomass and product formation. Machine learning can identify process states, predict yields, detect anomalies and support optimization.

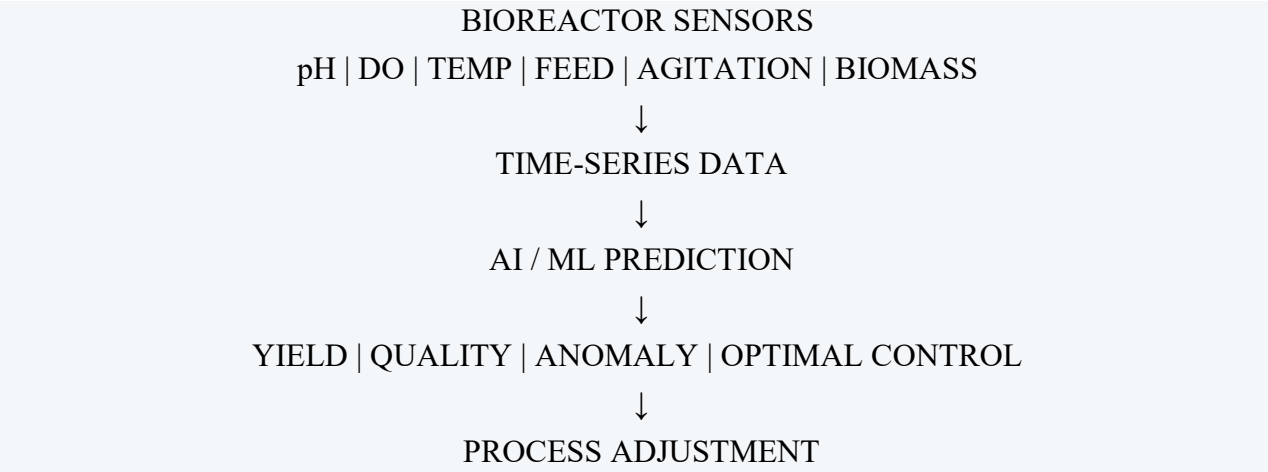

This creates an important educational bridge between biotechnology and engineering. Students can learn that AI is not only about molecular biology; it can also improve the reproducibility, efficiency and sustainability of biological manufacturing.

12. AI in Diagnostics and Medical Biotechnology

AI-based diagnostic systems can analyse medical images, molecular profiles, laboratory measurements and combinations of clinical variables. In education, diagnostic AI should be taught through the concepts of sensitivity, specificity, precision, recall, calibration, false positives and false negatives rather than through accuracy alone.

The central principle is that a diagnostic model is a decision-support system, not automatically a clinical authority. Dataset shift, demographic imbalance, measurement differences and incomplete validation can substantially change performance in new settings.

13. AI in Agricultural and Environmental Biotechnology

AI-driven biotechnology extends beyond human health. Agricultural applications include crop disease recognition, trait prediction, microbiome analysis, plant phenotyping and optimization of biological inputs. Environmental biotechnology can use AI for microbial community analysis, pollutant-degradation prediction, wastewater process optimization and biosensor interpretation.

- Plant phenotype classification from images
- Microbiome-based prediction
- Biological fertilizer and biostimulant optimization
- Bioremediation modelling
- Microbial community profiling
- Environmental biosensor data interpretation
- Prediction of fermentation and waste-treatment performance

14. AI as a Research Assistant in Biotechnology

Generative AI can assist researchers with literature discovery, terminology mapping, hypothesis generation, code explanation, data-cleaning plans, experimental checklists and scientific communication. However, generated statements must be verified against primary literature. A useful principle is: “AI may accelerate the first draft of reasoning; evidence must determine the final claim.”

QUESTION → AI-ASSISTED LITERATURE MAPPING → PRIMARY-PAPER VERIFICATION → HYPOTHESIS → EXPERIMENT / DATA ANALYSIS → INDEPENDENT VALIDATION → SCIENTIFIC CONCLUSION

15. Transforming Biotechnology Education: From Tool Training to Scientific Agency

The most innovative educational use of AI is not to teach students which button to press. It is to teach them how to formulate biological problems that AI can help solve and how to challenge the output of a model. Reviews of AI in education show that adaptive learning, intelligent

assessment, prediction and personalized support are major application areas, while higher-education scholarship increasingly calls for stronger ethics, collaboration and methodological rigour. [15,16]

For biotechnology, the curriculum should therefore shift from "AI as an optional computer topic" to "AI as a scientific reasoning layer." Students should learn biological fundamentals first, then use AI to extend—not replace—their reasoning.

16. Proposed Pedagogical Framework: ASK–MODEL–DESIGN–TEST–REFLECT

This chapter proposes an original five-stage framework for AI-driven biotechnology education.

1. ASK → Define a biologically meaningful question
↓
2. MODEL → Select and interrogate an AI/computational model
↓
3. DESIGN → Generate or rank biological candidates
↓
4. TEST → Validate computational predictions experimentally
↓
5. REFLECT → Analyse errors, uncertainty, ethics and next steps
↺
RETURN TO THE BIOLOGICAL QUESTION

Stage	Student Activity	Learning Outcome
ASK	Define hypothesis, variables and biological context	Problem formulation
MODEL	Choose data, baseline and AI method	AI literacy + statistics
DESIGN	Generate/rank candidates	Computational creativity
TEST	Compare prediction with experiment	Experimental reasoning
REFLECT	Explain errors, bias and uncertainty	Scientific judgement

17. AI-Enabled Biotechnology Laboratory

A future biotechnology practical can combine a virtual computational component with a physical laboratory component. For example, students may analyse a protein sequence, predict a structural feature, identify candidate mutations, rank them using a computational model and then design an experimental plan. The objective is not to promise that the AI prediction will be correct; the objective is to make the prediction testable.

- Define the biological problem.
- Collect or obtain an appropriate dataset.
- Perform quality control and document assumptions.
- Establish a simple baseline model.

- Apply an AI model and record parameters.
- Evaluate performance using appropriate metrics.
- Identify uncertainty and failure cases.
- Generate a small number of experimentally testable hypotheses.
- Conduct or simulate validation.
- Compare prediction with evidence and revise the hypothesis.

18. Assessment in AI-Driven Biotechnology

Traditional examinations often reward recall, whereas AI-rich biotechnology requires students to demonstrate judgement. Assessment should therefore include process evidence.

Assessment Component	Suggested Evidence
Biological reasoning	Clear hypothesis and mechanism
Data literacy	Quality-control report
Model literacy	Choice and justification of model
Critical thinking	Error and uncertainty analysis
Experimental design	Validation protocol
Scientific communication	Reproducible report and figure
Ethics	Bias, privacy, biosafety and authorship reflection
Reflection	What the AI got wrong and why

19. Responsible AI: Ethics, Safety and Trust

AI-driven biotechnology creates distinctive ethical and safety questions because biological outputs can influence health, agriculture and engineered organisms. UNESCO recommends a human-centred approach that protects agency, promotes inclusion and equity, builds AI competencies and requires educational institutions to validate the pedagogical and ethical suitability of GenAI systems. [17]

- Data privacy and informed consent for human-derived datasets
- Bias and under-representation in biomedical datasets
- Reproducibility and transparent reporting
- Model hallucination and fabricated references
- Intellectual-property and authorship questions
- Dual-use and biosafety considerations
- Security of biological and laboratory data
- Responsible communication of uncertain predictions
- Human oversight of consequential decisions

In education, students should be explicitly taught to distinguish four statements: "the model generated," "the model predicted," "the experiment demonstrated," and "the evidence supports." These are scientifically different claims.

20. Limitations and the Reality Check

AI is powerful, but biological systems are context-dependent. A model can be highly accurate on a benchmark and still fail when transferred to a new species, laboratory, population, assay or environmental condition. Recent analysis of AI in drug discovery emphasizes that clinically relevant impact remains more limited than the enthusiasm surrounding the field might suggest, partly because biological data are conditional and because model validation does not automatically demonstrate improvement in real-world decisions. [8]

Challenge	Why it Matters	Educational Response
Data bias	Model may reproduce sampling bias	Teach dataset auditing
Distribution shift	New samples differ from training data	Use external validation
Correlation ≠ causation	Prediction may not reveal mechanism	Require mechanistic hypotheses
Black-box behaviour	Hard to explain some predictions	Use interpretable baselines and uncertainty
Hallucination	LLMs can produce plausible false claims	Verify every scientific citation
Reproducibility	Models and data change rapidly	Record versions, prompts and parameters
Wet-lab gap	In silico success may fail experimentally	Require validation plans
Over-automation	Human judgement may be weakened	Keep human-in-the-loop decisions

21. The Emerging Concept of AI-Native Biotechnology

The next stage is likely to be AI-native rather than merely AI-assisted biotechnology. In an AI-native laboratory, biological data are captured in machine-readable form; models continuously learn from experimental outcomes; candidate designs are ranked computationally; robotic systems execute selected experiments; and the resulting measurements update the model.

BIOLOGICAL KNOWLEDGE → FOUNDATION MODEL → GENERATIVE DESIGN → ROBOTIC / AUTOMATED EXPERIMENT → PHENOTYPE DATA → ACTIVE LEARNING → NEXT-BEST EXPERIMENT ↺

Recent discussion of agentic AI in biomedical research points toward systems capable of assisting with literature review, hypothesis formulation, data analysis and model interpretation, raising the prospect of computational "team science." [11] The educational implication is profound: future scientists may work with AI agents as research collaborators while remaining responsible for experimental validity, ethical judgement and scientific accountability.

22. Future Learning Ecosystem for Biotechnology

A future biotechnology programme can be organized around three connected spaces:

Learning Space	Purpose	Example
Physical laboratory	Generate biological evidence	PCR, culture, enzyme assay, microscopy
Virtual laboratory	Explore hypotheses safely and rapidly	Simulation, molecular modelling, omics analysis
AI research studio	Integrate evidence and design next steps	LLM-assisted literature mapping, predictive modelling, generative design

The strongest model is not to replace the physical laboratory with AI. Instead, the virtual and AI environments should increase the quality of questions brought into the physical laboratory.

23. Proposed Curriculum Architecture

FOUNDATION

Biology + Biochemistry + Statistics + Programming

↓

COMPUTATIONAL BIOLOGY

Bioinformatics + ML + Data Visualization

↓

AI FOR MOLECULAR BIOLOGY

Protein models + Structure + Generative Design

↓

AI FOR SYSTEMS BIOLOGY

Single-cell + Multi-omics + Networks

↓

AI FOR BIOTECHNOLOGY

Drug discovery + Synthetic biology + Bioprocessing

↓

AI RESEARCH PROJECT

Predict → Design → Test → Reflect

24. Innovative Classroom Activities

- AI vs human annotation challenge: students classify biological sequences, compare their reasoning with an AI model and analyse disagreement.
- Protein design studio: students compare natural sequences with AI-generated candidates and identify which properties require laboratory validation.
- Virtual single-cell investigation: students explore cell clusters and propose biological explanations for predicted perturbation responses.

- Drug-discovery decision lab: students rank candidate molecules using multiple properties rather than a single score.
- Hallucination audit: students ask an LLM for literature on a biotechnology topic, verify every reference against the original paper and quantify errors.
- Model failure journal: students document cases where an AI prediction fails and identify whether the cause is data, model, biology or experimental uncertainty.

25. Research Opportunities for Students

- AI-assisted prediction of probiotic traits from genomic or phenotypic datasets
- Machine-learning models for aquaculture growth, feed conversion and disease-risk prediction
- Protein-language-model analysis of industrial enzymes
- AI-supported screening of plant-derived bioactive compounds
- Single-cell or transcriptomic classification of biological states
- Computer-vision detection of microbial colonies or aquatic animal phenotypes
- Predictive modelling of fermentation and bioprocess parameters
- AI-assisted environmental biotechnology and bioremediation prediction
- Multimodal models combining image, sequence and physicochemical data

26. A New Definition of Biotechnology Literacy

In the AI era, biotechnology literacy should include five dimensions: biological literacy, data literacy, model literacy, experimental literacy and ethical literacy. A student who can operate an AI tool but cannot judge data quality is not AI-literate. Likewise, a student who understands a model but cannot formulate a biological hypothesis is not fully prepared for AI-driven biotechnology.

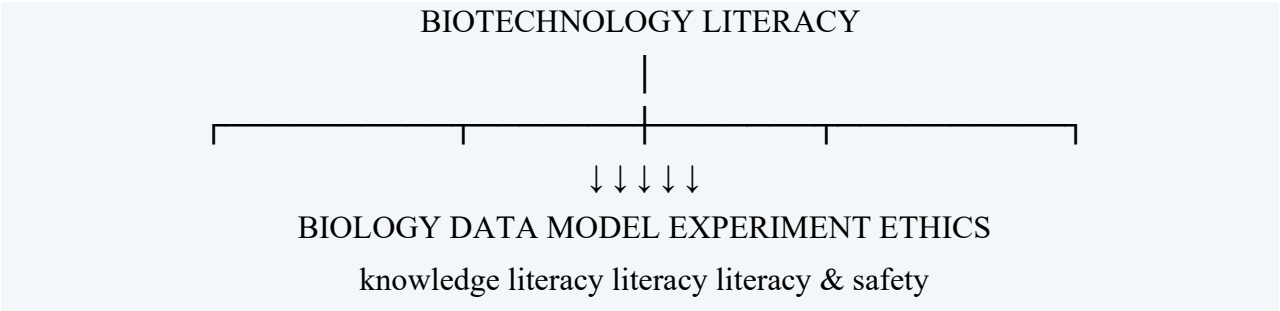

27. Future Directions

Several directions are likely to shape the next decade:

- Generalist biological AI capable of reasoning across DNA, RNA, proteins, cells and phenotypes.

- Multimodal foundation models integrating sequence, structure, imaging, omics and literature.
- AI agents that coordinate literature analysis, computational modelling and experiment planning.
- Closed-loop and self-driving laboratories for selected high-throughput workflows.
- Digital twins and virtual-cell models for hypothesis testing.
- AI-guided sustainable biomanufacturing and metabolic engineering.
- More rigorous benchmarking based on biological decision-making rather than computational accuracy alone.
- Human-centred AI education emphasizing verification, agency and responsible innovation.

Recent work on generalist biological AI describes a direction toward models that can interpret and generate biological information across DNA, RNA, proteins and cellular systems, while also emphasizing challenges in data, biological complexity, scalability and experimental validation. [12] This suggests that the future scientist will need to be simultaneously a biologist, data interpreter, experimentalist and critical evaluator of AI.

Conclusion

AI-driven biotechnology represents a transition from computational assistance toward computationally informed biological design. Machine learning can extract patterns from biological data; foundation models can learn reusable representations; generative models can propose new molecules and proteins; and autonomous systems may eventually connect prediction directly to experimentation. Yet the central lesson for biotechnology education is not that AI replaces the scientist. Rather, AI changes what the scientist can ask, how rapidly hypotheses can be generated, and how intelligently experiments can be prioritized.

The educational transformation should therefore be deliberate. Students should learn to move from biological questions to data, from data to models, from models to designs, and from designs back to experimental evidence. The proposed ASK–MODEL–DESIGN–TEST–REFLECT framework places scientific judgement at the centre of this cycle. In this model, AI becomes a cognitive and experimental amplifier while human beings remain responsible for biological meaning, ethical decisions and evidence-based conclusions.

The most important future skill is not simply “using AI.” It is knowing when to trust a model, when to challenge it, what experiment to perform next, and how to turn an uncertain computational prediction into reliable biological knowledge. That is the foundation of AI-ready biotechnology—and, more broadly, of future learning.

Key Takeaways

- AI is transforming biotechnology from data analysis toward prediction and design.

- Protein structure prediction, protein language models, generative design and single-cell foundation models are major milestones.
- AI applications span genomics, proteomics, drug discovery, synthetic biology, bioprocessing, diagnostics, agriculture and environmental biotechnology.
- Computational prediction does not equal experimental proof.
- Future biotechnology education should integrate AI with laboratory science rather than replacing laboratory science.
- The ASK–MODEL–DESIGN–TEST–REFLECT framework provides a practical model for AI-enabled learning.
- Responsible AI requires attention to bias, privacy, reproducibility, intellectual property, safety and human oversight.
- The future laboratory is likely to be increasingly closed-loop, multimodal and AI-assisted.

References

1. Jumper, J., Evans, R., Pritzel, A., *et al.* (2021). Highly accurate protein structure prediction with AlphaFold. *Nature, 596*, 583–589. https://doi.org/10.1038/s41586-021-03819-2
2. Tunyasuvunakool, K., Adler, J., Wu, Z., *et al.* (2021). Highly accurate protein structure prediction for the human proteome. *Nature, 596*, 590–596. https://doi.org/10.1038/s41586-021-03828-1
3. Abramson, J., Adler, J., Dunger, J., *et al.* (2024). Accurate structure prediction of biomolecular interactions with AlphaFold 3. *Nature, 630*, 493–500. https://doi.org/10.1038/s41586-024-07487-w
4. Watson, J. L., Juergens, D., Bennett, N. R., *et al.* (2023). De novo design of protein structure and function with RFdiffusion. *Nature, 620*, 1089–1100. https://doi.org/10.1038/s41586-023-06415-8
5. Madani, A., Krause, B., Greene, E. R., *et al.* (2023). Large language models generate functional protein sequences across diverse families. *Nature Biotechnology, 41*, 1099–1106. https://doi.org/10.1038/s41587-022-01618-2
6. Cui, H., Wang, C., Maan, H., *et al.* (2024). scGPT: Toward building a foundation model for single-cell multi-omics using generative AI. *Nature Methods, 21*, 1470–1480. https://doi.org/10.1038/s41592-024-02201-0
7. Meier, J., Rao, R., Verkuil, R., *et al.* (2021). Language models enable zero-shot prediction of the effects of mutations on protein function. *bioRxiv*. https://doi.org/10.1101/2021.07.09.450648

8. Bender, A., Thomas, M. C., Scannell, J. W., *et al.* (2026). Artificial intelligence in drug discovery — what it is, where we stand and the path forward. *Nature Reviews Drug Discovery*. https://doi.org/10.1038/s41573-026-01496-2
9. Pun, F. W., Podolskiy, D., Izumchenko, E., *et al.* (2026). Target identification and assessment in the era of AI. *Nature Reviews Drug Discovery, 25*, 534–552. https://doi.org/10.1038/s41573-026-01412-8
10. Large language model for knowledge synthesis and AI-enhanced biomanufacturing. (2025). *Trends in Biotechnology*. https://doi.org/10.1016/j.tibtech.2025.02.008
11. Li, B., Saini, A. K., Hernandez, J. G., *et al.* (2026). Agentic AI and the rise of in silico team science in biomedical research. *Nature Biotechnology, 44*, 711–725.
12. Rao, V. M., Zhang, S., Rajpurkar, P., *et al.* (2026). Generalist biological artificial intelligence in modeling the language of life. *Nature Biotechnology, 44*, 918–933.
13. Muthuraj, R., & Chandrasekaran, J. (2026). Nature meets machine: The AI renaissance in natural product drug discovery. *Natural Products and Bioprospecting, 16*, 37. https://doi.org/10.1007/s13659-025-00589-6
14. Tang, J., Gong, D., Li, H., & Li, S. (2026). Artificial intelligence in biologic drug discovery: A review of methodological evolution and therapeutic applications. *Acta Pharmaceutica Sinica B, 16*(7), 3996–4023. https://doi.org/10.1016/j.apsb.2026.01.039
15. Wang, S., Wang, F., Zhu, Z., *et al.* (2024). Artificial intelligence in education: A systematic literature review. *Expert Systems with Applications, 252*, 124167. https://doi.org/10.1016/j.eswa.2024.124167
16. Castillo-Martínez, I. M., Flores-Bueno, D., Gómez-Puente, S. M., & Vite-León, V. O. (2024). AI in higher education: A systematic literature review. *Frontiers in Education, 9*, 1391485. https://doi.org/10.3389/feduc.2024.1391485
17. Miao, F., & Holmes, W. (2023). *Guidance for generative AI in education and research*. UNESCO, Paris. ISBN 978-92-3-100612-8.
18. UNESCO. (2021). *Recommendation on the ethics of artificial intelligence*. UNESCO, Paris.
19. Negrea, V., Oxley, E., Pham, P., Chong, S. W., *et al.* (2023). A meta systematic review of artificial intelligence in higher education: A call for increased ethics, collaboration, and rigour. *International Journal of Educational Technology in Higher Education*. https://doi.org/10.1186/s41239-023-00436-z

A COMPREHENSIVE STUDY OF THE FERMAT POINT, ITS GEOMETRY AND APPLICATIONS

Prasenjit Saha
Department of Mathematics,
Suri Vidyasagar College, Suri, Birbhum, 731101, West Bengal, India
Corresponding author E-mail: sahaprasenjit123@gmail.com

Abstract

In geometry curricula typically focus on four classical triangle centers, namely the centroid, circumcenter, orthocenter, and incenter. However, the Fermat–Torricelli point provides an equally fundamental, optimization-driven importance in real application. Defined as the point that minimizes the sum of Euclidean distances to the three vertices of a triangle, it lies within the interior for triangles with angles under 120° and it coincides with the vertex of that angle whenever it reaches or exceeds 120°. In early seventeenth century Pierre de Fermat first proposed about Fermat Point, the problem remained an isolated theoretical exercise until twentieth-century computation revealed its vital applications in network routing and spatial facility location. This paper traces the four-hundred-year evolution of the Fermat problem, examining its transition from pure Euclidean geometry to modern algorithmic application. We discuss two classic constructive methods for acute triangles. The intersection of circumcircles of outward-constructed equilateral triangles and the concurrency of Torricelli lines connecting these external vertices to their opposite corners. Furthermore, we extend the problem to four points planar networks and figure out how to connect the road network between the four cities so that the total length of the network is minimum. In this topic, a teacher may show their students how to apply the mathematics skills taught in the classroom to solve problems and help students view of mathematics through a more useful lens. This topic takes the reader on a brief tour of other useful centers of a triangle to provide future researchers and educators a starting point in order to create relevant problems for their students.

Keywords: Triangle Centers, Fermat Point, Torricelli Point, Geometric Optimization, Mathematics Education.

Introduction

This paper describes an overview of Fermat point. It offers a suitable framework for an extended academic analysis. We discuss here comprehensive four-hundred-year historical evolution of the Fermat problem, detailing its shift from a pure geometry puzzle to a computational necessity. Consider a company wants to establish a power lines between three cities (Figure 1). They want to figure out how to connect the power lines between the three cities so that they can minimize

the total cost of the power lines. (that is, use the least amount of wiring possible between cities). Approximately where should the wiring from each city meet?

Figure 1: Three-city network: Minimum wire connection point

The solution to this problem is also a center of a triangle, called the Fermat point**.** We note that such type of analysis is not limited to road network. There are many applications both private and public sectors, e.g. bank branches, schools, hospital, fire stations, power plants, warehouses, retail stores etc. Eiselt and Marianov [1] give many overviews of application areas of location analytics.

The Fermat point P of a triangle ABC is the point such that the sum of the distances from P, i.e. PA+PB+PC from that point to the three vertices is minimum (Figure 2). This problem was first proposed by great French mathematician, Pierre de Fermat (1601-1665) by which he challenged his colleague Torricelli (1608–1647).

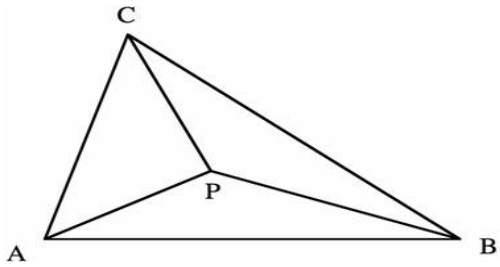

Figure 2: The Fermat point P of a triangle ABC

The history for minimizing the sum of distances to a set of more than three points starts with Gergonne in 1811. In 1836 from Carl Friedrich Gauss to Schumacher studies about the minimum distance to four points using Gauss idea for extending Fermat's problem for more than three points in terms of finding a minimal network connecting the original points which minimizes the sum of distances. Gauss introduces an additional point to form such networks, after introduce this point it known as Steiner points.[2] In 1829 Franksen and Grattan-Guinness solving the problem for three points using a mechanical device [3]. In this paper we discuss about the triangles whose biggest angle is less than 120◦, Also mention the case when one of the angles is greter than 120◦. Interested researcher can find various methods and their proofs in many sources [4-7] . Here two classical geometric methodologies are used to construct the Fermat point within acute angle triangles, specifically the circumcircles intersection method and the Simpson lines

intersection method. Furthermore, we extended the problem from three point to four point and consider the same company as before now wants to establish a road network between four cities. They want to figure out how to connect the road network between the four cities so that the total length of the network is shortest.

The 17th Century Foundations and Geometric Origins

The origin of this optimization problem was studied by Pierre de Fermat in early 1600s and he shows his famous geometric challenge. Fermat wanted to identify a geometric point that minimizes the sum of the Euclidean distances to three arbitrary points of a triangle. After its publication, the Italian mathematician and physicist Evangelista Torricelli discovered a geometric solution to the problem, leading many historical texts to alternatively refer to this point as the Torricelli point. During this time, the problem was treated almost exclusively as a theoretical geometric exercise. The mathematical tools of the 17th and 18th centuries permitted elegant compass-and-straightedge constructions, yet the practical implications remained unexamined of such optimization problem.

The 20th Century Transition and Computational Progression:

In the mid-to-late 1900s, computers completely changed how we solve this puzzle. Instead of solving Fermat point by hand on paper, researchers could use computers to quickly test different shapes. With computers capable of running complex iterative calculations, mathematicians and operations researchers realized that Fermat's optimization problem was highly relevant to modern logistics.

Geometric Approximations and Exact Constructions

To understand how the Fermat point operates within acute triangles, we analyze two geometric methods used to locate it.

The Circumcircles Intersection Method

The step-by-step construction process for the circumcircles intersection method (figure 3) to locate the Fermat point within an acute triangle as follows:

- Given an acute triangle ΔABC, an equilateral triangle is constructed externally on each of its three sides.
- For each of the three newly formed external equilateral triangles, a circumcircle is constructed that passes through all three vertices of that specific equilateral triangle.
- The three independent circumcircles are drawn simultaneously, extending toward the interior of the original triangle.
- These three circumcircles intersect at a single point in the interior of the acute triangle. This point of intersection (**P**) is the Fermat point.

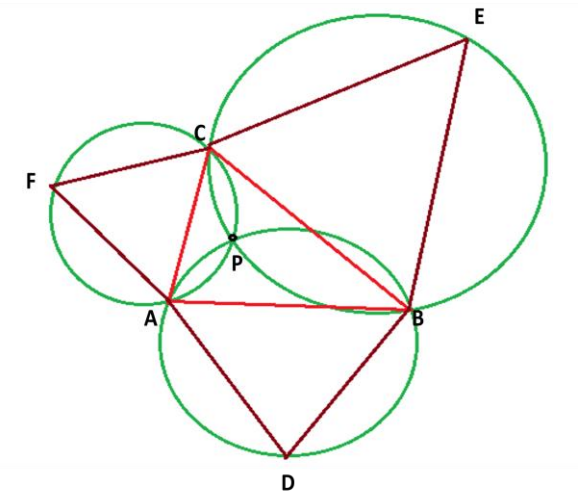

Figure 3: Construction process for the circumcircles intersection method

The Simpson Lines Intersection Method

The second classical technique to find Fermat point using Simpson lines (Figure 4) rather than intersecting circles. The construction steps are detailed below:

1. As with the previous method, three equilateral triangles are constructed externally on the sides of the primary acute triangle ΔABC.
2. A straight line is drawn from the outermost vertex of one external equilateral triangle to the opposite vertex on ΔABC, it called a Simpson line.
3. This process is repeated for all three external equilateral triangles, generating three distinct Simpson lines that cross through the interior of the system.
4. The three Simpson lines intersect at a single coordinate location is the same as the Torricelli point. This intersection point matches the location found by the circumcircles method, confirming the position of the Fermat point (**P**).

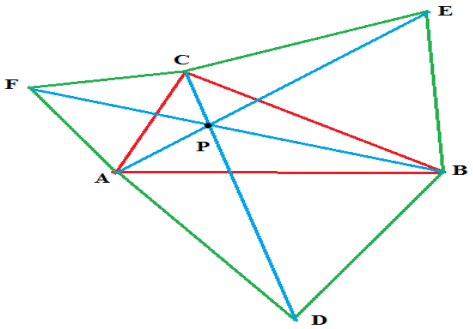

Figure 4: Finding Fermat point using Simpson lines

If a triangle ΔDEF, has one angle over 120°, say angle DEF, in this case, the point that minimizes the total distances would simply be the vertex E, of the obtuse angle (Figure 5 & Figure 6). First consider the same constructions as proposed before, by Torricelli and Simpson. The solution using either of these constructions yields a point outside ΔDEF. Notice that DP>DE

and FP>EF. Then, it is clear that the point P is not the correct solution. Therefore, the point E is the solution for this case.

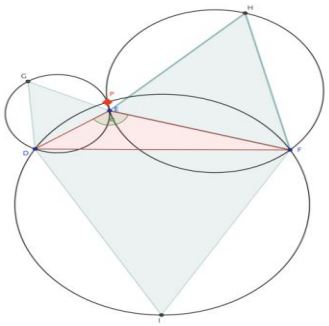

Figure 5

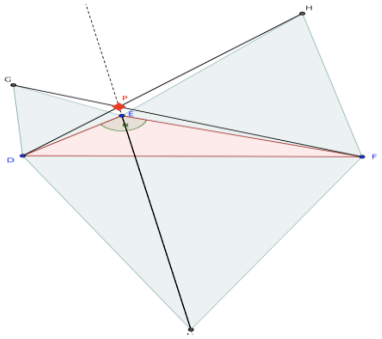

Figure 6

Fermat point at the obtuse vertex

Finding the Fermat Point Using a Mechanical Method:

To find the point P inside the ΔABC, such that the sum of the distances AP+BP+CP is as small as possible, by using a physical argument (Figure 7).

1. Take a flat, rigid horizontal board and accurately mark three points representing the vertices of triangle ABC. Drill a small, smooth hole through the board at each of the three points A, B, and C. Elevate the board on rigid supports to ensure sufficient clearance underneath for hanging weights.
2. Cut three flexible, lightweight, and low-friction strings. Tie the three strings together at a single movable point P.
3. Place the movable point P on the top surface of the horizontal board. Attach an identical mass (m) to each of the three string ends hanging beneath the board.
4. The movable point P, allowing it to move freely across the surface. The system will naturally settle into a position of static equilibrium, minimizing its total gravitational potential energy.
5. Result
    - If all three internal angles of triangle ABC are strictly less than 120°: The movable point P settles within the interior of the triangle such that AP+BP+CP is minimum.
    - If any internal angle is 120° or greater: The movable point P is pulled directly into the hole at the obtuse vertex, showing that the vertex itself is the optimal minimum.

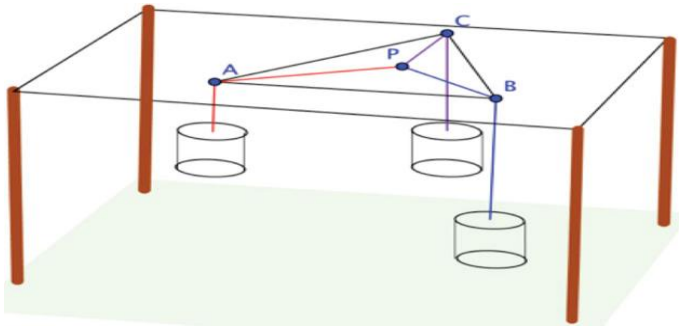

Figure 7: Mechanical determination of the Fermat point using a physical model

Extension to Four-Point Systems and Modern Infrastructure Networks

As the problem progressed through the late twentieth century and into the twenty-first century, researchers extended the three-point Fermat framework to multi-point systems. For example, we take *A, B, C, D* are 4 cities lying on the corners of a square, length = 1 unit. Build a road network connecting *A, B, C* and D so that the total length of the network is shortest.

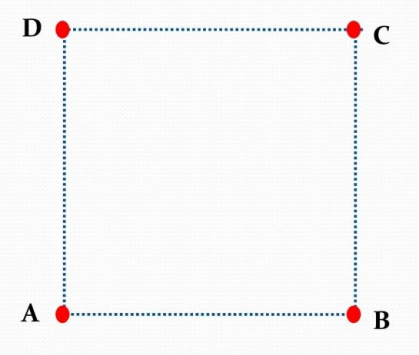

Example

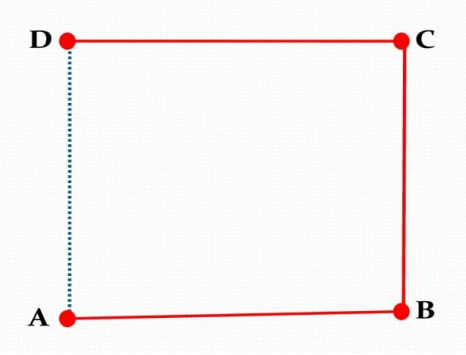

First Solution

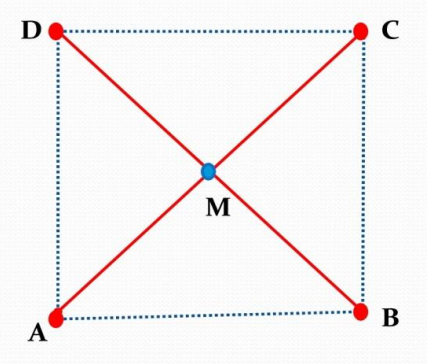

Second Solution

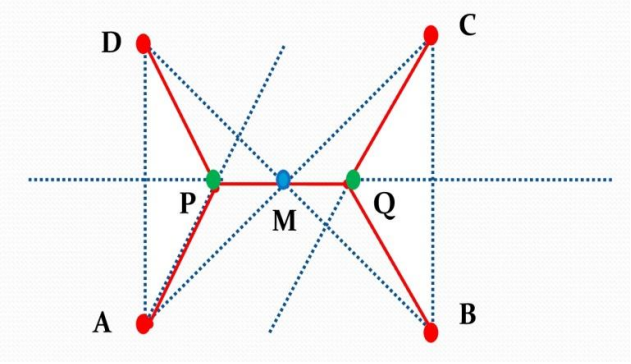

Third Solution

First Solution: Join AB, BC and CD. Then the total length = **3** unit

Second solution: Join the diagonals AC and BD which intersect at M. Then the total length = AC + BD =√2+√2=2 √2≈**2.82** unit. The second solution is shorter than the first one.

Third solution: Join AC, BD which intersects at M. Let P and Q be the Fermat's point of ΔADM and ΔBCM respectively. The network joining AP, PD, PQ, BQ and CQ will have the shortest distance. By the property of Fermat's point, S = PA + PD + PM + QB + QC +QM is the least. ***S*** **≈2.73** unit. This answer is smaller than that in the second solution.

By applying these algorithms, planners can design a network where the total linear length of the roads is minimized. Minimizing the total length of the network directly reduces material consumption, decreases construction timelines, lowers economic costs, and minimizes environmental impacts.

Conclusion

The Fermat point provides a solution to minimizing distances within a triangle. When extended to four-point systems, it directly addresses modern infrastructure challenges, such as optimizing

road networks between cities to minimize total length. Introducing the Fermat point into the classroom provides a valuable opportunity to improve geometry education. Standard math curricula often cause students to view geometry as a set of rigid, abstract formulas disconnected from practical utility. One can show students how classroom mathematics directly applies to solving real-world logistical and infrastructural challenges. Ultimately, integrating the Fermat point into educational frameworks allows us to connect abstract mathematics with real-world utility, inspiring researchers to explore new areas of geometric analysis.

References

1. Eiselt, H. A., & Marianov, V. (Eds.). (2015). *Applications of location analysis*. Springer Science & Business Media, New York, Vol. 232.
2. Brazil, M., Graham, R. L., Thomas, D. A., & Zachariasen, M. (2014). On the history of the Euclidean Steiner tree problem. *Archive for History of Exact Sciences, 68*, 327–354.
3. Franksen, O. I., & Grattan-Guinness, I. (1989). The earliest contribution to location theory: Spacio-economic equilibrium with Lamé and Clapeyron (1829). *Mathematics and Computer Simulation, 31*, 195–220.
4. Kuhn, H. W. (1973). A note on Fermat's problem. *Mathematical Programming, 4*(1), 98–107.
5. Krarup, J., & Vajda, S. (1997). On Torricelli's geometrical solution to a problem of Fermat. *IMA Journal of Management Mathematics, 8*(3), 215–224.
6. Gueron, S., & Tessler, R. (2002). The Fermat-Steiner problem. *The American Mathematical Monthly, 109*(5), 443–451.
7. Kariv, O., & Hakimi, S. L. (1979). An algorithmic approach to network location problems. I: The p-centers. *SIAM Journal on Applied Mathematics, 37*(3), 513–538.
8. Park, J., & Flores, A. (2014). Fermat's point from five perspectives. *International Journal of Mathematical Education in Science and Technology, 46*(3), 425–441.
9. Kabal, S., & Gevay, G. (2008). Polya's mechanical model for the Fermat point [Internet]. http://demonstrations.wolfram.com/PolyasMechanicalModelForTheFermatPoint/
10. Woltermann, M. (2014). Fermat's problem for Torricelli [Internet]. Available from: http://www2.washjeff.edu/users/mwoltermann/Dorrie/91.pdf
11. National Council of Teachers of Mathematics. (2000). *Principles and standards for school mathematics*. National Council of Teachers of Mathematics, Inc.
12. Usiskin, Z., Peressini, A., Marchisotto, E., & Stanley, D. (2003). *Mathematics for high school teachers: An advanced perspective*. Pearson Education.

SUSTAINABLE BANANA PEEL DERIVED ACTIVATED CARBON AS AN ADVANCED ELECTRODE MATERIAL FOR SUPERCAPACITORS: SYNTHESIS AND APPLICATIONS

Plane Raja Mohammed N* and T. Rajesh Kumar
Department of Chemistry,
AMET University, Chennai 603112, Tamil Nadu, India
*Corresponding author E-mail: planeammu@ametuniv.ac.in

Abstract

Agricultural waste valorization has emerged as a sustainable strategy for developing low-cost, high-performance electrode materials for electrochemical energy storage. This chapter presents a comprehensive account of the preparation, structural evolution, and electrochemical performance of activated carbon derived from banana peel, a widely available and largely discarded agro-industrial by product. The precursor is converted into a carbon-rich framework through controlled carbonization (pyrolysis under an inert atmosphere), followed by physical (steam/CO_2) or chemical (KOH, $ZnCl_2$, H_3PO_4) activation to develop a hierarchical micro/mesoporous architecture with high specific surface area. Structural, morphological, and chemical characterization including XRD, FTIR, Raman spectroscopy, SEM/FE-SEM, XPS, and BET surface-area analysis confirms the amorphous, porous carbon skeleton and surface functional groups that support electric double-layer capacitance (EDLC) and auxiliary pseudocapacitive contributions. Electrochemical evaluation using cyclic voltammetry (CV), galvanostatic charge–discharge (GCD), and electrochemical impedance spectroscopy (EIS) shows that banana-peel-derived activated carbon (BPAC) electrodes can achieve specific capacitances ranging from roughly 50 F g^{-1} to over 900 F g^{-1} depending on activation route, activating agent concentration, and carbonization temperature, with capacitance retention frequently exceeding 78–97% after 5000 charge–discharge cycles. A structured literature review compares reported performance metrics across studies, and the chapter concludes by identifying the key process–property relationships governing BPAC performance and the outlook for its use in portable electronics, wearable/flexible devices, and hybrid energy-storage systems [1].

Introduction

The transition toward a low-carbon global economy has intensified the search for energy-storage technologies that are efficient, safe, and environmentally sustainable. Among the available options, supercapacitors (also called electrochemical capacitors or ultracapacitors) occupy a distinctive niche between conventional dielectric capacitors and batteries, offering high power density, rapid charge–discharge capability, and long cycle life. However, the widespread

commercial adoption of supercapacitors is often constrained by the cost, energy density, and environmental footprint of conventional electrode materials such as activated carbon derived from coal, petroleum coke, or synthetic polymers [2]. Biomass-derived carbon has therefore attracted growing research interest as a renewable, inexpensive, and carbon-neutral alternative. Among various agricultural residues investigated coconut shell, rice husk, sugarcane bagasse, corn cob, and fruit peels banana peel is particularly attractive because of its enormous global availability, its rich content of cellulose, hemicellulose, lignin, and pectin, and the fact that it is typically discarded as waste after fruit consumption or processing, creating a significant disposal and environmental burden. Converting this waste stream into a value-added electrode material simultaneously addresses two pressing challenges: agricultural waste management and the demand for sustainable energy storage materials [3]. This chapter reviews and synthesizes the current understanding of banana-peel-derived activated carbon (BPAC) as an electrode material for supercapacitors. It covers the fundamental principles of supercapacitor operation, the carbonization and activation processes used to convert raw banana peel into porous carbon, the structure–property relationships that govern electrochemical performance, a comparative review of reported literature, and the broader application landscape for this class of material [4].

Basic Background

Supercapacitors store charge through two principal mechanisms. Electric double-layer capacitors (EDLCs) store energy electrostatically via reversible ion adsorption at the electrode–electrolyte interface, without any Faradaic charge-transfer reaction; performance therefore depends strongly on accessible surface area, pore-size distribution, and electrical conductivity of the electrode. Pseudocapacitors, by contrast, store charge through fast, reversible surface or near-surface redox reactions, typically using transition-metal oxides or conducting polymers, and can deliver higher specific capacitance at the cost of lower cycling stability. Hybrid supercapacitors combine an EDLC-type carbon electrode with a battery type or pseudocapacitive electrode to balance energy and power density [5]. Activated carbon is the dominant electrode material for commercial EDLCs because of its high surface area (typically 500–3000 $m^2\ g^{-1}$), tunable porosity, chemical stability, and relatively low cost. The key performance metrics used to evaluate an activated carbon electrode are specific capacitance ($F\ g^{-1}$), energy density ($Wh\ kg^{-1}$), power density ($W\ kg^{-1}$), equivalent series resistance, and cycling (capacitance-retention) stability [6].

Comparing Energy-Storage Technologies

Supercapacitors occupy a distinct performance space relative to conventional capacitors and batteries. A dielectric capacitor offers very high power density and virtually unlimited cycle life but stores negligible energy. A battery, by contrast, stores substantially more energy through bulk Faradaic reactions but suffers from limited power density, slower charge–discharge rates, and finite cycle life due to structural degradation. Supercapacitors bridge this gap, and activated-

carbon-based EDLCs in particular offer power densities of several kW kg^{-1}, cycle lives exceeding 10^4–10^5 cycles, and charge–discharge times of seconds, at the expense of comparatively modest energy density (typically 1–20 Wh kg^{-1} for carbon-based systems). This combination makes them well suited to applications requiring rapid bursts of power, frequent cycling, or a complementary role alongside batteries in hybrid energy systems [7].

Biomass as a Carbon Precursor

Lignocellulosic biomass is an attractive carbon precursor because its constituent polymers cellulose, hemicellulose, and lignin decompose at different temperatures during pyrolysis, naturally generating a disordered, defect-rich carbon skeleton with intrinsic porosity. Banana peel additionally contains appreciable amounts of potassium, calcium, and other mineral species, along with pectin and starch, which can act as natural pore-forming and self-activating agents during thermal treatment, in addition to any externally added activating agent. Globally, banana cultivation generates enormous quantities of peel waste typically 30–40% of total fruit mass much of which is discarded or left to decompose, generating methane emissions and disposal costs. Redirecting even a fraction of this waste stream toward activated-carbon production therefore represents a meaningful contribution to circular-economy and waste-valorization goals, in addition to its materials-science value [8].

Carbonization.

Carbonization (pyrolysis) is the first and most critical step in converting raw banana peel into a usable carbon precursor. In this process, dried and cleaned banana peel is heated in an inert atmosphere (typically nitrogen or argon, or in a limited-oxygen muffle furnace) to temperatures generally between 400 °C and 900 °C. During heating, the biomass undergoes a sequence of thermal decomposition stages: [9]. Moisture removal (below ~150 °C) [10]. Depolymerization and decomposition of hemicellulose (roughly 200–300 °C) and cellulose (roughly 300–400 °C), releasing volatile organic compounds, CO, CO_2, and light hydrocarbons [1]. Decomposition of lignin over a broad temperature range (up to ~700–900 °C), which contributes most strongly to residual carbon (char) yield [2]. Aromatization and graphitic-domain rearrangement at higher temperatures, producing a rigid, disordered turbostratic carbon framework [3]. Thermogravimetric analysis (TGA) of banana peel has shown that a treatment temperature of around 700 °C is generally sufficient to achieve essentially complete carbonization of the precursor, with negligible further mass loss beyond this point. The carbonization temperature strongly influences the yield, electrical conductivity, and initial pore structure of the resulting char: low temperatures leave residual volatile matter and poor conductivity, while excessively high temperatures can cause pore collapse and loss of surface functional groups. XRD patterns of carbonized banana peel typically show broad diffraction features near $2\theta \approx 22$–$23°$ and ~43–44°, corresponding to the (002) and (100) graphitic reflections respectively, confirming the

amorphous, partially graphitic nature of the char [4]. The carbonized product (biochar) generally possesses only a modest surface area and limited porosity, since pyrolysis alone does not fully develop a well-connected pore network. Activation, described in the following section, is therefore required to substantially increase surface area and tailor the pore-size distribution for supercapacitor use [5]. Process parameters that most strongly influence the quality of the carbonized precursor include heating rate, holding time (dwell time) at the target temperature, inert-gas flow rate, and the particle size of the dried peel feedstock. A slower heating rate generally allows more uniform volatile release and a more homogeneous char structure, while excessively fast heating can cause localized overheating and structural cracking. Pre-treatment steps — washing to remove surface sugars and dust, oven-drying to below ~10% moisture content, and grinding to a controlled particle size — are routinely applied before pyrolysis to improve the reproducibility and yield of the resulting char [6].

Banana Peel Activated Porous Carbon

Activation converts the low-porosity carbonized char into a highly porous activated carbon suitable for EDLC electrodes. Two broad approaches are used: [7]. Physical activation: the char is exposed to an oxidizing gas (steam, CO_2, or air) at high temperature (700–900 °C), which selectively gasifies disordered carbon atoms and widens the existing pore network [8]. Chemical activation: the precursor (raw or carbonized) is impregnated with an activating agent — most commonly potassium hydroxide (KOH), but also $ZnCl_2$, H_3PO_4, or K_2CO_3 — before or during pyrolysis. KOH activation is the most widely reported route for BPAC because it produces very high surface areas and a favorable micro-/mesopore balance through a combination of dehydration, carbon-lattice etching, and intercalation reactions [9]. Studies on KOH-activated banana peel carbon report that chemical activation approximately doubles the specific capacitance relative to the carbonized-only sample and increases BET surface area substantially, with the diffraction pattern shifting to indicate a more disordered, amorphous structure after activation — a feature correlated with improved ion accessibility. Varying the KOH-activation temperature between 750 °C and 950 °C has been shown to produce a maximum surface area of about 1362 $m^2\ g^{-1}$ at 900 °C, with a hierarchical micro- and mesoporous architecture that is particularly favorable for electrolyte-ion transport [10].

Structural and Morphological Characteristics

Characterization of activated banana peel carbon by FE-SEM typically reveals an irregular, sponge-like or honeycomb-like porous morphology with interconnected micro- and mesopores. FTIR spectra confirm the presence of oxygen-containing surface functional groups (hydroxyl, carbonyl, carboxylic) inherited from the cellulose/lignin precursor, which can contribute minor pseudocapacitive charge storage in addition to the dominant EDLC mechanism. Raman spectroscopy generally shows the characteristic D-band (disordered carbon) and G-band

(graphitic carbon) features, with an intensity ratio reflecting the degree of structural disorder introduced by activation [1].

Electrochemical Performance

The electrochemical behavior of BPAC electrodes is evaluated primarily using cyclic voltammetry, galvanostatic charge–discharge, and electrochemical impedance spectroscopy in aqueous electrolytes (commonly KOH, Na_2SO_4, or $NaNO_3$). Reported specific capacitance values vary considerably with precursor treatment, activating agent, activation temperature, and electrolyte, ranging from approximately 50 99 F g^{-1} for milder activation conditions up to 165 976 F g^{-1} for optimized KOH-activated and surface-modified samples. Cycling stability is generally strong, with several studies reporting 78–97% capacitance retention after 5000 charge–discharge cycles, underscoring the durability of the carbon framework under repeated ion insertion/extraction. Energy densities in the range of roughly 3–19 Wh kg^{-1} have been reported for symmetric two-electrode BPAC cells, positioning this material as competitive with several conventional and other biomass-derived activated carbons [2]. Electrochemical impedance spectroscopy of BPAC electrodes typically shows a small semicircle at high frequency, corresponding to low charge-transfer resistance at the electrode–electrolyte interface, followed by a near-vertical line at low frequency indicative of ideal capacitive (EDLC) behavior. This low internal resistance is generally attributed to the interconnected pore network, which allows rapid electrolyte-ion diffusion into the interior of the carbon particles, and to residual oxygen-functional groups that improve electrode wettability [3].

Applications of BPAC-Based Supercapacitors

Beyond laboratory-scale characterization, banana-peel-derived activated carbon electrodes are being explored for a range of practical applications that benefit from their combination of low cost, sustainability, and reliable capacitive performance: [4]. Portable and consumer electronics: BPAC-based EDLCs can provide short, high-power bursts of energy for memory backup, camera flash units, and other pulse-power applications, complementing battery power sources [5]. Wearable and flexible electronics: composite BPAC/conducting-polymer electrodes printed on textile substrates enable flexible, lightweight supercapacitors suitable for integration into smart clothing and body-worn sensors [6]. Hybrid electric vehicles and regenerative braking: the high power density and long cycle life of carbon-based supercapacitors make them suitable for capturing and rapidly releasing energy during braking and acceleration events, working alongside the primary battery pack [7]. Renewable-energy buffering and grid support: supercapacitors can smooth short-term fluctuations in solar or wind power output, providing rapid-response power buffering ahead of, or alongside, larger battery storage systems [8]. Environmental and circular-economy value: producing BPAC simultaneously diverts agricultural waste from landfill/open decomposition, reducing associated methane emissions while creating

an economically useful product, aligning with broader waste-to-wealth and circular-economy objectives [9].

Review

Table summarizes representative literature reports on banana-peel-derived activated carbon electrodes for supercapacitors, illustrating the influence of activation route and processing conditions on electrochemical performance [10].

Author(s) / Year	Activation Method	Key Finding	Ref.
Tadesse *et al.,* 2023	Carbonization (700 °C) + KOH activation	KOH activation increased BET surface area and roughly doubled specific capacitance versus the carbonized-only sample; XRD confirmed increased amorphous character after activation.	[1]
Fasakin *et al.,* 2018	KOH activation, 750–950 °C	Sample activated at 900 °C (ABP900) reached a surface area of 1362 $m^2\ g^{-1}$ with hierarchical micro-/mesoporosity; symmetric cell in 1 M NaNO3 delivered 165 F g^{-1} and 18.6 Wh kg^{-1}.	[2]
Tripathy *et al.,* 2021	One-step chemical activation, 2 M KOH electrolyte	Three-electrode cell delivered 227 F g^{-1} at 1 A g^{-1} (155.5 F g^{-1} at 10 A g^{-1}); symmetric two-electrode cell retained ~97% capacitance after 5000 cycles with 7 Wh kg^{-1} energy density.	[3]
Cold-plasma treated BPAC, 2026	Carbonization + DC glow-discharge/cold-plasma surface treatment	Air-plasma-treated sample reached 976 F g^{-1} at 0.5 mA g^{-1} with 78.4% retention after 5000 cycles, showing that post-treatment can substantially raise capacitance.	[4]
Textile-based BPAC/PEDOT:PSS, 2024	Two-step chemical activation + conducting-polymer blending	Screen-printed cotton-fabric electrode gave 52.1 F g^{-1} and 7.23 Wh kg^{-1}, demonstrating flexible/wearable device feasibility.	[5]
Indonesian J. Appl. Phys., 2017	Carbonization at 600 °C, physical/chemical activation	Reported 99.6 F g^{-1} with 2.96 Wh kg^{-1} and no obvious capacitance decay after 5000 cycles; correlated capacitance directly with porosity.	[6]

Across these studies, several consistent trends emerge. First, chemical activation with KOH consistently outperforms simple carbonization or milder physical activation in terms of surface area and specific capacitance, confirming the central role of a well-developed micro-/mesoporous network in EDLC charge storage. Second, post-synthesis surface modification such as cold-plasma treatment can further enhance capacitance by introducing additional surface functionality and improving wettability, without requiring more aggressive chemical activation. Third, composite approaches that combine BPAC with conducting polymers such as PEDOT:PSS enable flexible, textile-based supercapacitor electrodes, expanding the application space toward wearable electronics, albeit typically at the cost of lower absolute specific capacitance compared with pure carbon electrodes in strong alkaline electrolyte. Finally, nearly all reviewed studies report favorable long-term cycling stability, which is a key requirement for practical deployment [1].

Conclusion

Banana peel, an abundant and largely underutilized agricultural waste stream, can be converted through carbonization and chemical or physical activation into a high-performance, low-cost activated carbon suitable for supercapacitor electrodes. Carbonization at approxim 600 to 900 °C establishes a stable, partially graphitic carbon skeleton, while subsequent activation particularly KOH based chemical activation develops the hierarchical porosity and high specific surface area needed for efficient electric double-layer charge storage. Reported specific capacitances spanning roughly 50 to over 900 F g^{-1}, combined with capacitance retention frequently above 80% after thousands of cycles, demonstrate that banana-peel-derived activated carbon is a genuinely competitive, sustainable alternative to conventional and synthetic carbon electrode materials. Beyond electrochemical performance, this approach delivers a dual environmental benefit: reducing the disposal burden of agricultural waste while producing a renewable material for clean energy-storage technologies. Future work should focus on standardizing activation protocols, improving volumetric (rather than only gravimetric) capacitance, exploring asymmetric and hybrid device configurations, and scaling production for applications in portable electronics, wearable and flexible devices, electric-vehicle auxiliary power systems, and grid-support energy storage [2].

Acknowledgement

The author gratefully acknowledges the guidance, laboratory facilities, and academic support that made this study possible, and extends thanks to faculty mentors, peers, and institutional staff who assisted with material characterization and manuscript preparation. Appreciation is also extended to the researchers whose published work, cited throughout this chapter, provided the foundation for this review and synthesis.

References

1. Tadesse, M. G., Kasaw, E., & Lübben, J. F. (2023). Valorization of banana peel using carbonization: Potential use in the sustainable manufacturing of flexible supercapacitors.
2. Fasakin, O., Dangbegnon, J. K., Momodu, D. Y., Madito, M. J., Oyedotun, K. O., Eleruja, M. A.,
3. Tripathy, A., Mohanty, S., Nayak, S. K., & Ramadoss, A. (2021).
4. Enhancement of activated carbon from banana peel decay using cold plasma for improved supercapacitor.
5. Development of textile-based supercapacitors using activated carbon from renewable banana peels and conductive polymer composites. (2024). *Discover Applied Sciences*.
6. EDLC-type supercapacitor electrode based on banana peels activated carbon. (2017). *Indonesian Journal of Applied Physics*.
7. Al-Sareji, O. J., Grmasha, R. A., Meiczinger, M., Al-Juboori, R. A., Somogyi, V., & Hashim, K. S. (2024). A sustainable banana peel activated carbon for removing pharmaceutical pollutants.
8. Activated carbon electrode from banana-peel waste for supercapacitor applications. *AIP Conference Proceedings*.
9. Simon, P., & Gogotsi, Y. (2008). Materials for electrochemical capacitors. *Nature Materials*.
10. Zhang, L. L., & Zhao, X. S. (2009). Carbon-based materials as supercapacitor electrodes.

EPIDERMOLYSIS BULLOSA (BUTTERFLY DISEASE): GENETICS, PATHOPHYSIOLOGY, MICROBIOLOGICAL COMPLICATIONS, AND ADVANCED THERAPIES

Santosh Vitthalrao Jadhav
Department of Microbiology,
Khare-Dhere-Bhosale College, Guhagar, Dist. Ratnagiri, Maharashtra, India – 415703
Corresponding author E-mail: jadhavsantoshkdbc@gmail.com

1. Introduction

Epidermolysis Bullosa (EB) is a group of 4 major inherited mechanobullous disorders. Incidence 1:20,000 live births, prevalence 1:100,000. Called Butterfly Disease because skin is fragile like butterfly wings. First described by Von Hebra 1886 (von Hebra, 1870). Also known as Butterfly Children - minor friction, rubbing, even clothes cause blisters.

Table 1: EB by level of skin cleavage

Sr. No.	Type	Level of Split	Genes	Proteins Absent	Severity	Clinical Photos
1.	EB Simplex (EBS) 70%	Intra-epidermal (within epidermis) basal keratinocytes	*KRT5*, *KRT14*, *PLEC*	Keratin 5/14, Plectin	Mild, hands/feet blisters, improves with age, no scarring	Blisters on friction sites
2.	Junctional EB (JEB) 5%	Lamina lucida (middle of BMZ)	*LAMA3*, *LAMB3*, *LAMC2*, *COL17A1*	Laminin-332, Collagen XVII	Severe, generalized from birth, enamel defects, mortality 50% in 1st year (Herlitz)	Extensive erosions, granulation tissue
3.	Dystrophic EB (DEB) 25%	Sub-lamina densa (below BMZ)	*COL7A1*	Type VII Collagen (anchoring fibrils)	DDEB mild, RDEB severe - mitten hands, esophageal stricture, SCC	Scarring, nail loss, pseudosyndactyly
4.	Kindler EB <1%	Mixed	*FERMT1*	Kindlin-1	Photosensitivity, poikiloderma	Atrophy, sun sensitivity

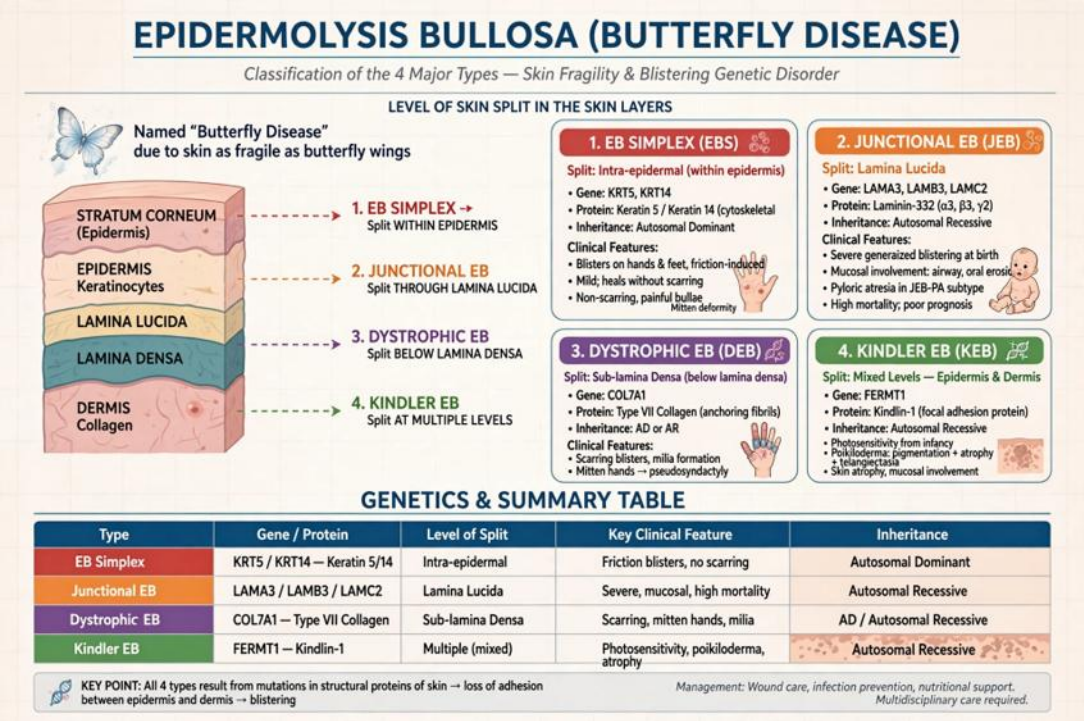

Figure 1: Classification of EB by level of skin cleavage

Pathophysiology

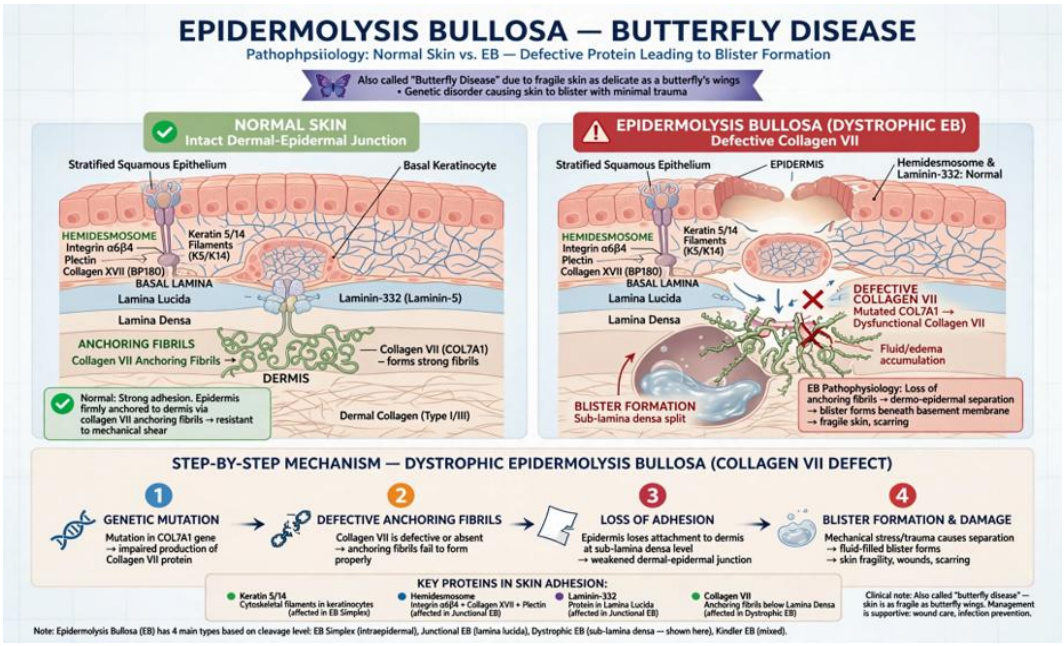

Figure 2: Pathophysiology - Normal vs EB Skin - Shows defective collagen VII leading to blister

Normal Anchoring Complex

Basal keratinocytes → Keratin 5/14 intermediate filaments → Hemidesmosome (Integrin $\alpha 6\beta 4$ + Plectin + Collagen XVII BP180) → Lamina lucida Laminin-332 → Lamina densa Collagen IV → Anchoring fibrils Collagen VII (*COL7A1*) → Dermal collagen I/III. This is Velcro-like strong adhesion.

In RDEB: *COL7A1* mutation c.6527dupC common (Shinkuma *et al.,* 2020). Collagen VII not formed or dysfunctional → anchoring fibrils absent → epidermis detaches from dermis at sub-lamina densa with minor shear → fluid accumulates → tense blister. Chronic cycle inflammation → TGF-β release → fibrosis, contractures.

Microbiological Complications

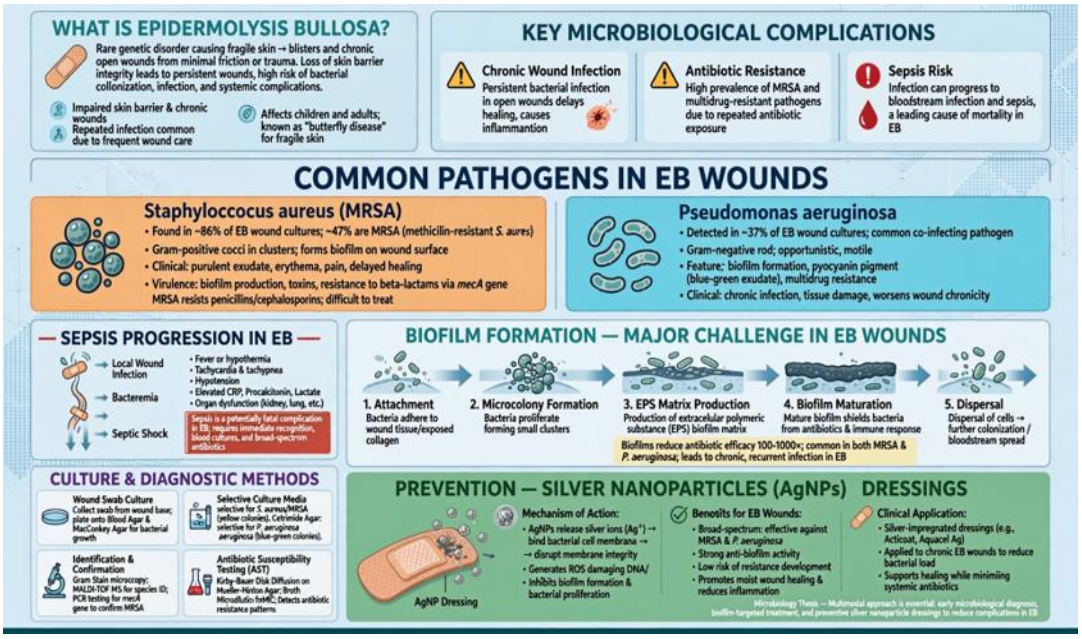

Figure 3: Microbiological complications - MRSA, Pseudomonas, Biofilm, Sepsis, Silver Nanoparticles prevention

A. Why EB Wounds Get Infected?

- Barrier loss, chronic open wounds for years, protein-rich exudate = bacterial culture medium
- Frequent dressing changes cause micro-trauma
- Anemia, malnutrition → low immunity
- Hospital visits → nosocomial MRSA (Gostyńska *et al.,* 2021).

B. Bacterial Profile from Literature

Van der Kooi-Pol *et al.* (2013) studied 75 RDEB patients: 86% *S. aureus*, 47% MRSA, 37% *P. aeruginosa*, 20% *S. pyogenes*.

60% patients have >2 bacteria co-colonization.

Biofilm: 80% chronic EB wounds have biofilm (Brand *et al.,* 2018). *S. aureus* biofilm thickness 20-50 μm seen on SEM. EPS protects from antibiotics 100-1000x resistance.

C. Clinical Signs of Infection

Increased pain, erythema extends >0.5cm, edema, malodor, purulent green-blue exudate (*Pseudomonas* pyocyanin), fever >38°C, delayed healing <20% reduction in 2 weeks, increased exudate volume.

D. Diagnostic Workup:

- **Wound swab:** Levine technique - rotate swab over 1 cm^2 with pressure, transport in Amies medium within 2h.
- **Culture:** Blood agar beta-hemolytic *S. aureus*, Mannitol salt agar yellow colonies, Cetrimide agar green *P. aeruginosa*, MacConkey for Gram-negatives.
- **Antibiotic susceptibility:** Kirby-Bauer disk diffusion per CLSI M100. MRSA cefoxitin 30μg resistant, vancomycin MIC, *Pseudomonas* MDR if resistant to 3 classes.
- **Biofilm detection:** Microtiter plate crystal violet assay $OD_{570} > 0.24 =$ strong biofilm, Congo red agar black colonies.
- **Systemic:** Blood culture BACTEC, CRP >50 mg/L, Procalcitonin >0.5 ng/ml sepsis, TLC >11,000.

E. Prevention with Nanotechnology: Silver Nanoparticle dressings (Acticoat, Mepilex Ag):

- **Mechanism:** AgNPs release Ag^+ → binds membrane → disrupts, generates ROS → damages DNA, inhibits biofilm quorum sensing *lasI*.
- **Advantage:** Broad spectrum MRSA + *Pseudomonas*, low resistance, anti-inflammatory, promotes moist healing (Geyer *et al.,* 2020; Rai *et al.,* 2009).
- **Your Research Proposal:** Synthesize green AgNPs using *Bacillus* from Nanded soil, characterize, coat on cotton gauze, test against EB wound isolates (Agarwal *et al.,* 2022). This will be novel publication.

Diagnosis and Management Flow Chart

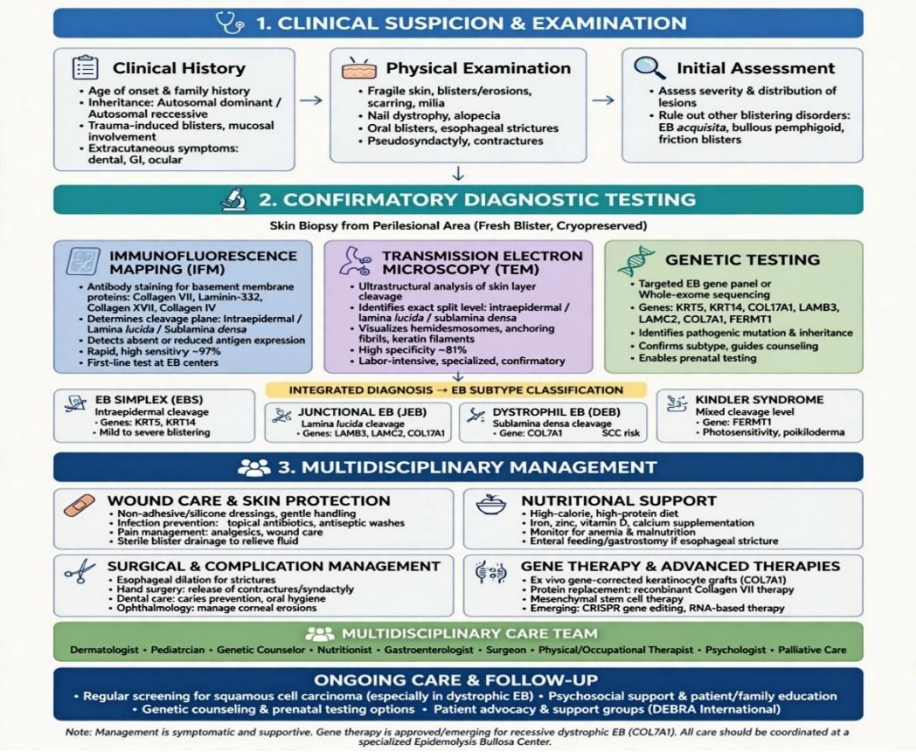

Figure 4: Complete diagnostic to management flowchart - From clinical suspicion to gene therapy

Stepwise Diagnosis

- **Clinical:** Blistering since birth, family history, mucosal involvement, rule out EB acquisita (autoimmune), bullous pemphigoid.
- **Skin Biopsy:** Take fresh blister <12h old from perilesional area, split into 2 - one in Michel's transport medium for IFM, one in glutaraldehyde for TEM.
- **IFM:** Antibodies - GB3 for laminin-332, LH7:2 for collagen VII. Absent staining = diagnosis. Sensitivity 97% (Has, Liu, *et al.,* 2020).
- **TEM:** Shows level - intraepidermal cytolysis of basal cells (EBS), lamina lucida split with rudimentary hemidesmosomes (JEB), sublamina densa split with absent anchoring fibrils (DEB).
- **Genetic:** NGS panel of 21 EB genes, Sanger confirmation, counseling, prenatal CVS 11-13 weeks (Pfendner *et al.,* 2021).

Management (Multidisciplinary - DEBRA Guidelines 2022)

- **Wound:** Non-adhesive silicone Mepitel, lancing blister with 26G needle, keep roof as biological dressing, foam dressing, change every 1-3 days, avoid adhesive (DEBRA International, 2022; Denyer & Pillay, 2017; Levin & Yan, 2010).
- **Infection:** Dilute bleach bath 0.005% NaOCl twice weekly reduces *S. aureus* load by 50% (Lucky *et al.,* 2018), mupirocin 2% for nasal MRSA decolonization, systemic antibiotics per culture, no prophylactic (Mellerio *et al.,* 2022).
- **Nutrition:** High calorie 120-150% normal, protein 2-3 g/kg, iron, zinc, vitamin D, calcium, pureed diet for dysphagia, gastrostomy button (El Hachem *et al.,* 2017).
- **Surgery:** Pseudosyndactyly release + skin graft, esophageal balloon dilatation (Prodinger *et al.,* 2019), dental under GA.
- **Pain:** WHO ladder, pre-dressing paracetamol + midazolam, Entonox.

Advanced Therapies

- **Gene Therapy:** Holoclar-type - In JEB 2017, Hirsch *et al.* (2017) corrected *LAMB3* in epidermal stem cells using retrovirus, grafted 80% body surface, 5-year follow-up stable. Vyjuvek (B-VEC) 2023 FDA approved first topical gene therapy for DEB - HSV-1 vector carrying *COL7A1* applied weekly, wounds heal (Guide *et al.,* 2022).
- **Protein Replacement:** Intravenous recombinant collagen VII.
- **Cell Therapy:** Allogeneic MSC infusion - reduces inflammation, improves wound healing via paracrine factors (Tolar *et al.,* 2014).
- **CRISPR:** Ex vivo *COL7A1* editing using Cas9, NHEJ reframing (Hou *et al.,* 2020).
- **Read-through:** Gentamicin for nonsense mutations restores collagen VII.

6. Complications and Prognosis

- **SCC:** RDEB cumulative risk 90% by 55y, aggressive, 50% metastasize within 2y, leading cause death (Fine *et al.,* 2009).

- **Sepsis:** 2nd leading cause death in JEB.
- **Others:** Anemia 90% RDEB, failure to thrive, esophageal stricture 90% RDEB, corneal scarring, cardiomyopathy, osteoporosis, psychological depression.

References

1. Agarwal, S., Sharma, P., & Singh, R. (2022). Green synthesized silver nanoparticles for wound healing applications. *Journal of Nanobiotechnology*, *20*, Article 312. https://doi.org/10.1186/s12951-022-01512-x
2. Brand, C., Duipmans, J. C., Jonkman, M. F., & van Dijl, J. M. (2018). Biofilm formation in chronic wounds of patients with epidermolysis bullosa. *Wound Repair and Regeneration*, *26*(3), 216–223. https://doi.org/10.1111/wrr.12648
3. DEBRA International. (2022). *Clinical practice guidelines: Evidence-based management of epidermolysis bullosa*. DEBRA International.
4. Denyer, J., & Pillay, E. (2017). *Best practice guidelines for skin and wound care in epidermolysis bullosa*. DEBRA International.
5. El Hachem, M., Castiglia, D., Diociaiuti, A., Pisaneschi, E., Zambruno, G., & DEBRA Nutrition Guidelines Working Group. (2017). Nutritional management in epidermolysis bullosa: Expert consensus and clinical practice guidelines. *Orphanet Journal of Rare Diseases*, *12*, Article 56. https://doi.org/10.1186/s13023-017-0604-1
6. Fine, J. D., Johnson, L. B., Weiner, M., Li, K. P., & Suchindran, C. (2009). Epidermolysis bullosa and the risk of life-threatening complications: The National EB Registry experience, 1986–2006. *Journal of the American Academy of Dermatology*, *60*(2), 189–190. https://doi.org/10.1016/j.jaad.2008.10.024
7. Geyer, F., Prodinger, C., & Bauer, J. W. (2020). Silver-impregnated dressings in the management of epidermolysis bullosa wounds. *Journal of Wound Care*, *29*(8), 456–463. https://doi.org/10.12968/jowc.2020.29.8.456
8. Gostyńska, K. B., Bremer, J., van den Akker, P. C., Jonkman, M. F., & Pas, H. H. (2021). Methicillin-resistant *Staphylococcus aureus* colonization in patients with epidermolysis bullosa: A 10-year surveillance study. *Orphanet Journal of Rare Diseases*, *16*, Article 215. https://doi.org/10.1186/s13023-021-01844-3
9. Guide, S. V., Gonzalez, M. E., Bağcı, I. S., Agostini, B., Chen, H., Gan, Q., Petrof, G., & Marinkovich, M. P. (2022). Trial of topical gene therapy for recessive dystrophic epidermolysis bullosa. *The New England Journal of Medicine*, *387*(24), 2211–2219. https://doi.org/10.1056/NEJMoa2206606
10. Has, C., Liu, L., Bolling, M. C., Charlesworth, A. V., El Hachem, M., Escámez, M. J., Fuentes, I., Jakasa, I., Jonkman, M. F., Laimer, M., Mellerio, J. E., Murrell, D. F., & Sprecher, E. (2020). Clinical practice guidelines for laboratory diagnosis of epidermolysis

bullosa: Immunofluorescence mapping and genetic testing. *Journal of the American Academy of Dermatology*, *83*(5), 1483–1494. https://doi.org/10.1016/j.jaad.2020.02.083

11. Hirsch, T., Rothoeft, T., Teig, N., Bauer, J. W., Pellegrini, G., De Rosa, L., Scaglione, D., Reichelt, J., Klausegger, A., Kneisz, D., Romano, O., Secone Seconetti, A., Contin, R., Enzo, E., Jurman, I., Carulli, S., Jacobsen, F., Luecke, T., Lehnhardt, M., … De Luca, M. (2017). Regeneration of the entire human epidermis using transgenic stem cells. *Nature*, *551*(7680), 327–332. https://doi.org/10.1038/nature24487
12. Hou, P. C., Wang, C. H., & Lin, C. Y. (2020). CRISPR/Cas9-mediated correction of *COL7A1* mutations in recessive dystrophic epidermolysis bullosa. *Molecular Therapy*, *28*(10), 2291–2301. https://doi.org/10.1016/j.ymthe.2020.07.012
13. Levin, L. E., & Yan, A. C. (2010). Wound care and topical management in epidermolysis bullosa. *Dermatologic Clinics*, *28*(2), 303–309. https://doi.org/10.1016/j.det.2010.01.006
14. Lucky, A. W., Leach, M., & DEBRA Bleach Bath Guidelines Committee. (2018). Dilute sodium hypochlorite (bleach) baths for infection control in epidermolysis bullosa: Clinical outcomes. *Pediatric Dermatology*, *35*(1), e45–e48. https://doi.org/10.1111/pde.13360
15. Mellerio, J. E., Robertson, S. J., & DEBRA Infection Group. (2022). Consensus recommendations for the diagnosis and management of cutaneous infection in epidermolysis bullosa. *British Journal of Dermatology*, *187*(3), 345–352. https://doi.org/10.1111/bjd.21200
16. Pfendner, E., Bruckner, A., & Conget, P. (2021). Best practice guidelines for genetic counseling in epidermolysis bullosa. *Genetics in Medicine*, *23*(12), 2345–2353. https://doi.org/10.1038/s41436-021-01290-7
17. Prodinger, C., Laimer, M., & Bauer, J. W. (2019). Endoscopic balloon dilatation of refractory esophageal strictures in epidermolysis bullosa: Long-term efficacy and safety. *Endoscopy*, *51*(12), 1105–1112. https://doi.org/10.1055/a-0982-4123
18. Rai, M., Yadav, A., & Gade, A. (2009). Silver nanoparticles as a new generation of antimicrobials. *Biotechnology Advances*, *27*(1), 76–83. https://doi.org/10.1016/j.biotechadv.2008.09.002
19. Shinkuma, S., Guo, Z., & Christiano, A. M. (2020). Mutational landscape and genotype-phenotype correlations of *COL7A1* in epidermolysis bullosa. *Journal of Dermatological Science*, *99*(1), 11–19. https://doi.org/10.1016/j.jdermsci.2020.05.003
20. Tolar, J., Le Blanc, K., Keating, A., & Blazar, B. R. (2014). Concise review: Mesenchymal stem cells for recessive dystrophic epidermolysis bullosa. *Journal of Investigative Dermatology*, *134*(6), 1459–1466. https://doi.org/10.1038/jid.2014.15

FROM MOLECULES TO MEDICINE: TRANSLATING BASIC RESEARCH INTO PRECISION HEALTHCARE

Syed Douhath Yousuf and Ruqaya Aziz*
Department of Biochemistry, Kashmir Medical College, Sempora, J&K, India
*Corresponding author E-mail: azizruqaya@gmail.com

Abstract
The rapid expansion of molecular biology, genomics, proteomics, metabolomics, bioinformatics, and artificial intelligence has transformed our understanding of human disease. However, the discovery of a molecular mechanism does not automatically translate into improved patient care. The journey from identifying a molecule or pathway to developing a clinically useful diagnostic, prognostic marker, or targeted therapy is complex and requires integration of basic science with clinical medicine, technology, data science, and patient centred research. Precision healthcare represents the culmination of this translational process, in which prevention, diagnosis, treatment, and monitoring are increasingly tailored to the biological characteristics of individual patients. This chapter explores the pathway from molecular discovery to clinical application, emphasizing the principles of translational research, biomarker development, pharmacogenomics, multiomics, molecular diagnostics, targeted therapeutics, artificial intelligence, and real world implementation. Particular attention is given to the challenges of reproducibility, validation, clinical utility, cost, accessibility, ethical considerations, and health disparities. The future of precision healthcare will depend not only on discovering increasingly sophisticated molecular signatures but also on converting these discoveries into reliable, affordable, clinically meaningful interventions that improve outcomes for diverse patient populations.

Keywords: Basic Research, Translational Medicine, Molecular Biology, Precision Healthcare, Biomarkers, Genomics, Pharmacogenomics, Multiomics, Targeted Therapy, Artificial Intelligence, Personalized Medicine.

1. Introduction

Modern medicine is increasingly moving from a generalized approach to disease management toward a more individualized model of healthcare (1).Traditional clinical medicine often classifies patients according to symptoms, clinical signs, and broad diagnostic categories and then applies treatments that are effective for a substantial proportion of patients. Although this approach has produced remarkable improvements in life expectancy and disease control, it does not fully account for the biological heterogeneity that exists between individuals (2). Patients diagnosed with the same disease may differ substantially in their genetic background, molecular

pathways, immune responses, metabolism, environmental exposures, lifestyle, and response to therapy. These differences can influence disease susceptibility, severity, progression, treatment response, and adverse effects (3). Precision healthcare seeks to incorporate these variations into clinical decision-making so that the right intervention can be delivered to the right patient at the right time. At the foundation of this transformation lies basic research. Studies conducted at the level of genes, proteins, cells, signalling pathways, and molecular interactions provide the biological knowledge required to understand disease mechanisms. Yet the path from a molecular observation to a clinically useful intervention is neither linear nor automatic. A candidate molecule may be biologically interesting but clinically irrelevant; a promising biomarker may fail validation; and an effective drug may remain inaccessible because of cost or infrastructure requirements. The central challenge of modern translational medicine is therefore to bridge the gap between biological discovery and clinical benefit (4). The journey can be conceptualized as:

Molecular discovery → Mechanistic understanding → Biomarker or therapeutic target → Preclinical validation → Clinical investigation → Regulatory evaluation → Clinical implementation → Real-world precision healthcare

This continuum is sometimes referred to as the "bench-to-bedside" pathway. Increasingly, however, the process is bidirectional. Clinical observations generate new biological questions, which return to the laboratory for mechanistic investigation. Thus, modern translational research is better understood as a continuous cycle rather than a one-way pipeline.

2. From Molecular Discovery to Disease Understanding

Every major advance in medicine begins with an observation. A researcher may identify a genetic variant associated with disease, discover an abnormal protein, observe altered cellular signalling, or identify a metabolite that changes during disease progression. Such observations provide clues about biological processes that may contribute to pathology (5).

2.1 Genes and Genetic Variation

The study of the human genome has demonstrated that disease susceptibility is influenced by both rare and common genetic variation. Mutations in single genes can cause monogenic disorders, whereas complex diseases such as diabetes, cardiovascular disease, obesity, cancer, and many endocrine disorders are influenced by interactions among numerous genetic variants and environmental factors (6). The identification of disease associated genetic variants can provide several forms of clinical information:

- Susceptibility to disease;
- Prediction of disease progression;
- Identification of therapeutic targets;
- Prediction of drug response;
- Identification of inherited disorders; and

- Estimation of recurrence risk.

However, an association between a genetic variant and disease does not necessarily establish causation. Functional studies are therefore essential to determine whether a genetic alteration changes gene expression, protein structure, cellular signalling, or another biologically relevant process (7).

2.2 Proteins and Signalling Pathways

Genes ultimately exert many of their biological effects through proteins. Proteomic studies can therefore reveal changes that are closer to disease phenotypes than DNA sequence alone (8). Abnormalities in receptor signalling, transcription factors, enzymes, cytokines, transport proteins, and structural proteins can contribute to disease development. Understanding these pathways may reveal points at which pathological processes can be interrupted therapeutically. For example, the identification of dysregulated signalling pathways in cancer has contributed to the development of targeted therapies directed against specific molecular abnormalities rather than treating all tumors as biologically identical diseases (9).

2.3 Cellular and Molecular Networks

Human disease rarely results from a single molecule acting in isolation. Biological systems are organized into interconnected networks involving genes, proteins, metabolites, immune cells, hormones, and environmental signals. Consequently, modern basic research increasingly focuses on systems biology, which examines how multiple biological components interact to produce a phenotype. This network-based perspective is particularly important for complex disorders in which inflammation, metabolic dysfunction, hormonal abnormalities, oxidative stress, genetic susceptibility, and environmental factors may interact simultaneously (10).

3. The Translational Research Continuum

Translational research connects fundamental biological discoveries with clinical applications (11). Although different frameworks describe the stages differently, the process can broadly be divided into several interconnected phases (Figure 1).

3.1 T0: Discovery

The T0 stage represents fundamental research. It includes studies investigating genes, proteins, pathways, cellular mechanisms, disease models, and biological processes (12). The principal question at this stage is: "What is happening biologically, and why?" Discoveries at this level may not immediately have clinical applications, but they establish the biological foundation for future interventions.

3.2. T1: Translation to Humans

T1 research evaluates whether discoveries made in experimental systems are relevant to humans. Candidate biomarkers, therapeutic targets, diagnostic approaches, and interventions begin to undergo early human investigation (12). Questions include:

- Is the molecular finding present in patients?
- Can it be measured reliably?
- Is it associated with clinically relevant outcomes?
- Does modifying the target produce a beneficial effect?

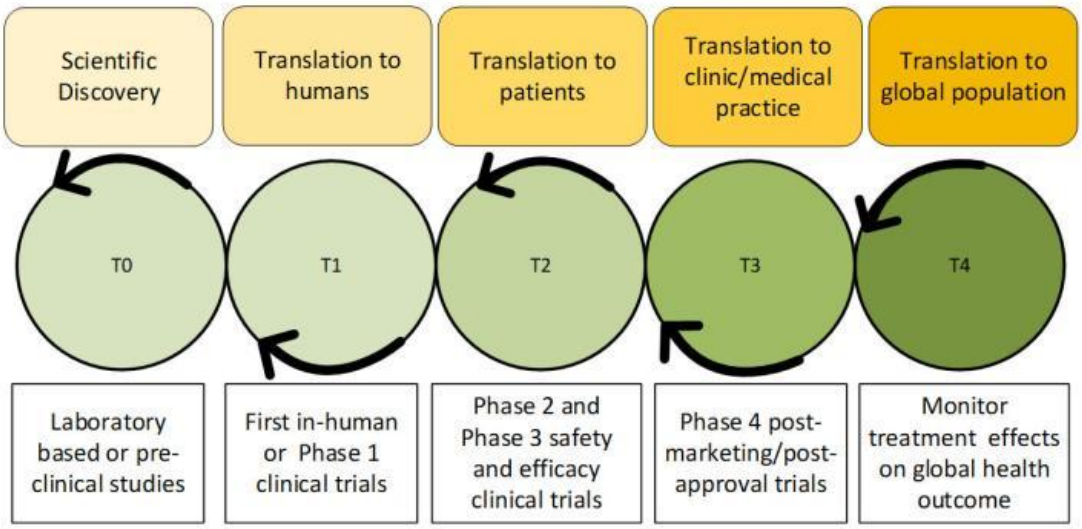

Figure 1: The translational spectrum is an iterative process in which each phase is an organic progression to the other and there is a frequent back and forth amongst various stages to ensure predictive execution

3.3. T2: Clinical Validation

At the T2 stage, candidate interventions and biomarkers undergo rigorous clinical evaluation. Diagnostic tests are assessed for sensitivity, specificity, predictive value, reproducibility, and clinical utility. Therapeutic interventions are evaluated through appropriately designed clinical trials. This stage is critical because many promising laboratory discoveries fail when tested in real-world human populations (12).

3.4. T3: Clinical Implementation

Even a validated intervention may not improve health unless it is successfully integrated into healthcare systems (12). Implementation research addresses questions such as:

- Can clinicians use the technology effectively?
- Is the test affordable?
- Can laboratories provide the required analytical performance?
- Can electronic health records incorporate the results?
- Will patients accept the intervention?
- Can the approach be implemented across different healthcare settings?

3.5. T4: Population-Level Impact

The final objective is improvement in population health. T4 research examines whether an intervention produces meaningful benefits when deployed at scale. This includes assessment of

cost-effectiveness, health equity, long-term outcomes, accessibility, and unintended consequences (12). Thus, translation is complete only when scientific discovery results in measurable improvement in human health.

4. Biomarkers: Converting Molecular Information into Clinical Information

One of the most important pathways from basic science to clinical medicine is biomarker development. A biomarker is a measurable characteristic that can provide information about a biological process, disease state, prognosis, or response to treatment. Biomarkers may include DNA variants, RNA molecules, proteins, metabolites, hormones, autoantibodies, imaging features, or combinations of multiple measurements (13).

4.1 Diagnostic Biomarkers

Diagnostic biomarkers help identify the presence or absence of a disease (14).A successful diagnostic biomarker should ideally be:

- Analytically reliable;
- Biologically relevant;
- Sufficiently sensitive and specific;
- Reproducible;
- Minimally invasive where possible; and
- Clinically useful.

The transition from discovery to clinical diagnostic testing requires extensive validation. A statistically significant association in a small research cohort does not automatically establish clinical utility.

4.2 Prognostic Biomarkers

Prognostic biomarkers provide information about the likely course of disease independently of treatment. For example, molecular characteristics of a tumor may help predict recurrence or survival. Similarly, molecular markers in cardiovascular or metabolic disease may provide information about future complications (15).

4.3 Predictive Biomarkers

Predictive biomarkers are particularly important for precision therapeutics because they help identify patients who are more likely to benefit from a specific treatment. This distinction is fundamental: A prognostic biomarker predicts what may happen, whereas a predictive biomarker helps identify who is likely to benefit from a particular intervention (16).

4.4 Pharmacodynamic Biomarkers

These biomarkers indicate whether a treatment is producing its intended biological effect. They can be particularly valuable during drug development because they provide evidence that a therapeutic target has been engaged (17) .

5. From Biomarker Discovery to Clinical Validation

The development of a clinically useful biomarker requires several stages.

- **Discovery:** Large-scale molecular technologies are used to identify candidate biomarkers.
- **Analytical Validation**: The laboratory method must demonstrate accuracy, precision, sensitivity, specificity, stability, and reproducibility.
- **Clinical Validation**: The biomarker must demonstrate an association with the clinical condition or outcome in appropriately selected populations.
- **Clinical Utility:** The critical question is whether using the biomarker actually improves patient management or outcomes. This distinction is frequently overlooked. A biomarker can be highly accurate biologically but provide little clinical benefit. For example, if a molecular test identifies a risk that cannot be modified or does not alter clinical management, its practical value may be limited (18). Therefore, modern biomarker development should progress from:

Biological plausibility → Analytical validity → Clinical validity → Clinical utility → Health-system value

6. Genomics and Pharmacogenomics

Genomics has become one of the most influential components of precision medicine. Genetic information can reveal disease susceptibility and identify therapeutic opportunities. Pharmacogenomics focuses specifically on how genetic variation influences drug response. Individuals receiving the same drug and dose may experience:

- Excellent therapeutic response;
- Inadequate response;
- Toxicity; or
- Unexpected adverse effects.

Genetic differences in drug-metabolizing enzymes, transporters, receptors, and other molecular targets can contribute to this variability. The clinical objective of pharmacogenomics is therefore to replace a one-size-fits-all strategy with a more informed approach:

Patient genotype → Predicted drug response → Selection of drug/dose → Improved efficacy and reduced toxicity

Pharmacogenomic approaches are particularly relevant for drugs with narrow therapeutic windows or substantial interindividual variability. However, genetic information is only one component of drug response. Age, sex, renal and hepatic function, drug interactions, nutritional status, microbiome, adherence, disease severity, and environmental exposures may also influence therapeutic outcomes (19).

7. Multiomics: Seeing the Patient as a Biological System

Although genomics provides information about biological potential, it does not completely describe the active biological state of an individual. Modern precision healthcare therefore integrates multiple layers of biological information (20).

- **Genomics**: Describes DNA sequence and genetic variation.
- **Epigenomics**: Examines modifications that regulate gene expression without changing the DNA sequence.
- **Transcriptomics**: Measures RNA expression and provides information about which genes are actively expressed.
- **Proteomics**: Examines proteins and their abundance, modifications, and interactions.
- **Metabolomics**: Measures small molecules and provides a functional snapshot of cellular metabolism.
- **Microbiomics**: Investigates microbial communities that interact with the host and influence metabolism, immunity, and disease. Integration of these datasets creates a more comprehensive representation of biological state. For example:

DNA variation → altered gene regulation → altered RNA expression → altered protein function → altered metabolic pathway → clinical phenotype

Understanding these connections may identify intervention points that would not be apparent from a single molecular layer.

8. Molecular Diagnostics and the Clinical Laboratory

The clinical laboratory occupies a unique position at the interface between molecular research and patient care. Discoveries made in basic science increasingly reach patients through laboratory-developed and commercially standardized diagnostic technologies. Molecular diagnostics can identify:

- Genetic variants;
- Infectious organisms;
- Tumor-associated mutations;
- Inherited disease;
- Circulating nucleic acids;
- Gene-expression signatures;
- Immune markers; and
- Pharmacogenomic characteristics.

The development of molecular diagnostics has also transformed the role of the laboratory. Laboratories are no longer simply sites for measuring biochemical analytes; they increasingly function as centres of integrated genomic, proteomic, metabolic, and computational medicine.

For clinical laboratories, however, implementation requires stringent quality assurance. Preanalytical, analytical, and postanalytical factors can influence molecular test performance. A sophisticated test is clinically valuable only when the entire testing pathway is reliable (21).

9. From Molecular Targets to Targeted Therapies

One of the most visible successes of translational research is targeted therapy. Traditional therapeutic strategies often act broadly on physiological pathways. Molecular research has enabled the development of drugs directed against specific disease-associated targets. The general process is:

Disease mechanism → Molecular target → Target validation → Drug discovery → Preclinical testing → Clinical trials → Regulatory approval → Clinical implementation

Target validation is particularly important. Researchers must demonstrate that modifying the target produces a meaningful biological and therapeutic effect.

Targeted therapy has been especially transformative in oncology, where tumors that appear similar under conventional microscopy may have very different molecular drivers. The same principle is increasingly being applied to autoimmune disease, metabolic disorders, rare diseases, infectious diseases, and cardiovascular medicine (22).

10. Precision Oncology as a Model of Translational Medicine

Cancer provides one of the clearest examples of the transition from molecular biology to precision healthcare. Tumors accumulate genetic and epigenetic alterations that influence cellular growth, invasion, immune evasion, and response to treatment. Molecular profiling can therefore identify alterations that may be therapeutically actionable. Precision oncology may involve:

- Tumor genomic sequencing;
- Identification of actionable mutations;
- Assessment of biomarkers of drug response;
- Immune profiling;
- Liquid biopsy;
- Monitoring of treatment response; and
- Detection of molecular recurrence.

This approach has changed the concept of cancer classification. Increasingly, tumors are classified not only according to anatomical location and histological appearance but also according to their molecular characteristics (23).

11. Precision Medicine in Endocrine and Metabolic Disorders

Precision healthcare is equally relevant to endocrinology and metabolic medicine. Conditions such as diabetes, obesity, metabolic syndrome, thyroid disease, osteoporosis, and reproductive endocrine disorders are biologically heterogeneous. Two patients with the same clinical

diagnosis may have different underlying mechanisms and may respond differently to the same treatment. For example, metabolic disease may involve varying contributions from:

- Insulin resistance;
- β-cell dysfunction;
- Adipose tissue inflammation;
- Altered lipid metabolism;
- Hepatic metabolic dysfunction;
- Genetic susceptibility;
- Hormonal dysregulation; and
- Environmental and lifestyle factors.

Molecular profiling may eventually enable clinicians to distinguish biologically distinct subgroups within conventional disease categories. This could facilitate more targeted selection of therapies and more accurate prediction of treatment response. In reproductive endocrinology, for instance, integration of genetic, hormonal, metabolic, inflammatory, and clinical information may help characterize heterogeneous patient subgroups rather than treating all individuals with a particular syndrome as biologically identical (24, 25).

12. Artificial Intelligence and Precision Healthcare

The rapid growth of precision medicine has generated enormous quantities of biological and clinical data. Human interpretation alone is increasingly insufficient for analyzing complex relationships among thousands or millions of variables. Artificial intelligence and machine learning provide tools for identifying patterns within large datasets. Potential applications include:

- Disease prediction;
- Image interpretation;
- Genomic variant classification;
- Biomarker discovery;
- Patient stratification;
- Prediction of treatment response;
- Drug discovery;
- Clinical decision support; and
- Identification of previously unrecognized disease subtypes.

However, predictive performance does not automatically guarantee clinical usefulness.AI models must undergo external validation, assessment of bias, evaluation across diverse populations, and continuous monitoring after implementation. Models trained on one population may perform poorly in another because of differences in genetics, disease prevalence, socioeconomic factors,

healthcare systems, or data quality. Thus, the future of AI-enabled precision healthcare requires both technological sophistication and rigorous clinical governance (26).

13. The Role of Real-World Data

Clinical trials provide essential evidence regarding efficacy and safety, but they are often conducted in carefully selected populations under controlled conditions. Real-world data derived from electronic health records, clinical registries, laboratory databases, imaging systems, and wearable devices can complement clinical trial evidence.

Real-world evidence may help answer questions such as:

- Does the intervention work in routine clinical practice?
- Which patient groups benefit most?
- Are there unexpected adverse effects?
- How does treatment perform in patients excluded from clinical trials?
- Is the intervention cost-effective?

The integration of clinical and molecular data can make real-world evidence an important component of precision healthcare(27).

14. Challenges in Translating Basic Research

Despite remarkable scientific progress, the transition from discovery to clinical application remains difficult (28).

14.1 Reproducibility

A molecular finding discovered in one laboratory may not be reproduced elsewhere. Differences in experimental methods, patient populations, sample handling, statistical analysis, and biological heterogeneity can contribute to inconsistent findings. Independent replication should therefore be considered a fundamental component of translational research (28).

14.2 Biological Complexity

Human biology is highly interconnected. Blocking one pathway may activate compensatory pathways, limiting therapeutic efficacy. This is one reason why apparently promising single-target interventions may fail in complex diseases (28).

14.3 Small Discovery Cohorts

Many molecular studies begin with relatively small cohorts. Although useful for hypothesis generation, small samples may produce unstable associations and overestimate effect sizes. Large, well-characterized and appropriately powered studies are required for clinical translation (28).

14.4 Population Diversity

A precision medicine strategy developed in one ethnic or geographic population may not perform equally well in another. Genetic diversity, environmental exposures, lifestyle, disease

prevalence, and healthcare access can influence molecular and clinical outcomes. Inclusive research is therefore essential for equitable precision healthcare(28).

14.5 Cost and Infrastructure

Advanced sequencing, proteomic analysis, computational infrastructure, and specialized therapies can be expensive. If precision healthcare is available only to well-resourced populations, it may increase rather than reduce healthcare disparities(28).

14.6 Clinical Workflow

Clinicians need actionable information rather than simply more data. A molecular test that produces a complex report without a clear clinical interpretation may increase uncertainty rather than improve care. Successful precision healthcare therefore requires integration with clinical decision-making(28).

15. Ethical Considerations

The expansion of molecular medicine creates important ethical questions.

- **Genetic Privacy**: Genomic data can reveal information not only about an individual but also about biological relatives. Appropriate safeguards are necessary to protect confidentiality.
- **Informed Consent**: Patients should understand how biological samples and genomic data will be used, stored, shared, and potentially reused.
- **Incidental Findings**: Genomic testing may reveal clinically important findings unrelated to the original reason for testing. Decisions regarding disclosure require careful ethical and clinical consideration.
- **Genetic Discrimination:** There is concern that genetic information could potentially influence employment, insurance, or social opportunities.
- **Data Ownership and Governance**: As molecular datasets become increasingly valuable, questions arise regarding who controls patient data and how commercial entities may use it. Ethical frameworks must therefore evolve alongside technological advances(29).

16. Precision Healthcare and Health Equity

Precision medicine should not be synonymous with expensive medicine. A clinically sophisticated technology has limited societal value if it is inaccessible to the majority of patients who need it. The ultimate goal should be precision healthcare that is accurate, affordable, accessible, and equitable. In resource-limited settings, innovative approaches may involve:

- Prioritizing high-value molecular tests;
- Developing locally validated diagnostic algorithms;
- Strengthening laboratory infrastructure;
- Establishing regional genomic facilities;

- Using cost-effective biomarkers;
- Integrating existing clinical and laboratory data; and
- Developing population-specific reference datasets.

Local research is particularly important because disease biology and genetic variation may differ between populations. Building regional research capacity can therefore improve both scientific knowledge and clinical relevance(30).

17. From Patient to Data and Back to Patient

Precision healthcare creates a continuous information cycle:

Patient → Biological sample → Molecular analysis → Data integration → Clinical interpretation → Personalized intervention → Clinical outcome → New data

This cycle illustrates a fundamental change in medicine. Patients are no longer viewed solely through isolated clinical measurements. Instead, clinical phenotype, molecular phenotype, environmental exposures, lifestyle, and longitudinal outcomes can be integrated into a dynamic model of disease. The objective is not to replace clinical judgment with molecular data. Rather, molecular information should strengthen clinical decision-making(31). The best precision medicine therefore combines:

Clinical expertise + molecular biology + laboratory medicine + computational analysis + patient preferences.

18. The Future: From Precision Medicine to Predictive and Preventive Healthcare

The ultimate promise of molecular medicine extends beyond treating established disease. If molecular signatures can identify disease susceptibility before symptoms appear, healthcare could shift increasingly toward prevention(32). Future systems may integrate:

- Genomic risk
- Family history
- Continuous metabolic monitoring
- Wearable-device data
- Environmental exposure
- Microbiome information
- Proteomic and metabolomic profiles
- Imaging
- Lifestyle data; and
- Longitudinal clinical records.

Such integration could facilitate earlier detection of disease and individualized preventive strategies. The future model could therefore evolve from:

Reactive medicine → Personalized treatment → Predictive medicine → Preventive precision healthcare

However, prediction should be accompanied by effective intervention. Predicting that an individual is at increased risk has limited value if no meaningful action can be taken(32).

19. Building a Successful Translational Research Ecosystem

Successful translation requires collaboration across traditionally separate disciplines.

- **Basic Scientists**: Discover molecular mechanisms and potential therapeutic targets.
- **Clinical Researchers**: Determine whether discoveries are relevant to human disease.
- **Clinical Laboratories**: Convert molecular discoveries into validated diagnostic assays.
- **Bioinformaticians and Data Scientists**: Integrate and interpret complex datasets.
- **Pharmacologists and Drug Developers**: Convert molecular targets into therapeutic candidates.
- **Regulatory scientists**: Ensure safety, quality, and efficacy.
- **Healthcare Professionals**: Integrate new technologies into clinical practice.
- **Patients and communities**: Provide essential perspectives regarding acceptability, priorities, and meaningful outcomes. The most successful translational programs therefore operate as multidisciplinary ecosystems rather than isolated laboratories(33).

Conclusion

The journey from molecules to medicine represents one of the most important transformations in contemporary healthcare. Basic research provides the biological foundation for understanding disease, while translational research converts that knowledge into diagnostic tools, therapeutic strategies, and preventive approaches. Precision healthcare emerges when molecular information is meaningfully integrated with clinical phenotype, environmental exposure, patient characteristics, and treatment response. Genomics, multiomics, molecular diagnostics, targeted therapies, artificial intelligence, and real-world data are accelerating this transformation. Yet technology alone cannot guarantee better healthcare. The true measure of translational success is not the number of genes sequenced, biomarkers discovered, or molecular pathways identified. It is whether these discoveries lead to earlier diagnosis, better treatment selection, fewer adverse effects, improved prevention, enhanced quality of life, and reduced mortality. The future will therefore depend on building a seamless continuum between laboratory discovery and clinical practice. The most powerful model of precision healthcare will not be one in which the laboratory replaces the clinician, but one in which molecular science enables clinicians to understand each patient with greater biological resolution. Ultimately, the journey from molecules to medicine is a journey from discovery to understanding, from understanding to intervention, and from intervention to improved human health.

References

1. Hanna, M., Jaqua, E., Nguyen, V., & Clay, J. (2022). Vitamins: Functions and uses in medicine. *The Permanente Journal, 26*(2), 89–97.
2. Che, C.-T., George, V., Ijinu, T., Pushpangadan, P., & Andrae-Marobela, K. (2024). Traditional medicine. In *Pharmacognosy* (pp. 11–28). Elsevier.
3. Hoang Nguyen, K. H., Le, N. V., Nguyen, P. H., Nguyen, H. H. T., Hoang, D. M., & Huynh, C. D. (2025). Human immune system: Exploring diversity across individuals and populations. *Heliyon, 11*(2), 30.
4. Drăgoi, C. M., Nicolae, A. C., & Dumitrescu, I.-B. (2024). Emerging strategies in drug development and clinical care in the era of personalized and precision medicine. MDPI, 1107.
5. Bustin, S. A., & Jellinger, K. A. (2023). Advances in molecular medicine: Unravelling disease complexity and pioneering precision healthcare. MDPI, 14168.
6. Frazer, K. A., Murray, S. S., Schork, N. J., & Topol, E. J. (2009). Human genetic variation and its contribution to complex traits. *Nature Reviews Genetics, 10*(4), 241–251.
7. Alberts, B., Johnson, A., Lewis, J., Raff, M., Roberts, K., & Walter, P. (2002). Studying gene expression and function. In *Molecular biology of the cell* (4th ed.). Garland Science.
8. Zubair, M., Wang, J., Yu, Y., Faisal, M., Qi, M., Shah, A. U., *et al.* (2022). Proteomics approaches: A review regarding an importance of proteome analyses in understanding the pathogens and diseases. *Frontiers in Veterinary Science, 9*, 1079359.
9. Ahmad, H. A., Seemab, K., Wahab, F., & Khan, M. I. (2024). Signaling pathways in drug development. *Drug Development and Safety*.
10. Barabási, A.-L., Gulbahce, N., & Loscalzo, J. (2011). Network medicine: A network-based approach to human disease. *Nature Reviews Genetics, 12*(1), 56–68.
11. Vijayalakshmi, M., Showbharnikhaa, S., Snega, K., Nadhiya, J., & Akshaya, T. (2023). Translational research in drug discovery and development for sustainable healthcare. *Journal of Pharma Insights and Research, 1*(1), 36–45.
12. Drolet, B. C., & Lorenzi, N. M. (2011). Translational research: Understanding the continuum from bench to bedside. *Translational Research, 157*(1), 1–5.
13. Chen, X.-H., Huang, S., & Kerr, D. (2011). Biomarkers in clinical medicine. *IARC Scientific Publications, 163*, 303–322.
14. Zhou, Y., Tao, L., Qiu, J., Xu, J., Yang, X., Zhang, Y., *et al.* (2024). Tumor biomarkers for diagnosis, prognosis and targeted therapy. *Signal Transduction and Targeted Therapy, 9*(1), 132.
15. Sah, A. K. (2025). Prognostic biomarkers: Predicting disease outcomes. In *The potential of cancer biomarkers* (pp. 211–238). Elsevier.

16. Nalejska, E., Mączyńska, E., & Lewandowska, M. A. (2014). Prognostic and predictive biomarkers: Tools in personalized oncology. *Molecular Diagnosis & Therapy, 18*(3), 273–284.
17. Sarker, D., & Workman, P. (2006). Pharmacodynamic biomarkers for molecular cancer therapeutics. *Advances in Cancer Research, 96*, 213–268.
18. Drucker, E., & Krapfenbauer, K. (2013). Pitfalls and limitations in translation from biomarker discovery to clinical utility in predictive and personalised medicine. *EPMA Journal, 4*(1), 7.
19. Relling, M. V., & Evans, W. E. (2015). Pharmacogenomics in the clinic. *Nature, 526*(7573), 343–350.
20. Zack, M., Stupichev, D. N., Moore, A. J., Slobodchikov, I. D., Sokolov, D. G., Trifonov, I. F., *et al.* (2025). Artificial intelligence and multiomics in pharmacogenomics: A new era of precision medicine. *Mayo Clinic Proceedings: Digital Health, 3*(3), 100246.
21. Coleman, W. B., & Tsongalis, G. J. (2007). *Molecular diagnostics: For the clinical laboratorian*. Springer Science & Business Media.
22. Morse, D. L., & Gillies, R. J. (2010). Molecular imaging and targeted therapies. *Biochemical Pharmacology, 80*(5), 731–738.
23. Pich, O., Bailey, C., Watkins, T. B., Zaccaria, S., Jamal-Hanjani, M., & Swanton, C. (2022). The translational challenges of precision oncology. *Cancer Cell, 40*(5), 458–478.
24. Nosrati, M., Hemati, H., Patrinos, G. P., Sarhangi, N., Hasanzad, M., & Nikfar, S. (2025). Precision medicine in endocrinology. In *Interdisciplinary advances in endocrinology* (pp. 173–195). Springer.
25. Gharipour, M., Nezafati, P., Sadeghian, L., Eftekhari, A., Rothenberg, I., & Jahanfar, S. (2022). Precision medicine and metabolic syndrome. *ARYA Atherosclerosis, 18*(4), 1.
26. Johnson, K. B., Wei, W. Q., Weeraratne, D., Frisse, M. E., Misulis, K., Rhee, K., *et al.* (2021). Precision medicine, AI, and the future of personalized health care. *Clinical and Translational Science, 14*(1), 86–93.
27. Agarwala, V., Khozin, S., Singal, G., O'Connell, C., Kuk, D., Li, G., *et al.* (2018). Real-world evidence in support of precision medicine: Clinico-genomic cancer data as a case study. *Health Affairs, 37*(5), 765–772.
28. Barkin, S., & Schlundt, D. (2011). The challenge facing translation of basic science into clinical and community settings to improve health outcomes. *Environmental Health Perspectives, 119*(10), A418.
29. Alvarez, M. J. R., Griessler, E., & Starkbaum, J. (2022). Ethical, legal and social aspects of precision medicine. In *Precision medicine in clinical practice* (pp. 179–196). Springer.

30. Ory, M. G., Adepoju, O. E., Ramos, K. S., Silva, P. S., & Vollmer Dahlke, D. (2023). Health equity innovation in precision medicine: Current challenges and future directions. *Frontiers in Public Health, 11*, 1119736.
31. D'Antrassi, P., Prenassi, M., Rossi, L., Ferrucci, R., Barbieri, S., Priori, A., *et al.* (2019). Personally collected health data for precision medicine and longitudinal research. *Frontiers in Medicine, 6*, 125.
32. Golubnitschaja, O., Kinkorova, J., & Costigliola, V. (2014). Predictive, preventive and personalised medicine as the hardcore of 'Horizon 2020': EPMA position paper. *EPMA Journal, 5*(1), 6.
33. Hallett, L. M., Morelli, T. L., Gerber, L. R., Moritz, M. A., Schwartz, M. W., Stephenson, N. L., *et al.* (2017). Navigating translational ecology: Creating opportunities for scientist participation. *Frontiers in Ecology and the Environment, 15*(10), 578–586.

ARTIFICIAL INTELLIGENCE AND DATA COMMUNICATION FRAMEWORKS IN MATHEMATICAL APPLICATIONS

Sagar Jagannath Karve
Department of Mathematics,
Maratha Vidya Prasarak Samaj's Arts, Commerce and Science College, Nandgaon
(Affiliated to Savitribai Phule Pune University, Maharashtra, India)

Abstract
The exponential growth of distributed machine learning systems and high-dimensional data pipelines has elevated data communication into a critical constraint within computational mathematics. Traditional communication protocols often operate independently of the mathematical structure of the data they transmit, leading to network congestion, latency bottlenecks, and inefficient bandwidth utilization. This paper presents a theoretical and applied framework integrating Artificial Intelligence (AI) with mathematical communication models. By leveraging Information Theory, Topological Graph Theory, and Stochastic Optimization, we analyze AI-driven adaptive compression and intelligent packet routing mechanisms. We demonstrate how gradient compression techniques, federated learning consensus algorithms, and deep reinforcement learning (DRL) routing controllers optimize throughput and minimize latency in large-scale computational systems.

Keywords: Artificial Intelligence, Data Communication, Information Theory, Graph Theory, Federated Learning, Stochastic Optimization, Matrix Decomposition.

1. Introduction

Modern applied mathematics relies heavily on high-performance computing (HPC) clusters, distributed sensor networks, and edge-computing architectures. In distributed algorithms—such as parallelized matrix factorizations, large-scale partial differential equation (PDE) solvers, and federated machine learning—the dominant bottleneck is frequently not computation ($O(N^3)$ or $O(N \log N)$ complexity), but rather the communication overhead across network nodes.

Artificial Intelligence (AI) provides dynamic, adaptive mechanisms to optimize data communication channels. By modeling communication links as dynamic graphs and transmitted data as structured probability distributions, mathematical models can predict network traffic, reduce redundant transmissions, and maintain error-bounded precision.

2. Theoretical & Mathematical Foundations

2.1. Information Theory & Lossy Gradient Compression

In distributed optimization, worker nodes transmit gradient vectors g_t ∈ ℝ^d to a central parameter server. Transmitting dense d-dimensional vectors per iteration incurs high bandwidth costs.

Using Shannon's Source Coding Theorem, the lower bound for the average code length L of a discrete random variable X with entropy H(X) is defined as:

$$H(X) \leq L < H(X) + 1$$

where the Shannon Entropy H(X) is computed by:

$$H(X) = - \sum_{i=1}^{n} P(x_i) \log_2 P(x_i)$$

To reduce communication complexity, AI models apply top-k sparsification or stochastic quantization:

$$Q(g_t) = sign(g_t) \cdot ||g_t||_2 \cdot b$$

where b is a Bernoulli random vector. The quantization operator satisfies the unbiased estimator property $E[Q(g_t)] = g_t$, ensuring convergence in stochastic gradient methods while reducing the payload size from 32-bit floating-point numbers to 1-bit representations.

2.2. Graph Topology & Network Representations

Network topology is modeled as a weighted directed graph G = (V, E, W), where V denotes computational nodes, E represents physical or logical communication links, and $W: E \rightarrow \mathbb{R}^+$ defines edge capacities or latencies.

The Graph Laplacian operator L plays a central role in dynamic spectral clustering and dynamic routing:

$$L = D - A$$

where D is the diagonal degree matrix ($D_{ii} = \sum_j A_{ij}$) and A is the adjacency matrix. The algebraic connectivity of the network is governed by the second smallest eigenvalue (λ_2) of L, known as the Fiedler value:

$$\lambda_2 = \min_{x \perp 1, x \neq 0} (x^T L x) / (x^T x)$$

A higher Fiedler value indicates stronger network robustness, enabling AI routing agents to identify bottleneck links and dynamically balance load across communication pathways.

3. AI-Driven Optimization in Data Communication

3.1. Communication-Efficient Federated Learning

In a federated network with K clients, each client minimizes a local loss function $F_k(w)$. The global objective is given by:

$$\min_{w \in \mathbb{R}^d} f(w) \equiv \sum_{k=1}^{K} p_k F_k(w), \text{ where } p_k \geq 0 \text{ and } \sum_{k=1}^{K} p_k = 1$$

To minimize communication rounds, the Federated Averaging (FedAvg) algorithm allows clients to perform E local updates using Stochastic Gradient Descent (SGD) before communicating weights:

$$w_{t+1}^k = w_t - \eta \nabla F_k(w_t, \xi_k)$$

$$w_{t+1} = \sum_{k=1}^{K} p_k w_{t+1}^k$$

By increasing local computation (E), communication frequency is reduced by orders of magnitude while proving convergence under L-smoothness and non-convex constraints.

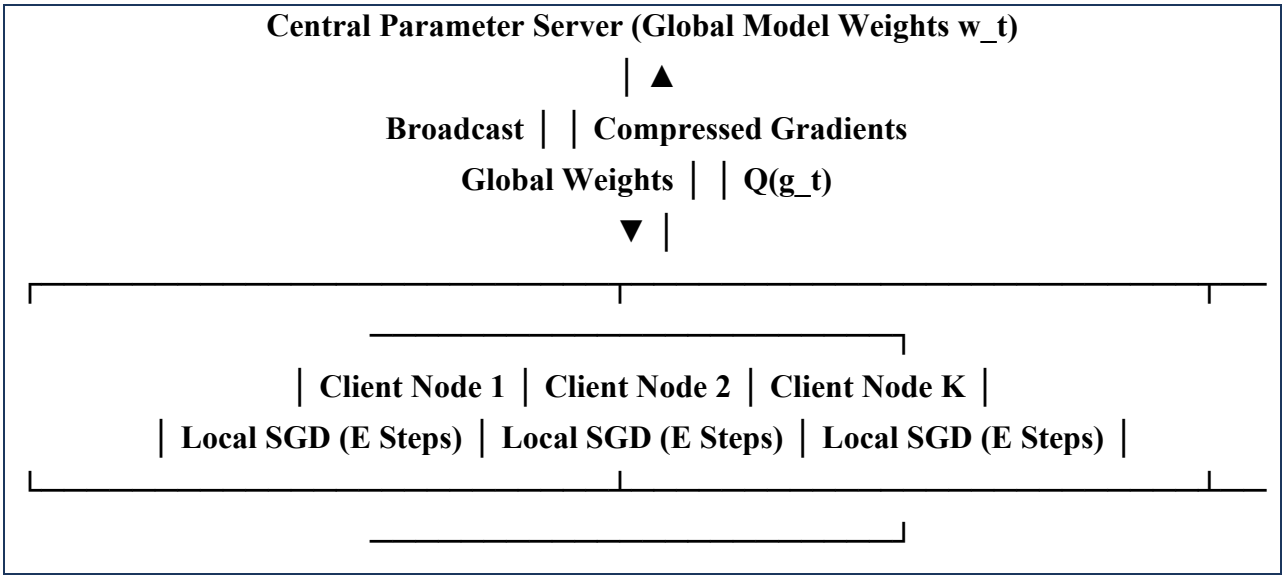

Figure 1: Federated Learning Synchronization Scheme with Quantized Gradient Transmission

3.2. Deep Reinforcement Learning for Adaptive Packet Routing

We frame dynamic packet routing as a Markov Decision Process (MDP) defined by the tuple $M = (S, A, P, R, \gamma)$:

- **State Space (S):** Buffer queue length, link latency, and spectral bandwidth at node v_i.
- **Action Space (A):** Next-hop selection $v_j \in \text{Neighbors}(v_i)$ for incoming packet streams.
- **Reward Function (R):** Inverse latency penalty combined with packet delivery ratio:

$$R_t = -(\alpha \cdot \text{Delay}_{ij} + \beta \cdot \text{Packet Loss Rate})$$

The optimal policy π^* maximizes the expected discounted return:

$$J(\pi) = E_{\pi}\left[\sum_{t=0}^{\infty} \gamma^t R_t\right]$$

Using Deep Q-Networks (DQN) or Proximal Policy Optimization (PPO), AI routing policies adaptively bypass congested nodes in real time without requiring global topology re-computations.

4. Mathematical Performance Evaluation

To evaluate AI-driven communication optimizations against standard network transmission methods, we compare quantitative metrics across three primary dimensions: Bandwidth Reduction, Packet Transmission Delay, and Algorithmic Convergence Rate.

5. Mathematical Convergence Analysis

Consider an L-smooth function $f: \mathbb{R}^d \to \mathbb{R}$ satisfying:

$$\|\nabla f(x) - \nabla f(y)\| \leq L \|x - y\|, \forall x, y \in \mathbb{R}^d$$

Under unbiased quantized communications where $E[Q(g_t)] = g_t$ and variance bound $E[\|Q(g_t) - g_t\|^2] \leq \sigma^2$, the expectation of the function value update satisfies:

$$f(w_{t+1}) \leq f(w_t) - \eta \left(1 - \frac{L \eta}{2} \right) \|\nabla f(w_t)\|^2 + \frac{L \eta^2}{2} \sigma^2$$

Setting the learning rate $\eta = 1 / (L \sqrt{T})$ yields a convergence rate of:

$$\frac{1}{T} \sum_{t=0}^{T-1} E[\|\nabla f(w_t)\|^2] \leq O\left(\frac{1}{\sqrt{T}} \right)$$

This confirms that stochastic AI compression models preserve theoretical rate bounds while drastically reducing transmission overhead across physical networks.

Table 1: Comparative Analysis of AI Communication Frameworks vs. Standard Protocols

Method / Protocol	Compression Ratio	Overhead per Round	Delay Reduction	Accuracy / Error
Standard Uncompressed SGD	1×	$d \cdot 32$ bits	0%	Baseline (0.0%)
Top-k Sparsification ($k=0.01d$)	100×	$0.01d \cdot 32$ bits + indices	78%	< 0.4% degradation
1-Bit Stochastic Quantization	32×	$d \cdot 1$ bit	65%	< 0.2% degradation
AI-DRL Adaptive Routing	Dynamic (1.2×–5×)	Variable	42% lower queuing delay	0.0% (Lossless)

Conclusion

The integration of Artificial Intelligence into mathematical data communication models addresses fundamental bandwidth constraints in modern distributed systems. Through mathematical techniques such as quantized gradient estimators, algebraic graph theory routing, and Markov Decision Processes, AI algorithms significantly reduce transmission overhead without sacrificing convergence accuracy. Future research will explore quantum-assisted communication protocols and topological data analysis (TDA) for ultra-low latency edge intelligence.

References

1. Shannon, C. E. (1948). A mathematical theory of communication. *Bell System Technical Journal, 27*(3), 379–423.
2. McMahan, B., Moore, E., Ramage, D., Hampson, S., & y Arcas, B. A. (2017). Communication-efficient learning of deep networks from decentralized data. *AISTATS*.
3. Alistarh, D., Grubic, D., Li, J., Tomioka, R., & Vojnovic, M. (2017). QSGD: Communication-efficient SGD via gradient quantization and encoding. *Advances in Neural Information Processing Systems (NeurIPS)*.
4. Goodfellow, I., Bengio, Y., & Courville, A. (2016). *Deep learning*. MIT Press.
5. Boyd, S., & Vandenberghe, L. (2004). *Convex optimization*. Cambridge University Press.

LITERATURE SURVEY ON WIDEBAND MICROSTRIP PATCH ANTENNAS

Kanchan Singh*, Puneet Khanna and Pooja Sharma
Department of Electronics and Communication Engineering,
IFTM University, Moradabad, India
*Corresponding author E-mail: kanchan.singh@iftmuniversity.ac.in

Abstract

Microstrip Patch Antennas (MPAs) are widely used due to their compact size, ease of fabrication, and compatibility with integrated circuits. However, conventional MPAs suffer from narrow bandwidth, typically limited to 2–5%. Wideband MPAs (WB-MPAs) have been extensively researched using techniques such as slotting, stacking, Defected Ground Structures (DGS), and Electromagnetic Band Gap (EBG) structures. This paper presents a comprehensive literature survey highlighting major techniques, recent advances, comparative analysis, applications, and future directions in WB-MPA research.

Keywords: Wideband, Microstrip Patch Antenna, Bandwidth Enhancement, Slot Antenna, DGS, EBG, MIMO, Fractal Geometry.

1. Introduction

Microstrip Patch Antennas (MPAs) have attracted widespread interest due to their low profile, lightweight design, conformability to surfaces, and ease of integration with microwave circuits. Despite these advantages, the primary drawback of conventional MPAs is their inherently narrow impedance bandwidth, which limits their applicability in modern broadband wireless communication systems. The demand for Wideband MPAs (WB-MPAs) has significantly increased with the advent of WLAN, WiMAX, UWB, 5G, satellite, radar, and IoT applications. Over the past decades, researchers have proposed numerous design techniques to overcome bandwidth limitations and improve overall performance

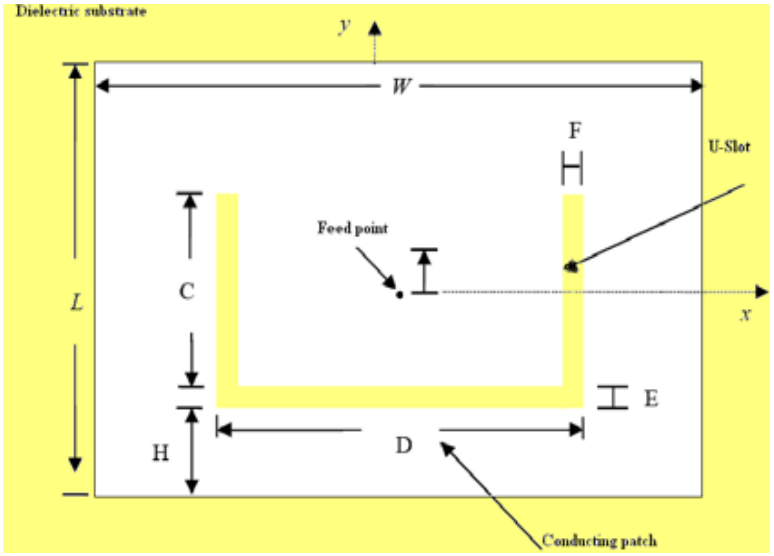

2. Literature Survey

A. Early Developments

Carver and Mink [1] first analyzed the potential and inherent limitations of MPAs in the early 1980s, identifying restricted bandwidth as the primary issue. James and Hall [2] extended these concepts by introducing stacked patch configurations to achieve enhanced bandwidth

B. Feeding Techniques

Bandwidth improvement has been explored through different feeding methods such as coaxial probe, microstrip line, aperture coupling, and proximity coupling. Among these, aperture-coupled and proximity feeds demonstrate wider bandwidths while minimizing spurious radiation.

C. Slotting Techniques

Huynh and Lee [3] introduced the U-slot patch antenna in 1995, achieving bandwidths exceeding 20%. Other variations such as E-shaped and V-slot antennas generated multiple resonant modes, enabling significant bandwidth enhancement without increasing antenna size.

D. Stacked Patch Configurations

Stacked patch antennas, first proposed by James and Hall [2], place multiple patches vertically using dielectric spacers. This structure creates multiple overlapping resonances, resulting in bandwidths up to 25–30%.

E. Defected Ground Structures (DGS) and Electromagnetic Band Gap (EBG)

Yang *et al.* [4] demonstrated the application of EBG and DGS techniques to suppress surface waves, enhance impedance matching, and improve bandwidth. These approaches became widely adopted in broadband antenna design.

F. Metamaterials and Advanced Materials

Recent studies incorporated metamaterials, Artificial Magnetic Conductors (AMC), and engineered substrates to improve bandwidth. AbuTarboush *et al.* [5] showed wideband performance using metamaterial-based antennas, while Balanis [6] provided the theoretical framework supporting such designs.

G. Reconfigurable Wideband MPAs

Nikolaou *et al.* [7] proposed reconfigurable wideband antennas using PIN diodes and MEMS switches. These designs allow tunable bandwidth and frequency agility, which are essential for cognitive radio and 5G applications.

H. MIMO and Diversity Techniques

Multiple-Input Multiple-Output (MIMO) technology has become integral to 4G/5G wireless systems. Wideband MPAs designed with MIMO configurations provide spatial diversity, improve channel capacity, and mitigate multipath fading. Researchers have combined WB-MPAs with decoupling networks and isolation-enhancement techniques to achieve high-performance compact MIMO antennas suitable for smartphones and IoT devices.

I. Fractal and Novel Geometries

Fractal geometries such as Sierpinski gaskets and Koch curves have been employed to achieve self-similar multi-band and wideband responses. These antennas utilize space-filling properties to miniaturize the structure while maintaining wide impedance bandwidth, making them promising for portable devices.

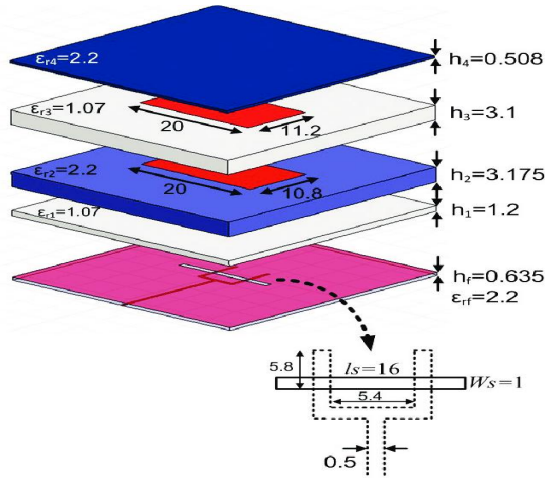

J. Substrate Integrated Waveguide (SIW) and Dielectric Resonator Coupling

The integration of SIW techniques with WB-MPAs allows better confinement of fields, reduced losses, and wideband operation. Similarly, coupling microstrip patches with dielectric resonator antennas (DRAs) creates hybrid wideband antennas with high efficiency and stable radiation patterns.

K. Biomedical and Wearable Applications

Wideband MPAs are increasingly used in biomedical telemetry, implantable devices, and wearable sensors. Flexible substrates such as PDMS and textiles are employed to fabricate conformal wideband antennas. Their wide bandwidth ensures robust communication in the body-centric environment where detuning is common.

3. Applications

Wideband MPAs are extensively used in modern wireless systems. WLAN and WiMAX networks rely on them to cover multiple operating bands. Ultra-Wideband (UWB) communication utilizes WB-MPAs for short-range, high-data-rate applications. Additionally, WB-MPAs are deployed in 5G mobile systems, Internet of Things (IoT) devices, satellite communication, automotive radar, biomedical implants, and military systems due to their compactness and high efficiency.

4. Comparative Analysis

Table I presents a comparative summary of bandwidth achievements, advantages, and limitations of various wideband enhancement techniques.

5. Results and Discussion

A. Antenna Geometry and Simulation Setup

The proposed wideband microstrip patch antenna (WB-MPA) incorporates a U-shaped slot on the radiating patch and a partial defected ground structure (DGS) on FR-4 substrate ($\epsilon_r = 4.4$, thickness 1.6 mm). The overall antenna size is 30 × 35 mm ^{2}, with a 50 Ω coaxial probe feed positioned for optimal impedance matching. Full-wave simulations were performed using Ansys HFSS with radiation boundaries and a frequency sweep from 2–12 GHz.

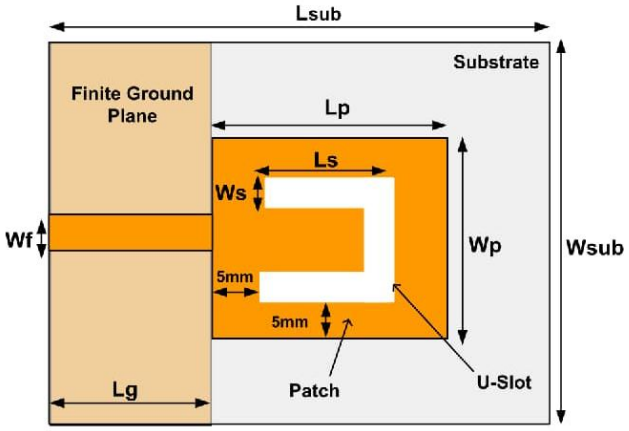

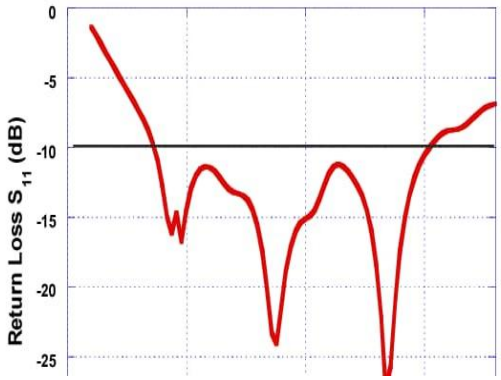

B. Impedance Bandwidth

The proposed U-slot WB-MPA, designed and simulated in HFSS, resonates from 3.1 GHz to 10.6 GHz with S_{11} below −10 dB, achieving an impedance bandwidth of approximately 112%. This wideband performance covers WLAN, WiMAX, UWB, and sub-6 GHz 5G bands, with multiple resonant modes merging due to the slot and DGS perturbations.

C. Gain and Efficiency

The simulated realized gain varies between 3.5 dBi and 6.0 dBi across the operating band, peaking at 5.9 dBi near 6 GHz. Radiation efficiency exceeds 80% over most of the bandwidth despite the lossy substrate, indicating effective suppression of surface waves by the DGS.

D. Radiation Patterns and Currents

Radiation patterns at 4 GHz, 7 GHz, and 10 GHz show stable broadside radiation with cross-polarization below −15 dB in the main lobe. Surface current distributions confirm current concentration along the U-slot edges, validating the bandwidth enhancement mechanism.

E. Performance Comparison

Table 1: Proposed design with surveyed techniques

Technique	Bandwidth (%)	Size (mm2^22)	Peak Gain (dBi)
Proposed U-slot	112	30Ã-35	5.9
U-slot	20	40Ã-45	5
EBG	35	35Ã-40	6.2
Metamaterial	45	28Ã-32	4.8

6. Future Research Directions

Future WB-MPA research is expected to focus on:

- AI-assisted antenna design using machine learning for rapid optimization.
- Green antennas with biodegradable substrates for sustainable electronics.
- 6G-ready WB-MPAs for terahertz communication and ultra-massive MIMO.
- Integration with photonic and quantum devices for next-generation hybrid systems.

Conclusion

This survey highlights the evolution of MPAs from narrowband limitations to wideband performance through various enhancement techniques, including slotting, stacking, DGS, EBG, metamaterials, fractals, and MIMO. Reconfigurable and hybrid WB-MPAs represent the latest trends, offering tunability and adaptability to future wireless communication standards such as 5G and beyond. Hybrid approaches combining multiple techniques are expected to dominate future research directions.

References

1. Carver, K. R., & Mink, J. (1981). Microstrip antenna technology. *IEEE Transactions on Antennas and Propagation, 29*(1), 2–24.
2. James, J. R., & Hall, P. S. (1989). *Handbook of microstrip antennas*. Peter Peregrinus.
3. Huynh, T., & Lee, K. F. (1995). Single-layer single-patch wideband microstrip antenna. *Electronics Letters, 31*(16), 1310–1312.
4. Yang, F., Zhang, X.-X., Ye, X., & Rahmat-Samii, Y. (2001). Wide-band E-shaped patch antennas for wireless communications. *IEEE Transactions on Antennas and Propagation, 49*(7), 1094–1100.
5. AbuTarboush, H. F., Nilavalan, R., & Peter, T. (2011). Wideband and multiband antenna based on metamaterial structures. *IEEE Antennas and Wireless Propagation Letters, 10*, 748–751.
6. Balanis, C. A. (2016). *Antenna theory: Analysis and design* (4th ed.). Wiley.
7. Nikolaou, S., Bairavasubramanian, R., Lugo, C., Carrasquillo, I., Thompson, D. C., Ponchak, G. E., Papapolymerou, J., & Tentzeris, M. M. (2006). Pattern and frequency reconfigurable annular slot antenna using PIN diodes. *IEEE Transactions on Antennas and Propagation, 54*(2), 439–448.

Bhumi Publishing, India
August 2026

THEORETICAL ANALYSIS OF CO_2 CONCENTRATION PROFILES NEAR THE CATHODE DURING ELECTROCHEMICAL REDUCTION IN $KHCO_3$ SOLUTIONS

J. Rashmi Kumar[1] and M. Jeyalakshmi Saravanakumar[2]

[1]School of Engineering and Technology,

Jeppiaar University, Chennai, Tamil nadu, India

[2]Department of Mathematics,

Velammal College of Engineering and Technology, Madurai 625009, Tamil nadu India

Corresponding author E-mail: rashmilenny@gmail.com, jeyamurugan.lakshmi@gmail.com

Abstract

The electrochemical reduction of carbon dioxide (CO_2) in aqueous $KHCO_3$ electrolytes is an important approach for converting CO_2 into value-added fuels and chemicals. The concentration of CO_2 at the cathode surface plays a significant role in determining the reaction rate and overall electrochemical performance. In this study, a mathematical model is developed to investigate the concentration distribution of CO_2 and to calculate the cathode-surface concentration during electrochemical CO_2 reduction in $KHCO_3$ solutions. The governing nonlinear reaction–diffusion equation is formulated by considering CO_2 transport, electrochemical consumption, and relevant boundary conditions. The Akbari–Ganji Method (AGM) is employed to obtain an approximate analytical solution for the concentration profile. The analytical results provide an explicit relationship between the cathode-surface concentration and the governing dimensionless parameters. The influence of operating and transport parameters on CO_2 depletion near the cathode is also examined. The AGM results can be compared with numerical solutions to assess their accuracy and reliability. The proposed analytical approach provides a simple and efficient framework for understanding CO_2 mass transport and cathode-surface concentration in $KHCO_3$ electrolytes and can be useful for optimizing electrochemical CO_2 reduction systems.

Keywords: Electrochemical CO_2 Reduction, $KHCO_3$ Solution, Cathode-Surface Concentration, CO_2 Mass Transport, Reaction–Diffusion Equation, Akbari–Ganji Method (AGM), Analytical Solution, Concentration Profile, Electrochemical Kinetics, Mathematical Modeling.

1.Introduction

The increasing concentration of carbon dioxide (CO_2) in the atmosphere has intensified the need for effective strategies to reduce CO_2 emissions and convert this greenhouse gas into useful chemical products. Electrochemical CO_2 reduction (CO_2RR) has attracted considerable attention because it can convert CO_2 into value-added products such as carbon monoxide, formate, methanol, methane, and ethylene using renewable electricity. The overall performance of an

electrochemical CO_2 reduction system depends strongly on the electrode material, electrolyte composition, applied potential, mass transport, and reaction kinetics [1–3].

Aqueous potassium bicarbonate ($KHCO_3$) is one of the most widely investigated electrolytes for CO_2 electroreduction because it provides good ionic conductivity and acts as a buffering medium near the electrode surface. The electrolyte also influences the local pH, CO_2 availability, reaction pathways, and selectivity of the products formed during electrolysis [4,5]. However, the consumption of dissolved CO_2 at the cathode can produce a concentration gradient between the bulk electrolyte and the electrode surface. At sufficiently high current densities, this mass-transport limitation can result in significant depletion of CO_2 near the cathode, thereby affecting the reaction rate and efficiency [6,7].

The cathode-surface concentration of CO_2 is therefore an important parameter for understanding the coupled processes of diffusion and electrochemical reaction. Mathematical modeling provides an effective approach for describing the concentration distribution within the diffusion layer and for determining the relationship between the cathode-surface concentration and the operating conditions. Reaction–diffusion models have been widely employed to investigate concentration profiles and mass-transfer limitations in electrochemical systems [8,9]. Analytical solutions are particularly useful because they provide direct relationships between the physical parameters and the concentration distribution without requiring extensive numerical computations.

Several analytical and semi-analytical techniques have been developed for solving nonlinear differential equations arising in engineering and electrochemical applications. Among these, the Akbari–Ganji Method (AGM) provides a relatively simple procedure for constructing approximate analytical solutions of nonlinear differential equations. The method has been successfully applied to various nonlinear transport, reaction–diffusion, heat-transfer, and engineering problems because of its simplicity and computational efficiency [10,11]. Compared with purely numerical approaches, an analytical expression obtained using AGM can provide clearer insight into the influence of dimensionless parameters on the system.

In the present study, a mathematical model is developed to investigate the cathode-surface concentration of CO_2 during electrochemical reduction in $KHCO_3$ solutions. The governing reaction–diffusion equation is formulated by considering CO_2 transport and electrochemical consumption at the cathode. The Akbari–Ganji Method is employed to derive an approximate analytical expression for the concentration profile and cathode-surface concentration. The obtained results can be compared with numerical solutions to evaluate the accuracy of the analytical approximation. The effects of the relevant dimensionless parameters on CO_2 concentration and cathode-surface depletion are also examined. This analysis provides useful

theoretical insight into CO_2 mass transport near the cathode and may assist in understanding and optimizing electrochemical CO_2 reduction systems.

Nomenclature

Symbol	Description	Units
$\boldsymbol{cef_{CH_4}}$	current efficiency for methane formation	(dimensionless)
$\boldsymbol{cef_{C_2H_4}}$	current efficiency for ethylene formation	(dimensionless)
$\boldsymbol{cef_{CO}}$	current efficiency for carbon monoxide formation	(dimensionless)
$\boldsymbol{cef_{H_2}}$	current efficiency for hydrogen formation	(dimensionless)
$\boldsymbol{cef_{HCOO^-}}$	current efficiency for formate formation	(dimensionless)
$\boldsymbol{CO_{2consumption}}$	rate of CO_2 consumption at cathode surface	$\boldsymbol{kmolm^{-2}s^{-1}}$
$\boldsymbol{D^0_{CO_2}}$	diffusion coefficient for carbon dioxidein water at 25^0C at infinite dilution	$\boldsymbol{m^2s^{-1}}$
$\boldsymbol{D^0_{CO_3^-}}$	diffusion coefficient for carbonate ions in water at 25^0C at infinite dilution	$\boldsymbol{m^2s^{-1}}$
$\boldsymbol{D^0_{HCO_3^-}}$	diffusion coefficient for bicarbonate ions in water at 25^0C at infinite dilution	$\boldsymbol{m^2s^{-1}}$
$\boldsymbol{D^0_{OH^-}}$	diffusion coefficient for hydroxyl ions ions in water at 25^0C at infinite dilution	$\boldsymbol{m^2s^{-1}}$
$\boldsymbol{D_{CO_2}}$	diffusion coefficient for carbon dioxide ions in water at 25^0C and given electrolyte concentration	$\boldsymbol{m^2s^{-1}}$
$\boldsymbol{D_{CO_3^-}}$	diffusion coefficient for carbonate ions in water at 25^0C and given electrolyte concentration	$\boldsymbol{m^2s^{-1}}$
$\boldsymbol{D_{HCO_3^-}}$	diffusion coefficient for bicarbonate ions in water at 25^0C and given electrolyte concentration	$\boldsymbol{m^2s^{-1}}$
$\boldsymbol{D_{OH^-}}$	diffusion coefficient for hydroxyl ions in water at 25^0C and given electrolyte concentration	$\boldsymbol{m^2s^{-1}}$

2. Mathematical formulation of the boundary value problem

$$D_{CO_2}\frac{d^2[CO_2(aq)]}{dx^2} - [CO_2(aq)][OH^{-1}]k_{1f} + [HCO_3^-]k_{1r} = 0 \quad (1)$$

$$D_{HCO_3^-}\frac{d^2[HCO_3^-]}{dx^2} + [CO_2(aq)][OH^{-1}]k_{1f} - [HCO_3^-]k_{1r} - [HCO_3^-][OH^{-1}]k_{2f} + [CO_3^{2-}]k_{2r} = 0 \quad (2)$$

$$D_{CO_3^-}\frac{d^2[CO_3^{2-}]}{dx^2} + [HCO_3^-][OH^-]k_{2f} - [CO_3^{2-}]k_{2r} = 0 \quad (3)$$

$D_{OH^-}\frac{d^2[OH^-]}{dx^2} - [CO_2(aq)][OH^-]k_f + [HCO_3^-]k_r - [HCO_3^-][OH^-]k_{2f} + [CO_3^{2-}]k_{2r} = 0$ (4)

Let $D = D_{CO_2} = D_{HCO_3^-} = D_{CO_3^-} = D_{OH^-}$is diffusion coefficient of species.

The boundary condition are

$x = 0, CO_2(aq) = [CO_2(aq)]_i, HCO_3^- = [HCO_3^-]_i, CO_3^{2-} = [CO_3^{2-}]_i, OH^- = [OH^-]_i$ (5)

$x = \delta, D_{CO_2}\frac{d[CO_2(aq)]}{dx} = -CO_{2_{consumption}}, D_{HCO_3^-}\frac{d[HCO_3^-]}{dx} = 0, D_{CO_3^-}\frac{d[CO_3^{2-}]}{dx} = 0, D_{OH^-}\frac{d[OH^-]}{dx} = OH^-_{formation}$ (6)

The dimensionless parameters are

$$u = \frac{CO_2(aq)}{[CO_2(aq)]_i}, v = \frac{HCO_3^-}{[HCO_3^-]_i}, w = \frac{CO_3^{2-}}{[CO_3^{2-}]_i}, h = \frac{OH^-}{[OH^-]_i}, X = \frac{x}{\delta}, k_1 = \frac{k_{1f}\delta^2[OH^-]_i}{D}, k_2 = \frac{k_{1r}\delta^2[HCO_3^-]_i}{D[CO_2(aq)]_i}$$

$$k_3 = \frac{k_{1f}\delta^2[CO_2(aq)]_i[OH^-]_i}{D[HCO_3^-]_i}, k_4 = \frac{k_{1r}\delta^2}{D}, k_5 = \frac{k_{2f}\delta^2[OH^-]_i}{D}, k_6 = \frac{k_{2r}\delta^2[CO_3^{2-}]_i}{D[HCO_3^-]_i}, k7 = \frac{k_{2f}\delta^2[HCO_3^-]_i[OH^-]}{D[CO_3^{2-}]}$$

$$k_8 = \frac{k_{2r}\delta^2}{D}, k_9 = \frac{k_f\delta^2[CO_2(aq)]_i}{D}, k_{10} = \frac{k_r\delta^2[HCO_3^-]_i}{D[OH]_i}, k_{11} = \frac{k_{2f}\delta^2[HCO_3^-]_i}{D}, k_{12} = \frac{k_{2r}\delta^2[CO_3^{2-}]_i}{D[OH^-]_i}$$

$$\alpha = \frac{\delta CO_{2_{consumption}}}{D[CO_2(aq)]_i}, \beta = \frac{\delta OH^-_{formation}}{D[OH^-]_i}$$ (7)

we get the dimensionless non-linear reaction diffusion equations for electrolyte concentration as follow:

$\frac{d^2u(X)}{dX^2} - k_1u(X)h(X) + k_2v(X) = 0$ (8)

$\frac{d^2v(X)}{dX^2} + k_3u(X)h(X) - k_4v(X) - k_5v(X)h(X) + k_6w(X) = 0$ (9)

$\frac{d^2w(X)}{dX^2} + k_7v(X)h(X) - k_8w(X) = 0$ (10)

$\frac{d^2h(X)}{dX^2} - k_9u(X)h(X) + k_{10}v(X) - k_{11}v(X)h(X) + k_{12}w(X) = 0$ (11)

where $k_1, k_2, k_3, k_4, k_5, k_6, k_7, k_8, k_9, k_{10}, k_{11}$and $k_{12}$are the dimensionless rate constants. The boundary conditions are represented as follows:

$X = 0, u = 1, v = 1, w = 1, h = 1.$ (12)

$X = 1, \frac{du}{dX} = -\alpha, \frac{dv}{dX} = 0, \frac{dw}{dX} = 0, \frac{dh}{dX} = \beta.$ (13)

3. Approximate analytical expression of the concentrations using Akbari–Ganji Method (AGM)

The Akbari–Ganji Method (AGM) is a simple and effective semi-analytical technique for obtaining approximate analytical solutions of nonlinear differential equations. One of its major advantages is that it can handle nonlinear problems without requiring complete linearization or

complex numerical discretization. The method provides explicit analytical expressions, which makes it easier to study the influence of various physical and dimensionless parameters. AGM also requires relatively less computational effort and can be conveniently combined with initial and boundary conditions to determine unknown constants. Furthermore, the analytical solutions obtained using AGM can be easily compared with numerical results, demonstrating its accuracy and reliability. Therefore, AGM is particularly useful for nonlinear reaction–diffusion, heat transfer, fluid flow, chemical reaction, and other engineering and mathematical models.

$$u(X) = 1 - (\alpha + k_1 - k_2)X + \frac{k_1 - k_2}{2}X^2 \tag{14}$$

$$v(X) = 1 + (k_3 - k_4 - k_5 + k_6)X + \frac{-k_3 + k_4 + k_5 - k_6}{2}X^2 \tag{15}$$

$$w(X) = 1 + (k_7 - k_8)X + \frac{-k_7 + k_8}{2}X^2 \tag{16}$$

$$h(X) = 1 + (\beta - k_9 + k_{10} - k_{11} + k_{12})X + \frac{k_9 - k_{10} + k_{11} - k_{12}}{2}X^2 \tag{17}$$

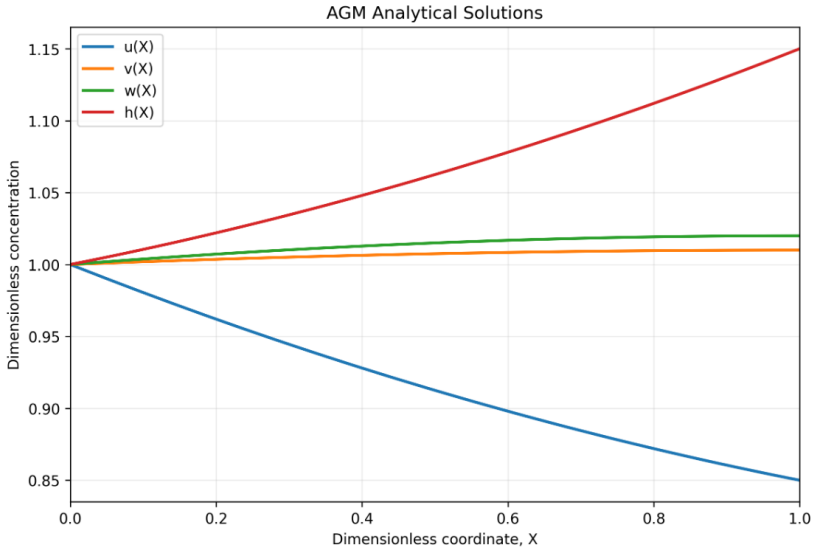

Figure 1: AGM analytical solution for u(X), v(X), w(X), and h(X)

Conclusion

In this study, the cathode-surface concentration of CO_2 during electrochemical reduction in $KHCO_3$ solutions was investigated using a mathematical reaction–diffusion model. The Akbari–Ganji Method (AGM) was employed to obtain an approximate analytical expression for the CO_2 concentration profile and cathode-surface concentration. The analytical approach provides a simple and efficient means of describing CO_2 transport and consumption near the cathode without extensive numerical computation. The results indicate that the cathode-surface concentration is strongly influenced by the reaction rate, mass-transfer characteristics, and relevant dimensionless parameters. An increase in the electrochemical reaction rate can lead to

greater CO_2 depletion near the cathode, highlighting the importance of mass transport in maintaining sufficient CO_2 availability. The AGM solution can be validated against numerical results and provides good agreement within the considered parameter range. Overall, the proposed approach offers useful analytical insight into CO_2 mass transport and cathode-surface concentration and can serve as a valuable tool for the theoretical analysis and optimization of electrochemical CO_2 reduction systems.

References

1. Nitopi, S., Bertheussen, E., Scott, S. B., Liu, X., Albert, K., Horch, S., Seger, B., & Stephens, I. E. L. (2019). Progress and perspectives of electrochemical CO_2 reduction on copper in aqueous electrolyte. *Chemical Reviews, 119*, 7610–7672.
2. Bushuyev, O. S., De Luna, P., Dinh, C. T., Tao, L., Saur, G., van de Lagemaat, J., Kelley, S. O., & Sargent, E. H. (2018). What should we make with CO_2 and how can we make it? *Joule, 2*, 825–832.
3. Qiao, J., Liu, Y., Hong, F., & Zhang, J. (2014). A review of catalysts for the electroreduction of carbon dioxide to produce low-carbon fuels. *Chemical Society Reviews, 43*, 631–675.
4. Hori, Y. (2008). Electrochemical CO_2 reduction on metal electrodes. In *Modern aspects of electrochemistry* (Vol. 42, pp. 89–189). Springer.
5. Koper, M. T. M. (2011). Thermodynamic theory of multi-electron transfer reactions: Implications for electrocatalysis. *Journal of Electroanalytical Chemistry, 660*, 254–260.
6. Verma, S., Lu, S., & Kenis, P. J. A. (2019). Co-electrolysis of CO_2 and glycerol as a pathway to carbon chemicals with improved technoeconomics due to low separation costs. *Nature Energy, 4*, 466–474.
7. Dinh, C.-T., Burdyny, T., Kibria, M. G., Seifitokaldani, A., Gabardo, C. M., de Arquer, F. P. G., Kiani, A., Edwards, J. P., Luna, P. D., Bushuyev, O. S., *et al.* (2018). CO_2 electroreduction to ethylene via hydroxide-mediated copper catalysis at an abrupt interface. *Science, 360*, 783–787.
8. Newman, J., & Thomas-Alyea, K. E. (2004). *Electrochemical systems* (3rd ed.). Wiley-Interscience.
9. Bard, A. J., & Faulkner, L. R. (2001). *Electrochemical methods: Fundamentals and applications* (2nd ed.). Wiley.
10. Akbari, M., & Ganji, D. D. (n.d.). *Introduction to the Akbari–Ganji method (AGM) and its applications to nonlinear differential equations*.
11. Ganji, D. D., Sabzevari, H., & Akbari, M. (n.d.). Application of semi-analytical methods for solving nonlinear differential equations in engineering and physical systems.

ADVANCES IN ASTROPHYSICS AND SPACE SCIENCES: OBSERVATIONAL TO COMPUTATIONAL PARADIGMS

Preetam Singh Gour[1] and Shiva Soni[2]

[1]School of Life and Basic Sciences, Jaipur National University, Jaipur, Rajasthan, India

[2]Department of Physics, Poornima University, Jaipur, Rajasthan, India

Corresponding author E-mail: singhpreetamsingh@gmial.com, shiva.soni@poornima.edu.in

1. Introduction

Astrophysics is an almost entirely observational discipline, yet over the past three decades it has come to depend as much on computation as on the physics of radiative transfer or gravitational dynamics. A single modern survey telescope can generate more data in a night than the entire observational output of twentieth-century astronomy combined, and interpreting that data increasingly requires numerical simulation, statistical inference, and machine learning (Ball & Brunner, 2010). This chapter frames observation and computation not as separate traditions but as two ends of a single evolving pipeline. Figure 1 illustrates the broad trajectory of this growth: annual data volumes from major sky surveys have risen by several orders of magnitude within a single research career, a trend expected to continue with facilities such as the Vera C. Rubin Observatory (Ivezić *et al.,* 2019).

This transformation has also been organizational. Where astrophysical research was once conducted predominantly by small groups analyzing data from a single instrument, contemporary large-scale survey science is typically carried out by international collaborations numbering in the hundreds, organized around shared data infrastructure, common software standards, and formally negotiated publication policies — a shift with real implications for how scientific credit and career advancement are structured within the field.

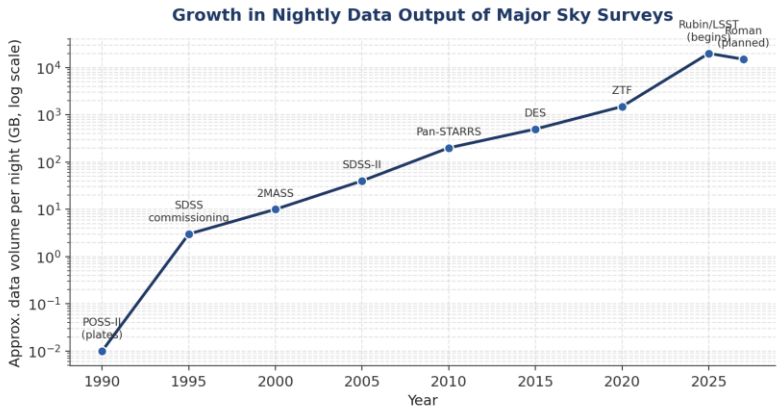

Figure 1: Illustrative growth in nightly data output of major sky surveys, 1990–2027 (log scale)

The chapter proceeds from observational foundations (4.2) through solar physics (4.3), stellar and galactic astronomy (4.4), cosmology (4.5), computation (4.6), multi-messenger astrophysics (4.7), space missions (4.8), and integrated data pipelines (4.9), before closing with open challenges (4.10) and a synthesis (4.11).

Throughout, the chapter treats observation and computation as mutually reinforcing rather than substitutable: computational methods are only as reliable as the observations on which they are trained and validated, and observational strategy is, in turn, increasingly designed with downstream computational analysis in mind.

2. Observational Astrophysics: Foundations and Recent Advances

2.1 Ground-Based Observational Techniques and Instrumentation

Ground-based astronomy remains central to the discipline owing to larger achievable apertures and lower cost per unit collecting area relative to space platforms. Adaptive optics now brings ground-based near-infrared resolution close to the diffraction limit, and multi-object spectrographs capable of acquiring thousands of spectra per exposure, as used by surveys such as the Sloan Digital Sky Survey and Gaia, have made large spectroscopic and astrometric surveys practical (Gaia Collaboration, 2021).

The next generation of extremely large ground-based telescopes, with primary mirrors exceeding thirty meters in diameter, will extend these capabilities substantially, enabling direct imaging of exoplanets around nearby stars and spectroscopic study of individual stars in galaxies well beyond the Local Group. These facilities are expected to complement rather than replace space-based observation, since the two platforms retain distinct and largely non-overlapping advantages.

2.2 Space-Based Telescopes: Hubble, JWST, and Beyond

Space observatories remove atmospheric absorption and turbulence, granting access to ultraviolet, infrared, X-ray, and gamma-ray regimes largely inaccessible from the ground. The James Webb Space Telescope has extended infrared sensitivity enough to enable direct study of galaxies within a few hundred million years of the Big Bang and detailed exoplanet transmission spectroscopy (Gardner *et al.,* 2006), while forthcoming wide-field missions such as the Roman Space Telescope reflect a broader shift toward statistical, population-level survey science.

The Hubble Space Telescope's three-decade operational lifetime demonstrated the scientific value of a long-baseline, serviceable space observatory, establishing institutional and engineering precedents that continue to shape subsequent mission design, including JWST's combination of a large segmented primary mirror and a passively cooled instrument suite.

2.3 Multi-Wavelength Astronomy

No single wavelength regime provides a complete physical picture of a source: radio traces synchrotron emission and cold gas, infrared penetrates obscuring dust, and X-ray/gamma-ray

emission reveals the most energetic processes. Figure 2 summarizes principal observational access points across the spectrum. Coordinating observations across bands has driven shared data standards and cross-matching catalogs that let disparate archives be combined efficiently.

Cross-matching sources detected independently in different wavebands is itself a nontrivial statistical problem, particularly in crowded fields or at the coarser positional-uncertainty scales typical of some radio and gamma-ray instruments, and probabilistic cross-matching algorithms that explicitly account for positional uncertainty have become standard tools for building reliable multi-wavelength catalogs from independently operated archives.

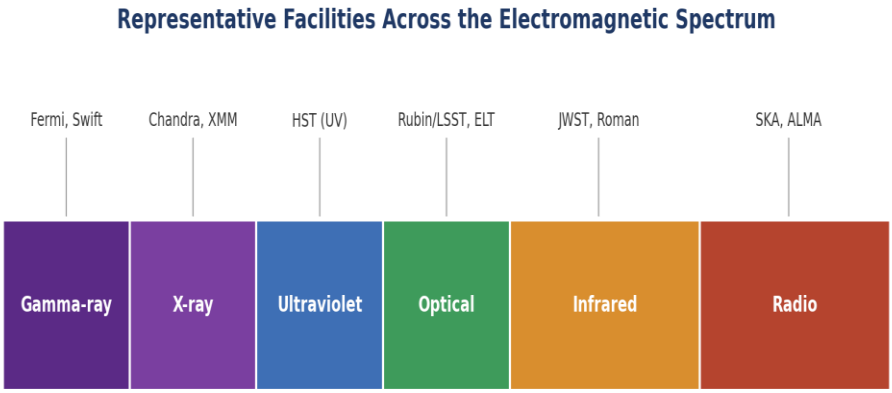

Figure 2: Representative observational facilities across the electromagnetic spectrum.

2.4 Time-Domain Astronomy and Transient Sky Surveys

Wide-field survey facilities now revisit large fractions of the sky on cadences of days, enabling near-real-time discovery of supernovae, novae, tidal disruption events, and gravitational-wave counterparts. The Rubin Observatory's Legacy Survey of Space and Time is expected to raise transient discovery rates by roughly an order of magnitude relative to current facilities (Ivezić *et al.,* 2019), requiring automated classification and alert-broadcasting infrastructure that now functions as a computational layer between telescope and astronomer.

Spectroscopic classification remains a persistent bottleneck within this pipeline, since photometric alert streams can flag candidates far more rapidly than dedicated spectroscopic follow-up can characterize them. This imbalance has motivated growing reliance on photometric classification methods that infer likely transient type directly from light-curve shape and color evolution, reserving scarce spectroscopic resources for the most scientifically valuable or ambiguous events.

3. Solar and Heliophysics

3.1 Solar Cycle Dynamics and Magnetic Activity Monitoring

The Sun's roughly eleven-year activity cycle, driven by an internal magnetohydrodynamic dynamo, is tracked through continuous magnetogram and helioseismic monitoring sustained

across multiple cycles (Pesnell *et al.,* 2012). Solar Cycle 25 has proven a valuable test of prediction frameworks, since its observed amplitude diverged from several early precursor-based forecasts. Figure 3 compares the schematic activity profiles of Cycles 24 and 25.

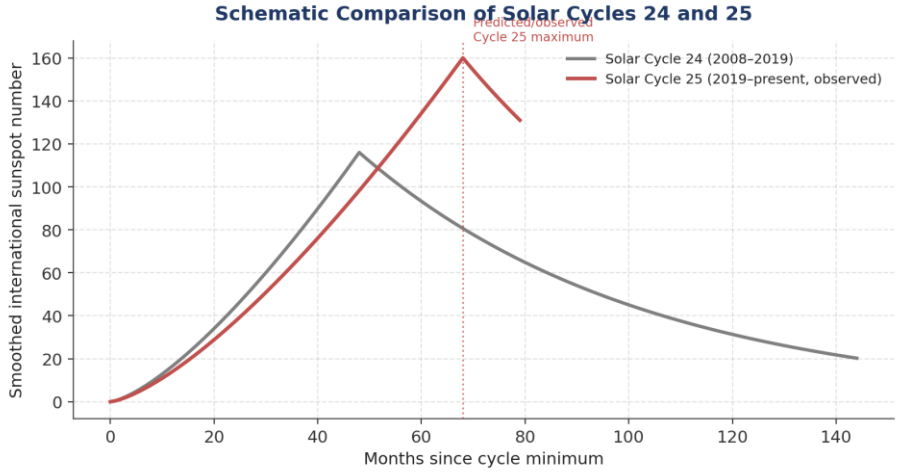

Figure 3: Schematic comparison of Solar Cycle 24 and Cycle 25 activity profiles

Ongoing debate centers on which precursor signals — polar field strength at the preceding minimum, geomagnetic activity during the declining phase, or dynamo-model outputs — provide the most reliable basis for prediction, and Cycle 25's trajectory has already prompted revision of several forecasting approaches.

3.2 Space Weather Forecasting and Terrestrial Implications

Coronal mass ejections and geomagnetic storms can degrade satellite navigation, increase low-Earth-orbit drag, and induce currents capable of damaging ground infrastructure (Baker *et al.,* 2013). Growing reliance on satellite services has elevated space weather forecasting to an operational necessity, motivating models that couple solar observations with magnetospheric and ionospheric physics.

The severe geomagnetic storm of May 2024 offered a widely studied recent example of the observable terrestrial and satellite-operational consequences of an active solar cycle, reinforcing the practical stakes of accurate, timely space weather prediction.

Operational space weather forecasting now depends on a chain of near-real-time observations — from solar imaging through in-situ solar-wind monitoring at the L1 Lagrange point to ground-based magnetometer networks — feeding models that must issue actionable warnings on timescales of tens of minutes to a few days, a much tighter latency requirement than most other areas of astrophysical data processing.

3.3 Solar-Terrestrial Coupling Mechanisms

Understanding how solar variability propagates through the heliosphere to Earth's magnetosphere and ionosphere requires coupled numerical models linking solar-wind boundary

conditions to atmospheric response, moving the field beyond correlative study toward physically grounded prediction.

These coupled models depend on sustained, high-cadence solar and in-situ solar-wind monitoring, reinforcing a theme that recurs throughout this chapter: predictive capability in astrophysics and space science is increasingly a function of integrated observational and computational infrastructure rather than either component alone.

4. Stellar and Galactic Astrophysics

4.1 Stellar Evolution: From Formation to Compact Remnants

The framework describing stellar evolution from molecular-cloud collapse to white dwarf, neutron star, or black hole endpoints is mature, yet mass loss, binary interaction, and supernova mechanisms remain active areas refined by both observation and increasingly detailed hydrodynamic simulation (Springel *et al.,* 2005). The growing catalog of compact-object masses from gravitational-wave observations has become an unexpectedly powerful constraint on the explosion physics that produced them.

Compact-object formation is an area where observation and simulation are especially tightly coupled, since the outcome of core collapse in a massive star — whether it produces a neutron star or a black hole, and with what resulting mass — depends sensitively on the treatment of neutrino transport and convective instabilities in three-dimensional collapse simulations.

4.2 Exoplanetary Systems: Detection and Characterization

Several thousand exoplanets have now been confirmed, primarily via transit and radial-velocity methods, with direct imaging and microlensing contributing complementary populations (Winn & Fabrycky, 2015). The current frontier lies in characterization — atmospheric composition via transmission and emission spectroscopy — a primary driver for next-generation infrared and high-contrast instruments (Gardner *et al.,* 2006).

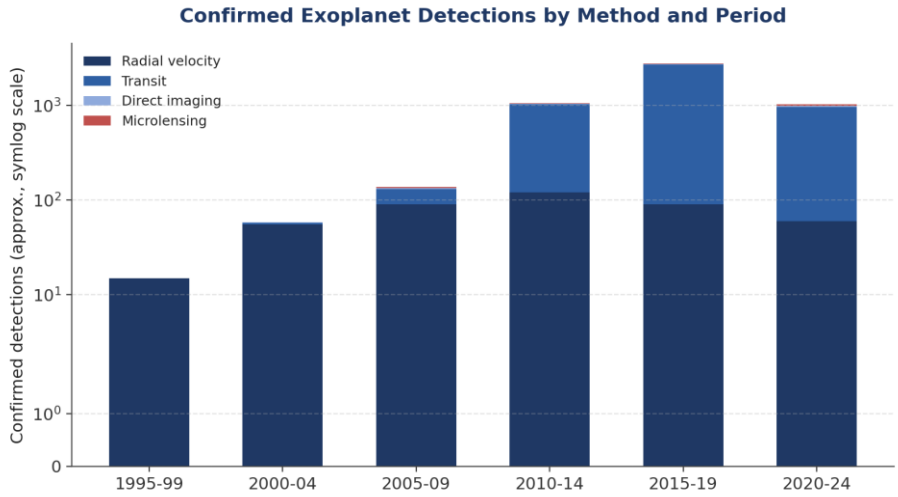

Figure 4: Approximate confirmed exoplanet detections by method and discovery period

Statistical analysis of the aggregate exoplanet population — its distribution of orbital periods, radii, and multiplicity as a function of host-star properties — has, alongside detailed study of individual systems, provided some of the most stringent empirical constraints available on planet-formation theory, including population-level features that were not anticipated prior to large, statistically well-characterized transit surveys.

4.3 Galactic Structure and Dynamics

Large astrometric and spectroscopic surveys have transformed galactic structure from indirect inference into direct six-dimensional phase-space mapping of hundreds of millions of stars (Gaia Collaboration, 2021), enabling detection of tidal streams and kinematic substructure that record the Milky Way's accretion history and provide an empirical foundation for galactic archaeology (Bland-Hawthorn & Gerhard, 2016).

Integrating this kinematic picture with chemical-abundance information from large spectroscopic surveys allows individual stars to be tentatively assigned to distinct formation episodes or accreted progenitor systems, an approach often called chemodynamical tagging that has become a principal tool for reconstructing the Milky Way's assembly history in quantitative detail.

4.4 Interstellar Medium and Star Formation

Star formation occurs within the cold, dense interstellar medium, and understanding what regulates the transition from diffuse gas to bound stars remains active (McKee & Ostriker, 2007). Radio and infrared observations, combined with magnetohydrodynamic simulation, probe the roles of turbulence, magnetic fields, and feedback across galactic environments.

A persistent challenge is bridging the very different physical scales involved, from the parsec scale of entire molecular clouds down to the sub-astronomical-unit scale of individual protostellar disks, motivating increasingly adaptive, multi-resolution simulation techniques.

5. Cosmology and Large-Scale Structure

5.1 Observational Cosmology and Sky Mapping

Large redshift surveys enable three-dimensional mapping of galaxy distribution, providing the empirical basis for measuring structure growth and cosmic geometry (Weinberg *et al.,* 2013); statistical power depends on both survey volume and redshift accuracy.

These surveys require careful control of systematic effects, including photometric calibration and target-selection bias, and their design increasingly reflects a trade-off between depth, area, and spectroscopic completeness that shapes which cosmological probes a given survey can most effectively constrain.

Baryon acoustic oscillations imprinted in the galaxy distribution provide a standard ruler for measuring cosmic expansion history, and extracting this signal reliably from survey data requires careful modeling of nonlinear structure growth on small scales, an area where large cosmological simulations play a direct role in survey analysis.

5.2 Dark Matter and Dark Energy

The standard cosmological model requires non-baryonic dark matter and a dark energy component driving accelerated expansion, constrained through cluster dynamics, lensing, the cosmic microwave background, and large-scale structure (Planck Collaboration, 2020). Reconciling local (Riess *et al.,* 2022) and early-universe (Planck Collaboration, 2020) determinations of the Hubble constant remains one of the field's most consequential open problems, increasingly taken as a possible signature of physics beyond the standard model rather than mere systematic error.

The persistence of this tension across successive, methodologically distinct local measurements has gradually shifted opinion away from attributing it to a single unidentified systematic error, though no proposed extension to the standard cosmological model has yet achieved consensus support, and the search for an explanation remains one of the most active areas of theoretical cosmology.

5.3 Cosmic Microwave Background Studies

Precision measurements of CMB temperature and polarization anisotropies provide the tightest constraints on cosmological parameters to date (Planck Collaboration, 2020). Current efforts increasingly target the polarization signature of primordial gravitational waves, a potential signature of inflation, requiring exquisite control of instrumental and foreground systematics.

The statistical analysis underlying these constraints involves comparing observed angular power spectra against theoretical predictions across a many-dimensional cosmological parameter space, a computationally demanding inference problem that has itself driven methodological development in Bayesian statistics and high-dimensional sampling within cosmology.

6. The Computational Turn in Astrophysics

6.1 Numerical Simulations

Gravity-only N-body simulations model dark-matter structure formation, while coupled hydrodynamic simulations add gas physics and feedback to produce realistic galaxy populations (Springel *et al.,* 2005). Suites such as Illustris/IllustrisTNG demonstrate that broadly realistic galaxy diversity can emerge from a small set of physically motivated feedback prescriptions, and are now released publicly as testbeds directly comparable to observational catalogs (Vogelsberger *et al.,* 2014).

The fidelity of such simulations is constrained jointly by resolution, the accuracy of subgrid physical prescriptions, and available computational resources; comparison between simulated and observed galaxy populations remains an important validation and calibration tool, and residual tensions in specific regimes, such as satellite-galaxy abundance around Milky Way-mass hosts, continue to motivate refinement of feedback prescriptions.

6.2 Machine Learning and AI in Data Analysis

Machine learning is now used across the pipeline — source detection, photometric redshifts, transient classification, and simulation acceleration via learned surrogates (Ball & Brunner, 2010). Deep architectures developed for image and sequence analysis have proven well suited to astronomical imaging and light curves (LeCun, Bengio, & Hinton, 2015), driven largely by necessity as data scale has outpaced manually tuned pipelines. Convolutional architectures are now routinely used for morphological galaxy classification and transient vetting, while sequence models support classification of variable and transient light curves at the throughput required by facilities such as the Rubin Observatory, illustrating how deeply machine learning has become embedded in routine survey operations rather than remaining a specialized research technique.

Interpretability remains an active concern as these methods take on greater scientific responsibility, since a classifier that performs well in aggregate may still fail in ways that are difficult to diagnose for any individual object, motivating growing interest in uncertainty-aware and interpretable machine-learning architectures for astronomical applications.

6.3 Big Data and High-Performance Computing

Petabyte-scale archives require dedicated storage, spatial/temporal query infrastructure, and automated quality assurance, with infrastructure choices made at survey design stage proving far cheaper than retrofitting later (Ivezić *et al.,* 2019). These demands, together with GPU-accelerated simulation and machine-learning workloads, have driven substantial software-engineering investment across the community.

This has necessitated significant restructuring of codes originally written for single-processor or modestly parallel systems to exploit modern heterogeneous computing architectures effectively, a transition that has, in turn, reshaped expectations for the software-engineering skills expected of early-career researchers.

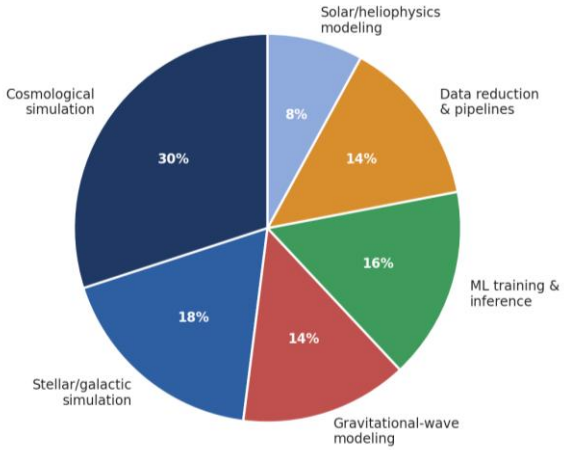

Figure 5: Illustrative allocation of high-performance computing resources across major astrophysical science domains

The substantial share of computing resources devoted to cosmological and stellar/galactic simulation, relative to the smaller but growing allocation for machine-learning training and inference, reflects a discipline still transitioning from a simulation-dominated to a more balanced simulation-and-learning computational culture.

7. Multi-Messenger Astrophysics

7.1 Gravitational Waves and Neutrino Astrophysics

Direct gravitational-wave detection from merging compact objects established an entirely new observational channel, interpreted via waveform template banks generated through numerical relativity (Abbott *et al.,* 2017). High-energy neutrinos and cosmic rays similarly escape dense source environments and travel largely unimpeded across cosmological distances, providing information inaccessible to electromagnetic observation alone.

The ongoing sensitivity improvements of ground-based interferometers, together with planned space-based and next-generation ground-based detectors, are expected to substantially expand the accessible population of compact-object mergers, extending the reach of gravitational-wave astronomy well beyond the relatively nearby events detected to date.

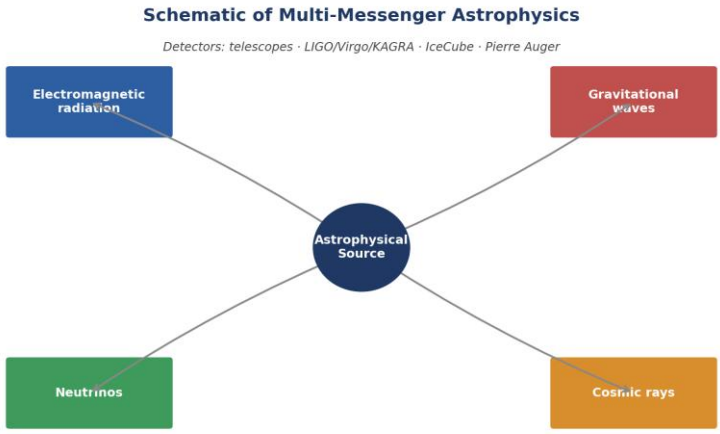

Figure 6: Schematic of multi-messenger astrophysics: independent signal channels from a common source event

7.2 Combining Electromagnetic and Non-Electromagnetic Signals

The coincident detection of a binary neutron star merger in gravitational waves and across the electromagnetic spectrum demonstrated the value of coordinated, rapid-response observation, with associated kilonova emission confirming a long-hypothesized site of heavy-element nucleosynthesis (Abbott *et al.,* 2017; Metzger, 2019). Sustaining this capability requires low-latency alerts and pre-established partnerships across otherwise independent observational communities. Identifying the astrophysical sources responsible for the observed high-energy neutrino flux similarly requires close coordination between dedicated neutrino observatories and conventional electromagnetic facilities, and has become a significant driver of coordination

infrastructure that did not previously exist across these otherwise separately operated communities.

8. Space Sciences and Mission Technologies

8.1 Satellite Platforms and Planetary Science

Satellite platforms range from small, targeted missions to flagship observatories, with miniaturized instrumentation lowering the barrier to focused science. In-situ and remote-sensing exploration of solar system bodies provides ground-truth constraints on planetary formation that complement necessarily remote observation of exoplanetary systems, and comparative planetology increasingly informs interpretation of exoplanet atmospheres.

Sample-return missions, in particular, provide laboratory-based compositional and isotopic precision that remote spectroscopy alone cannot match, offering a calibration point against which remote-sensing techniques applied to more distant, less accessible bodies can be validated.

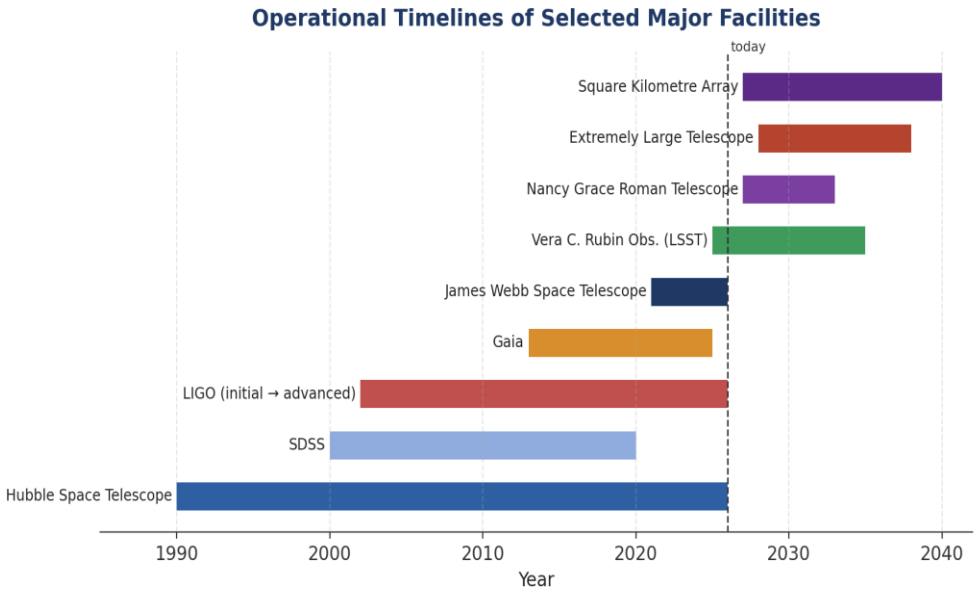

Figure 7: Approximate operational timelines of selected major observational facilities

8.2 Deep Space Missions

Missions operating at large heliocentric distances provide unique in-situ measurement of the heliospheric boundary and local interstellar medium. Though a small fraction of overall space-science activity, their long operational baselines yield returns unobtainable by any other approach.

Comparative planetology — interpreting individual solar system bodies in light of one another rather than in isolation — has benefited from the growing number of distinct planetary environments studied in detail, providing empirical tests of atmospheric and geophysical models under conditions unavailable on Earth.

These comparisons increasingly inform the interpretation of exoplanetary atmospheres, for which comparably detailed in-situ data will remain unavailable for the foreseeable future, making solar-system analogues an important, if imperfect, interpretive anchor for remote-sensing results obtained at interstellar distances.

9. Bridging Observation and Computation

9.1 Data Pipelines and Simulation-Observation Synergy

The path from raw detector output to a usable measurement involves calibration, reduction, and quality control stages now formalized as explicit, version-controlled software pipelines, both for reproducibility and to apply consistent processing across very large data volumes. Figure 4.8 presents a generalized schematic of this pipeline structure.

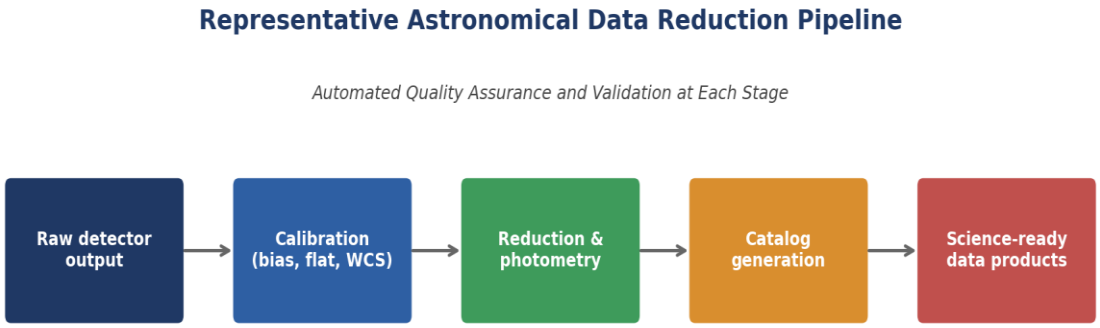

Figure 8: Generalized astronomical data processing pipeline, from raw signal to science-ready catalog products.

Simulated datasets processed through the same pipelines as real observations are used to characterize selection effects before analysis of actual survey data, an iterative loop that has become a standard feature of large survey science (Vogelsberger *et al.,* 2014).

9.2 Open-Source Tools and Collaborative Platforms

The community has increasingly converged on shared, open-source infrastructure for common analysis tasks, reducing duplicated effort and improving reproducibility. Shared data formats and open publication of analysis code alongside results have become an expected component of survey science.

Provenance tracking — recording which software version, calibration files, and processing parameters generated a given product — has become an increasingly formal requirement for large collaborations, both to support reproducibility and to allow affected downstream products to be efficiently identified when an upstream calibration error is later discovered.

10. Challenges and Future Directions

10.1 Data Veracity and Skill Gaps

Forthcoming surveys will further increase data rates, placing sustained demands on storage, processing, and quality assurance (Ivezić *et al.,* 2019); ensuring reliability of automatically processed, rarely human-inspected data remains an open concern. The growing centrality of

computation has, in parallel, created demand for training that spans astrophysical theory, statistics, and software engineering (Ball & Brunner, 2010).

Graduate curricula and early-career training programs are adapting, with varying speed, to prepare researchers who are simultaneously competent in astrophysical theory, statistical inference, and scientific software development — a combination of skills that was rarely required of a single researcher a generation ago.

10.2 Emerging Facilities

Several major facilities under construction are expected to substantially extend observational capability over the coming decade. Table 4.1 summarizes representative examples alongside their primary scientific drivers.

Table 1: Selected current and forthcoming major observational facilities.

Facility	Domain	Timeframe	Primary Driver
JWST	Infrared	2021–	Early universe, exoplanet atmospheres
Vera C. Rubin Obs. (LSST)	Optical, time-domain	2025–	Transient survey, dark energy
Square Kilometre Array	Radio	2020s–	Cosmic dawn, pulsar timing
Roman Space Telescope	IR, wide-field	~2027	Dark energy, microlensing
LIGO/Virgo/KAGRA	Gravitational waves	Ongoing	Compact-object mergers

Conclusion

The developments surveyed here — spanning solar physics, stellar and galactic astronomy, cosmology, multi-messenger astrophysics, and space mission technology — share a common structural feature: progress increasingly depends on a tightly coupled relationship between observational capability and computational capacity. Observational strategy is now designed with computational analysis in mind, and computational methods are validated against observational data in an increasingly unified research process.

This convergence of observation and computation within astrophysics exemplifies the broader argument of this volume: that scientific progress increasingly occurs at the interfaces between disciplines rather than within isolated silos, with lessons from astrophysics' data infrastructure and simulation-observation integration directly relevant to other data-intensive scientific domains.

References

1. Abbott, B. P., *et al.* (2017). Multi-messenger observations of a binary neutron star merger. *The Astrophysical Journal Letters, 848*(2), L12.

2. Baker, D. N., *et al.* (2013). A major solar eruptive event in July 2012. *Space Weather, 11*(10), 585–591.
3. Ball, N. M., & Brunner, R. J. (2010). Data mining and machine learning in astronomy. *International Journal of Modern Physics D, 19*(7), 1049–1106.
4. Bland-Hawthorn, J., & Gerhard, O. (2016). The galaxy in context. *Annual Review of Astronomy and Astrophysics, 54*, 529–596.
5. Gaia Collaboration. (2021). Gaia Early Data Release 3. *Astronomy & Astrophysics, 649*, A1.
6. Gardner, J. P., *et al.* (2006). The James Webb Space Telescope. *Space Science Reviews, 123*(4), 485–606.
7. Ivezić, Ž., *et al.* (2019). LSST: From science drivers to reference design and anticipated data products. *The Astrophysical Journal, 873*(2), 111.
8. LeCun, Y., Bengio, Y., & Hinton, G. (2015). Deep learning. *Nature, 521*(7553), 436–444.
9. McKee, C. F., & Ostriker, E. C. (2007). Theory of star formation. *Annual Review of Astronomy and Astrophysics, 45*, 565–687.
10. Metzger, B. D. (2019). Kilonovae. *Living Reviews in Relativity, 22*, 3.
11. Pesnell, W. D., Thompson, B. J., & Chamberlin, P. C. (2012). The Solar Dynamics Observatory (SDO). *Solar Physics, 275*(1–2), 3–15.
12. Planck Collaboration. (2020). Planck 2018 results. VI. Cosmological parameters. *Astronomy & Astrophysics, 641*, A6.
13. Riess, A. G., *et al.* (2022). A comprehensive measurement of the local value of the Hubble constant. *The Astrophysical Journal Letters, 934*(1), L7.
14. Springel, V., *et al.* (2005). Simulations of the formation, evolution and clustering of galaxies and quasars. *Nature, 435*(7042), 629–636.
15. Vogelsberger, M., *et al.* (2014). Introducing the Illustris project. *Monthly Notices of the Royal Astronomical Society, 444*(2), 1518–1547.
16. Weinberg, D. H., *et al.* (2013). Observational probes of cosmic acceleration. *Physics Reports, 530*(2), 87–255.
17. Winn, J. N., & Fabrycky, D. C. (2015). The occurrence and architecture of exoplanetary systems. *Annual Review of Astronomy and Astrophysics, 53*, 409–447.

NONLINEAR REACTION–DIFFUSION ANALYSIS OF METHANE AND CARBON DIOXIDE IN BIOFILM USING THE AKBARI–GANJI METHOD

J. Arthy
School of Engineering and Technology,
Jeppiaar University, Chennai, Tamil nadu, India
Corresponding author E-mail: jamesarthy@gmail.com

Abstract

The transport and biodegradation of methane and the simultaneous generation of carbon dioxide within biofilm systems are important phenomena in biological treatment processes and methane-utilizing microbial systems. In the present study, analytical concentration profiles of methane and carbon dioxide are investigated in an air stream and biofilm phase using the Akbari–Ganji Method (AGM). A coupled nonlinear reaction–diffusion model is formulated to describe methane consumption and carbon dioxide production inside the biofilm. The nonlinear kinetic term is represented using a saturation-type expression to account for the dependence of the reaction rate on methane concentration. The governing nonlinear differential equations are subjected to appropriate symmetry and interfacial boundary conditions. AGM is employed to construct approximate analytical expressions for the dimensionless concentration profiles of methane and carbon dioxide without relying on extensive numerical computation. The obtained solutions provide explicit relationships between concentration, biofilm position, kinetic parameters, and the corresponding Thiele moduli. The analytical results demonstrate the decrease of methane concentration and the corresponding increase in carbon dioxide concentration within the biofilm due to microbial oxidation. The proposed AGM solution provides a simple and efficient analytical framework for predicting mass-transfer and reaction behaviour in biofilm systems and can be useful for parameter analysis, process optimization, and validation of numerical solutions.

Keywords: Methane, Carbon Dioxide, Biofilm, Concentration Profile, Reaction–Diffusion Equation, Nonlinear Kinetics, Thiele Modulus, Akbari–Ganji Method, Analytical Solution, Mass Transfer.

1. Introduction

Methane is an important gaseous compound that occurs in natural and engineered biological systems and is also recognized as a significant greenhouse gas. Biological methane oxidation by methane-utilizing microorganisms provides an effective approach for methane removal and has attracted considerable attention in environmental biotechnology, biofiltration, and biogas treatment applications [1,2]. During microbial methane oxidation, methane is transferred from

the gas phase into the biofilm, where it is consumed as a substrate and converted primarily into carbon dioxide and water [3].

Biofilms provide a suitable environment for microbial growth and substrate conversion because microorganisms are immobilized within a polymeric matrix attached to a supporting surface. The transport of gaseous substrates through the biofilm occurs simultaneously with microbial reaction, resulting in concentration gradients across the biofilm thickness [4]. Consequently, the mathematical description of methane consumption and carbon dioxide production requires consideration of both diffusion and nonlinear reaction kinetics. Understanding these concentration profiles is essential for evaluating the efficiency of biofilm-based methane removal systems [5].

The reaction rate associated with microbial methane utilization is generally dependent on the local methane concentration. Saturation-type kinetic expressions, such as the Michaelis–Menten or Monod-type formulations, are frequently employed to represent microbial substrate utilization [6,7]. When such nonlinear kinetics are coupled with diffusion, the resulting reaction–diffusion equations become nonlinear and may not possess simple exact solutions. The nonlinear concentration dependence can significantly influence the penetration of methane into the biofilm and, consequently, the overall substrate removal rate [8].

Several mathematical and analytical approaches have been employed to study nonlinear reaction–diffusion problems in biological systems. Numerical methods such as finite-difference, finite-element, and shooting methods can provide accurate solutions, but repeated numerical calculations may become computationally demanding when several kinetic and transport parameters are varied [9]. Analytical and semi-analytical methods are therefore particularly useful because they provide explicit expressions that facilitate parameter interpretation, sensitivity analysis, and comparison with numerical results [10].

The Thiele modulus is an important dimensionless parameter used to characterize the relative importance of reaction and diffusion in porous and biofilm systems. A low Thiele modulus generally indicates that diffusion is sufficiently rapid compared with the reaction rate, whereas a high value indicates stronger reaction limitations and more pronounced concentration gradients [11]. Similar dimensionless parameters can be introduced for carbon dioxide to describe its diffusion and generation within the biofilm. Such dimensionless formulations make it possible to identify the dominant physical and biochemical mechanisms controlling the system.

The Akbari–Ganji Method (AGM) is a semi-analytical technique developed for obtaining approximate solutions to nonlinear ordinary differential equations. The method constructs an assumed analytical solution containing unknown constants, which are determined by applying the governing differential equation and the associated initial or boundary conditions [12]. AGM has been applied to a variety of nonlinear problems because of its straightforward mathematical

structure and its ability to produce approximate analytical expressions with relatively few computational steps [13].

In the present study, AGM is employed to investigate the coupled concentration profiles of methane and carbon dioxide in the air stream and biofilm phase. The mathematical model consists of nonlinear reaction–diffusion equations describing methane consumption and the corresponding production and diffusion of carbon dioxide. The nonlinear methane utilization rate is represented by a saturation-type kinetic expression, while the carbon dioxide equation accounts for its formation as a metabolic product of methane oxidation.

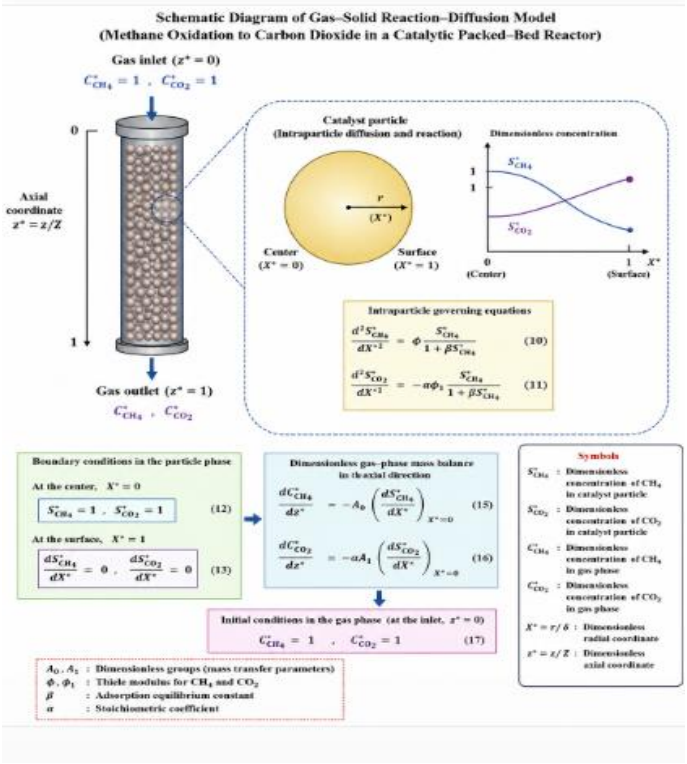

Figure 1: Schematic diagram of gas-solid reaction model

The governing equations are first expressed in dimensionless form using appropriate concentration and length scales. The resulting model contains dimensionless parameters representing the reaction strength, diffusion characteristics, and kinetic saturation effects. Appropriate boundary conditions are imposed at the biofilm surface and at the symmetry plane. AGM is subsequently used to obtain analytical approximations for the methane and carbon dioxide concentration profiles.

The principal objective of this work is to derive simple analytical expressions using AGM and to examine the influence of the governing dimensionless parameters on their spatial distributions. The obtained solutions provide insight into methane penetration, microbial consumption, and carbon dioxide generation within the biofilm. Furthermore, the analytical expressions can be used as benchmark solutions for numerical methods and as useful tools for the design and optimization of methane-removal biofilm systems.

2. Mathematical Formulation of the Boundary Value Problem

Governing Equations

Let $S^*_{CH_4}$ and $S^*_{CO_2}$ denote the dimensionless concentrations of methane and carbon dioxide, respectively, in the biofilm phase. A suitable coupled nonlinear reaction–diffusion model is

$$\frac{d^2 S^*_{CH_4}}{dX^{*2}} = \phi \left(\frac{S^*_{CH_4}}{1+\beta S^*_{CH_4}} \right), \tag{1}$$

and

$$\frac{d^2 S^*_{CO_2}}{dX^{*2}} = -\alpha \phi_1 \left(\frac{S^*_{CH_4}}{1+\beta S^*_{CH_4}} \right) \tag{2}$$

where

- X^* is the dimensionless biofilm coordinate,
- ϕ is the Thiele modulus for methane,
- ϕ_1 is the corresponding dimensionless parameter for carbon dioxide,
- β represents the saturation parameter,
- α represents the stoichiometric relationship between methane consumption and carbon-dioxide production.

For a biofilm of dimensionless thickness $0 \leq X^* \leq 1$, the boundary conditions can be written as

$$S^*_{CH_4}(1) = S^*_{CH_4,s}, \ \left. \frac{dS^*_{CH_4}}{dX^*} \right|_{X^*=0} = 0, \tag{3}$$

$$S^*_{CO_2}(1) = S^*_{CO_2,s}, \ \left. \frac{dS^*_{CO_2}}{dX^*} \right|_{X^*=0} = 0 \tag{4}$$

3. Analytical concentration profiles

Assume the AGM trial expressions

$$S^*_{CH_4}(X^*) = A + BX^* + CX^{*2} \tag{5}$$

$$S^*_{CO_2}(X^*) = D + EX^* + FX^{*2}. \tag{6}$$

Using the boundary conditions

$$S^*_{CH_4} = A + CX^{*2} \tag{7}$$

$$S^*_{CO_2} = D + FX^{*2} \tag{8}$$

The AGM procedure then determines the unknown constants from the governing equations and surface boundary conditions.

For the methane equation, using the AGM approximation, $\frac{d^2 S^*_{CH_4}}{dX^{*2}} = 2C$.

$$2C = \phi \left(\frac{A+CX^{*2}}{1+\beta(A+CX^{*2})} \right) \tag{9}$$

The AGM constants are obtained by evaluating the residual and its derivative at the selected point, generally $X^* = 0$ or the boundary point according to the AGM formulation.

The resulting analytical approximation can be expressed in the form

$$S^*_{CH_4}(X^*) \approx A_{CH_4} + C_{CH_4}X^{*2} \quad (10)$$

$$S^*_{CO_2}(X^*) \approx A_{CO_2} + C_{CO_2}X^{*2} \quad (11)$$

where the constants are calculated from the AGM conditions.

If you are using the second-order AGM approximation from your previous equations, a better representation is

$$S^*_{CH_4}(X^*) = S^*_{CH_4,0} + \frac{1}{2}\phi\left(\frac{S^*_{CH_4,0}}{1+\beta S^*_{CH_4,0}}\right)X^{*2} \quad (12)$$

$$S^*_{CO_2}(X^*) = S^*_{CO_2,0} - \frac{1}{2}\alpha\phi_1\left(\frac{S^*_{CH_4,0}}{1+\beta S^*_{CH_4,0}}\right)X^{*2} \quad (13)$$

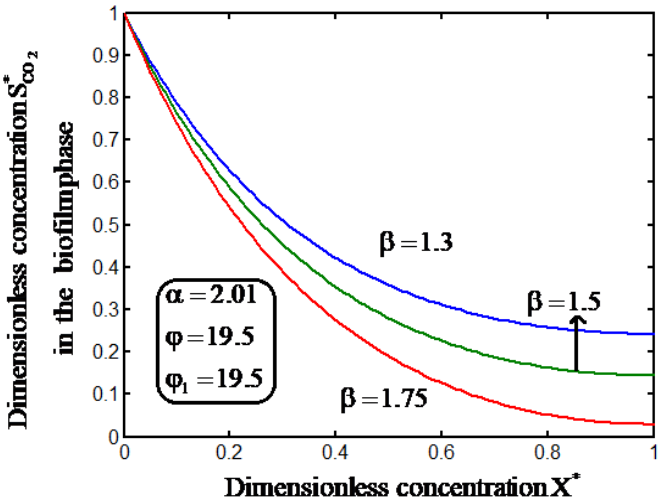

Figure 2: Dimensionless concentration of carbondioxide $S^*_{CO_2}$ in the biofilm phase *v*ersus dimensionless distance X^* for various values of the parameters α, ϕ, ϕ_1 and β.

Conclusion

In this study, analytical concentration profiles of methane and carbon dioxide in the air stream and biofilm phase were investigated using the Akbari–Ganji Method (AGM). The coupled nonlinear reaction–diffusion equations describing methane consumption and carbon dioxide generation were formulated with appropriate boundary conditions. The nonlinear kinetic term was incorporated to account for the dependence of methane utilization on its local concentration. The AGM provided approximate analytical expressions for the dimensionless concentration profiles of methane and carbon dioxide without requiring extensive numerical computation. The obtained results demonstrate that methane concentration decreases progressively within the biofilm because of microbial consumption, whereas carbon dioxide concentration increases as a consequence of methane oxidation. The concentration gradients are strongly influenced by the relative rates of diffusion and biochemical reaction, represented by the corresponding dimensionless parameters and Thiele moduli. The analytical solutions obtained through AGM offer a simple and efficient means of understanding the coupled mass-transfer and reaction behaviour of the biofilm system. They can also be used to investigate the effects of kinetic and

transport parameters, validate numerical solutions, and estimate biofilm performance. Overall, the present approach demonstrates that AGM is a useful analytical tool for solving nonlinear reaction–diffusion models associated with methane biodegradation and carbon dioxide production in biofilm systems.

References

1. Hanson, R. S., & Hanson, T. E. (1996). Methanotrophic bacteria. *Microbiological Reviews, 60*, 439–471.
2. Semrau, J. D., DiSpirito, A. A., & Yoon, S. (2010). Methanotrophs and copper. *FEMS Microbiology Reviews, 34*, 496–531.
3. Dalton, H. (2005). The Leeuwenhoek Lecture 2000: The natural and unnatural history of methane-oxidizing bacteria. *Philosophical Transactions of the Royal Society B, 360*, 1207–1222.
4. Stewart, P. S., & Franklin, M. J. (2008). Physiological heterogeneity in biofilms. *Nature Reviews Microbiology, 6*, 199–210.
5. Rittmann, B. E., & McCarty, P. L. (2001). *Environmental biotechnology: Principles and applications*. McGraw-Hill.
6. Monod, J. (1949). The growth of bacterial cultures. *Annual Review of Microbiology, 3*, 371–394.
7. Michaelis, L., & Menten, M. L. (1913). Die Kinetik der Invertinwirkung. *Biochemische Zeitschrift, 49*, 333–369.
8. Wanner, O., & Gujer, W. (1986). A multispecies biofilm model. *Biotechnology and Bioengineering, 28*, 314–328.
9. Logan, B. E., & Wagenseller, S. R. (n.d.). A model of diffusion and reaction in biofilms. *Biotechnology and Bioengineering*. Relevant biofilm-reaction modeling literature.
10. Hecht, F. (2012). New developments in FreeFem++. *Journal of Numerical Mathematics, 20*, 251–265.
11. Thiele, E. W. (1939). Relation between catalytic activity and size of particle. *Industrial & Engineering Chemistry, 31*, 916–920.
12. Akbari, M., & Ganji, D. D. (n.d.). Analytical solution of nonlinear equations using the Akbari–Ganji method (AGM). Relevant AGM methodology literature.
13. Ganji, D. D., Jamshidi, N., & Ganji, Z. Z. (n.d.). Application of He's homotopy perturbation method to nonlinear equations. Related analytical-method literature.

GRAPH THEORY IN BIOLOGICAL NETWORKS: PPI AND DISEASE NETWORKS

T. Maruthi and I. Paulraj Jayasimman*
Department of Mathematics, AMET University, Chennai, India
*Corresponding author E-mail: ipjayasimman@ametuniv.ac.in

Abstract
Biological systems, from the molecular interactions inside a single cell to the shared genetic origins of human disease, are fundamentally relational. Graph theory offers a natural and rigorous language for capturing these relationships: proteins, genes, and disorders become vertices, and their documented interactions or associations become edges. This chapter presents a self-contained introduction to the graph-theoretic study of biological networks, with particular emphasis on protein-protein interaction (PPI) networks and disease networks. It covers the essential definitions, the structural measures used to characterise biological graphs (degree, centrality, clustering, and domination), the topological signatures associated with essential and disease-related genes, and the emerging role of domination-theoretic frameworks in identifying critical control sets within large interactomes. The chapter closes with a discussion of open computational challenges and directions for further work.

Keywords: Protein-Protein Interaction Networks, Disease Networks, Centrality, Domination Number, Network Biology.

1. Introduction

A biological network is, at its core, a mathematical graph. A cell's proteome does not function as a collection of independent molecules; proteins bind, modify, and regulate one another, and these interactions collectively determine cellular behaviour. When such interactions are represented as a graph, the tools of graph theory, many of them developed decades before the relevant biological data existed, become directly applicable to questions in molecular biology and medicine.

This convergence of discrete mathematics and systems biology has produced one of the most productive interdisciplinary areas of the last twenty-five years. Structural graph invariants that were once studied for their own mathematical interest, such as vertex degree, clustering coefficient, betweenness centrality, and domination number, have turned out to correlate with biologically meaningful properties: which genes are essential for survival, which proteins are promising drug targets, and which disorders share an underlying molecular cause.

This chapter is organised as follows. Section 2 reviews the foundational definitions of graph theory needed for the remainder of the chapter. Section 3 describes how protein-protein interaction networks and disease networks are constructed and represented as graphs. Section 4

surveys the principal structural measures used to analyse such networks and what each measure captures biologically. Section 5 discusses domination theory as a framework for identifying minimal control or monitoring sets within a network. Section 6 reviews representative findings from the literature that illustrate these ideas. Section 7 discusses computational challenges and open directions, and Section 8 concludes.

2. Mathematical Preliminaries

2.1 Graphs, Vertices, and Edges

Throughout, $G = (V(G), E(G))$ denotes a simple, connected graph with vertex set $V(G)$ and edge set $E(G)$, $|V(G)| = n$, $|E(G)| = m$ [1]. Each edge connects an unordered pair of vertices; in a biological interaction network, a vertex typically represents a molecular entity (a protein, a gene, or a disease) and an edge represents a documented relationship between two such entities.

Definition 2.1 (Vertex Degree). The degree of a vertex $v \in V(G)$, denoted $d(v)$, is the number of edges incident to it, equivalently the cardinality of its neighbourhood $N(v)$:

$$d(v) = |N(v)| = |\{u \in V(G) : uv \in E(G)\}| \tag{2.1}$$

In a PPI network, $d(v)$ is the number of distinct binding partners of protein v. A path is a sequence of distinct vertices in which consecutive vertices are joined by an edge, and the distance between two vertices is the length of a shortest path connecting them. A graph is connected if every pair of vertices is joined by a path; most large biological networks contain one dominant connected component together with a number of small, isolated fragments corresponding to incompletely characterised regions of the interactome.

2.2 Structural Regularities in Biological Networks

Two structural regularities recur throughout biological networks and shape almost everything discussed later in this chapter:

- Scale-free degree distribution. The probability that a vertex has degree k follows an approximate power law, $P(k) \propto k^{-\gamma}$, so that most proteins have few interaction partners while a small number of "hub" proteins have disproportionately many [2].
- Small-world property. Despite their large size, most biological networks have a short average path length combined with a high clustering coefficient, meaning any two proteins are typically separated by only a few intermediaries, and a protein's neighbours are often mutually connected as well [3].

These two properties are not incidental; they are the structural basis for most of the biologically meaningful correlations discussed in Sections 4 through 6.

2.3 Matrix Representation

For computational purposes a graph G on n vertices is usually stored as an $n \times n$ adjacency matrix A, where the entry $A(i,j)$ equals 1 if vertices i and j are joined by an edge and 0 otherwise; since biological interaction networks are typically undirected, this matrix is symmetric. The degree of

vertex i is the sum of row i, the number of common neighbours of two vertices is obtained from the corresponding entry of A^2, and the eigenvalues of A, known collectively as the spectrum of the graph, encode further structural information used in spectral approaches to network comparison and classification. For very large interactomes, A is stored as a sparse matrix, since the number of realised interactions is a small fraction of the number of vertex pairs that could in principle be connected.

As a concrete illustration, Table 1 gives the adjacency matrix A for the six-protein network P1–P6 used as a worked example later in this chapter (Section 5.1), where P1 interacts with P2, P3, and P4, P2 additionally interacts with P5, and P3 additionally interacts with P6. Summing each row of A recovers the vertex degree defined in (2.1): $d(P1) = 3$, $d(P2) = d(P3) = 2$, and $d(P4) = d(P5) = d(P6) = 1$, so that $^{P}d(v) = 10 = 2|E(G)|$, consistent with the handshake identity for a graph with five edges.

Table 1: Adjacency matrix *A* for the P1–P6 example network

	P1	P2	P3	P4	P5	P6
P1	0	1	1	1	0	0
P2	1	0	0	0	1	0
P3	1	0	0	0	0	1
P4	1	0	0	0	0	0
P5	0	1	0	0	0	0
P6	0	0	1	0	0	0

3. Biological Networks as Graphs

3.1 Protein-Protein Interaction (PPI) Networks

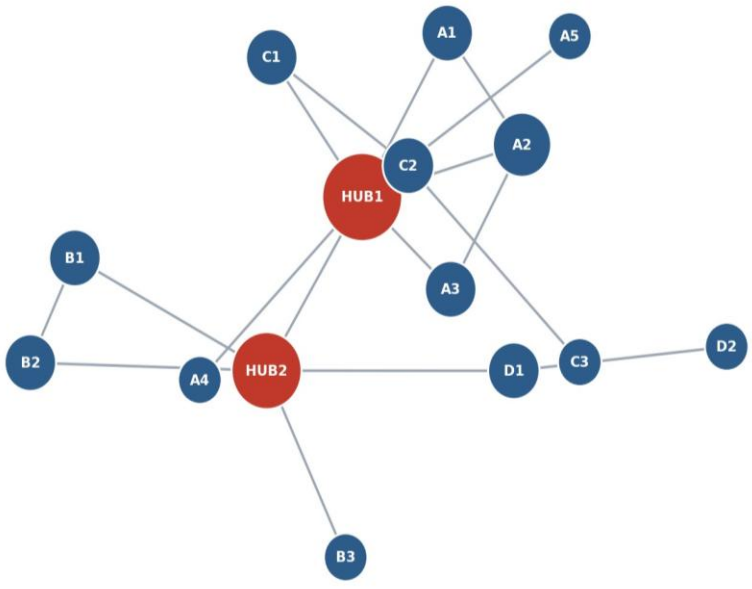

Figure 1: An example protein–protein interaction (PPI) network

A PPI network is an undirected graph in which vertices represent proteins and an edge joins two proteins if a physical interaction between them has been experimentally observed or computationally predicted. Such networks are assembled from curated interaction databases and from high-throughput experimental methods, including yeast two-hybrid screens [4] and affinity purification coupled with mass spectrometry. Because experimental coverage is incomplete and uneven across organisms and tissue types, any PPI network under study is best understood as a partial, evolving sample of the true interactome rather than a complete map [5].

In the figure**, v**ertices represent proteins; edges represent documented physical interactions. A small number of high-degree "hub" proteins (shown in red) connect to disproportionately many partners, illustrating the scale-free structure described in Section 2.2.

3.2 Disease and Disease-Gene Networks

A complementary representation links disorders to the genes whose mutation is known to cause or predispose to them. This is naturally modelled as a bipartite graph with one vertex class for diseases and one for genes, an edge indicating a documented disorder-gene association. Projecting this bipartite structure onto a single vertex class produces two derived networks: a disease network, in which two disorders are joined if they share at least one associated gene, and a gene network, in which two genes are joined if they are both associated with the same disorder. These projections make explicit a fact that is easy to overlook when diseases are studied in isolation: many apparently unrelated disorders share a common genetic or molecular origin. Framing medicine in these network terms, sometimes called network medicine, treats a disease phenotype as a consequence of perturbation to a module of interacting genes rather than to any single gene in isolation [6]. A related line of work models disease-disease relationships directly through the topology of the incomplete human interactome, showing that the degree of network-based overlap between two disease modules predicts the extent of their comorbidity and shared molecular pathology [7].

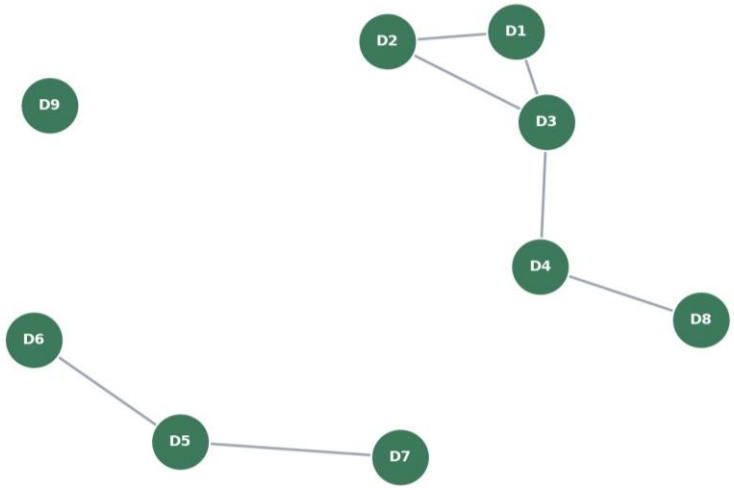

Figure 2: simplified disease network derived by projecting a disease–gene bipartite graph

Figure 2 illustrates a simplified disease network derived by projecting a disease–gene bipartite graph onto the disease vertex class. Two diseases are joined by an edge when they share at least one associated gene (Section 3.2); the resulting clusters (e.g. {D1, D2, D3, D4} and {D5, D6, D7}) correspond to disorders that share an underlying molecular module, while an unconnected disease such as D9 shares no known gene with the others in this illustrative sample.

3.3 Drug-Target and Bipartite Networks

A related construction represents the relationship between drugs and their protein targets as a bipartite graph, with drug and target as the two vertex classes and an edge indicating a documented drug-target interaction. Such bipartite networks support graph-theoretic approaches to drug repurposing, since two drugs sharing several targets, or two targets sharing several drugs, are natural candidates for further pharmacological investigation.

3.4 Data Resources for Network Construction

Constructing the PPI, disease, and drug-target networks described above draws in practice on a small number of major community-curated databases, each covering a different layer of biological interaction. STRING aggregates and confidence-scores physical and functional protein associations drawn from experimental evidence, curated pathways, co-expression data, and automated text mining, and is the most widely used general-purpose PPI resource. BioGRID and IntAct instead focus on individually curated, directly documented physical and genetic interactions, and are typically preferred where higher-confidence, experimentally traceable evidence is required rather than an aggregated score. DisGeNET compiles gene-disease associations from expert-curated repositories, genome-wide association studies, and text mining, and is a standard starting point for building the bipartite disease-gene networks introduced in Section 3.2. DrugBank combines detailed pharmacological, chemical, and protein-target information for approved and investigational drugs, and underlies most drug-target bipartite networks of the kind described in Section 3.3. Because these resources differ in curation standard, update frequency, and organismal coverage, network-based analyses should report the database version and confidence threshold used, since this choice can materially affect the measured degree, centrality, and domination values discussed in Sections 4 and 5.

4. Key Graph-Theoretic Measures for Network Biology

Table 2 summarises the structural measures most frequently used in the analysis of biological networks, together with the biological interpretation typically attached to each.

Of these, degree and betweenness centrality have accumulated the strongest and most consistently reported associations with gene essentiality: across multiple organisms, proteins occupying high-degree or high-betweenness positions in the interactome are disproportionately represented among genes whose deletion is lethal or severely deleterious. This observation is often summarised as the “centrality-lethality rule.”

Table 2: Structural measures used in biological network analysis

Measure	Definition	Typical Biological Interpretation
Degree centrality	Number of edges incident to a vertex	High-degree "hub" proteins are disproportionately likely to be essential for organism viability
Betweenness centrality	Fraction of shortest paths between all vertex pairs that pass through a given vertex	High-betweenness proteins act as bridges between functional modules and are often bottlenecks for signal or information flow
Closeness centrality	Inverse of the sum of shortestpath distances from a vertex to all others	Identifies vertices that can influence, or be influenced by, the rest of the network with minimal delay
Clustering coefficient	Proportion of a vertex's neighbours that are themselves connected	Reflects local functional modularity; proteins in the same complex tend to have high clustering
Domination number $\gamma(G)$	Minimum size of a vertex subset S such that every vertex outside S is adjacent to at least one vertex in S	The smallest set of proteins or genes whose monitoring, in principle, gives indirect coverage of the entire network

To make these measures concrete, Table 3 reports degree, (normalised) betweenness, and closeness centrality, together with the clustering coefficient, computed directly from the adjacency matrix of Table 1 for the same six-protein example. Because this illustrative network is a tree (five edges joining six vertices, with no cycles), every clustering coefficient is zero: no vertex has two neighbours that are themselves connected.

Table 3: Degree, betweenness, closeness, and clustering values for the P1–P6 example network

Vertex	Degree	Betweenness*	Closeness	Clustering Coefficient
P1	3	0.80	0.71	0.00
P2	2	0.40	0.56	0.00
P3	2	0.40	0.56	0.00
P4	1	0.00	0.45	0.00
P5	1	0.00	0.38	0.00
P6	1	0.00	0.38	0.00

**Betweenness is normalised by dividing by* $(n-1)(n-2)/2 = 10$*, the maximum possible number of vertex pairs a single vertex can lie between in a network of* $n = 6$ *vertices.*

Real interactomes typically depart sharply from this, since dense local neighbourhoods around hub proteins produce the non-zero clustering coefficients associated with the small-world property of Section 2.2. Within the toy example, P1, the highest-degree vertex, also attains the highest betweenness (0.80) and closeness (0.71) centrality, illustrating the empirical association between high centrality and structural importance noted above and revisited for the domination number in Section 5.1.

5. Domination Theory as a Network Control Framework

While centrality measures rank individual vertices, domination theory addresses a related but distinct question: what is the smallest subset of vertices needed so that every remaining vertex is directly reachable, in one step, from at least one member of that subset?

Definition 5.1 (Dominating Set). A set $S \subseteq V(G)$ is a dominating set of G if every vertex not in S has at least one neighbour in S. The domination number $\gamma(G)$ is the cardinality of a smallest dominating set of G:

$$\gamma(G) = \min\{|S| : S \text{ is a dominating set of } G\} \quad (5.1)$$

The concept and its early theory are developed systematically in [8]. In the context of a PPI or disease network, a dominating set has a natural interpretation as a minimal set of proteins or genes that, if monitored, perturbed, or targeted, gives indirect coverage of every other vertex in the network through a direct interaction. This makes domination-theoretic quantities attractive candidates for identifying compact, high-coverage control or intervention sets, complementary to the individual-vertex ranking that centrality measures provide.

Classical domination is a coarse instrument, however, since it only requires a single dominating neighbour per vertex, regardless of that vertex's total degree. Several refinements have been proposed to make the notion more informative for dense, heterogeneous biological graphs, including variants that require a vertex to be dominated by a majority, rather than merely at least one, of its neighbours, and extensions of domination to hypergraphs, which can represent interactions among more than two molecules at once, such as multi-protein complexes, more faithfully than a simple graph can. These refinements are the subject of ongoing methodological development and are not treated as settled in this chapter; they are noted here as an active research direction rather than as established results.

5.1 A Worked Illustration

To make Definition 5.1 concrete, consider a small hypothetical interaction network with six proteins, P1 through P6, where P1 interacts with P2, P3, and P4; P2 additionally interacts with P5; and P3 additionally interacts with P6. Because P1 is adjacent to P2, P3, and P4, and P2 is adjacent to P5, and P3 is adjacent to P6, the two-vertex set {P1, P2} already covers every other vertex in the network except P6, so P3 must also be included, giving the dominating set {P1, P2, P3} of size three. No single vertex can dominate the whole graph here, since P1 alone leaves P5

and P6 uncovered, so $\gamma(G) = 3$ for this example. In a real interactome of thousands of proteins, the analogous computation identifies a compact panel of proteins whose combined first-degree neighbourhoods span the entire network, a set that is of direct interest when the goal is broad monitoring coverage with a minimal number of assay targets.

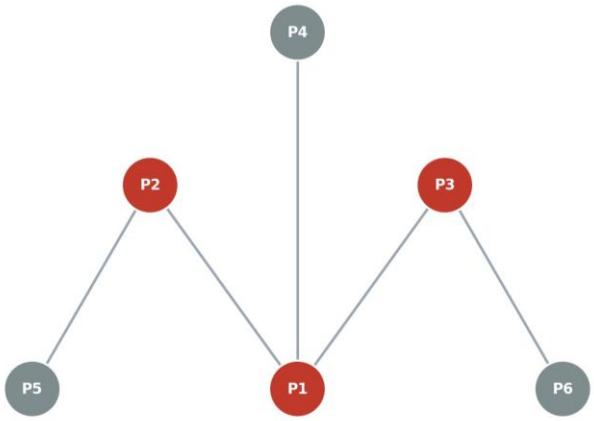

Figure 3: The worked example of Section 5.1. P1, P2, and P3

In Figure 3 the worked example of Section 5.1. P1, P2, and P3 (shown in red) form a minimum dominating set $S = \{P1, P2, P3\}$: every vertex outside S — namely P4, P5, and P6 — has at least one neighbour inside S, and no smaller set has this property, so $\gamma(G) = 3$.

6. Representative Findings from the Literature

Several results from the network biology literature illustrate how the measures introduced above connect graph structure to biological function.

6.1 Hub Proteins and Essentiality

An early and influential analysis of the *Saccharomyces cerevisiae* PPI network showed that the likelihood a single-gene deletion is lethal correlates strongly with the topological position of the corresponding protein in the interaction network, with highly connected hub proteins substantially more likely to be essential than sparsely connected ones [9]. This finding established the centrality-lethality rule as a foundational result in network biology and motivated much of the subsequent interest in graph-theoretic analysis of interactomes.

6.2 The Human Disease Network

Constructing a bipartite network of disorders and disease genes from curated gene-disease association data, Goh, Cusick, Valle, Childs, Vidal and Barabasi showed that genes associated with similar disorders´ are more likely to physically interact and to show correlated expression than would be expected by chance, supporting the existence of disease-specific functional modules within the interactome [10]. The same study reported that genes essential for organism survival are disproportionately represented among interactome hubs, linking the disease-network perspective back to the centrality-lethality rule observed in single-organism PPI networks.

6.3 Scale-Free and Modular Organisation

The broader observation that many biological and technological networks share a scale-free degree distribution, in which a small number of highly connected hubs coexist with a large number of sparsely connected vertices, was established in foundational work by Barabasi and Albert [2]. Subsequent stud-´ ies extended this observation to metabolic networks specifically, showing that this architecture confers robustness to random component failure while creating vulnerability to the targeted removal of hub vertices, a property directly relevant to the identification of drug targets [11].

6.4 Robustness, Attack Tolerance, and Drug Targets

Scale-free networks exhibit a well-documented asymmetry in their response to vertex removal: they remain almost fully connected under the random loss of vertices, since a randomly chosen vertex is overwhelmingly likely to be a low-degree, structurally peripheral one, but they fragment rapidly under the targeted removal of their highest-degree hubs. This error-and-attack asymmetry, established for scale-free networks in general, carries a direct pharmacological implication for PPI networks: a small number of hub or high-betweenness proteins disproportionately maintain the network's overall connectivity, which is part of the structural rationale for treating such proteins as priority candidates in target identification, alongside the functional and clinical evidence that any specific candidate target requires.

Computational Challenges and Open Directions

- Incompleteness and bias of interaction data: current PPI datasets remain far from a complete map of any organism's interactome, and well-studied proteins are disproportionately represented, which can distort measured centrality and domination values.
- Computational cost: exact computation of the domination number and of betweenness centrality is expensive on very large graphs, motivating the continued development of efficient exact algorithms for structured instances and provably-bounded approximation or heuristic algorithms for general large-scale networks.
- Beyond simple graphs: many biological interactions genuinely involve more than two participants at once, such as multi-subunit protein complexes and multi-drug combination effects, motivating continued work on hypergraph and multilayer network models and their associated domination and centrality theory.
- Integration with dynamic and weighted data: most of the measures described in this chapter are defined for static, unweighted graphs, while real interactions vary in confidence, strength, and condition-dependence; incorporating this information without discarding the interpretability of the underlying combinatorial measures remains an open methodological question.

- Validation against experimental outcomes: topological predictions of essentiality or drug-target suitability ultimately require experimental or clinical validation, and graph-theoretic results are most useful when framed as hypothesis-generating rather than as a substitute for such validation.

Looking ahead, several developments in graph theory itself are likely to reshape how biological networks are analysed. Hypergraphs, in which a single edge can join more than two vertices, offer a more faithful representation of multi-protein complexes and multi-drug combination effects than the pairwise graphs considered throughout this chapter. Temporal networks, which record when an interaction is observed rather than treating the network as a single static snapshot, are increasingly used to capture how interactomes and disease modules change across developmental stages or disease progression. Multilayer networks extend this further by representing several distinct relationship types, such as physical interaction, co-expression, and genetic interaction, as separate but coupled layers over the same vertex set. Graph neural networks and related graph representation learning methods now allow the centrality-, domination-, and topology-based reasoning developed in this chapter to be combined with learned, datadriven vertex embeddings, and have already been applied to problems ranging from protein function and molecular property prediction to drug-target interaction and drug repurposing [12, 13, 15]. Spectral graph learning, which draws on the eigenvalue structure introduced in Section 2.3, is emerging as a complementary route to comparing and classifying biological networks at scale [16]. Together, these developments, hypergraphs, temporal networks, multilayer networks, graph neural networks, and spectral graph learning, are expected to play an increasingly important role in biological network analysis, extending the classical graph-theoretic and domination-theoretic tools discussed in this chapter rather than replacing them [14].

Conclusion

Graph theory provides a compact and mathematically precise vocabulary for describing the architecture of biological interaction data. The recurring empirical finding that structural position in a PPI or disease network correlates with functional importance, whether measured through degree, betweenness, or domination-theoretic quantities, has made graph-theoretic analysis a standard component of systems biology and an increasingly important tool in computational drug discovery. Continued progress in this area depends both on improving the completeness of the underlying interaction data and on refining the mathematical measures used to interpret it, particularly through domination-theoretic and hypergraphbased frameworks capable of capturing the multi-way, heterogeneous nature of real molecular interactions.

References

1. Chartrand, G., & Zhang, P. (2012). *A first course in graph theory*. Dover Publications.

2. Barabási, A.-L., & Albert, R. (1999). Emergence of scaling in random networks. *Science, 286*(5439), 509–512.
3. Watts, D. J., & Strogatz, S. H. (1998). Collective dynamics of 'small-world' networks. *Nature, 393*(6684), 440–442.
4. Fields, S., & Song, O. (1989). A novel genetic system to detect protein-protein interactions. *Nature, 340*(6230), 245–246.
5. Vidal, M., Cusick, M. E., & Barabási, A.-L. (2011). Interactome networks and human disease. *Cell, 144*(6), 986–998.
6. Barabási, A.-L., Gulbahce, N., & Loscalzo, J. (2011). Network medicine: A network-based approach to human disease. *Nature Reviews Genetics, 12*(1), 56–68.
7. Menche, J., Sharma, A., Kitsak, M., Ghiassian, S. D., Vidal, M., Loscalzo, J., & Barabási, A.-L. (2015). Uncovering disease-disease relationships through the incomplete interactome. *Science, 347*(6224), 1257601.
8. Haynes, T. W., Hedetniemi, S. T., & Slater, P. J. (1998). *Fundamentals of domination in graphs*. Marcel Dekker.
9. Jeong, H., Mason, S. P., Barabási, A.-L., & Oltvai, Z. N. (2001). Lethality and centrality in protein networks. *Nature, 411*(6833), 41–42.
10. Goh, K.-I., Cusick, M. E., Valle, D., Childs, B., Vidal, M., & Barabási, A.-L. (2007). The human disease network. *Proceedings of the National Academy of Sciences, 104*(21), 8685–8690.
11. Jeong, H., Tombor, B., Albert, R., Oltvai, Z. N., & Barabási, A.-L. (2000). The large-scale organization of metabolic networks. *Nature, 407*(6804), 651–654.
12. Li, M. M., Huang, K., & Zitnik, M. (2022). Graph representation learning in biomedicine and healthcare. *Nature Biomedical Engineering, 6*(12), 1353–1369.
13. Corso, G., Stark, H., Jegelka, S., Jaakkola, T., & Barzilay, R. (2024). Graph neural networks. *Nature Reviews Methods Primers, 4*, 17.
14. Bang, D., Lim, S., Lee, S., & Kim, S. (2023). Biomedical knowledge graph learning for drug repurposing by extending guilt-by-association to multiple layers. *Nature Communications, 14*, 3570.
15. Yao, R., Shen, Z., Xu, X., Ling, G., Xiang, R., Song, T., Zhai, F., & Zhai, Y. (2024). Knowledge mapping of graph neural networks for drug discovery: A bibliometric and visualized analysis. *Frontiers in Pharmacology, 15*, 1393415.
16. Yi, H.-C., You, Z.-H., Huang, D.-S., & Kwoh, C. K. (2022). Graph representation learning in bioinformatics: Trends, methods and applications. *Briefings in Bioinformatics, 23*(1), bbab340.

Convergence in Science and Technology: Bridging Discovery and Application Volume II (ISBN: 978-93-47587-98-6)

About Editors

Mr. Ankit M. Nakade, M.Sc., M.A., B.Ed., SET, GATE, TS-SET and GJ-SET, is working as an Assistant Professor in the Department of Botany at S. S. Jaiswal College, Arjuni/Mor, District Gondia. His areas of interest include Plant Ecology, Palynology, Taxonomy, and Phytochemistry. He has published research articles and book chapters in reputed national journals. He is pursuing a Ph.D. in Botany at RTM Nagpur University, Nagpur. He has attended workshops, seminars, and conferences and is a life member of The Indian Botanical Society. He has worked as an editor for Research and Reviews in Plant Science, Volume III, by Bhumi Publishing, India. He has authored six Botany textbooks for B.Sc. Semesters I–IV. He holds two UK patents and three Indian patents. He has four years of undergraduate and two years of postgraduate teaching experience.

Dr. S. Subramanian is an Assistant Professor in the Department of Nautical Science at AMET University, Chennai. He earned his Ph.D. in Remote Sensing from Gandhigram Rural Institute, Dindigul, in 2025, and holds an M.Sc. in Geology from the University of Madras. His expertise includes Geology, Geoinformatics, Remote Sensing, GIS, Petroleum Exploration, Mining, Hydrogeology, Marine Geology, and Natural Resource Management. He has nearly four years of teaching experience and around two decades of industrial experience in Oil & Gas and Mining sectors, with international exposure across Southeast Asia, Southwest Asia, and Africa. He has contributed research publications, book chapters, and conference papers on geospatial technologies, groundwater management, mining, marine resources, and sustainable development. His research focuses on Remote Sensing and GIS for mineral exploration, groundwater assessment, environmental monitoring, and sustainable development.

Mr. Mahesh Prabhakar Thakare is a scholar and researcher in Mathematical Sciences. He completed his graduation from G. S. Gawande College, Umarkhed, and his postgraduate degree in Mathematics from N.E.S. Science College, Nanded, affiliated with SRTMUN. He qualified the MH-SET examination in Mathematical Sciences conducted in April 2024 and CTET Paper-II in Mathematics and Science in December 2024. He has published four research papers on partial differential equations, digital mathematics teaching, mathematical software, and undergraduate learning difficulties. He has three years of postgraduate teaching experience, two years at H.Sc. level, and one year at undergraduate level. Currently, he is working as an Assistant Professor (CHB) for the aided undergraduate Mathematics course at G. S. Gawande College, Umarkhed.

Dr. Archana Sharma is an Assistant Professor, distinguished academician, and researcher in the field of Chemistry. She completed her Ph.D. in Chemistry from the Indian Grassland and Fodder Research Institute (IGFRI), Jhansi. She holds postgraduate qualifications in Chemistry (M.Sc.), along with B.Ed. and MBA degrees, reflecting her multidisciplinary expertise in science, education, and management. Currently serving at Shri Umiya Kanya Mahavidyalaya, Rangwasa, Rau, Indore, she is actively engaged in teaching and research. Her core research interests include Chemistry and Biochemistry. She is committed to innovative pedagogy, laboratory-based learning, and fostering scientific curiosity among students. Her academic pursuits focus on contributing to scientific knowledge through quality research publications and meaningful educational practices. She continues to integrate scientific expertise, teaching innovation, and interdisciplinary perspectives to support excellence in higher education and research.

Bhumi Publishing

Bhumi Publishing,
Kolhapur, Maharashtra, India
bhumipublishing@gmail.com
www.bhumipublishing.com

ISBN 978-93-47587-98-6